THE COMBUSTION OF WOOD, MAINLY AS ASSESSED BY FLUIDISED-BED DIFFERENTIAL THERMAL ANALYSIS, WITH PARTICULAR REFERENCE TO RUBBER WOOD

A thesis presented for the degree of
Doctor of Philosophy in Chemical and Process
Engineering in the University of Canterbury,
Christchurch, New Zealand

by

Tan Ah Goh
1986

Dedicated to my mother, wife and children

ACKNOWLEDGEMENTS

The author would like, first of all, to thank Dr J.B. Stott for his supervision of this work in which he has shown great interest and provided valuable assistance. He would also like to thank Mr I.A. Gilmour for his help while Dr Stott was away on sabbatical leave.

Nearly all the technical needs in this work, including building the DTA apparatus, were provided by the technical staff of this department. They did a wonderful job and to them, the author extends his sincere thanks.

The author acknowledges the assistance provided by : (1) Dr D.E. Rogers and Dr R.H. Newman of the Department of Scientific and Industrial Research (Lower Hutt), the former in TG analysis of Rubber wood in a Stanton Redcroft thermobalance and the latter in examining the volatile products using ^{13}C NMR spectroscopy, (2) Dr C.J. Easton of the Chemistry Department of this University, in examining the volatile products using proton NMR spectroscopy and (3) Mrs J.A. Penman of the Geography Department, in the use of the digitiser.

The financial support of the New Zealand government by way of a Commonwealth Scholarship is gratefully acknowledged.

The author wishes to express his gratitute to his employer, the Rubber Research Institute of Malaysia, for giving him the opportunity to pursue this work and for providing most of the test materials. He is also indebted to some of his colleagues there for their help in preparing and shipping the test materials.

Finally, a word of thanks to all those who have given me a hand, besides the ones already mentioned.

CONTENTS

	Page
ABSTRACT	i
1. INTRODUCTION	1
1.1 Background	1
1.2 Objective	2
1.3 Method of Study	2
1.4 Scope	5
2. BASIC INFORMATION ON WOOD AND ITS COMBUSTION	6
2.1 Struture	6
2.2 Chemical Composition	7
2.3 Combustion	8
3. APPARATUS AND TEST MATERIALS	10
3.1 Apparatus	10
3.1.1 Furnace	10
3.1.2 Reactor	12
3.2 Test Materials	17
3.2.1 Rubber wood	17
3.2.2 Tropical hardwoods	22
3.2.3 Wood components	24
SECTION I : DIFFERENTIAL THERMAL ANALYSIS	
4. DIFFERENTIAL THERMAL ANALYSES IN AN INERT ENVIRONMENT	29
4.1 Trial Runs	29
4.2 Experimental Procedure	31
4.3 Individual Wood Components	34
4.3.1 Cellulose	34
4.3.2 Hemicelluloses	36
4.3.3 Acid Lignin	39
4.3.4 Extractives	40
4.4 Rubber Wood	42
4.4.1 Main Features of a Rubber Wood DTA Curve	42
4.4.2 Effect of Particle Size	43

Page

4.4.3 Effect of Gas Flowrate 54
4.4.4 Interpretation of DTA curves 54
4.4.5 DTA curves of Air-dry Wood 62
4.4.6 Comparison between Wood from Different Trees 62
4.4.7 Comparison between Fresh and Mouldy Wood 67
4.4.8 Comparison with Other Wood Species 70
5. ANALYSIS OF PYROLYSIS PRODUCTS 75
5.1 Collecting Device 75
5.2 Procedure 78
5.3 Yields of Pyrolysis Products 79
5.4 Examination of Liquid Fractions 85
6. DIFFERENTIAL THERMAL ANALYSIS IN AN OXIDATIVE ENVIRONMENT 93
6.1 Blank Runs 93
6.1.1 ΔT within Bed 93
6.1.2 ΔT between Beds 96
6.2 Experimental Procedure 96
6.3 Individual Wood Components 100
6.3.1 Cellulose 100
6.3.2 Acid Lignin 106
6.3.3 Extractives 108
6.4 Rubber Wood 110
6.4.1 Effect of Particle Size 110
6.4.2 Effect of Oxygen Concentration of Fluidising Gas 113
6.4.3 Heat of Reaction 125
6.4.4 Comparison with other Wood Species 129
6.4.5 Comparison between Wood from Different Trees 140
6.4.6 Comparison between Fresh and Mouldy Wood 142
6.4.7 Effect of Chemical Treatment 144
6.5 Temperature Drop across Reactor 147

Page

SECTION II : THERMOGRAVIMETRY

7. THERMOGRAVIMETRY 151
   7.1 Brief Introduction 151
   7.2 Analysis using Stanton Redcroft TG-750 Thermobalance 152
      7.2.1 In Nitrogen 154
      7.2.2 In Air 157
   7.3 Analysis using DTA Apparatus 157
      7.3.1 Wood Components 162
      7.3.2 Rubber Wood and other Wood Species 164
   7.4 Char Yields from Flash Pyrolysis 171
   7.5 Ash Determination 173

SECTION III : BURNING OF WOOD BLOCKS IN AN INCINERATOR

8. BURNING OF WOOD BLOCKS IN AN INCINERATOR 177
   8.1 Method of Study 177
      8.1.1 Apparatus 177
      8.1.2 Test Materials 179
      8.1.3 Experimental Procedure 180
   8.2 Results 182
      8.2.1 Rate of Burning 182
      8.2.2 Burner Temperatures 187
      8.2.3 Flue Gas Analysis 187
      8.2.4 Mass Balance 197
      8.2.5 Heat Balance 201

9. DISCUSSION AND CONCLUSIONS 205

REFERENCES 212

APPENDICES 216

ABSTRACT

The combustion characteristics of Rubber wood were studied using differential thermal analysis (DTA) carried out in fluidised-beds. Test samples up to 10 mm in diameter and fluidising gas of different oxygen concentrations were used. A number of tropical hardwoods were included in the study for comparison. Prior to the above study, investigations on the thermal behaviour of Rubber wood in an inert environment, in particular, the effect of particle size, were carried out. The particle sizes used ranged from smaller than 150 mesh to 19 mm diameter.

The yields of the various degradation products and the temperature range within which they were formed were noted. The liquid and gaseous products were analysed, the former qualitatively (by proton and ^{13}C NMR spectroscopy) and the latter quantitatively (by GLC).

Thermogravimetric analyses of the test materials were performed in both inert and oxidative environments to provide information complementary to those obtained from DTA, in particular, char yield and burning time in a stationary bed.

The ash contents of the wood species under study were determined. The adverse effect of ash on wood combustion was demonstrated in combustion experiments carried out in a down-draught incinerator using 5 cm thick blocks. Besides Rubber wood, three other species were used, including radiata Pine.

CHAPTER 1

INTRODUCTION

1.1 BACKGROUND

Malaysia is the world's leading producer of natural rubber, a commodity produced by the rubber tree (**Hevea brasiliensis**). Around 2.1 million hectares of her land is under rubber cultivation, occupying 6.4% of the land area. The method of harvesting this crop consists in slicing away a thin piece of the bark using a specially made knife. The process is known as tapping. A white, sticky liquid called latex* oozes out of the inner bark and is collected in a cup placed beneath the tapping panel. Tapping is normally carried out in the morning and the latices from all the trees in a particular field or plantation are collected before noon and processed before being exported. There are two common methods of processing natural rubber latices. In one of them, they are coagulated using formic acid, the coagulants are then pressed into sheets before being hung up and dried by smoke emitted from fuelwood. Rubbers produced in this way are known as Ribbed Smoked Sheets. In the other method, which is more widely used by the bigger producers, the latices are converted into coagulants as before, the coagulants are then reduced into crumbs mechanically before being dried in dryers using one or more oil-fired burners. The resultant product is marketed under the name Standard Malaysian Rubber, or SMR.

The economic life span of rubber trees is 25-30 years, at the end of which they are felled to make way for replanting. At the time of felling, the diameter of the tree trunk varies from around 20 cm to 40 cm, depending on the type of clone,+ soil fertility, etc. The amount of wood produced annually from the felling of old rubber trees has been estimated at around 6 million tonnes in Peninsular Malaysia (Tan and Chang, 1973). Among its more important uses today are as fuelwood

---

*Plural : latices.
+A clone is a vegetatively propagated plant with the same genetic constitution as the mother plant or seedling.

and for the making of charcoal, pulp and paper and furniture (Tan et al., 1981).

During the oil crisis of the seventies, most of the SMR producers in the country encountered the problem of increased fuel cost and uncertainty of supplies. It was soon realised that the petroleum-based fuels cannot be depended on for too long and an alternative source of energy would have to be found for drying their rubbers. A material much talked about as a likely alternative, especially in the long term, is Rubber wood, i.e. the wood derived from the rubber tree. Unlike petroleum, Rubber wood is renewable and is a by-product of the natural rubber industry itself. Besides, there is usually a good supply of other cellulosic materials almost all year round, e.g. Oil palm wood, Coconut wood and off-cut timbers, which could be used as a supplement for Rubber wood when the latter is in short supply. The switch to using biomass as the energy resource for drying SMR would save the country an estimated 30 million litres of diesel fuels a year (Khoo, 1982).

1.2 Objective

Although Rubber wood has long been used as fuel, virtually no published information is available on its combustion characteristics. It is doubtful if studies have ever been made on this subject. Such information will be of great help in the design of suitable burners for the wood. The primary objective of this work is therefore to study the combustion characteristics of Rubber wood and to compare them with those of other wood species from the tropics.

1.3 Method of Study

The method of study used is called differential thermal analysis, or DTA. Basically, it involves the continuous recording of the temperature difference between a test sample

and an inert reference material heated at a constant rate as a function of temperature or time. A change in the sample temperature with respect to the reference temperature signifies a reaction taking place in the sample. A schematic diagram of a typical DTA apparatus is shown in Figure 1 while an idealised DTA curve is provided in Figure 2. The measurement of temperature difference rather than temperatures has the advantage that it gives a greater sensitivity and permits detection of small temperature changes resulting from the physico-chemical transformations of substances during heating (Nguyen et al., 1981). This technique was developed around the turn of the century and its early use was mainly confined to research in metallurgy and clay minerals but in the course of time its fields of application became wider and covered such materials as soils, minerals, inorganic chemicals, polymers and solid fuels (Smothers and Chiang, 1966). Among those who have used it to study the thermal behaviours of wood and related materials are Arseneau (1961), Eickner (1962), Domburg et al.(1968), Chow and Pickles (1971) and Shafizadeh and DeGroot (1976). This technique has also been employed in the thermal analysis of coal, by workers including Stott and Baker (1953), Berkowitz (1958) and Rogers (1984).

In conventional DTA, both the test sample and the reference material remain stationary throughout the experiment. In both of them, a temperature gradient exists between the external boundary and the centre. In the case of the sample, this can be quite steep especially in runs conducted in an oxidative environment and may mask some of the temperature-dependent reactions. To overcome this problem, the present study was carried out in fluidised beds which have a uniform temperature. Fluidised-bed DTA was developed by Basden (1960a&b) who also built a calorimeter operating on the same principle (Basden, 1967a). An added advantage of this technique is that it is not necessary to use a uniform heating rate as in conventional DTA, in view of the high heat transfer

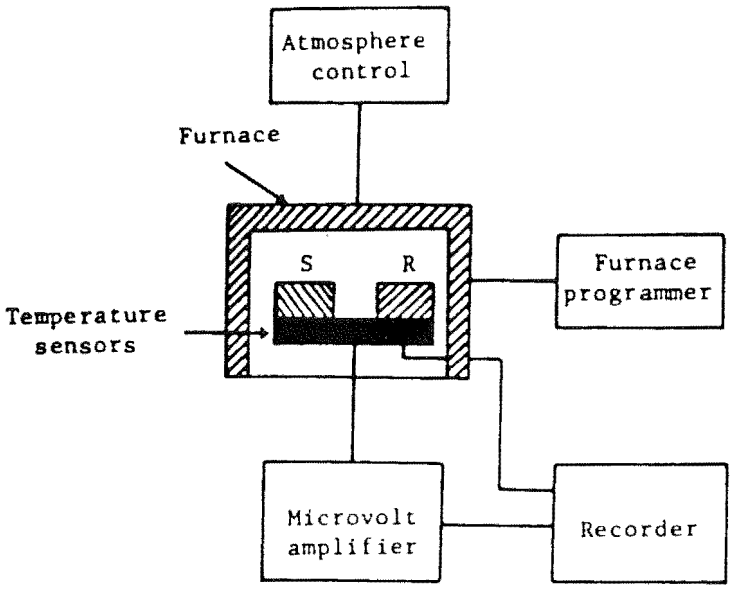

Figure 1. Schematic diagram of a typical DTA apparatus. S=Sample, R=Reference. After Wendlandt (1974)

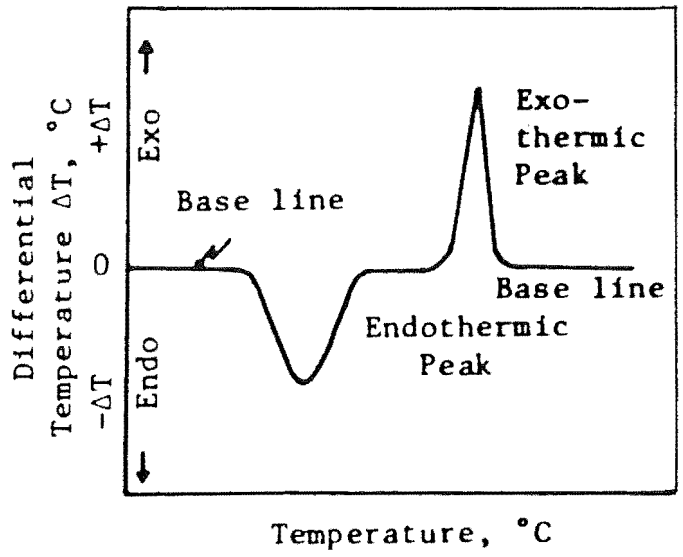

Figure 2. An idealised DTA curve. After Schwender (1968)

coefficients which exist between the beds and the containing walls. Furthermore a larger apparatus can be built, which would allow bigger wood pieces and also larger sample sizes to be used.

For combustion to take place, air or oxygen must be present in the sample chamber. Therefore, the study of the combustion characteristics of Rubber wood requires that the DTA experiments be carried out in an oxidative environment.

1.4 Scope

Although the main emphasis of this work lies in studying the combustion characteristics of Rubber wood, other areas of investigation which are of relevance were also carried out to provide additional information. These included DTA in an inert environment, analysis of the gases evolved during pyrolysis, monitoring of the weight loss during pyrolysis and combustion (thermogravimetry) and ash determination. The burning of 5 cm thick blocks in a down-draught incinerator was also investigated.

The terminology used in the present study was that recommended by the Nomenclature Committee of the International Conference of Thermal Analysis or ICTA (MacKenzie, 1971) while the results were reported in accordance with the guidelines of the Standardisation Committee of the same organisation (McAdie, 1967).

CHAPTER 2

BASIC INFORMATION ON WOOD AND ITS COMBUSTION

The basic information about wood and its combustion are provided here to facilitate a better understanding of the work being undertaken.

2.1 Structure

Wood is composed of elongated cells which are mostly oriented in the longitudinal direction of the stem. These cells vary in shape and functions, which include providing support to the tree and avenues for the transportation and storage of foodstuff. The flow of fluids from cell to cell occurs through openings in their walls known as pits.

The woods of coniferous trees or softwoods, differ in cell type and also in cell function from those of deciduous trees or hardwoods (Figure 3). Softwoods consist of 90% to 95% tracheids which are long and slender cells with flattened

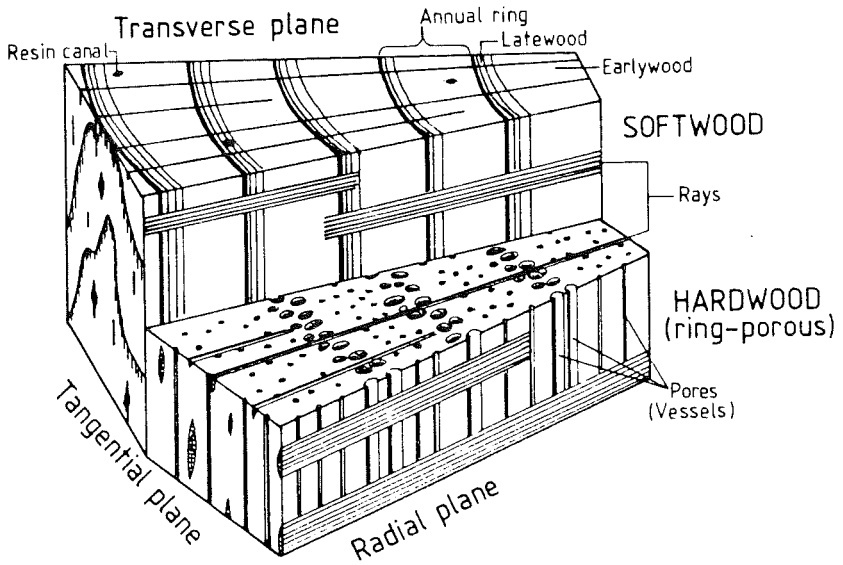

Figure 3. Structures of hardwoods and softwoods. After Fengel and Wegener (1984)

or tapered closed edges. The thick-walled latewood tracheids provide strength while the spacious early wood tracheids mainly conduct water and minerals within the tree. The storage and conduction of foodstuff takes place within the parenchyma cells which are oriented radially, forming rays. In hardwoods, the fibres are the basic tissues which function as supporting cells. Distributed within the wood are numerous conducting cells known as vessels or pores which are long pipes with open or perforated ends. The fibres of hardwoods have thicker walls but smaller lumina compared with the tracheids of softwoods. In some tropical hardwoods, there is a high percentage of longitudinal parenchyma.

2.2 Chemical Composition

The main constituents of wood, on a dry basis, are :

(1) Cellulose
(2) Hemicelluloses
(3) Lignin
(4) Extractives

Cellulose, the hemicelluloses and lignin are the cell-wall components whereas the extractives are not. Hardwoods contain around 40% cellulose, 33% hemicelluloses, 20% lignin and 7% extractives and ash while softwoods contain around 40% cellulose, 26% hemicelluloses, 26% lignin and 7% extractives and ash (Shafizadeh and Degroot, 1976).

Cellulose is the main component of the cell wall. It is a homopolysaccharide composed of β-D-glucopyranose units which are linked together by (1-->4)-glycosidic bonds. It is distinguished from the other polysaccharides in wood in that it yields only D-glucose on hydrolysis. It has the elementary formula $C_6H_{10}O_5$.

The hemicelluloses are heteropolysaccharides and are

easily hydrolysed by dilute acids. They are also soluble in aqueous alkaline solutions. Acetyl-4-O-methylglucuronoxylan, or xylan, is the major component in hardwoods while its counterpart in softwoods is the glucomannans or mannan (Shafizadeh and DeGroot, 1976). On hydrolysis, xylan yields D-xylose while mannan produces D-mannose. Xylan has the elementary formula $C_5H_8O_4$ (Tillman, 1978).

Lignin is an amorphous, aromatic compound built up of phenylpropane units (Sjostrom, 1981). It is characterised by the presence of methoxyl (OCH_3) and hydroxyl (OH) groups. It is an almost insoluble material but may be isolated from extractive-free wood as an insoluble residue after hydrolytic removal of the polysaccharides. It gives the cell wall its characteristics as regards strength, density and swelling properties. Its elementary formula is $C_9H_{10}O_3(OCH_3)_{0.9-1.7}$ (Tillman, 1978)

The extractives are not an essential structural part of the cell wall and can be extracted with water or organic solvents. Those which are soluble in organic solvents include resin and fatty acids and their esters, waxes, unsaponifiable substances and colouring matters. The water-soluble materials include inorganic salts, sugars, polysaccharides, cycloses and cyclitols, and some phenolic substances. Some of the substances which are soluble in organic solvents are also soluble in water, and vice versa.

Elementally, wood is composed of about 50% carbon, 6% hydrogen and 44% oxygen, on a weight basis. Only a minor difference exists in the elementary compositions of different wood species (Wenzl, 1970).

2.3 Combustion

When wood is heated above a certain temperature, it undergoes a degradation process known as pyrolysis during

which gases and vapours (often collectively referred to as the volatiles) are released, leaving behind a carbonaceous residue or char. The relative proportions of these products are dependent on the composition of the fuel, the reaction temperature, the rate of heating and the availability of oxygen (Evans et al., 1981). The vapours consist of water, organic compounds and tar and may be condensed to form a liquid fraction. In an oxidative environment, some of the gases and vapours burn with a flame which occurs entirely in the gas phase. The residual char, on the other hand, burns by surface oxidation, which is a slower process. Rapid oxidation of the char results in glowing combustion. In both cases, the final products are water and carbon dioxide. A small amount of ash is also produced. The combustion process is shown in Figure 4. If insufficient oxygen is present in the combustion chamber, this can lead to cracking of some of the volatiles to form soot particles.

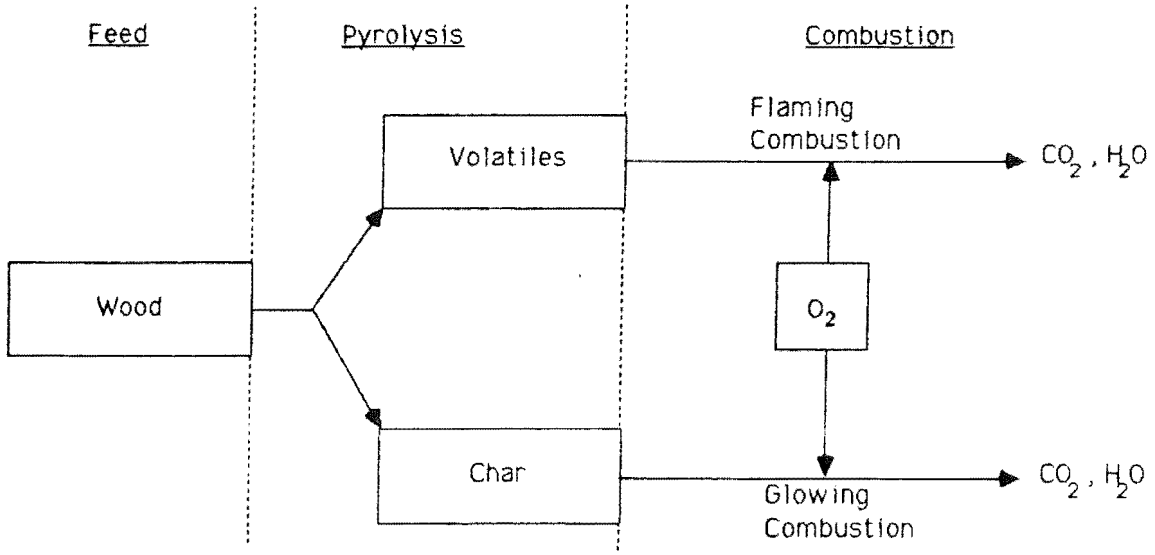

Figure 4. Wood combustion process. After Tillman (1978)

CHAPTER 3

APPARATUS AND TEST MATERIALS

3.1 Apparatus

The apparatus consists essentially of a furnace and a reactor. A brief description of each of them follows.

3.1.1 Furnace

The furnace is illustrated in Figure 5. It is hexagonal in shape and has an internal volume of 0.032 m^3. Its casing, including the lid, was constructed from 3 mm thick mild steel plate. It is insulated all round inside with 'Kaowool' ceramic fibre to a thickness of 45 mm except in the lid where the insulation is slightly thicker (53 mm). This insulating material, which comes in the form of a white blanket of various thicknesses, has a relatively low thermal capacity and conductivity compared with most of the conventional furnace lining materials. Four rows of insulating bricks are stacked on the inside of the furnace in the manner shown in the diagram. They form the sides and hold the heating elements. They sit on a layer of firebricks of height 40 mm placed at the bottom of the furnace. On top of the firebricks are two pieces of insulating bricks, each measuring 114mmx228mmx37mm. They are placed side by side and the reactor sits on them. To further reduce heat losses, the exterior walls of the furnace were lined with aluminium foil followed by a layer of fibre glass of thickness 50 mm. A piece of calico cloth was wrapped round the furnace to hold the external insulation. The internal dimensions of the furnace are : height 385 mm, length of a side 180 mm and distance between two opposite sides 310 mm.

The lid of the furnace contains six holes, two of diameter 42 mm and four of diameter 15 mm. The purpose of

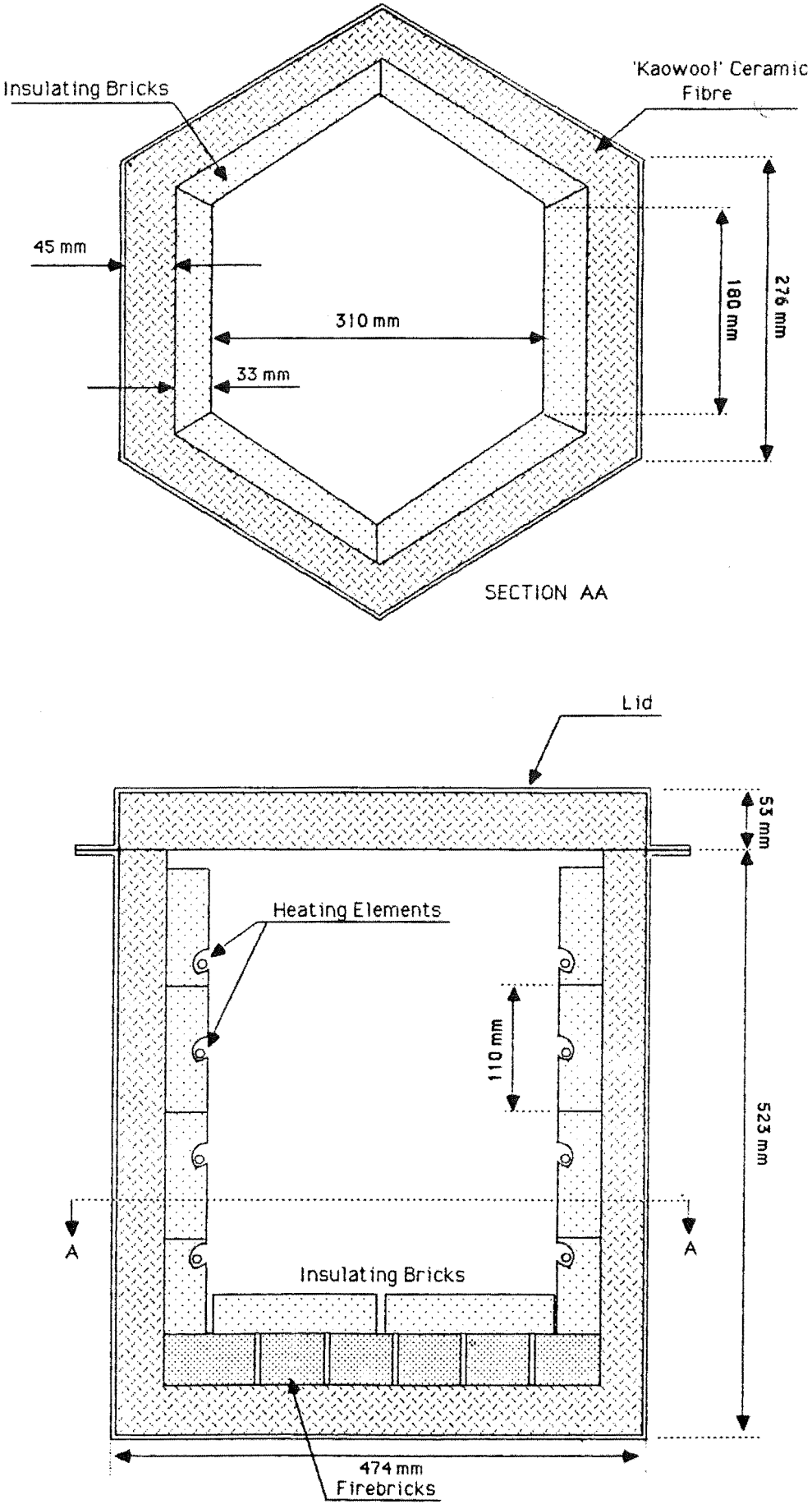

Figure 5. Schematic representation of furnace

these holes is to enable the two reaction tubes and also four stainless steel rods welded to the reactor to pass through, as shown in Figure 6. A thread was made at the end of each of the stainless steel rods so that the reactor can be bolted to the lid and lifted up for fan cooling at the end of each run (Figure 7). In this way, two or three runs can be carried out in a day as compared with only one if the reactor is allowed to cool down in the furnace. The lid contains the required mechanism for it to be lifted up with the aid of a crane.

The furnace is heated by four pieces of heating element inserted inside the grooves of the insulating bricks. Power supply to the furnace is regulated by a transformer which helps ensure that the heating elements are not overloaded. After a few trial runs, it was found that 3.5 kW was the correct power input to use, both from the viewpoint of duration of a run and safety of operation. The rate of heating of the reactor corresponding to this power input is around 5.5^{o}C/min.

3.1.2 Reactor

The reactor consists of three components. These are (1) the reaction tubes, (2) a stainless steel block and (3) a stand.

3.1.2.1 Reaction Tubes

The two reaction tubes are shown in Figure 8. They were made from SANDVIK 253MA stainless steel which is characterised by good structural stability at high temperatures and high resistance to oxidation and carburisation. The dimensions of each of them are : external diameter 33.4 mm, internal diameter 26.6 mm and height 497 mm. The distance separating them, centre to centre, is 70 mm. They are connected to a common stainless steel gas inlet coil through the use of a T-junction. The gas inlet coil has an external diameter of

Figure 6. Furnace lid and accessories.

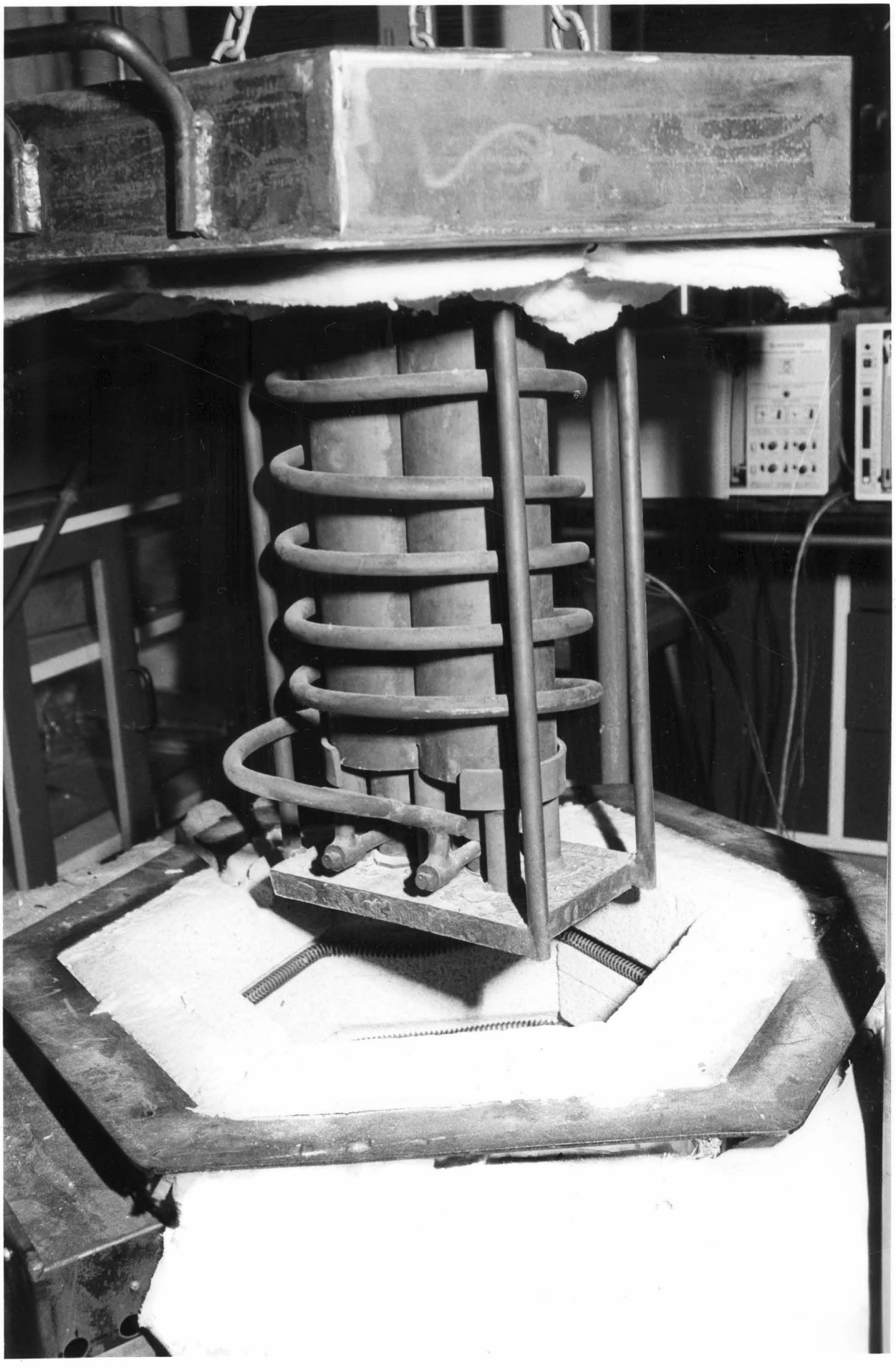

Figure 7. Reactor lifted up for fan cooling.

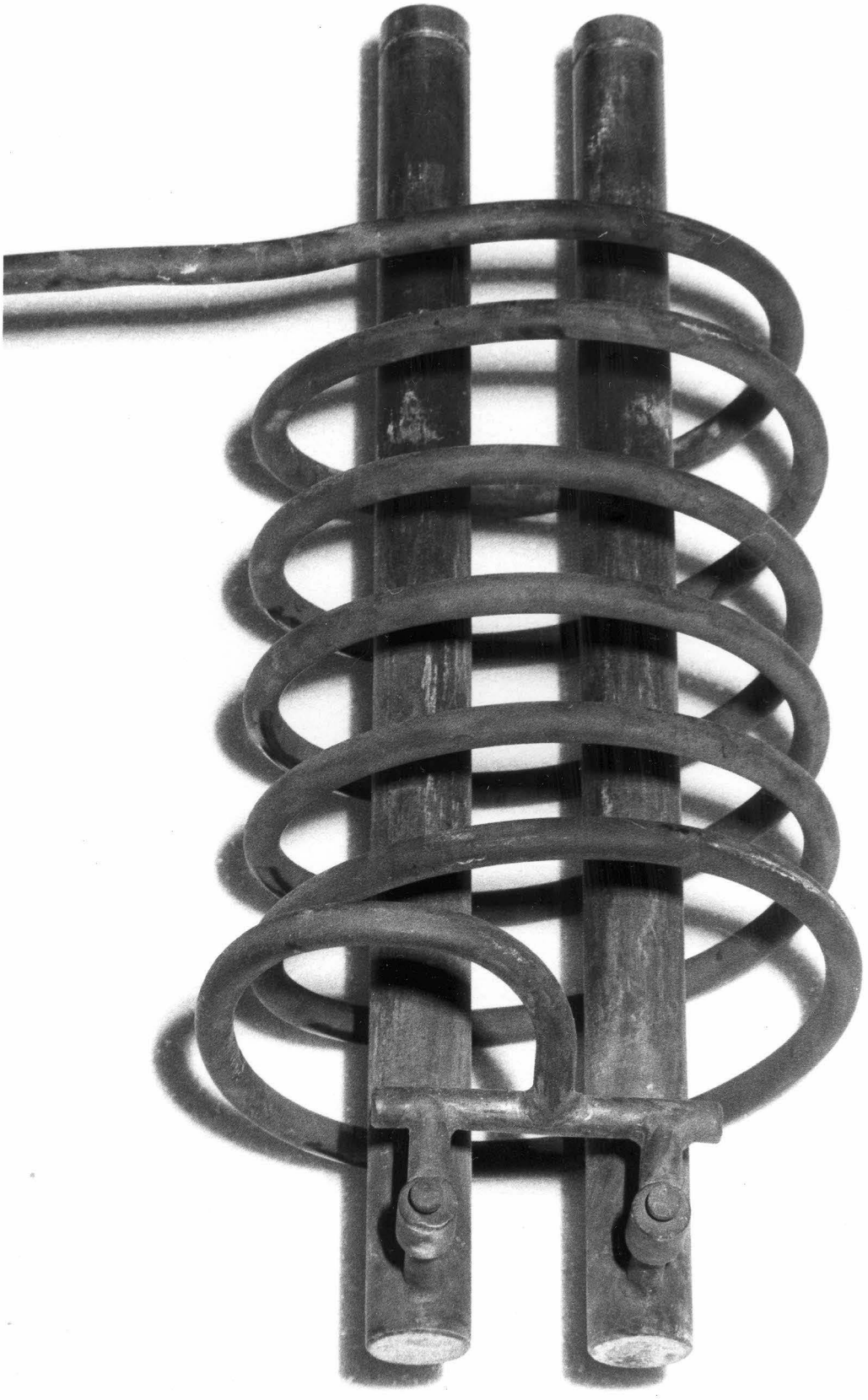

Figure 8. Reaction tubes and gas coil.

12.7 mm, an internal diameter of 10.0 mm and a length of 4.5 m and goes round the reaction tubes six times before ending up at the T-junction. The inlet gas passes through an orifice of diameter 1.6 mm and length 2 mm before entering each tube, as illustrated in Figure 9. The two orifices help keep the gas flowrates in the two tubes uniform. Without them, problems of uneven gas flowrates were encountered.

The gas distributor consists of a circular piece of 'Kaowool' ceramic fibre of thickness 13 mm. It was cut out from a blanket using a wad punch. It rests on a stainless steel frame of height 125 mm placed at the bottom of each tube. Its diameter at the time of preparation is 32 mm. By making it slightly oversized, it stays firmly in place when pushed down the tube with the aid of a rod. The frame consists essentially of two 25 mm diameters steel rings welded to the ends of two steel wires, each of length 120 mm and diameter 3 mm. It contains a metal strip welded across the two wires at a height of 9 cm to enable it to be taken out of the tube when required. The whole unit, i.e. the two reaction tubes plus the accessories, weighs 4.0 kg.

A considerable amount of time was spent in looking for a suitable gas distributor for use in the experiments. Several types or systems were tried out. 'Kaowool' ceramic fibre, in the form described above, was found to be the best for the following reasons :

- it is thermally stable
- it is not attached permanently to the tube
- it is easy to make, install and replace
- it is non fragile
- it does not allow fine solids to pass through
- because of its thickness, a considerable pressure drop exists across it, which is desirable to achieve equal gas flow through the openings
- it is relatively inexpensive

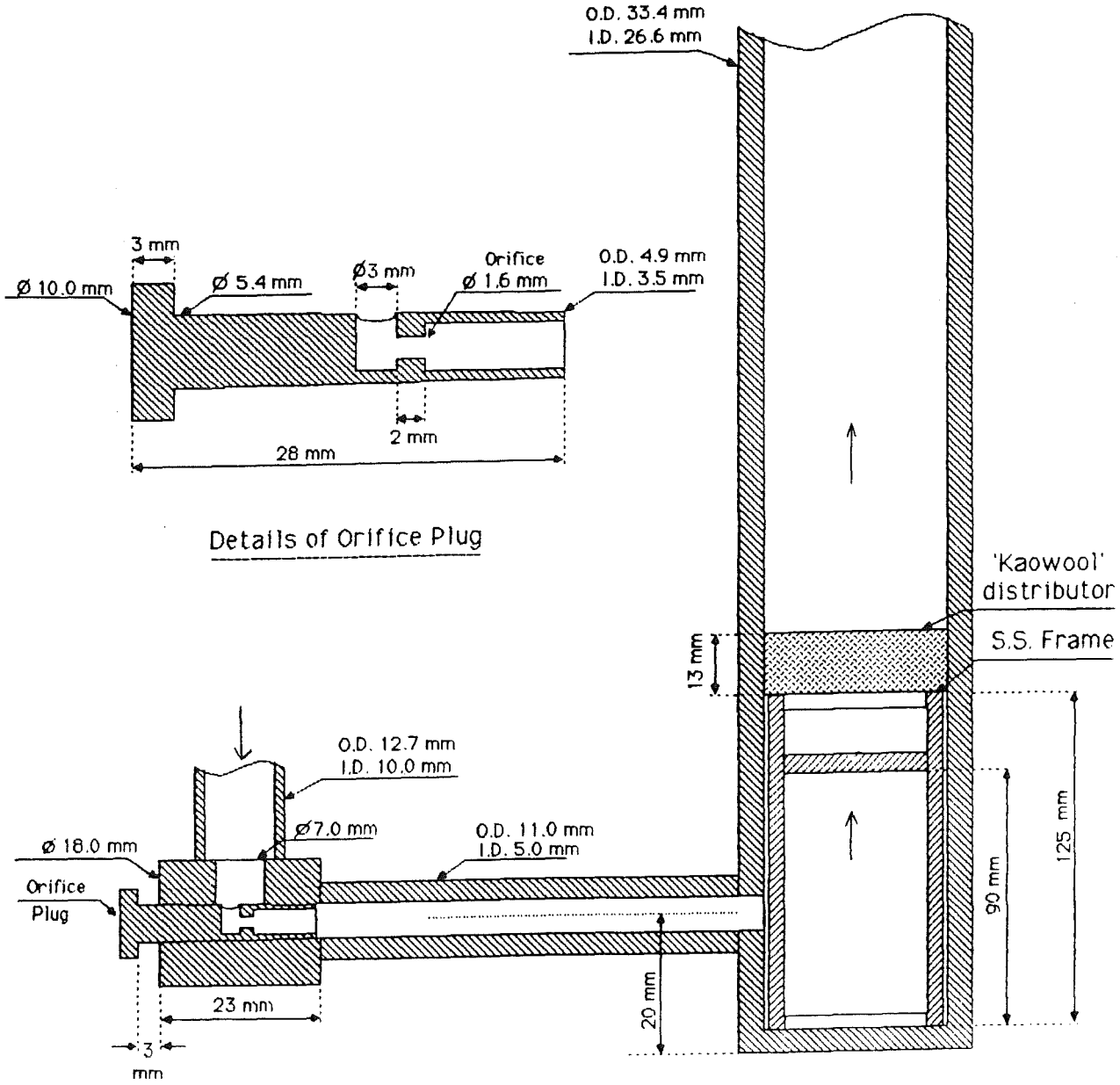

Figure 9. Details of gas inlet

3.1.2.2 Stainless Steel Block

The stainless steel block is shown in Figure 10. It was made from the welding together of two stainless steel tubes, each of external diameter 89.0 mm, internal diameter 39.4 mm and height 297 mm and having a segment cut off. The distance between the centres of the two tubes is 71 mm. It weighs 21.5 kg and serves as a heat sink.

3.1.2.3 Reactor Stand

The reactor stand is shown in Figure 11. It consists of four parts, viz (1) a mild steel base of length 210 mm, width 136 mm and thickness 19 mm, (2) four stainless steel rods of diameter 12.7 mm and height 472 mm welded to the shorter sides of the base, (3) six stainless tubes of external diameter 21.5 mm, internal diameter 13.5 mm and height 68 mm welded to the top face of the base and (4) a stainless steel strip of width 25 mm and thickness 4.5 mm welded around the tubes to form a barrier. The weight of the stand is 5.5 kg.

The assembled unit is shown in Figure 12 and represented schematically in Figure 13. In it, the two reaction tubes pass through the two holes in the stainless steel block. The annular space between each tube and the steel block is filled with powdered magnesia (magnesium oxide) and sealed at the ends by steel rings. A section of length 132 mm of each tube protrudes out of the block. However, only half of this section projects out of the lid. The steel block sits on the six pillars of the stand and is kept in place by the barrier. The weight of the assembled unit is 31.0 kg.

The thermal capacity, i.e. mass x specific heat, of the reactor is 19.84 kJ/K. If all the power input to the furnace (3.5 kW) goes into heating the reactor, its rate of temperature rise would be 10.58^{o}C/min. However, in practice,

Figure 10. Stainless steel block.

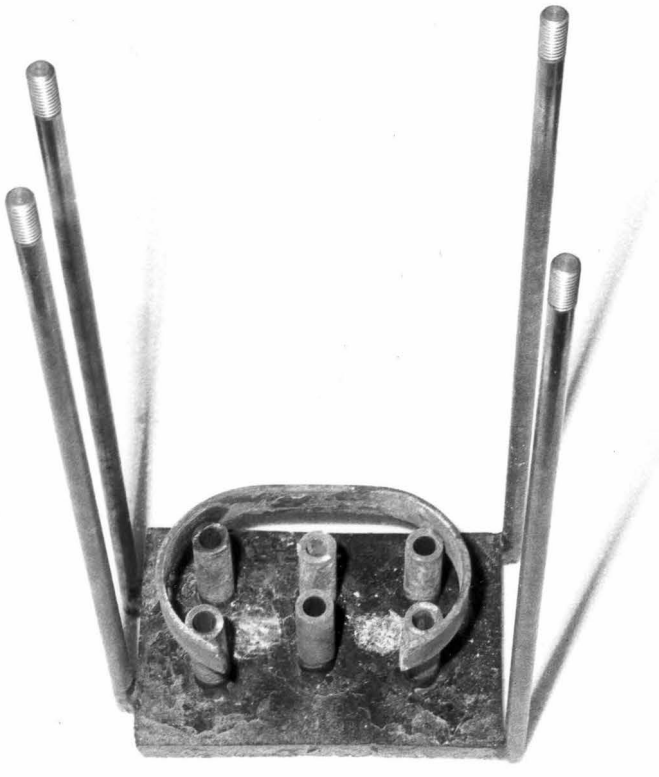

Figure 11. Reactor stand

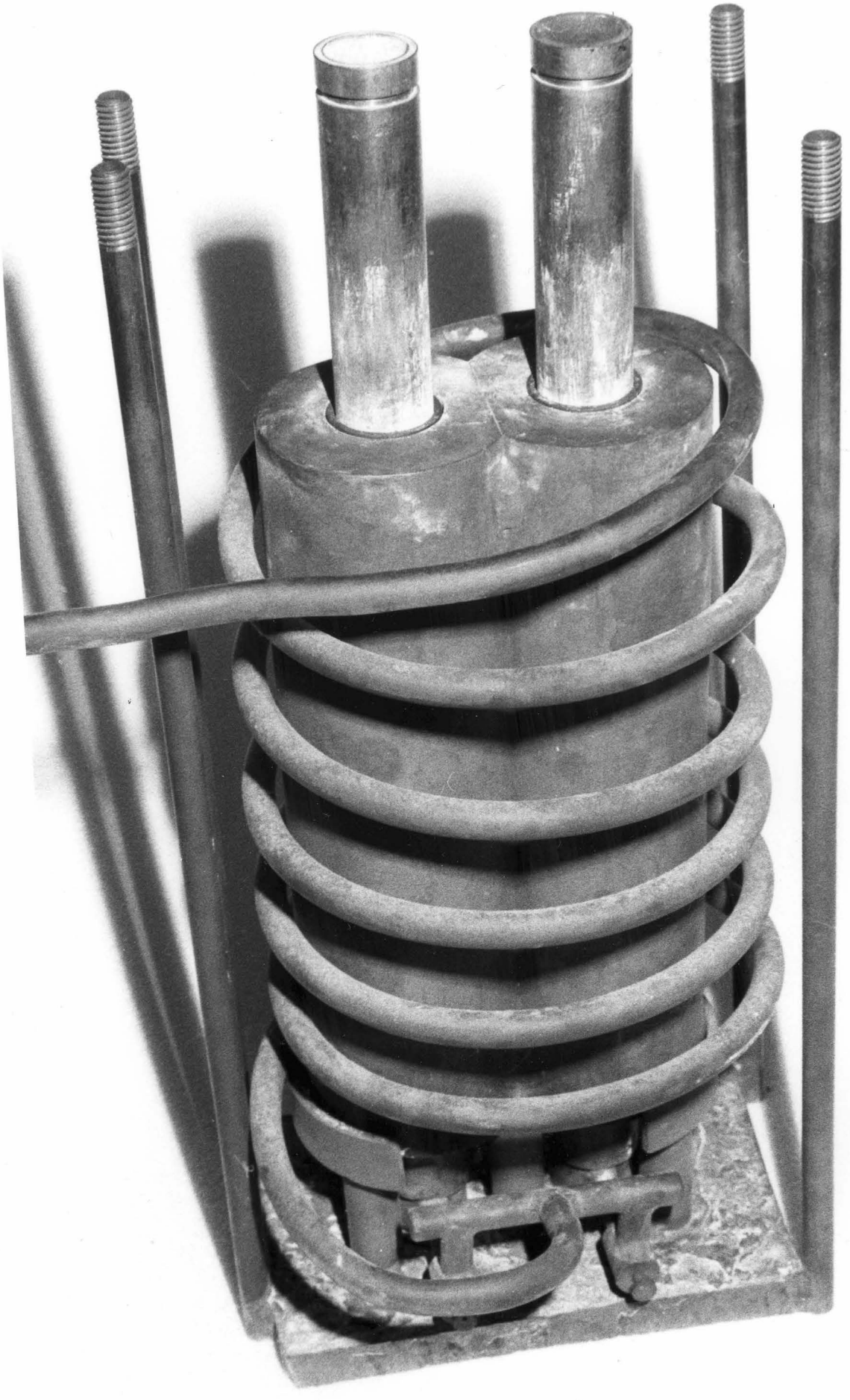

Figure 12. Assembled unit.

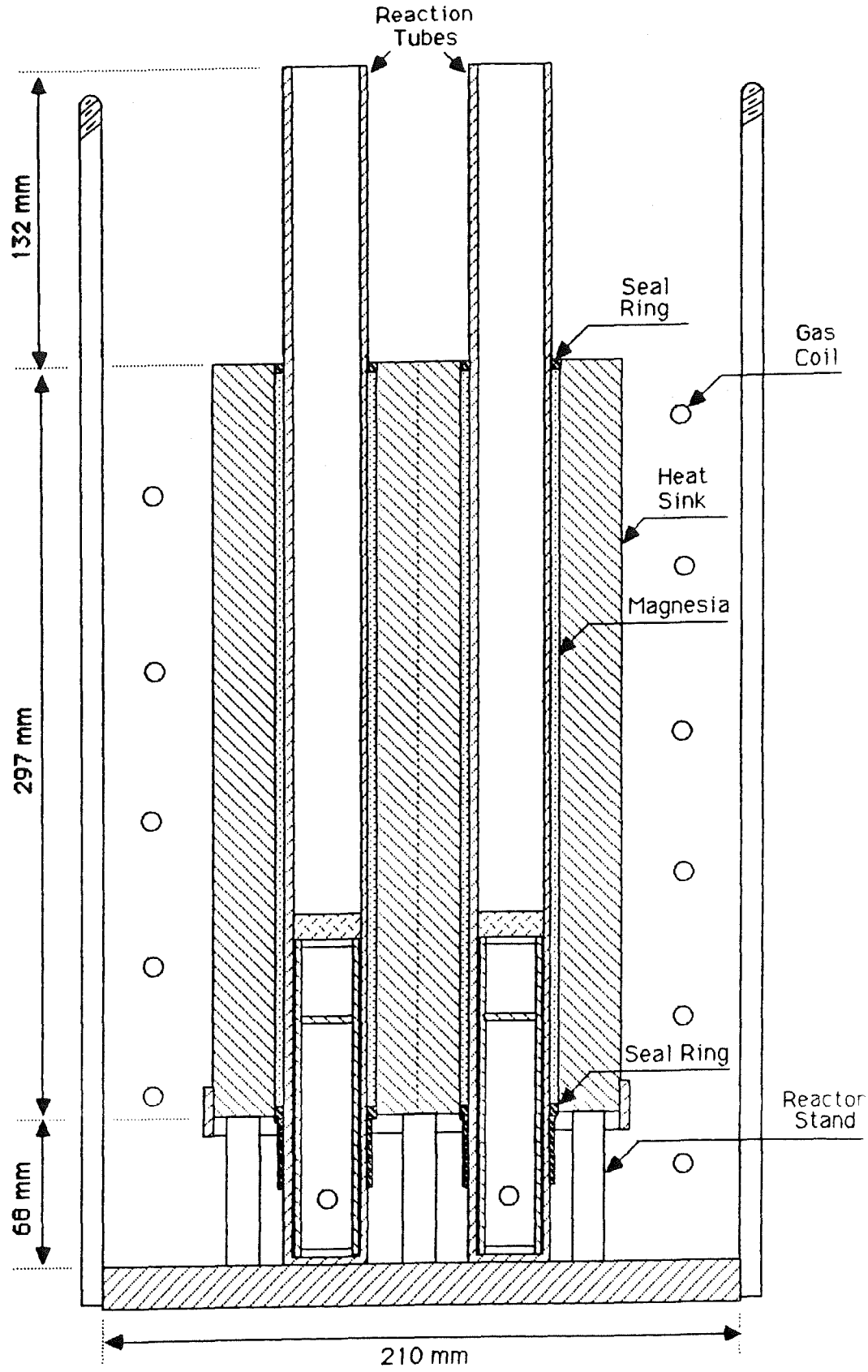

Figure 13. Schematic representation of assembled unit

a heating rate of around 5.5°C/min was obtained. This would mean that just over half the power input to the furnace goes into heating the reactor.

3.2 Test Materials

3.2.1 Rubber Wood

3.2.1.1 Extraction and Drying

Rubber wood is a hardwood and test pieces were obtained from the plantation of the Rubber Research Institute of Malaysia at Sungei Buloh, on the outskirt of Kuala Lumpur. Four old trees, one each from clones **Tjir 1, PR 107, RRIM 605** and **RRIM 623**, were felled using a chain saw. From each tree, four sections - each of thickness 5 cm, were obtained from the trunk at a height of around 1.7 m from the stump. Two of the sections from each tree were put in a dryer soon after extraction. The drying temperature was maintained at a constant value of 80°C. After one week of drying, the wood pieces were taken out and allowed to cool down for a moment before being packed in polythene bags. The other two sections from each tree were kept in a poorly ventilated and humid place for two weeks before being dried and packed in the same way as for the other sections. They were mouldy before being put into the dryer. All the wood pieces were air-freighted to the author as soon as they were packed. The average diameters of the wood sections from the four trees were as follows : **Tjir 1** 23.4 cm, **PR 107** 20.0 cm, **RRIM 605** 20.8 cm and **RRIM 623** 19.0 cm. The measurements did not include the bark which was left intact in the wood.

For ease of reference, the non-mouldy wood sections are referred to as fresh wood. Figure 14 shows how the mouldy and the fresh wood looked when cut through. The fresh wood had a uniform, creamy appearance whereas the mouldy wood was brownish in colour with blue patches here and there. In practice, Rubber wood is normally air-dried for some time, either in the open or under cover, before being used as fuel.

Figure 14. Appearances of fresh and mouldy wood sections

Fungal attack invariably occurs in the wood during drying because of its high starch content and lack of natural toxicants. The degree of infestation can vary from negligible to as severe as that encountered in the mouldy sections. This explains why both fresh and mouldy Rubber wood were used in the present study.

The reason for taking test pieces from several trees and belonging to different clones is to ensure that the work is not confined to an odd tree or clone, i.e. one which does not exhibit the general characteristics of the majority of the other trees or clones. However, this does not amount to studying the clonal variation in combustion characteristics of Rubber wood as such an exercise would require the use of a greater number of clones and also more test materials from each of them. This is beyond the scope of the present study.

3.2.1.2 Sample Preparation

For particle sizes below 4 mm in diameter, the samples were prepared by passing wood chips through a hammermill and separating the broken down pieces into various fractions using Endecotts vibrating test sieves. The hammermill was fitted with a screen containing 4 mm diameter openings. The percentages by weight of the different fractions obtained from a batch of **Tjir 1** wood chips were as follows :

< 150	mesh	particles	-	4.68%
-72+150	"	"	-	9.34%
-36+72	"	"	-	16.82%
-18+36	"	"	-	39.75%
-10+18	"	"	-	27.10%
-5+10	"	"	-	2.30%
>5	"	"	-	0.00%

In the above tabulation, '-5+10 mesh particles' denotes those particles which pass through the 5-mesh screen but are

retained on the 10-mesh screen. The apertures of the sieves used are given below :

Mesh Number	Aperture, mm
5	3.35
10	1.68
18	0.85
36	0.42
72	0.21
150	0.105

Particles of larger diameters were cut out directly from a disc of thickness 11-15 mm using a set of hole saws (Figure 15). The advantages of using these tools in sample preparation include : (1) they give a uniform particle size, (2) little time is required and (3) wastage is kept to a minimum. Wood pieces of 5 mm, 10 mm and 19 mm diameters were prepared in this way. Figure 16 shows the relative sizes of some of the samples prepared.

3.2.1.3 Density Determination

A disc of width 14-15 mm was obtained from a fresh as well as from a mouldy wood section from each tree using a bandsaw. Six cylindrical wood pieces were cut out randomly from each disc using a hole saw of diameter 19 mm. The actual dimensions of each wood piece (altogether 48 of them) were measured with the aid of a micrometer. The weights of all the wood pieces were determined after which they were put in an oven maintained at 105^{o}C until their weights were constant. This came about within 24 hours of putting them in the oven. The weights of the oven-dried wood pieces were recorded. The density of each wood piece prior to oven-drying was calculated from:

$$\text{Density} = \frac{\text{weight of wood}}{\text{volume of wood}}$$

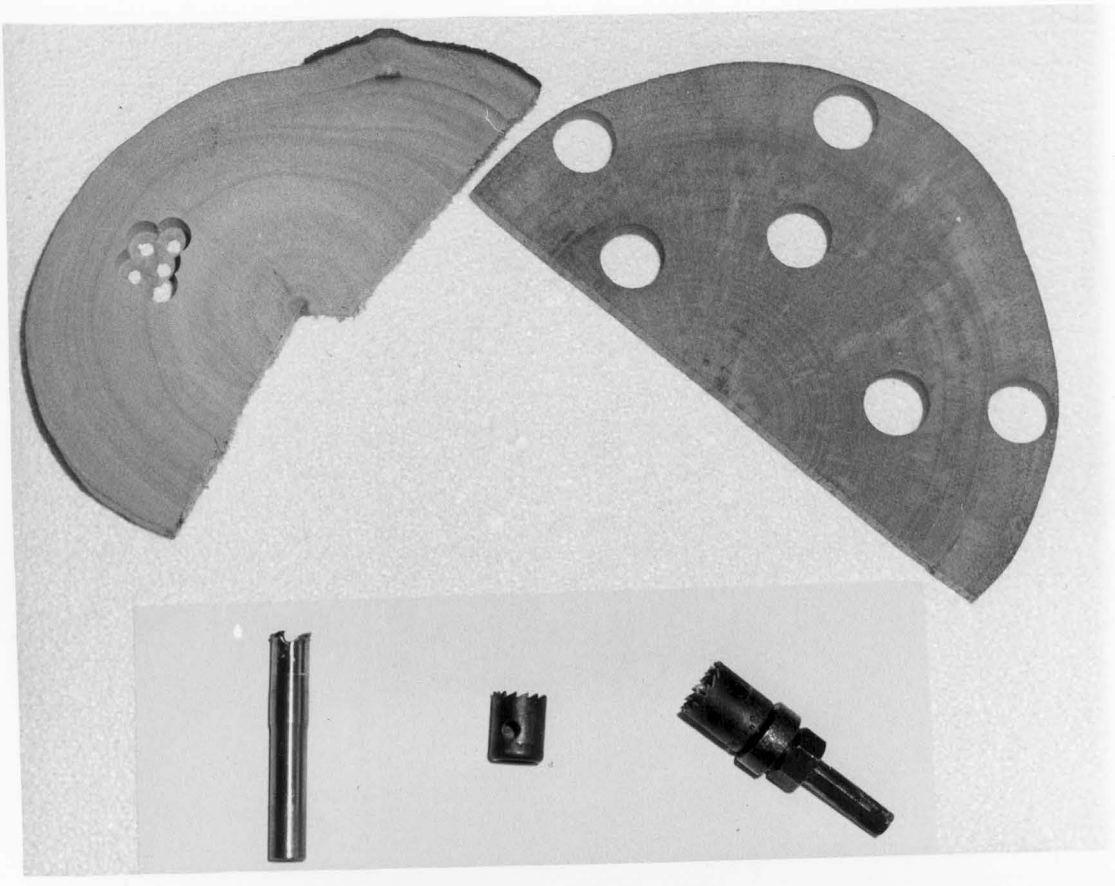

Figure 15. Hole saws

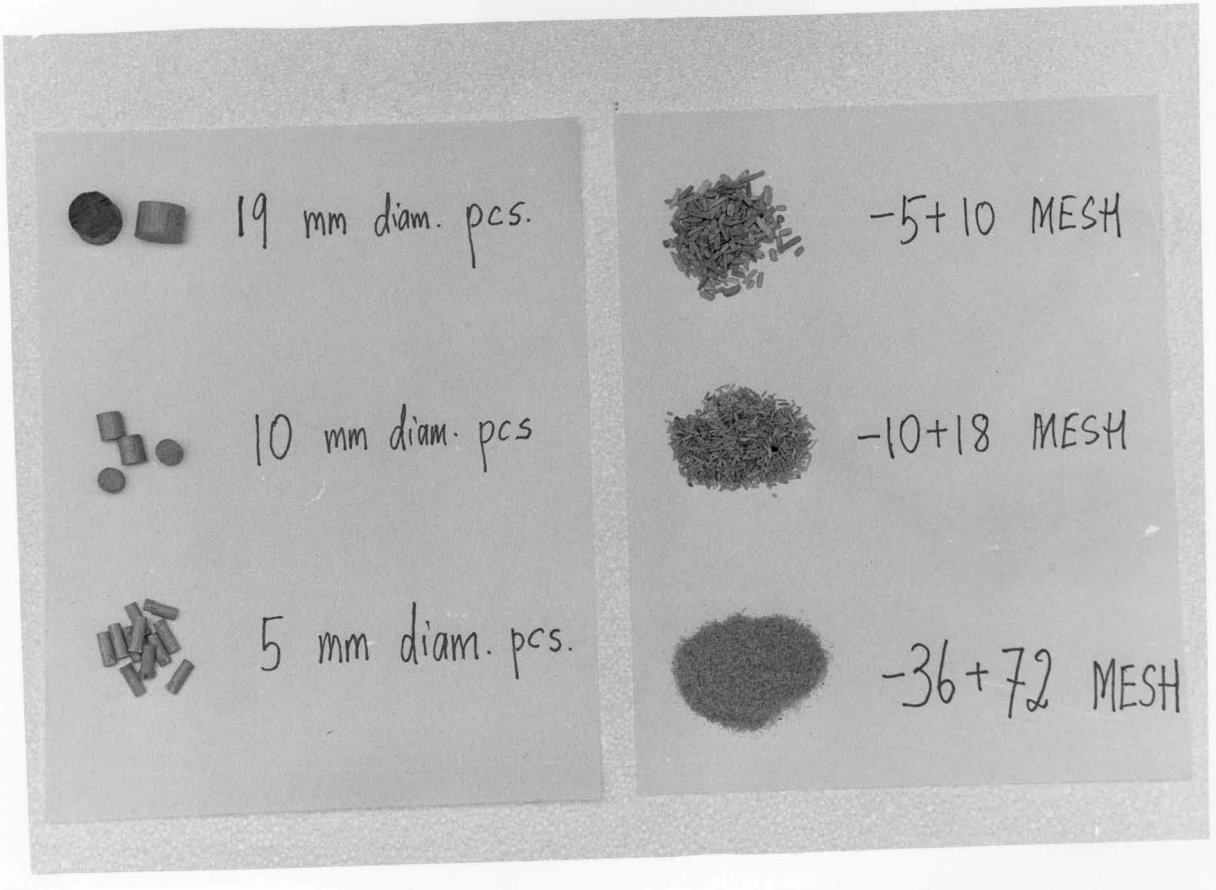

Figure 16. Rubber wood of different particle sizes.

and its moisture content, or MC, from:

$$MC = \frac{\text{initial weight - oven-dried weight}}{\text{oven-dried weight}} \times 100\%$$

It will be noticed that the moisture content of each wood piece was expressed as a percentage of the oven-dried wood. This is the common practice in the timber trade. The mean densities and moisture contents of the wood pieces from the various discs are presented in Table 1 while the individual values are given in Appendix 1. As shown in the table, the mean densities of the fresh wood pieces ranged from 630 kg/m^3 (**RRIM 623**) to 690 kg/m^3 (**PR 107**) and those of the mouldy wood pieces from 570 kg/m^3 (**RRIM 623**) to 640 kg/m^3 (**PR 107**). For the same tree, the mean density of the mouldy pieces was lower than that of the fresh pieces, by between 4% (**Tjir 1**)

Table 1. Densities of Rubber Wood Test Pieces

Source of wood	Mean density kg/m^3	Mean moisture content % of oven-dry wood
Tjir 1		
Fresh pcs	647	7.67
Mouldy pcs	619	7.96
PR 107		
Fresh pcs	694	8.23
Mouldy pcs	624	8.20
RRIM 605		
Fresh pcs	655	8.15
Mouldy pcs	581	8.36
RRIM 623		
Fresh pcs	627	8.26
Mouldy pcs	571	8.26

and 11% (**RRIM 605**). This difference was found to be insignificant, on the basis of the 5% level of significance, in the case of wood derived from the **Tjir 1** tree but significant in those obtained from the other three trees (Appendix 2). The mean density of all the fresh wood pieces was 656 kg/m^3 and that of the mouldy pieces 599 kg/m^3. The moisture contents of the wood pieces varied only very slightly, from 7.2% to 8.6% in the fresh pieces and from 7.6% to 8.8% in the mouldy pieces.

3.2.1.4 Chemical Composition

The chemical composition of Rubber wood, as determined by the Forest Research Institute of Malaysia (Peel, 1956), is as follows :

Component	% by weight
Cellulose	43.9
Lignin	23.3
Pentosan	18.0
Water solubles	6.0
Others	8.8

Pentosan is a portion of the hemicelluloses consisting chiefly of xylose and arabinose.

The ultimate analysis of Rubber wood, as done by the Chemistry Department of the University of Otago from two samples of **Tjir 1**'s fresh wood, is shown below :

Element	% by weight
C	48.99
O	43.97
H	5.91
Ash	1.14

3.2.2 Tropical Hardwoods

The tropical hardwoods test pieces were obtained in the form of hand samples, each of dimensions 75mmx100mmx18mm. They were prepared from kiln-dried timbers by the Forest Research Institute of Malaysia at Kepong. Altogether 16 pieces were obtained, each from a different species. Their moisture contents and densities were determined in the same way as that for Rubber wood, except that only one 19 mm diameter piece was cut out from each of them instead of six. The moisture contents of the wood pieces, as determined, varied from 8.0% to 11.9%. For comparison of densities, the wood pieces need to have a uniform moisture content. For this reason, besides the actual density, the density at 15% MC of each wood piece was calculated from :

$$\text{Density at 15\% MC} = \frac{1.15 \times \text{oven-dried weight}}{\text{original volume}}$$

The reason for using 15% as the reference moisture content for density calculation was because published values on densities of tropical hardwoods at this moisture content are available for comparison (Lee et al., 1965). The results obtained are presented in Table 2, in order of density. The densities of the test pieces were in the same order as those published in the literature, except for those of Pulai, light red Meranti, and Ramin which were 20-25% higher than the published values and those of Mengkulang and Mersawa which were 15-25% lower. Other properties of these wood species, including uses, can be found in the various Timber Trade Leaflets published by the Malaysian Timber Industry Board, Kuala Lumpur.

Two agricultural by-products of Malaysia were included in the study. These were Oil palm wood (**Elaeis guineensis**) and Coconut wood (**Cocos nucifera**). They are an important source

Table 2. Moisture Contents and Densities of Tropical Hardwoods Samples

Timber name	Botanical name	MC, %	Density kg/m^3	
			Actual	At 15% MC
Jelutong	Dyera costulata	9.44	424	445
Mengkulang	Heritiera spp.	10.24	470	490
Pulai	Alstonia spp.	10.41	485	505
Mersawa	Anisoptera spp.	10.70	536	557
Meranti, light red	Shorea spp.	10.45	585	610
Meranti, dark red	Shorea spp.	11.77	625	643
Sepetir	Sindora spp.	9.42	642	675
RUBBER WOOD*	Hevea brasiliensis	8.08	656	698
Nyatoh	Spp. of Sapotaceae	10.17	702	732
Keruing	Dipterocarpus spp.	9.85	760	796
Tualang	Koompassia excelsa	10.52	778	810
Ramin	Gonystylus spp.	7.95	772	822
Tembusu	Fagraea spp.	10.25	798	833
Merbau	Intsia palembanica	10.76	838	871
Kempas	Koompassia malaccensis	11.17	844	873
Chengal	Balanocarpus heimii	11.90	895	920
Balau	Shorea spp.	11.57	975	1005

*from results obtained earlier.

of biomass since oil palm covers 1.3 million hectares of land in Malaysia while coconut occupies 400000 hectares. Although commonly referred to as wood, they are, strictly speaking, derived from palms and not trees. Therefore differences in structure and chemical composition can be expected between them and the normal types of wood. A section of a trunk of thickness 5 cm and diameter 30 cm was obtained for each of them. They were oven-dried, packed and air-freighted to the author in the same way as for the fresh Rubber wood test pieces. Their densities and moisture contents, as received, were as follows:

Species	MC, %	Density, kg/m^3	
		Actual	At 15% MC
Oil palm wood	9.05	185	196
Coconut wood	8.57	948	1004

3.2.3 Wood Components

3.2.3.1 Cellulose

Filter paper is often used as the source of cellulose in the thermal studies of cellulosic materials (Broido, 1976; Rothermel, 1976 ; Shafizadeh and DeGroot, 1976). In the present investigation, Whatman No.542 ashless filter papers and extraction thimbles were used. They were cut into roughly 1 cm by 1 cm square pieces.

3.2.3.2 Extractives

(i) Water solubles

The water-soluble extractives were isolated from those fractions of Tjir 1's fresh wood which passed through the 18-mesh screen. The wood particles were mixed with eight times their weight of distilled water in a bowl and the contents were boiled for an hour on a hot plate. They were then filtered on a 12 cm diameter Buchner funnel with the aid

of a water pump. The process of boiling in water and filtration was repeated twice. Following this, the combined filtrates were evaporated to near dryness on a hot plate before being poured into a porcelain crucible and dried at 105°C in an oven. The final product consisted of a layer of dark brown solid adhering to the bottom of the crucible. It had to be broken up into small pieces by scraping with a spatula.

(ii) Benzene/ethanol solubles

The extractives soluble in organic solvents were isolated from the fresh wood of **Tjir 1** (-36+72 mesh particles) by Soxhlet extraction. The solvent used consisted of a mixture of two parts by volume of benzene and one part by volume of ethanol. After four hours of extraction, the extract was left uncovered in a fume cupboard overnight during which time most of the solvent evaporated off. The remaining portion was then dried at around 100°C in an oven for a few hours. The final product consisted of a sticky and dark brownish substance approaching a paste.

The extracted wood was left in a fume cupboard overnight before being dried at 105°C in an oven to ensure that it was solvent-free. It was then mixed with distilled water and boiled for an hour before being filtered on a Buchner funnel. This step was repeated twice. The final residue was dried at 105°C in an oven and was designated as 'extractive free' wood.

3.2.3.3 Hemicelluloses

A major portion of the hemicelluloses in hardwoods can be extracted using aqueous alkaline solutions. The method used here was adapted from Browning (1967).

About 20 gm of the extractive-free wood was mixed with 250 ml of 24% w/w potassium hydroxide solution in a flask, and

after the air in it had been replaced by nitrogen, was stoppered and left to stand for 24 hours. The contents of the flask were then filtered on a Buchner funnel. The filtrate was poured into 1000 ml of ethanol cooled down to 5°C. The precipitate formed was recovered by filtration, washed with distilled water and ethanol and vacuum-dried in a desiccator at room temperature. The final product appeared like small, brown granules.

The wood residue was washed repeatedly with distilled water before being dried at 105°C in an oven. It was designated as 'wood free of extractives and hemicelluloses' although it still contained those hemicelluloses which are insoluble in alkalis.

3.2.3.4 Lignin

The methods generally used for the extraction of lignin from wood are those based on hydrolysis and solution of the polysaccharides with strong mineral acids and recovering the residue. During isolation by acid hydrolysis, the lignin is altered and is no longer identical to the protolignin in the wood. The method used here for its isolation from Rubber wood was adapted from Browning (1967).

About 30 gm of the extractive-free wood was added to 300 ml of 72% sulphuric acid in a beaker surrounded by ice. The mixture almost immediately turned into a black slurry. It was stirred gently for about a minute (during which time its temperature rose to 41°C) before being allowed to stand for 2 hours with occasional stirring. Following this, it was diluted with 600 ml of distilled water and the contents were filtered on a Buchner funnel. The filtration was rather slow despite the use of a water pump. The black residue was transferred to a flask containing 300 ml of 3% sulphuric acid and the mixture was refluxed for 4 hours. After cooling down, the contents of the flask were filtered in the same way as

before. The residue was recovered and washed with hot distilled water until the filtrate was virtually free of acid. The final residue was dried at 105°C in an oven. It consisted of a coarse, black powder and was designated as 'acid lignin', since sulphuric acid was used in its preparation.

SECTION I

DIFFERENTIAL THERMAL ANALYSIS

CHAPTER 4

DIFFERENTIAL THERMAL ANALYSIS IN AN INERT ENVIRONMENT

4.1 Trial Runs

In the DTA runs of Rubber wood conducted in an oxidative environment (Chapter 6), both the sample and the reference beds were fluidised using sand as the inert material. The resultant DTA curves contained large and well-defined reaction peaks. This was not the case when the runs were carried out in an inert environment. The reaction peaks were small in size and ill-defined, as shown in Figure 17. This is because the heat of pyrolysis is only a small fraction that of combustion. As an illustration, the heat of pyrolysis of cellulose is 370 kJ/kg (Tang, 1972) compared with its heat of combustion of 16000 kJ/kg (Susott et al., 1975). Thus, for DTA runs in an inert atmosphere, there was a need to modify the experimental technique to bring about larger and clearer reaction peaks on the resultant curves.

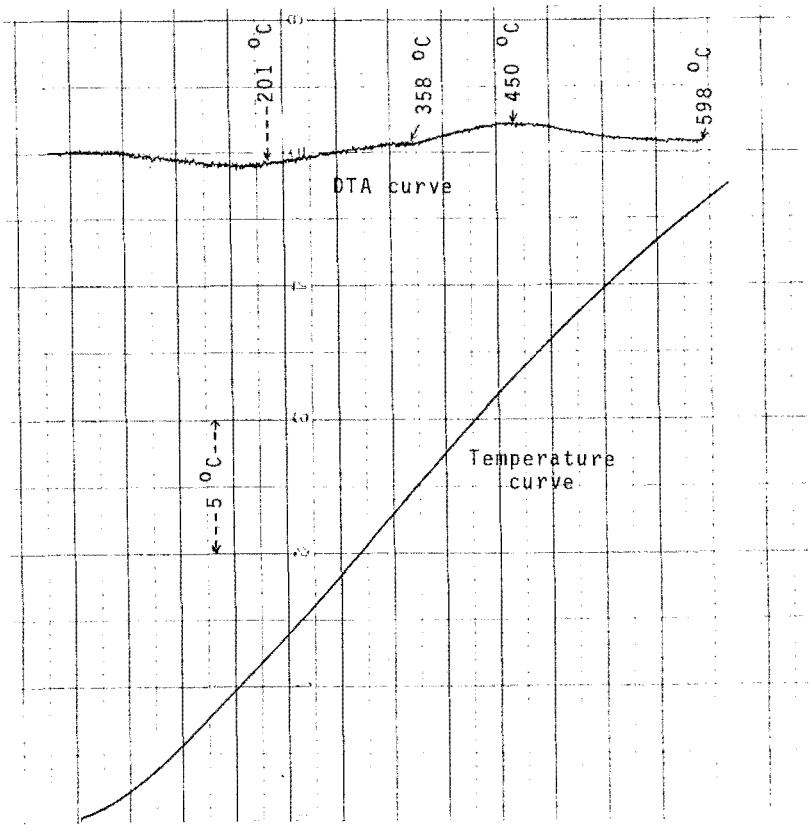

Figure 17. DTA curve in N_2 of a Rubber wood sample which was fluidised with sand during the run

Firstly, the feasibility of conducting fluidised-bed runs without the use of an inert material in the sample bed was investigated. This was found to be not feasible because the Rubber wood particles would not fluidise but instead 'channels' were formed in the bed, allowing the fluidising gas to escape. It was then decided to keep the sample bed, again containing only the test sample, static while keeping the reference bed fluidised. This was achieved by using a lower gas flowrate (0.8 lit/min instead of 4 lit/min) and aluminium oxide (-100+240 mesh fraction) as the reference material instead of sand which is much denser and therefore requires a higher gas velocity to fluidise. The resultant DTA curves were smooth and contained distinct and reasonably large reaction peaks, as shown in Figure 18. Even minor reactions peaks were clearly projected on the curves. Although this technique may not ensure that temperatures within the bed are

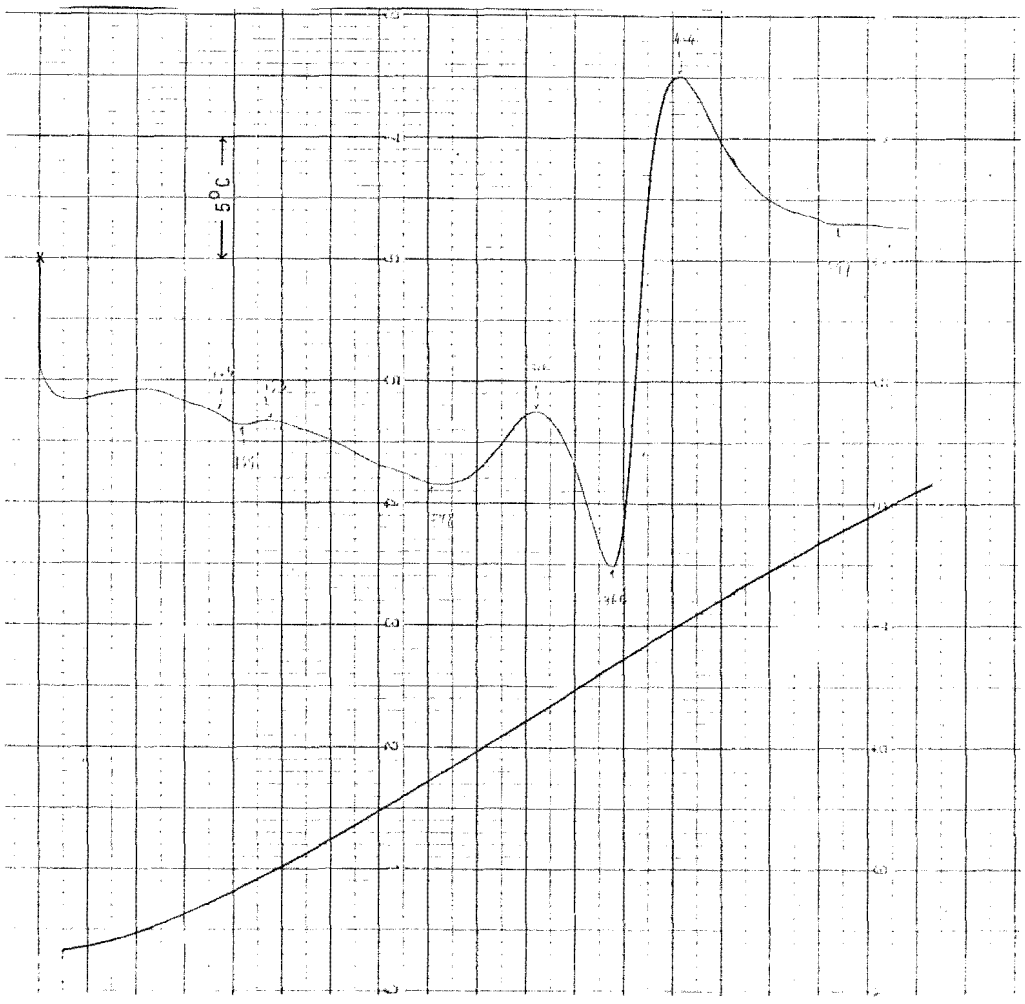

Figure 18. DTA curve in N_2 of a Rubber wood sample which remained stationary during the run

as uniform as when it is fluidised, the results were so consistent between duplicate runs that it was adopted. The reliability of the resultant curves was investigated by experiments in which the position of the differential thermocouple in the solid sample was changed. These experiments are described in Section 4.4.2 and the results obtained showed that these curves are a reliable indication of thermal changes in the wood.

4.2 Experimental Procedure

Described here is the general experimental procedure. Specific details, including sample size, are provided in the individual sections.

The experimental set-up is shown in Figure 19. The test sample, which was oven-dried at 105^{o}C for 16-24 hours, was placed in the sample tube while 5 gm of aluminium oxide was placed in the reference tube. Standing on each distributor was a stainless steel frame similar to the one used as support under the bed. In effect, each distributor was sandwiched between two steel frames which prevented it from being displaced. Three sheathed chromel/alumel thermocouples of diameter 1 mm and length 70 mm were used for measuring temperatures. Two of them were wired together to form a differential thermocouple. One member of the differential thermocouple was inserted into the test sample while the other member was placed in the reference tube with its sensing tip situated about 5 mm above the surface of the bed. The reason for not inserting the thermocouple in the reference tube into the bed was because the resultant DTA curve was smoother with the thermocouple tip located above the bed than within the bed, as shown in Figure 20. The third thermocouple was placed in the reference tube for measuring the reference bed temperature and is referred to as the temperature thermocouple. All the thermocouples were inserted into the tubes through holes in the metal strips of the steel frames to

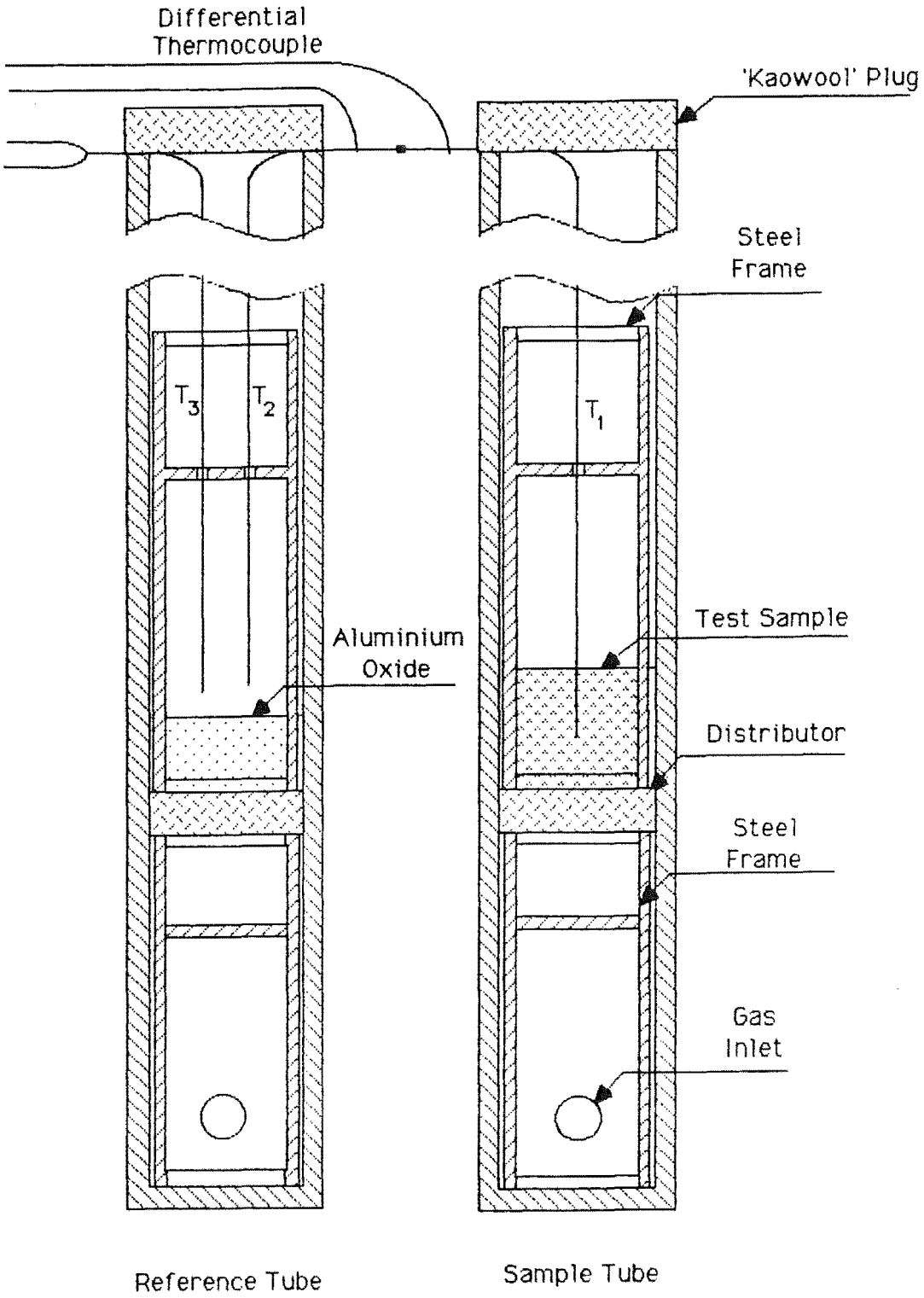

Figure 19. Experimental set-up for DTA in an inert atmosphere

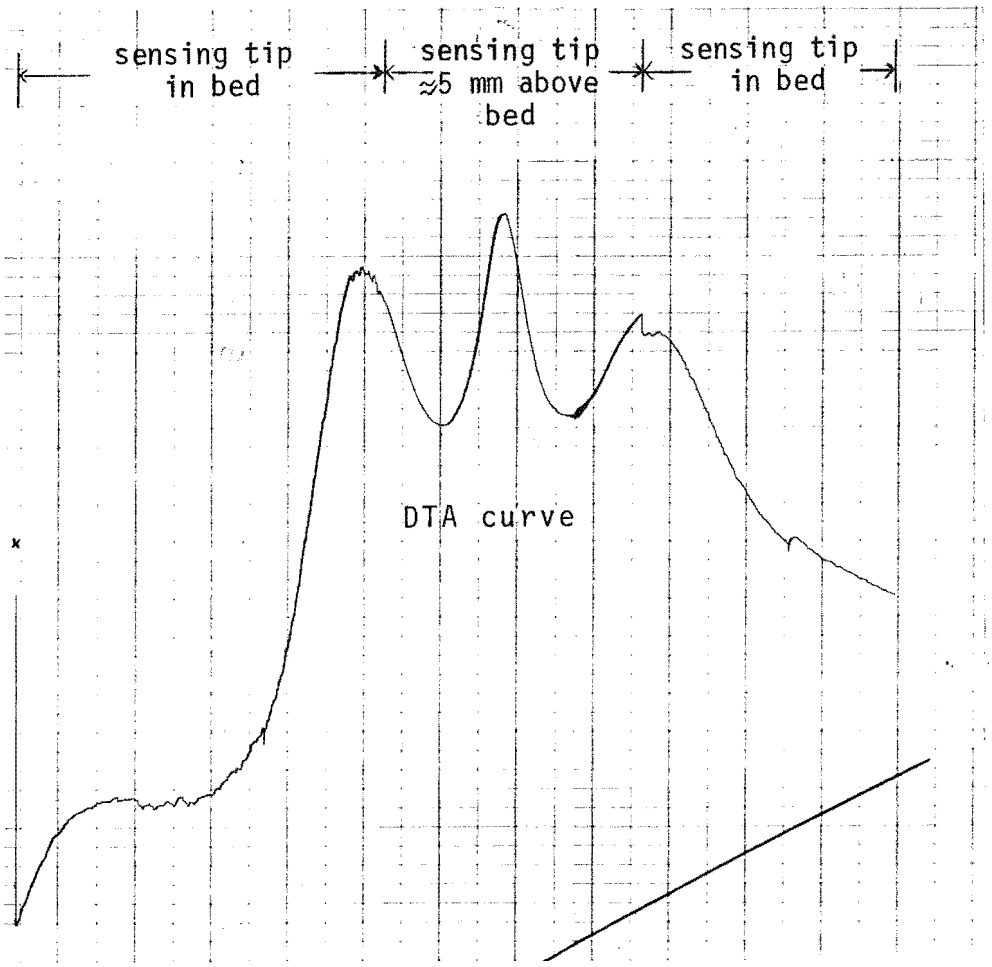

Figure 20. DTA curve in N_2 of a Rubber wood sample obtained from a trial run

restrain their movement. A Watanebe hot-pen recorder (model Servocorder SR 6312) was used to record the differential temperature between the two beds as well as the reference bed temperature as a function of time. A piece of 'Kaowool' of thickness 13 mm and diameter 32 mm (similar to the ones used as distributors) was placed on top of each tube to prevent surrounding air currents from getting into it and affecting the experiment. Nitrogen (of 99.995% purity and containing less than 10 ppm of oxygen) from a gas cylinder was passed through the two tubes with a combined flowrate in the cold of 0.8 lit/min. A vertical 'Quickfit' flowmeter (Figure 21), connected between the nitrogen cylinder and the reactor, was used to measure the gas flowrate. The reactor was heated at the rate of around 5.5^{o}C/min. The reference bed was fluidised

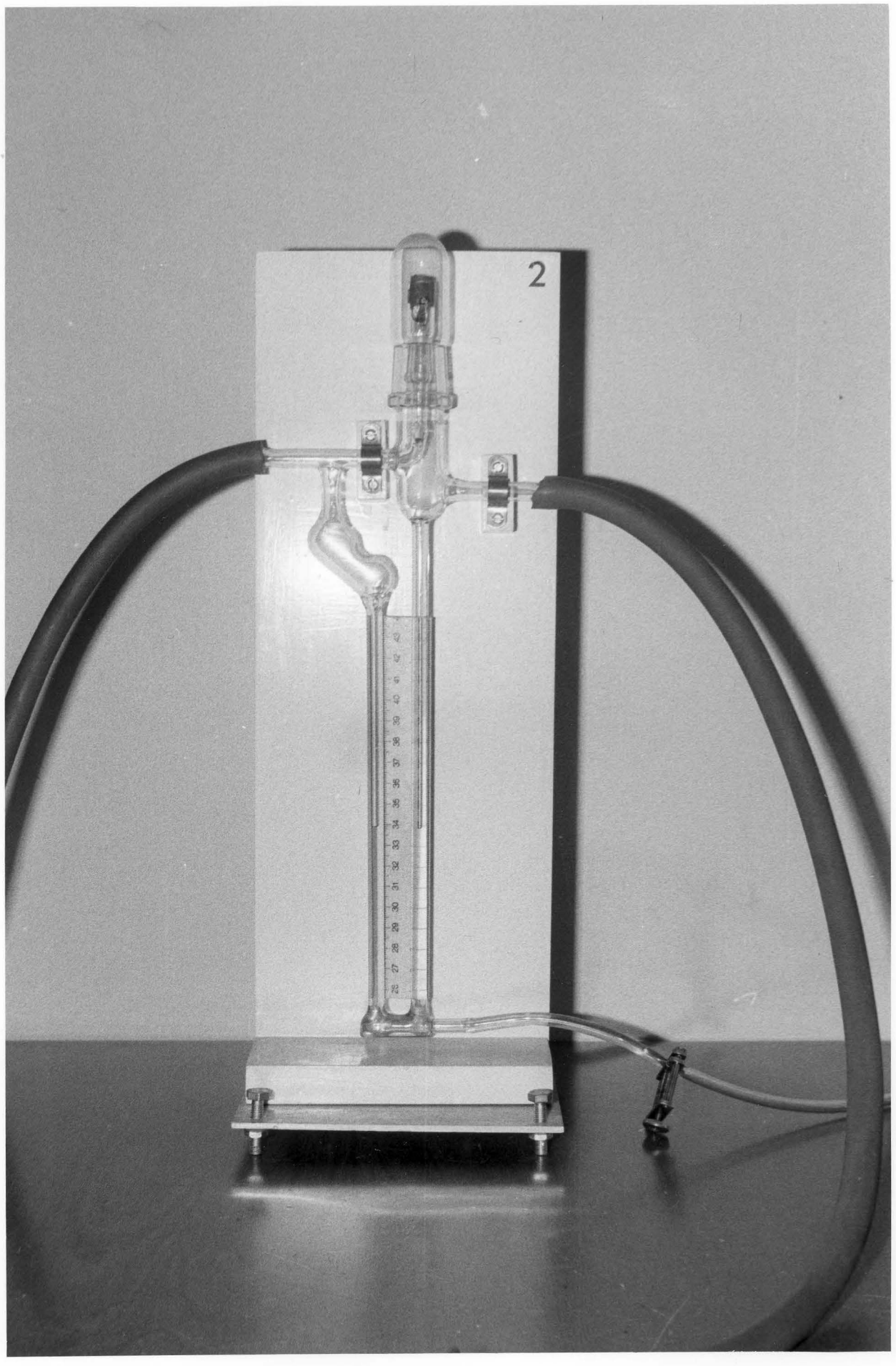

Figure 21. A vertical Quickfit flowmeter.

from the outset while the sample bed remained stationary throughout the run. When the reference bed temperature exceeded 500°C, the experiment was stopped as it had come to an end. This came about 90-120 minutes after it was started, depending on the initial temperature of the reactor. Normally the afternoon and evening runs took a shorter time to complete as the reactor was still quite warm when used.

Restart Procedure: When the reactor had cooled down, the steel frame in the sample tube was taken out and the residual char sucked out using a vacuum cleaner. The frame was then replaced and a new test sample introduced into the tube. The distributors and aluminium oxide were replaced only when needed as they are relatively stable thermally.

4.3 Individual Wood Components

4.3.1 Cellulose

A 1-gm sample (filter paper) was used and the resultant DTA curve is shown in Figure 22. In the diagram, the upper curve is the differential temperature curve while the lower one is the reference temperature curve. The X-axis represents time which increases from left to right. The Y-axis represents the potential difference between the measuring tip and the reference junction of the thermocouple or, in the case of the differential thermocouple, the potential difference between the two measuring tips. The readings were in millivolts and their temperature equivalents were obtained from the appropriate conversion table. Within the temperature range 0-600°C, the relationship between them is practically linear which means that the shapes of the two curves are not affected by a change in the parameter of the Y-axis from millivolts to degrees celsius. In this run, as in most of the other runs in N_2, the following full scale ranges were used : 50 mV for the reference temperature curve and 2 mV for the differential temperature curve. For the type of thermocouples used, 1 mV is equivalent to approximately 25°C.

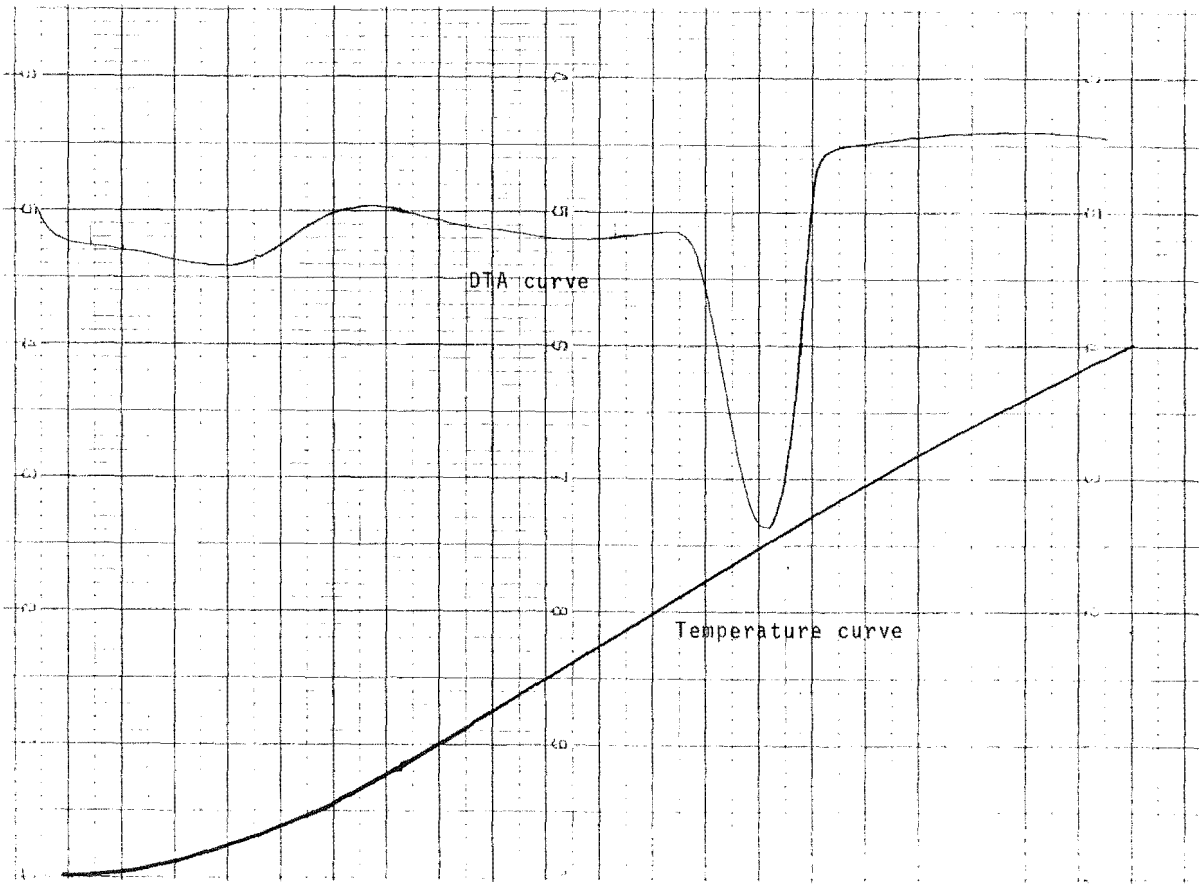

Figure 22. DTA curve in N_2 of cellulose (original)

To make the curves a little bit easier to read, they were re-plotted with the aid of a digitiser, a computer and a Hewlett-Packard plotter (model 7225A) so that the reference temperature formed the X-axis and the differential temperature the Y-axis. This is shown in Figure 23 which contained only one curve. In fact, the data were stored in the computer and this has the added advantage that each curve can be re-plotted as often as one wishes and, if necessary, on a different scale. The portion of the curve below 100°C was not reproduced because it contained only the drying curve of the re-absorbed moisture. Moreover, it would be rather difficult to reproduce this portion because of its non-linearity. The DTA curves resulting from runs using other materials were re-plotted in a similar manner.

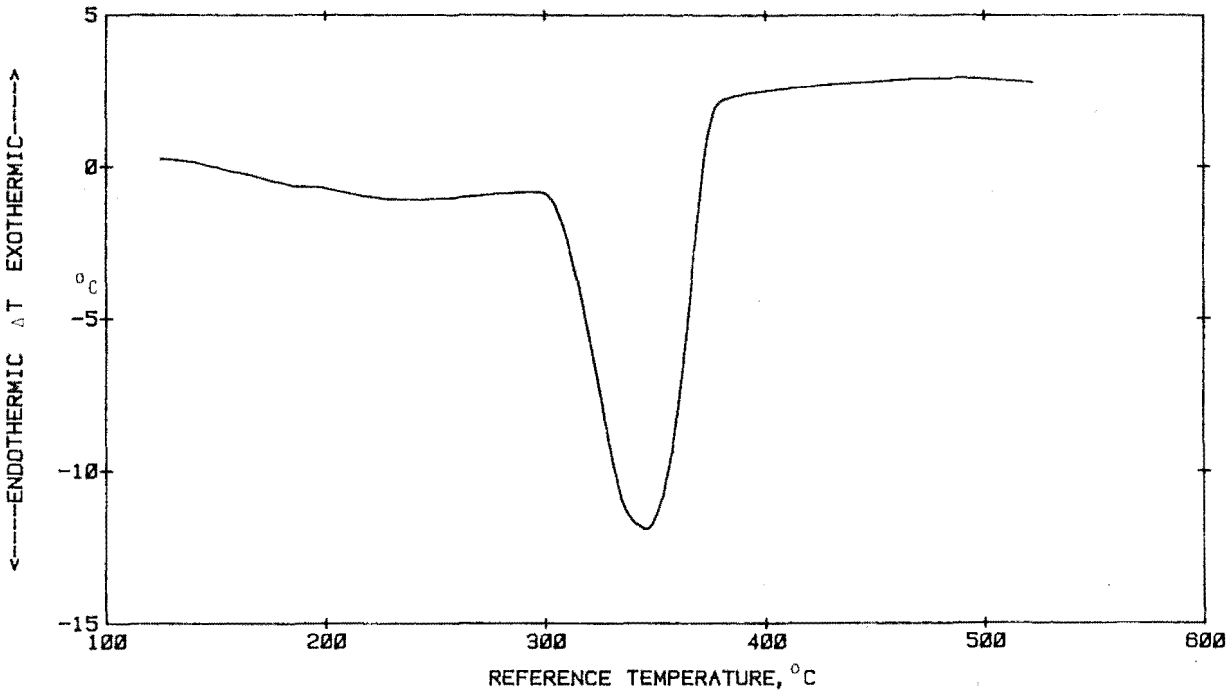

Figure 23. DTA curve in N_2 of cellulose (re-plotted)

As shown in Figure 23, the DTA curve of cellulose is dominated by a strong endotherm which extended from around 300°C to 380°C, peaking at about 345°C.* Except for a slight variation in the peak temperature, the results obtained were consistent with those obtained by other workers, including Tang (1972), Miller and Turner (1972) and Shafizadeh and DeGroot (1976). Kosik et al.(1972) attributed this endotherm to depolymerisation of the cellulose and volatilisation of the products, i.e. levoglucosans.

4.3.2 Hemicelluloses

Owing to the small amount of test material available, a special stainless steel tube of internal diameter 16 mm, thickness 1 mm and height 12 mm was made to house the sample. This is illustrated in Figure 24. The height of the sample, which weighed 0.6 gm, was 10 mm. Without the use of the tube, the test sample would only have a height of 2.8 mm, making it rather difficult for the thermocouple's sensing tip to be placed within it.

---

*Unless otherwise stated, temperatures assigned to reaction peaks are those of the reference bed. To obtain the actual sample temperatures, add the corresponding differential temperatures, which can have a negative value.

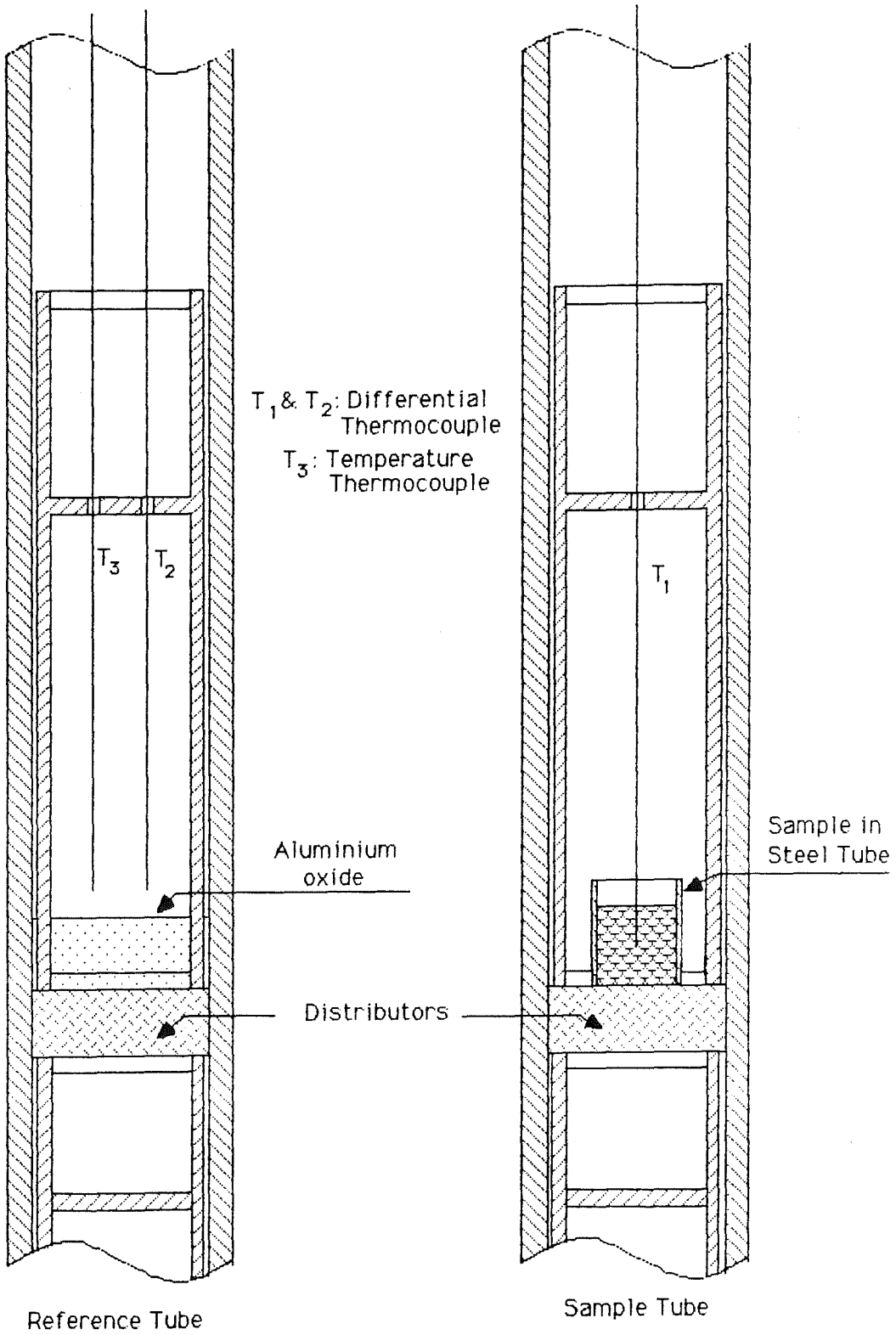

Figure 24. Experimental set-up for DTA of the hemicelluloses

The resultant DTA curve contained a strong and fairly sharp exotherm between 200°C and 275°C, a weak exotherm between 270°C and 310°C and possibly a weak but broad endotherm just below 200°C (Figure 25). The first exotherm peaked at about 240°C and the second one at about 285°C. In the case of the first exotherm, the rise in temperature was gradual initially but became more rapid on reaching 220°C. In the literature, most of the studies on thermal degradation of hardwood hemicelluloses were confined to xylan, the main component. Kosik et al.(1968) obtained two reaction peaks for xylan - an exotherm between 180°C and 280°C and an endotherm between 280°C and 400°C. Shimizu (1975), however, obtained an endotherm between 210°C and 250°C and an exotherm between 250°C and 300°C. The two sets of results were quite different and this could be due to a difference in the experimental conditions or the way the samples were prepared. Shafizadeh and DeGroot (1976), using xylan isolated from cotton wood, obtained a similar DTA curve to that of Shimizu. It is interesting to note that the DTA curve of the hemicelluloses obtained in the present study contained two exotherms, one of

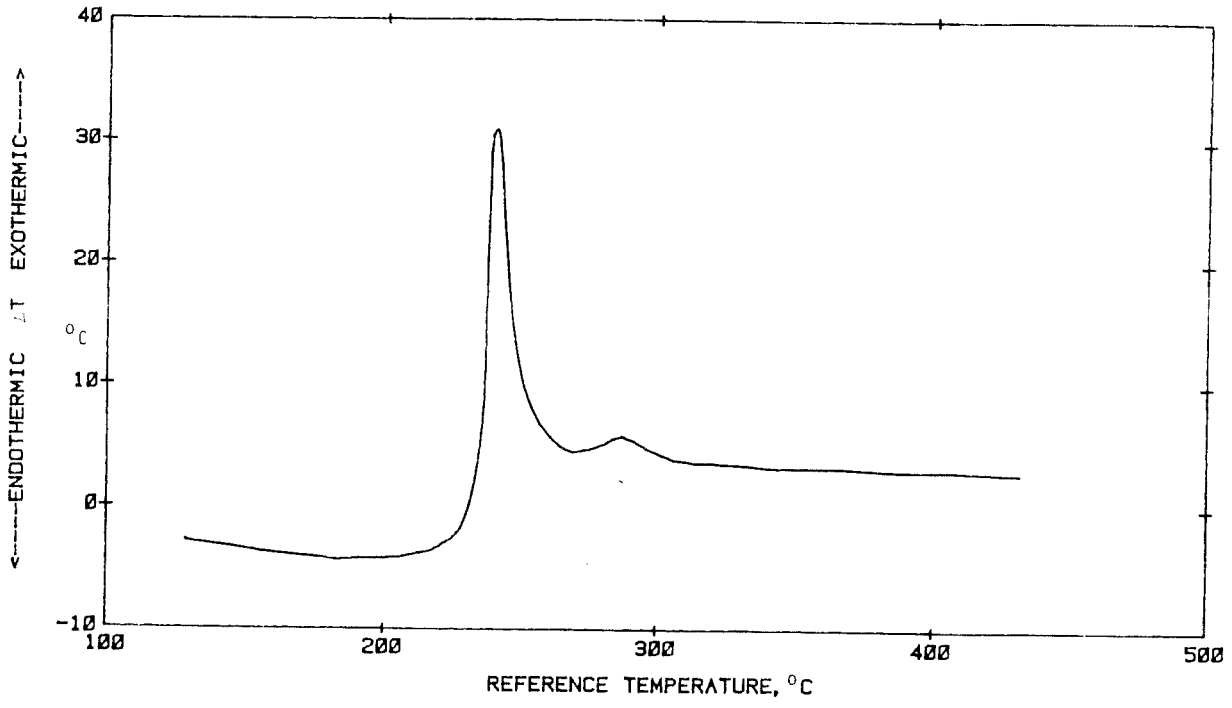

Figure 25. DTA curve in N_2 of the hemicelluloses

which is present in the DTA curve of xylan obtained by Kosik et al.(1968) and another in that of the same material obtained by Shimizu (1975) and Shafizadeh and DeGroot (1976).

4.3.3 Acid Lignin

Figure 26 shows the DTA curve of acid lignin obtained using a 1 gm sample. It consisted essentially of a broad exotherm between 260°C and 500°C with its peak situating at about 380°C. Eickner (1962) obtained similar results, except for a slight variation in the peak temperature. Tang (1972), using helium as the carrier gas, obtained a weak endotherm between 190°C and 345°C and a strong exotherm between 345°C and 500°C. Domburg et al.(1972), using samples prepared from Spruce (a softwood) and Aspen (a hardwood), obtained a broad exotherm which peaked at around 360°C and which contained a small depression at about 420°C. Thus, the DTA curve of acid lignin obtained in the present study closely resembled those obtained by other workers. The slight difference could be due to a variation in the experimental technique or in the compositions of the test samples since they were prepared from different wood species.

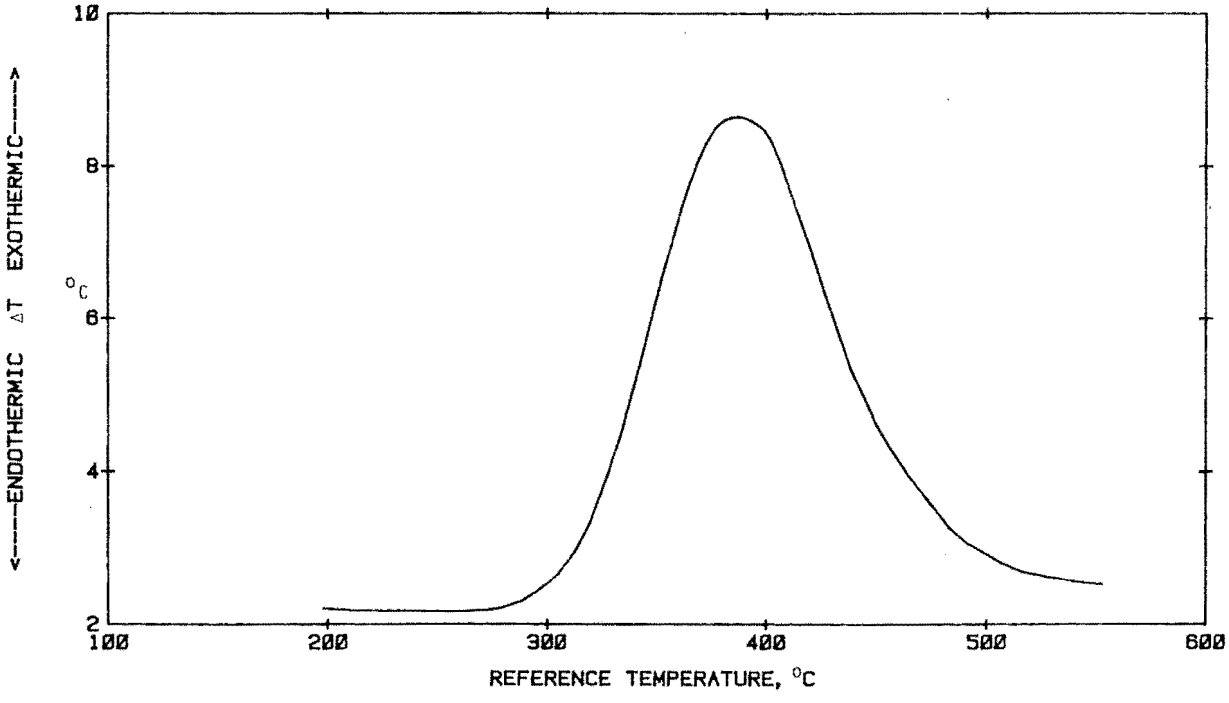

Figure 26. DTA curve in N_2 of acid lignin

4.3.4 Extractives

4.3.4.1 Hot water extract

The DTA curve of the water solubles obtained using a test sample of 2.2 gm is shown in Figure 27. It contained a fairly strong endotherm between 140°C and 245°C, a strong exotherm between 245°C and 325°C and a weak exotherm around 350°C. The endotherm peaked at about 185°C and the strong exotherm at about 290°C. As different wood species contains different types of extractives, it would be futile to compare the DTA curve obtained here with those obtained by other workers using samples prepared from other wood species. Moreover, literature on thermal behaviour of wood extractives in an inert environment is scanty. Similar results were obtained in the repeat run.

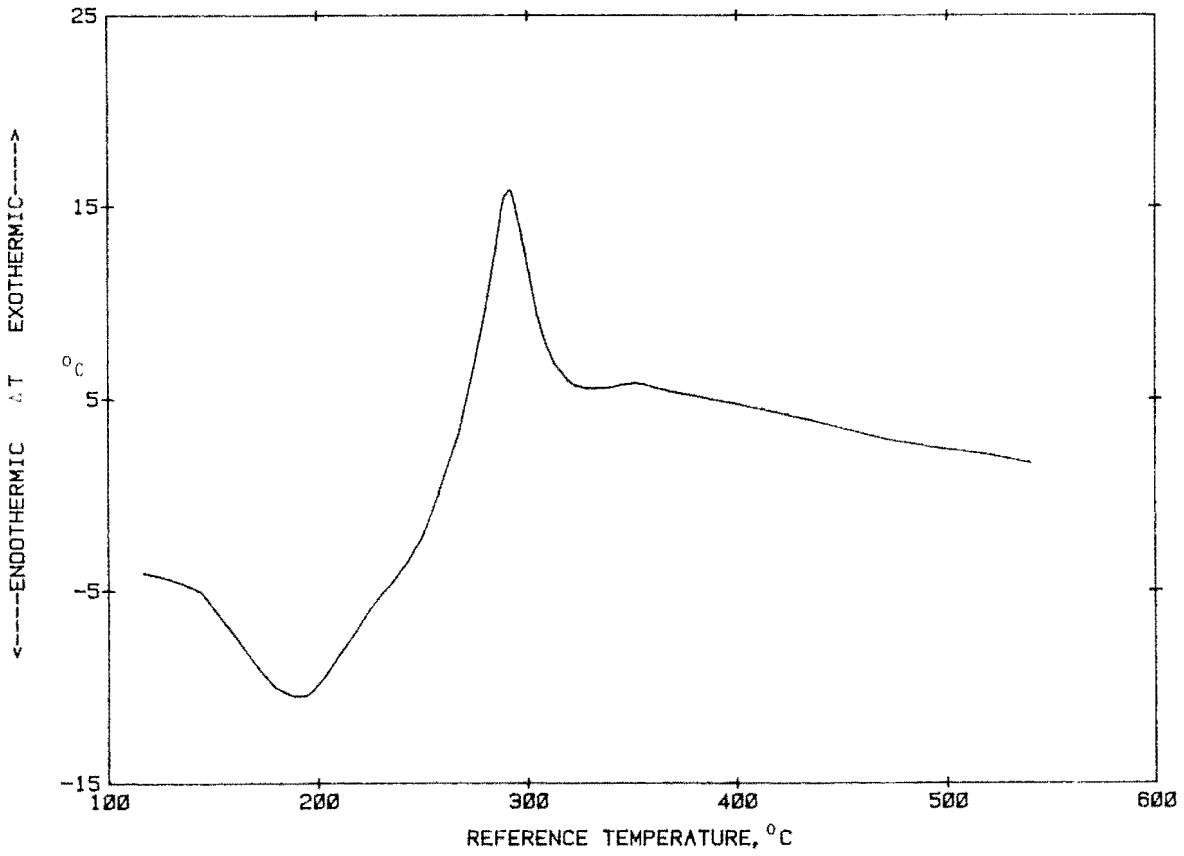

Figure 27. DTA curve in N_2 of the water solubles

4.3.4.2 Benzene/ethanol extract

The test sample was placed in a stainless steel container of internal diameter 11.5 mm, thickness 1 mm and height 14 mm. Its weight, which was determined as the difference between the weights of the container with and without the sample, was 0.6 gm.

Half way through the run, at about 180°C, the sample began to swell and the contents of the container eventually spilled outside. When this happened, the DTA trace lost its smoothness and continued its course on a somewhat zig-zag manner, as shown in Figure 28. No much useful information can be derived from the resultant curve, except that heat was released when the swelling occurred. The same thing happened in the repeat run.

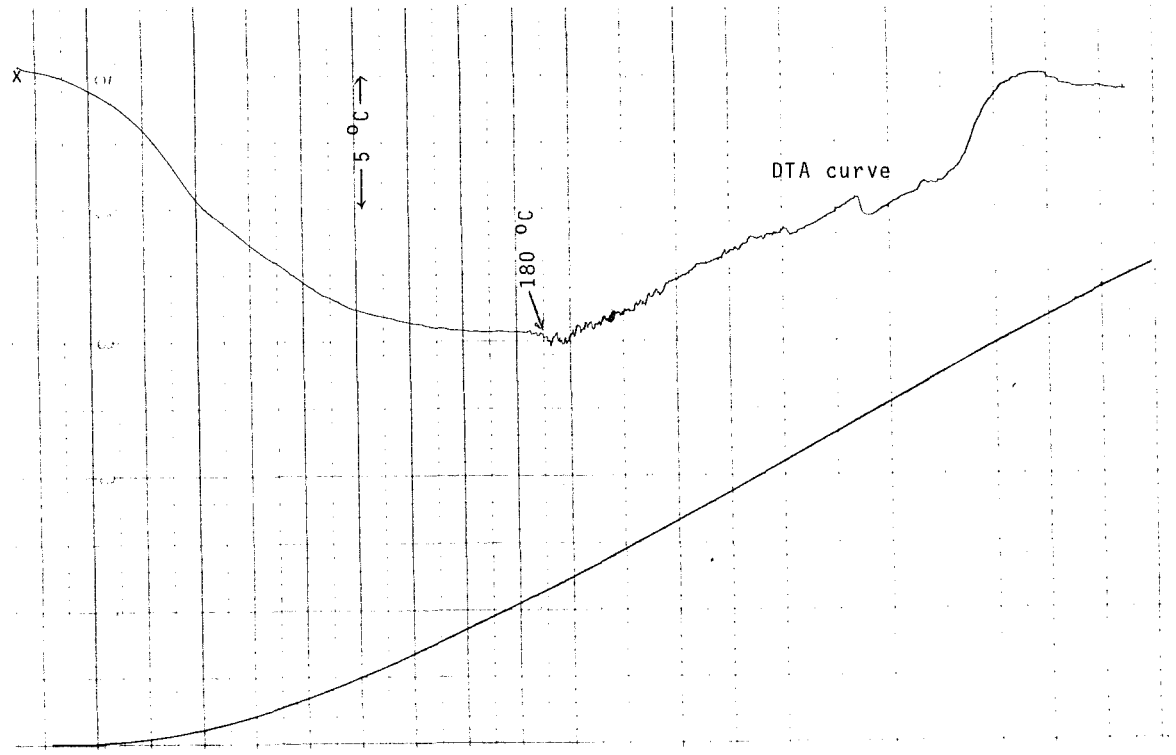

Figure 28. DTA curve in N_2 of the benzene/ethanol extract

4.4 Rubber Wood

Unless otherwise stated, the test samples were obtained from the fresh wood sections of **Tjir 1.** The reason behind this choice was because they were the biggest of all the wood sections available and thus provided the most material for testing.

4.4.1 Main features of a Rubber wood DTA Curve

Figure 29 shows the DTA curve of a 3-gm sample of Rubber wood of particle size -36+72 mesh. The height of the sample bed was 20 mm. The main features of the curve are as follows:

- a weak endotherm between 130°C and 155°C (marked 'A').
- part of an endotherm which stretched from 155°C to 240°C ('B').
- an exotherm which peaked at about 320°C ('C').
- an endotherm which peaked at about 360°C ('D').
- an exotherm which peaked at about 400°C ('E').
- a weak endotherm at around 490°C ('F').

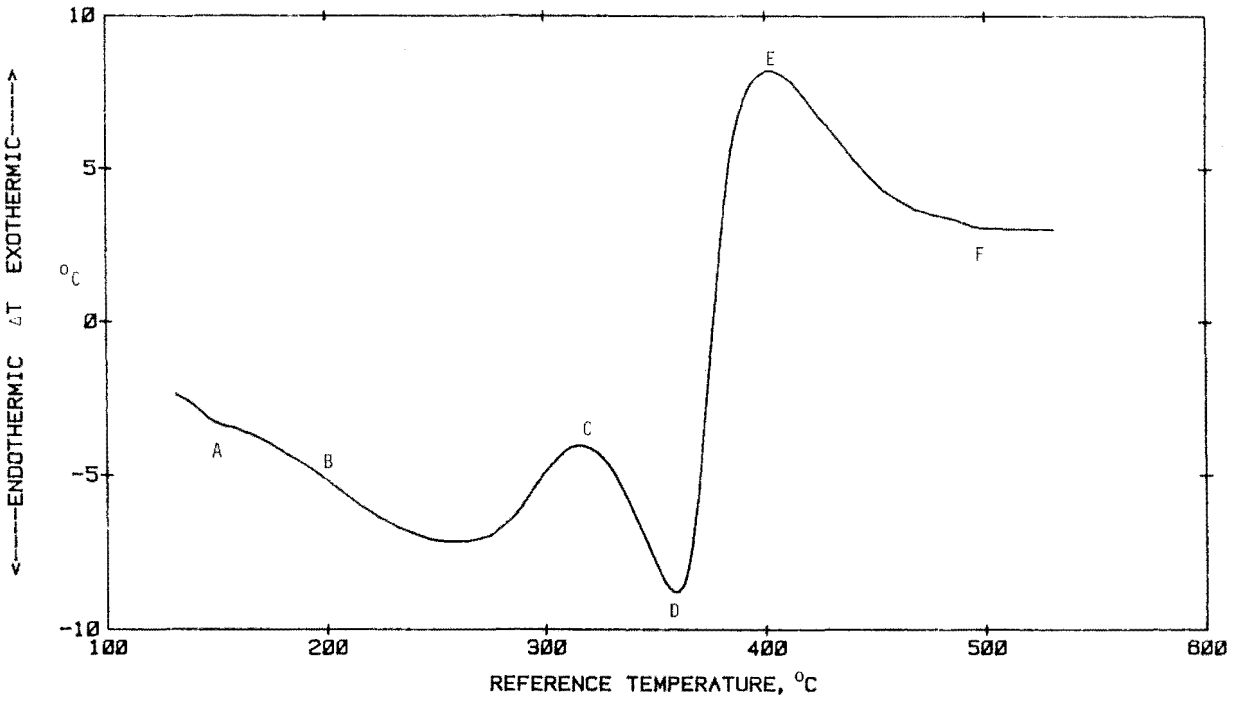

Figure 29. Main features of a DTA curve of Rubber wood (-36+72 mesh particles)

Except for Endotherms A and F which existed as individual peaks, the other reaction peaks overlapped with each other. Interpretation of the curve will be made in Section 4.4.4 when more information is available.

In a repeat run, visual observations of the experiment were made with the aid of a torchlight. To allow viewing into the sample tube, the top 'Kaowool' plug was not used in this run. It was noted that :

- an 'aromatic' smell was emitted from the sample tube from about 145°C.
- from around 190°C, smoke began to be emitted and its intensity increased with increasing temperature.
- the sample had turned slightly brownish at 220°C. The 'aromatic' smell was still present.
- as the temperature increased, the sample became darker and visibility in the sample tube poorer because of the smoke cloud. At about 290°C, the sample was no longer visible.
- visibility was partially restored at 390°C as a result of the smoke subsiding. By then, the sample had turned into char.
- visibility was much improved at 420°C. However, a small amount of smoke continued to be emitted.

The visual observations provided valuable information which will be of great help in the interpretation of the DTA curve of Rubber wood. For example, it was observed that charring of the wood occurred mainly between 290°C and 390°C which corresponds to the formation of Endotherm D.

4.4.2 Effect of Particle Size

Figure 30 shows the DTA curves of five Rubber wood samples of particle sizes ranging from <150 mesh to 10 mm diameter. Each of the samples weighed 3 gm. The height of the 5 mm and 10 mm diameter test pieces was approximately 11 mm. For ease of reference, the reaction peaks are labelled 'A'

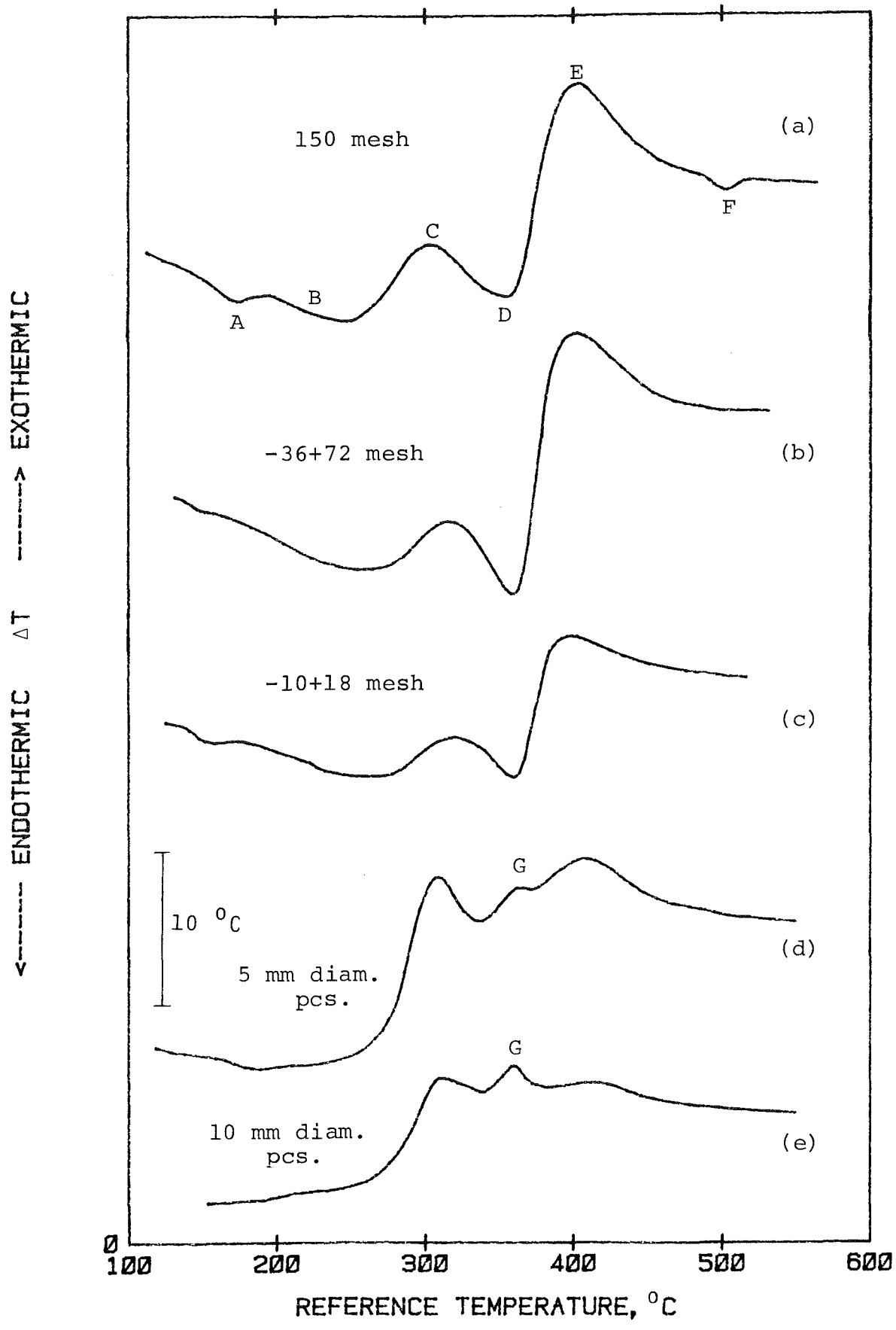

Figure 30. DTA curves in N_2 of Rubber wood of different particle sizes

to 'F' in Curve (a). It can be seen that the DTA curves of the < 150 mesh, -36+72 mesh and -10+18 mesh fractions were almost similar in shape, the only noticeable difference being that Endotherms A and F were more prominent in the DTA curve of the < 150 mesh fraction than in those of the other two fractions. The DTA curves of the 5 mm and 10 mm diameter pieces were fairly similar but were quite different from those of the other three samples. Each of them contained an extra exotherm between 340°C and 380°C (marked 'G') which was more conspicuous in the DTA curve of the 10 mm diameter pieces than in that of the 5 mm diameter pieces. Exotherm C was more prominent while Endotherm A was located at a higher temperature (190°C) in these curves than in the other three curves. Except in Curve (a), Endotherm F was barely visible or non-existent in the other curves.

The above results were obtained from runs in which the thermocouple's sensing tip was placed within the sample bed, in effect, surrounded by the wood particles. It would be interesting to compare these results with those obtained with the thermocouple's sensing tip placed within a single test piece. This can only be done for the larger wood pieces in which a hole can be made to house the thermocouple's sensing tip. Runs of this nature were carried out using 5 mm, 10 mm and 19 mm diameter single pieces of height 14 mm. The experimental set-up is illustrated in Figure 31. In the case of the 5 mm and 10 mm diameter pieces, a hole of diameter 1.5 mm was drilled to a depth of 7 mm into which the thermocouple was inserted. By making a small kink around the tip of the thermocouple before insertion, a tight grip was obtained between the thermocouple and the sample and this prevented the latter from falling off. The sample was then lowered into the sample tube and came to rest on the distributor. In the case of the 19 mm diameter test piece, a 2 mm diameter hole of depth 7 mm was made. It was dropped into the sample bed before the thermocouple was inserted into it. As it was relatively stable in view of its broad base, there was no need

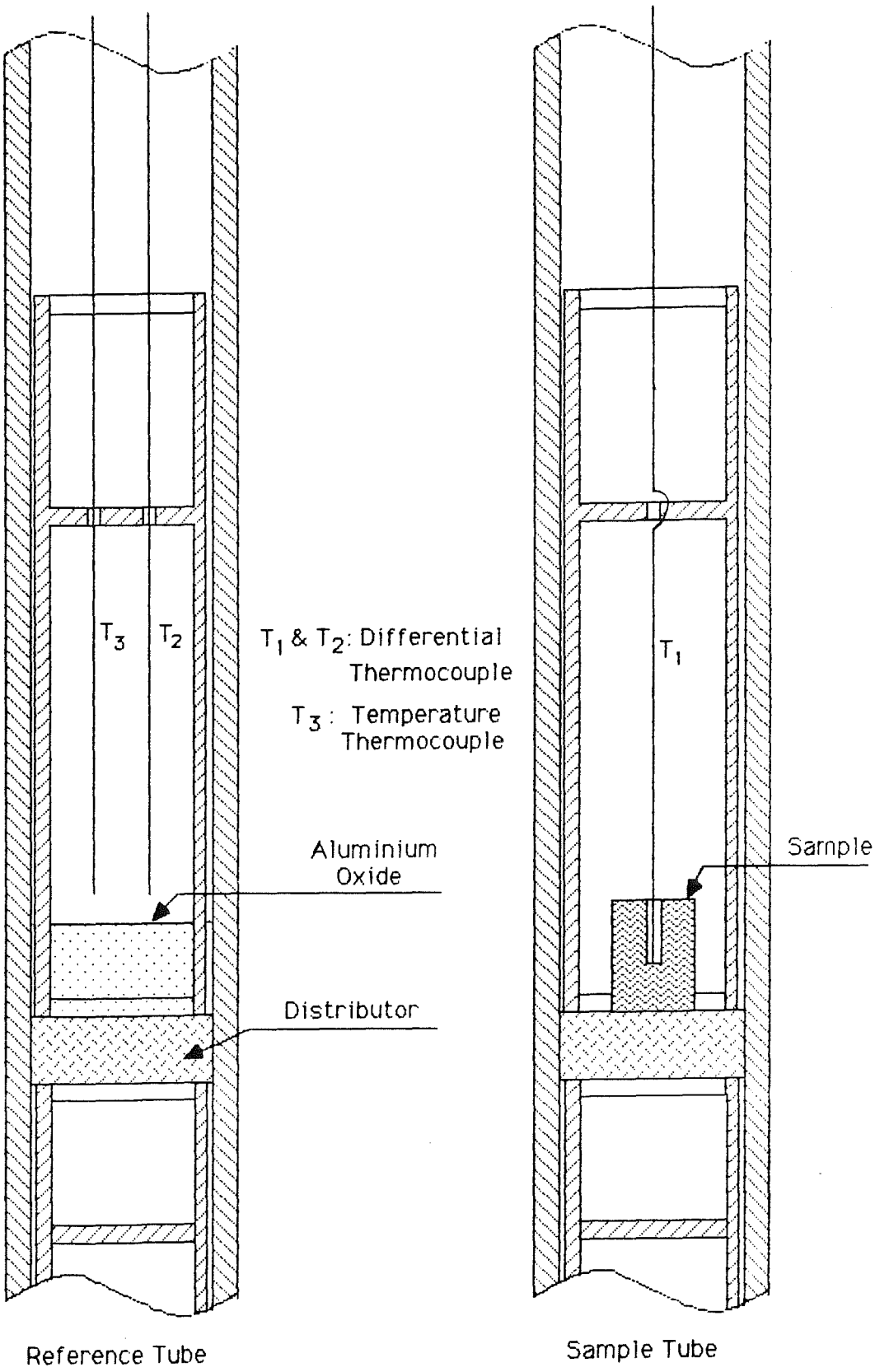

Figure 31. Experimental set-up for DTA of a single test piece

to make a kink in the thermocouple to provide a tight grip between them. In this run, no steel frame was used in the sample bed because the test piece would not be able to squeeze pass it. The weights of the 5 mm, 10 mm and 19 mm diameter test pieces were 0.19 gm, 0.70 gm and 2.58 gm respectively.

The DTA curves resulting from the new runs are presented in Figure 32. For ease of reference, the reaction peaks are labelled 'A' to 'G' in Curve (c). Except for a difference in size, the three curves were fairly similar in that the same reaction peaks were present in all of them. The most glaring difference between them lies in the relative size of Peak G which increased with increasing particle size, apparently at the expense of the exotherm to its right, i.e. Peak E. There was a close resemblance between the DTA curve of the 5 mm diameter piece and that obtained earlier for the same particle size using a 3 gm sample. The DTA curve of the 10 mm diameter piece, however, was more well-defined than the one obtained earlier although there was no basic difference in their shapes. Similarly, the reaction peaks in the DTA curve of the 19 mm diameter piece were large and well-defined. It therefore appears that in DTA of wood involving larger particle sizes, there is a clear advantage in using single test pieces with the thermocouple inserted into the sample.

The internal variation in thermal behaviour of a 19 mm diameter test piece was investigated by carrying out further runs. The experimental set-up for one of them is shown in Figure 33. Two 2-mm diameter holes were drilled in the test piece (obtained from a **PR 107** disc) to a depth of 7 mm, one in the middle and the other 2 mm from the edge. Two differential thermocouples were used, one inserted across the middle hole of the sample and the reference tube(T_1 & T_3) and the other across the outer hole and the reference tube (T_2 & T_4). Two DTA curves were thus obtained in this run (Figure 34), one from each differential thermocouple - Curve (a) from the first one and Curve (b) from the second one. It will be

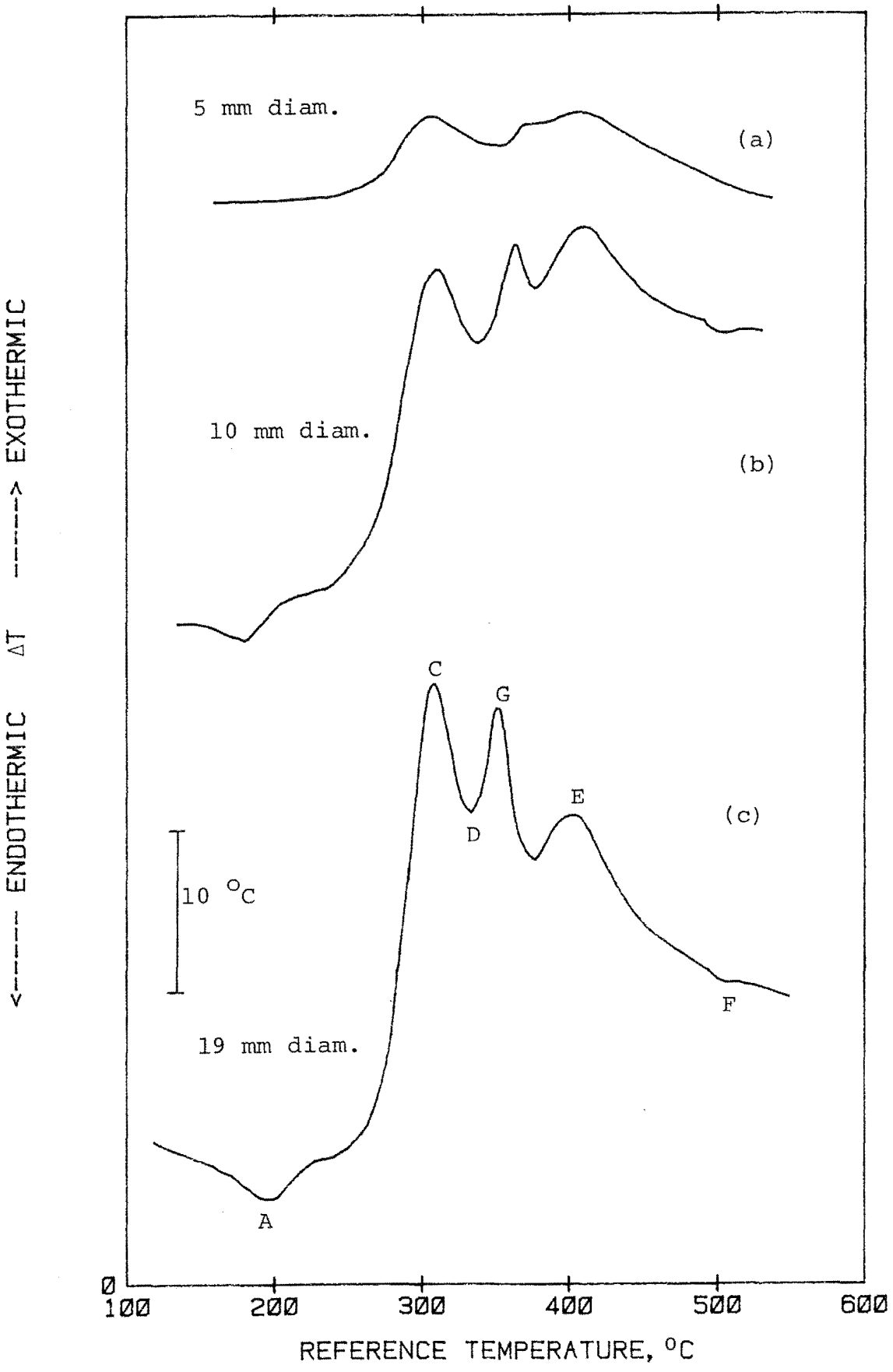

Figure 32. DTA curves in N_2 of Rubber wood of various diameters (single pc.)

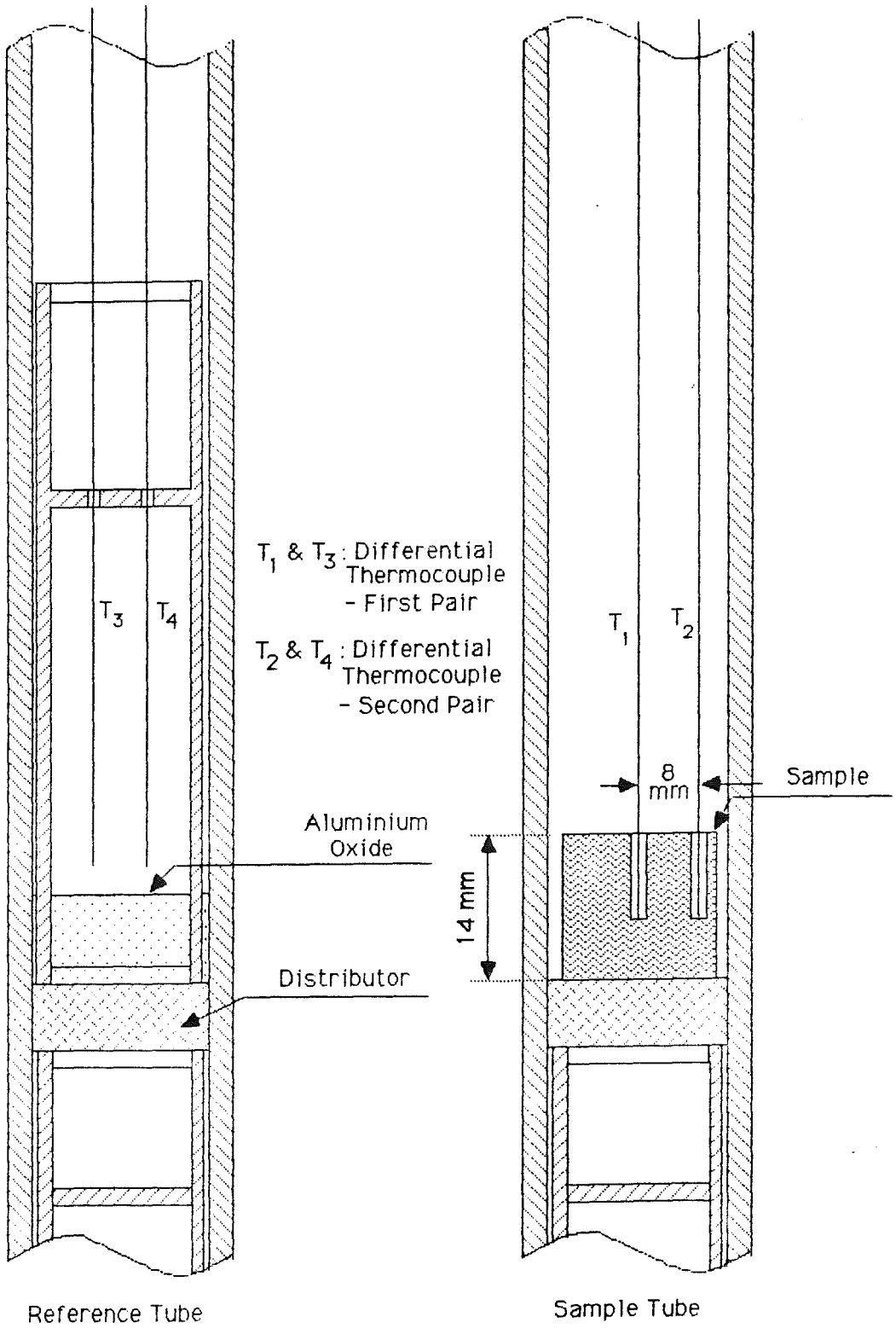

Figure 33. Experimental set-up of run to study the variation in thermal behaviour within a 19 mm diam. pc.

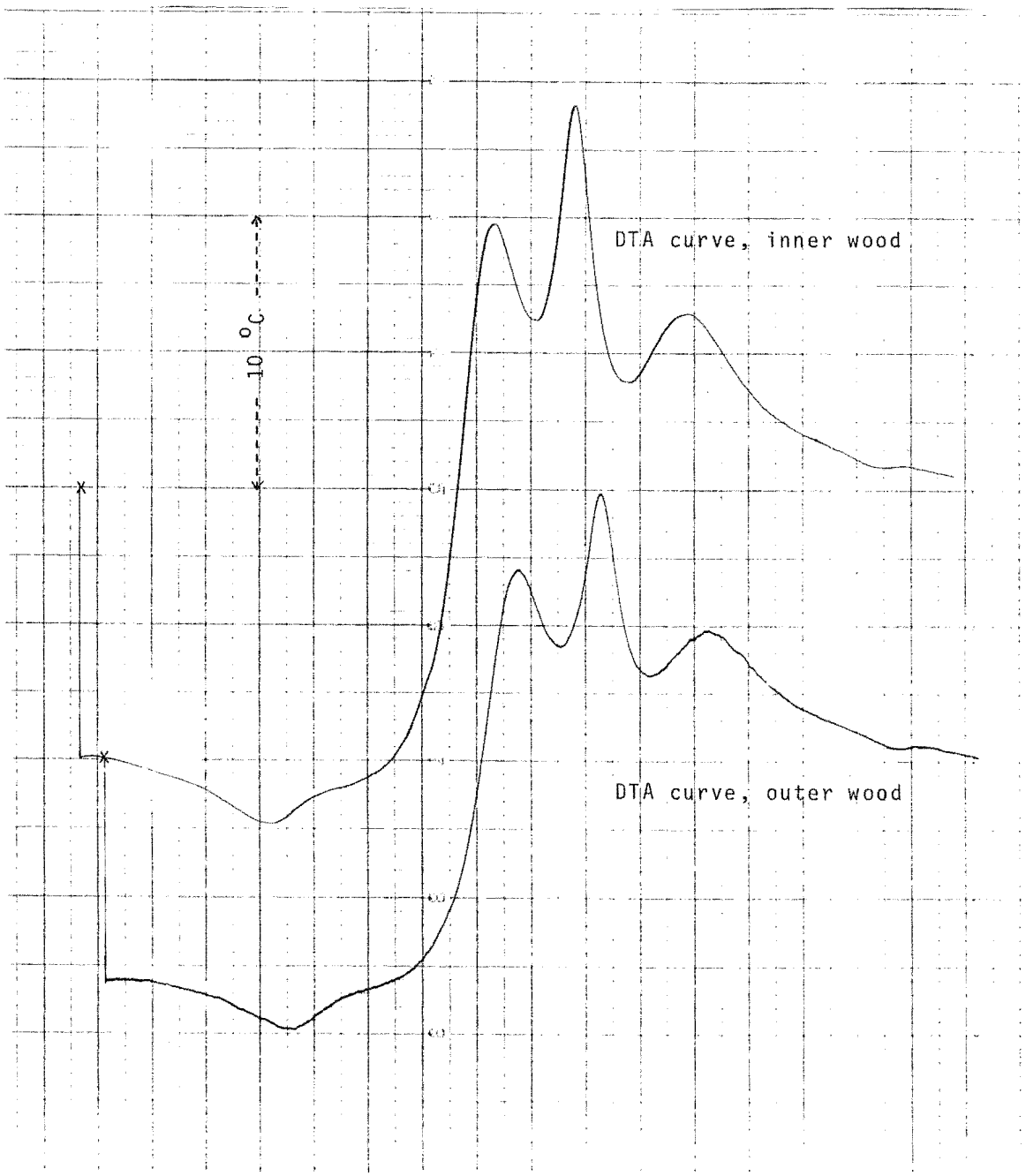

Figure 34. DTA curves in N_2 of the inner and the outer wood of a 19 mm diam. pc.

seen that the two curves were similar in shape. The only difference between them lies in the heights of the reaction peaks which were greater in Curve (a) than in Curve (b). For example, the height of Peak C (from Point B) in Curve (a) is 21°C as against 15°C in Curve (b). This seems to be due to the outer wood dissipating the heat of reaction to the surroundings more easily than the inner wood. There appeared to be very little time lag between the two curves. This was examined in greater details in another run in which the temperature difference between the inner and the outer wood was recorded as a function of the reference temperature by the experimental set-up shown in Figure 35. As shown in the resultant DTA curve (Figure 36), the temperature difference (T_1-T_2) between the two reference points in the wood increased from 0.5°C at 35°C to 5.3°C at 220°C before levelling off. The increase up to 145°C occurred almost at a steady rate. As the main pyrolysis reactions took placed at higher temperatures (above 240°C), this temperature difference is evidently due to the time lag in heat transfer from the outer to the inner part of the wood. As the heating rate was around 5.5°C/min, the time lag at 220°C between the two reference points in the sample was approximately 1 minute. The peaks exhibited in the curve arose from the difference in the rates of heat dissipation to the surroundings between the inner and the outer wood. The maximum temperature difference recorded during the run was about 7°C. A temperature difference of 3°C existed between the two reference points in the char. It is interesting to note that this curve is fairly similar in shape to the ones obtained earlier with the differential thermocouple inserted across the sample and the reference tube (see Figure 32). Similar results were obtained in the repeat runs. It is thus seen that although a temperature difference existed between the inner and the outer wood of a solid sample, there was very little difference in their thermal behaviours.

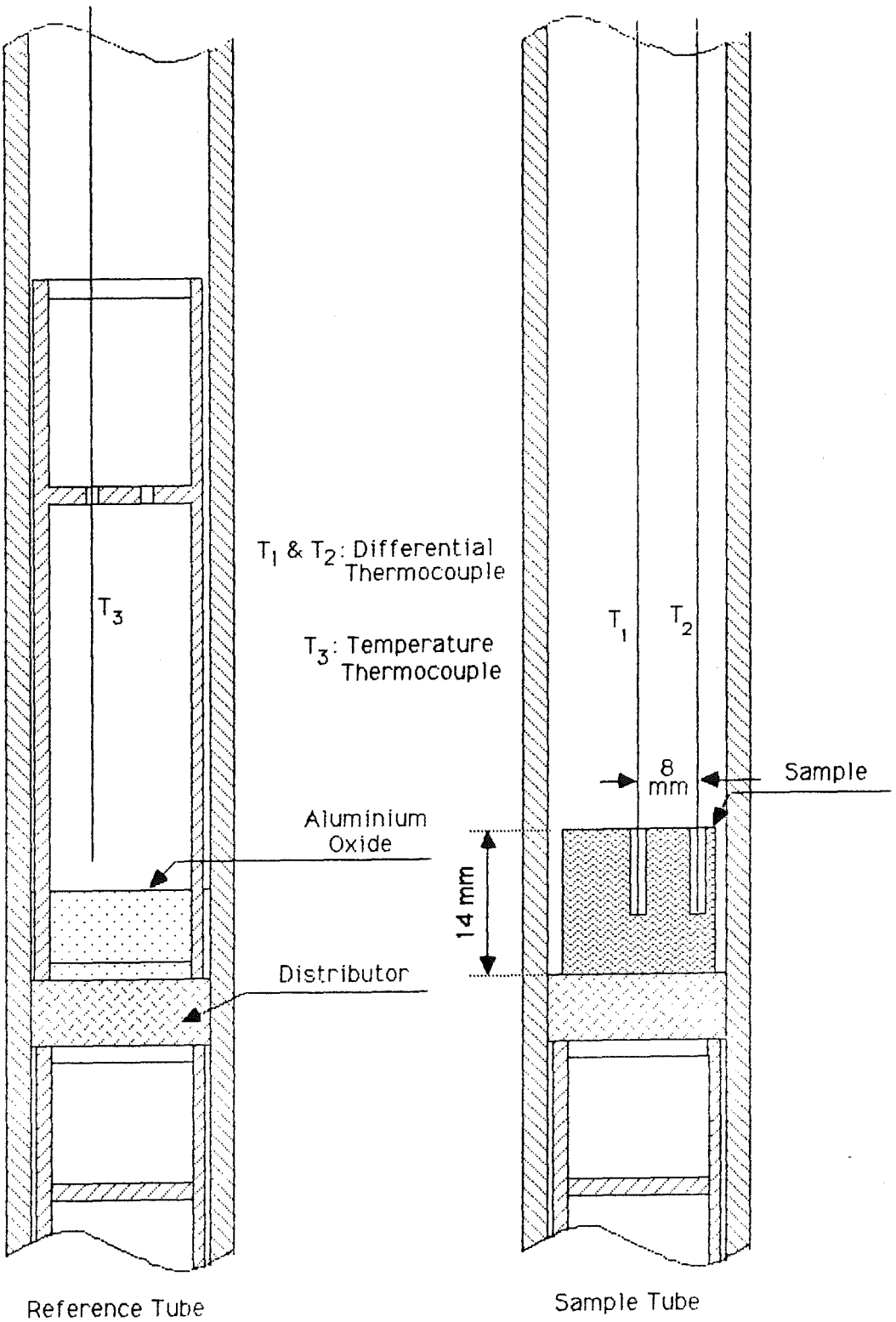

Figure 35. Experimental set-up of run to measure the temperature difference between the inner and the outer wood of a 19 mm diam. pc.

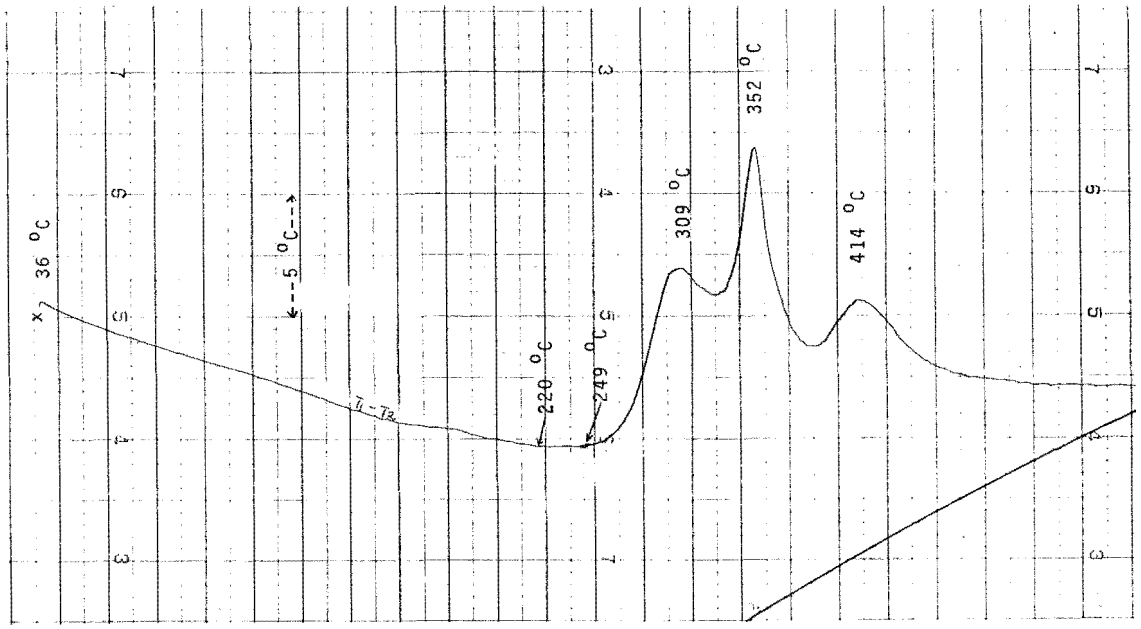

Figure 36. DTA curve showing the temperature difference between the inner and the outer wood of a 19 mm diameter piece

The above experiments show that the thermal analysis of Rubber wood, and perhaps wood in general, is dependent on particle size. This could be due to a difference in the pyrolysis pathways or to reactions between the volatile products within the sample, or both. In any case, in reporting the results of DTA experiments, it is important to specify the particle size used. Similarly, the comparison of the thermal behaviours of different wood species can only be meaningful if the experiments are conducted under similar conditions, including the use of a uniform particle size. Very little literature is available on the effect of particle size on the thermal behaviour of wood. The few studies which have been reported were confined to relatively small particle sizes, certainly no where near the largest size used in the present study. Finally, a remark about the overall effect of the pyrolysis reactions taking place in each sample. From the shapes of their DTA curves, it appears that the pyrolysis of the 5 mm, 10 mm and 19 mm diameter samples had an overall exothermic effect. It is not certain if the same thing can be said for the samples of smaller particle sizes.

4.4.3 Effect of Gas Flowrate

The effect of gas flowrate on the thermal behaviour of Rubber wood was investigated for the -36+72 mesh fraction. Three gas flowrates were used, viz 0.05 lit/min, 0.2 lit/min and 0.8 lit/min. A uniform sample size of 3 gm was used in these runs. The resultant DTA curves are presented in Figure 37. For ease of reference, the reaction peaks are labelled 'A' to 'F' in Curve (a). It can be seen that lowering the gas flowrate from 0.8 lit/min to 0.05 lit/min resulted in (1) the formation of an extra peak between 350°C and 390°C, (2) Endotherm A appearing at a higher temperature and (3) Endotherm B becoming less prominent. To a large extent, lowering the gas flowrate produced the same effect as increasing the particle size.

A similar investigation was carried out for cellulose. As shown in Figure 38, lowering the gas flowrate from 0.8 lit/min to 0.05 lit/min resulted in an exotherm being formed at around 380°C (marked 'H'). However, this exotherm is relatively small in size compared with the endotherm preceeding it.

4.4.4 Interpretation of DTA Curves

Interpretation of the DTA curves of Rubber wood based solely on information derived from those of the individual wood components was not as easy as it was thought to be because of overlapping reactions. To provide further information, two additional sets of runs were carried out using (1) mixtures of individual wood components and (2) Rubber wood samples (-36+72 mesh fraction) minus one or more components.

The DTA curves resulting from the first set of runs are presented in Figure 39. For ease of reference, the reaction peaks are labelled 'A' to 'E'. Comparing Curves (a) and (b),

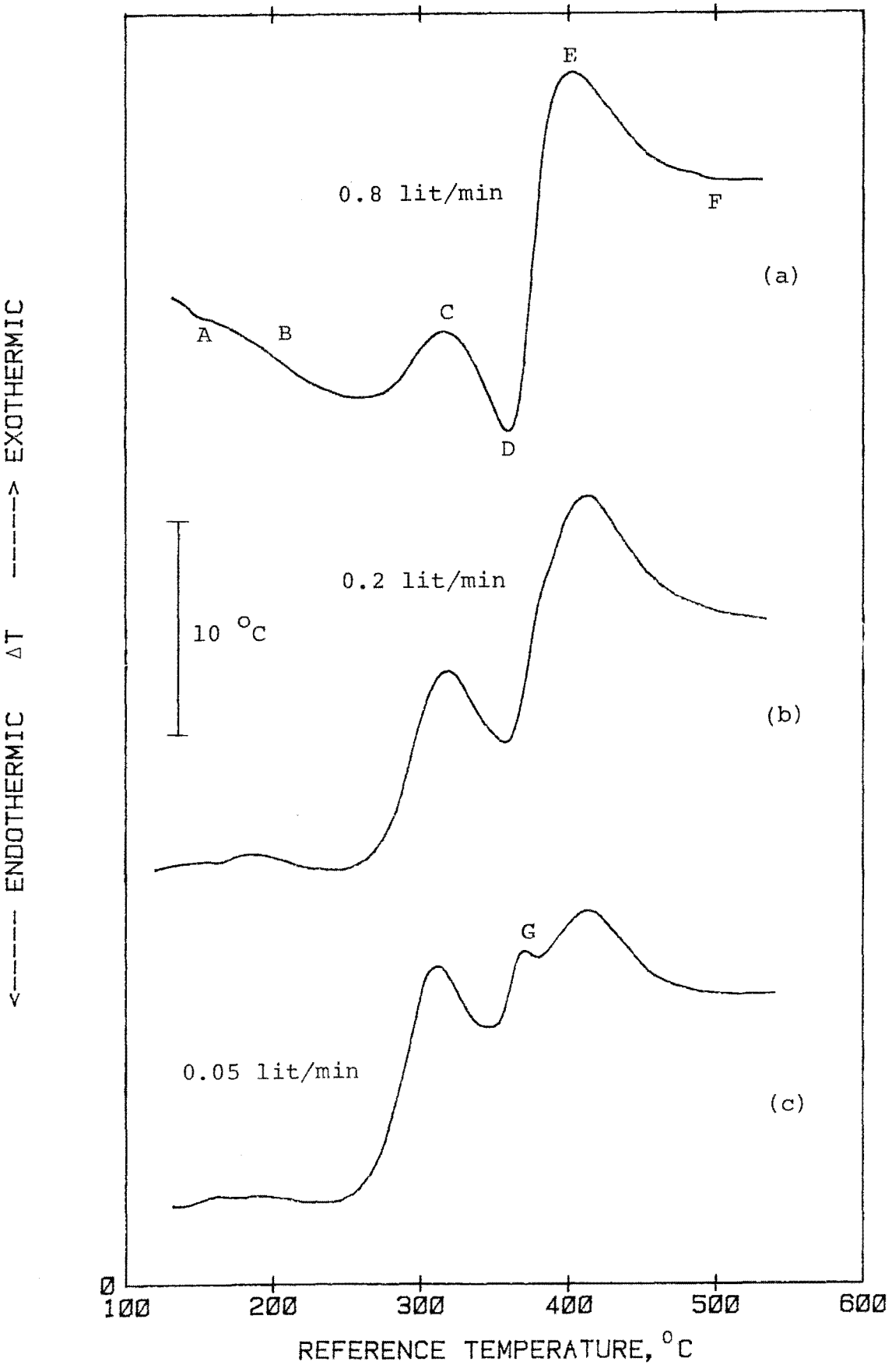

Figure 37. DTA curves in N_2 of Rubber wood (-36+72 mesh) obtained from runs using different gas flowrates

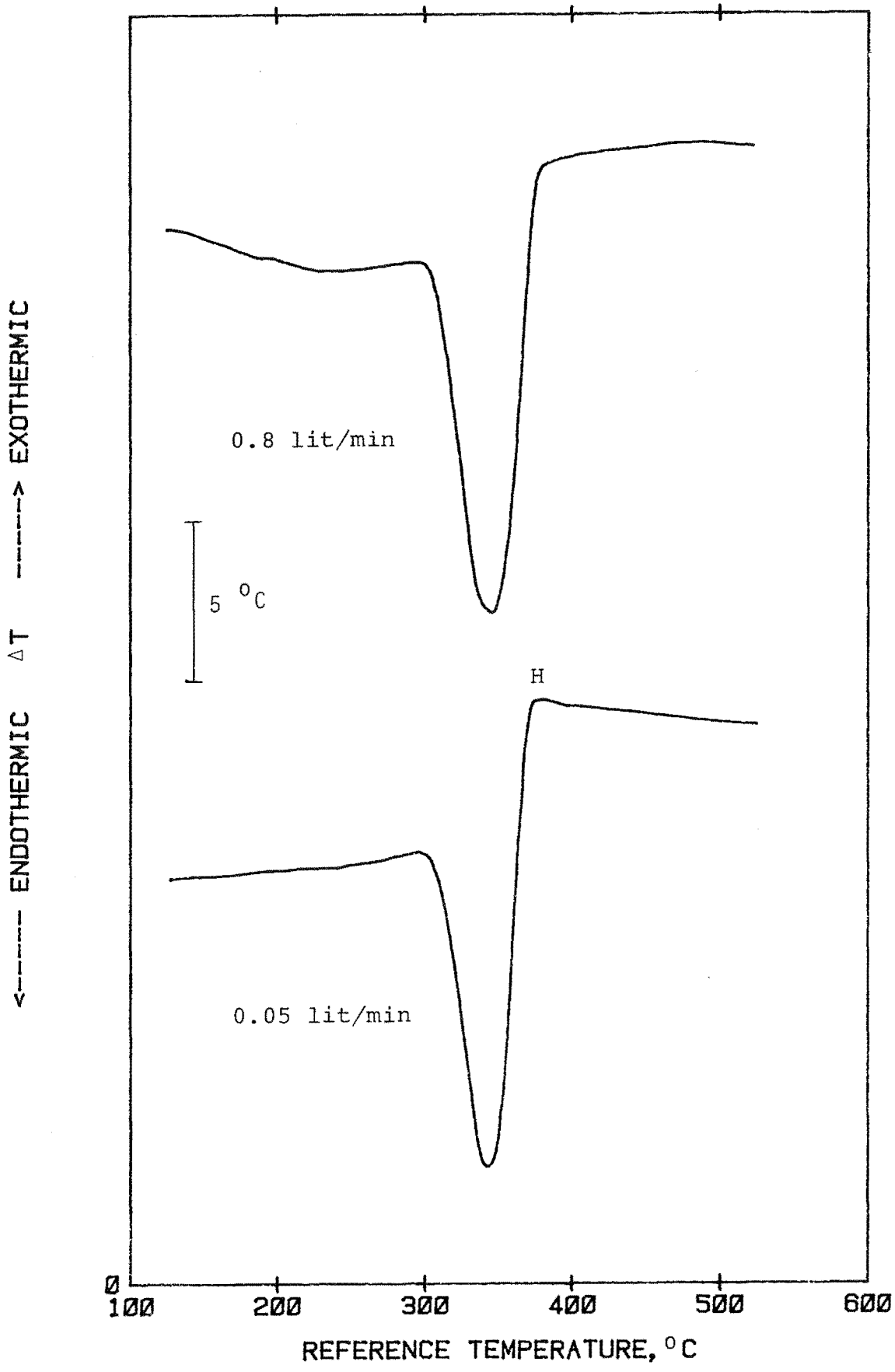

Figure 38. DTA curves in N_2 of cellulose obtained from runs using different gas flowrates

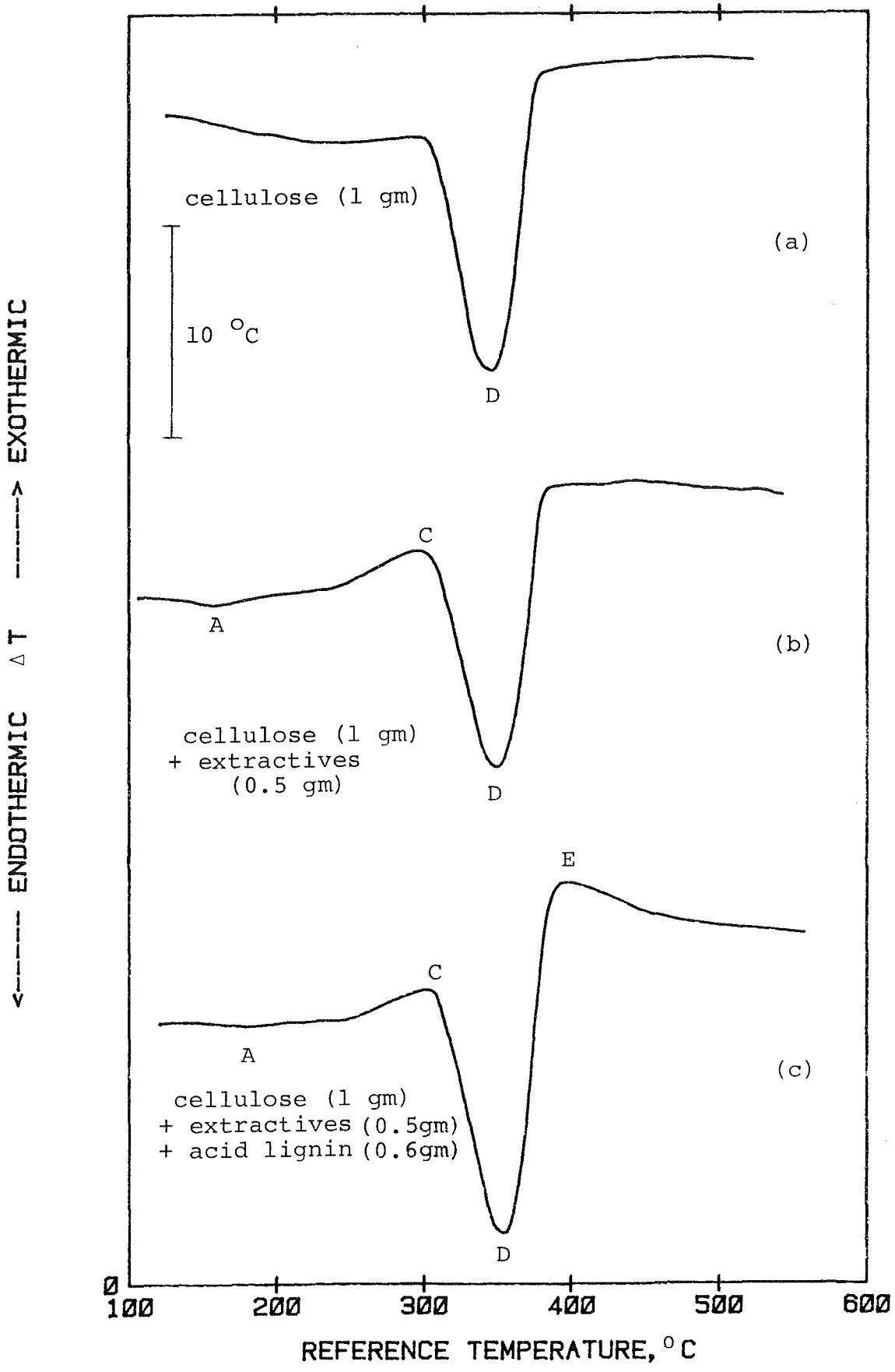

Figure 39. DTA curves in N_2 of mixed wood components

it is clear that Endotherm A and Exotherm C are attributed to the water-solubles. This is consistent with the results obtained earlier for the hot water extract as a single component (see Figure 27). The inclusion of acid lignin in the mixture resulted in an extra exotherm being formed, at around 400°C. In fact, only part of the lignin exotherm appeared in the curve, the remainder having been masked by the strong cellulose endotherm (see Figure 26). Figure 40 shows the resultant DTA curves from the second set of runs. Curves (a) and (b) are almost similar, indicating that the effect of the benzene/alcohol solubles on the thermal behaviour of Rubber wood is not great. By removing the water solubles from the wood, Exotherm C was greatly reduced in size while there was an increase in the size of Endotherm D, as shown in Curve (c). Endotherm A completely disappeared from the curve. It seems obvious that Endotherm A and part of Exotherm C are attributed to the water solubles. This is in agreement with the results obtained earlier. By removing some of the hemicelluloses from the extractive-free wood, Exotherm C virtually disappeared from the curve, as shown in Curve (e). It would therefore appear that part of Exotherm C is attributed to the hemicelluloses. However, the DTA curve of the hemicelluloses obtained earlier (see Figure 25) contained a rather strong exotherm between 200°C and 275°C which is not exhibited in any of the curves in Figure 40. The reason for this discrepancy is not entirely clear. Curve (e) is essentially the DTA curve of cellulose plus lignin since the other components have been removed from the wood. It closely resembled that of Curve (c) in Figure 39. This shows, first of all, that Endotherm D is attributed to cellulose and Exotherm E to lignin and, secondly, that removal of the extractives and hemicelluloses from the wood did not greatly change the nature of the remaining components. As for Endotherm F, it is rather difficult to pinpoint exactly the component responsible for it as it is very small and does not always show up in the DTA curves of Rubber wood. However, the fact that it is more prominent in the DTA curve of the <150

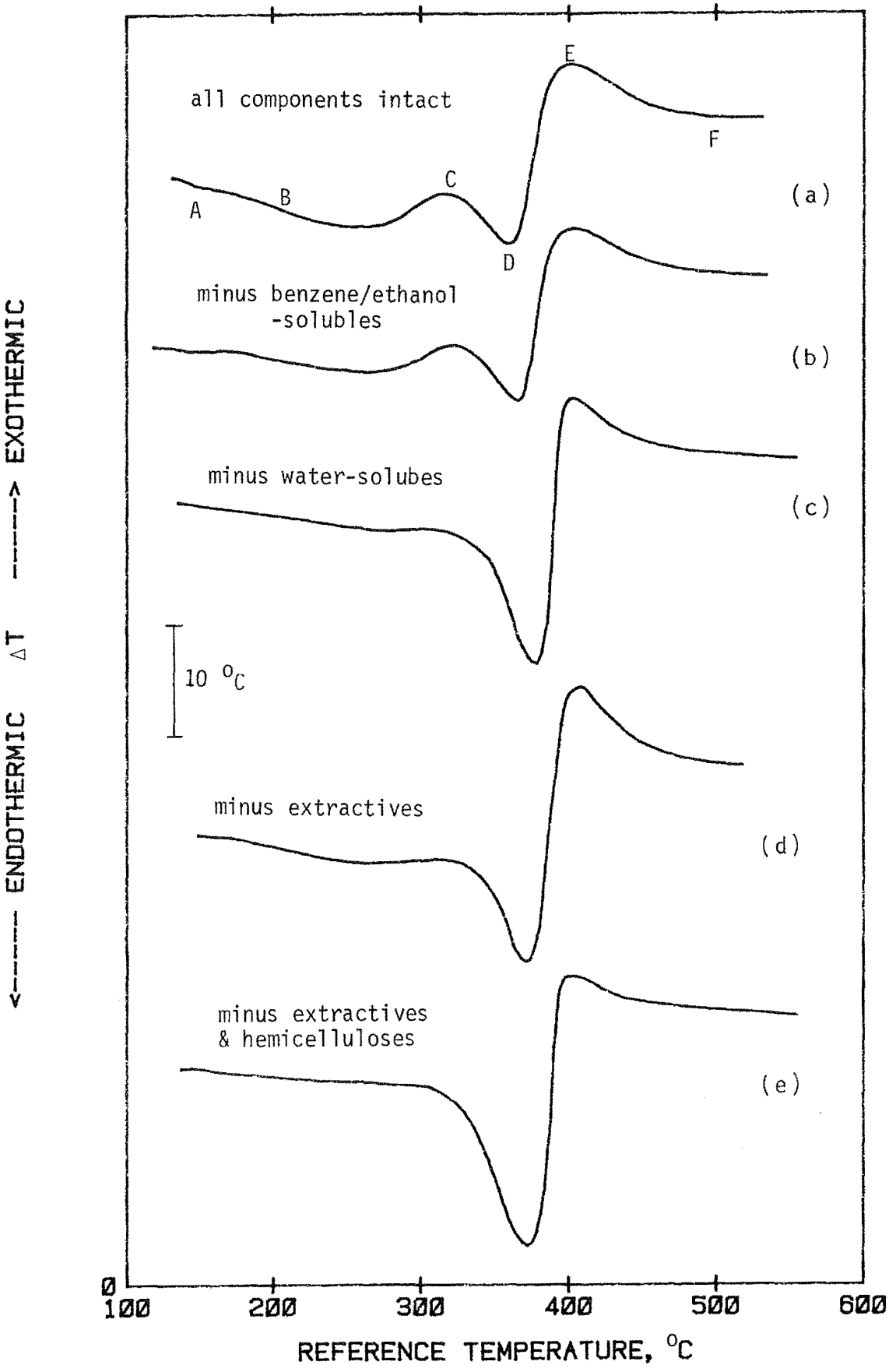

Figure 40. DTA curves in N_2 of Rubber wood (-36+72 mesh) minus one or more components

mesh fraction, which consisted mainly of the fines, seems to suggest that it is most likely due to the extractives. Endotherm B, which extended from around 160°C to 240°C, within which an 'aromatic' smell and smoke were emitted from the sample tube, appears to be due to the extractives and probably some of the hemicelluloses as well.

Next is the question of the extra peak (Exotherm G) which was present only in the DTA curves of the larger wood pieces. It is suspected that this is related to the water-soluble extractives since their DTA curve contained such a peak, although a small one (see Figure 27). To gather further evidence before drawing a conclusion, runs were carried out using 10 mm and 19 mm diameter single test pieces which had some of their water-solubles removed by soaking or boiling in water. As usual, the test samples were oven-dried before use. The resultant DTA curves are compared with those of the wood pieces with their water-solubles intact in Figure 41. It will be seen that by removing a portion of the water-solubles from the wood, Exotherm G was greatly reduced in size - to just a shoulder or a bulge. This serves to confirm that Exotherm G is indeed attributed to the water-soluble extractives. However, based on the information available, including the extractive content of the wood, it is more likely that the peak in question is due to reactions between the volatile products of the extractives and those of the other components within the sample than to the thermal decomposition of the extractives. In smaller wood particles, the volatile products formed easily escape to the surroundings and therefore have little chance to react. If, however, the run is conducted using a very low gas flowrate, the volatile products will have time to react within the bed before escaping. This is probably why an extra peak was formed in the DTA curve of the -36+72 mesh fraction when the gas flowrate was reduced from 0.8 lit/min to 0.05 lit/min (see Figure 37).

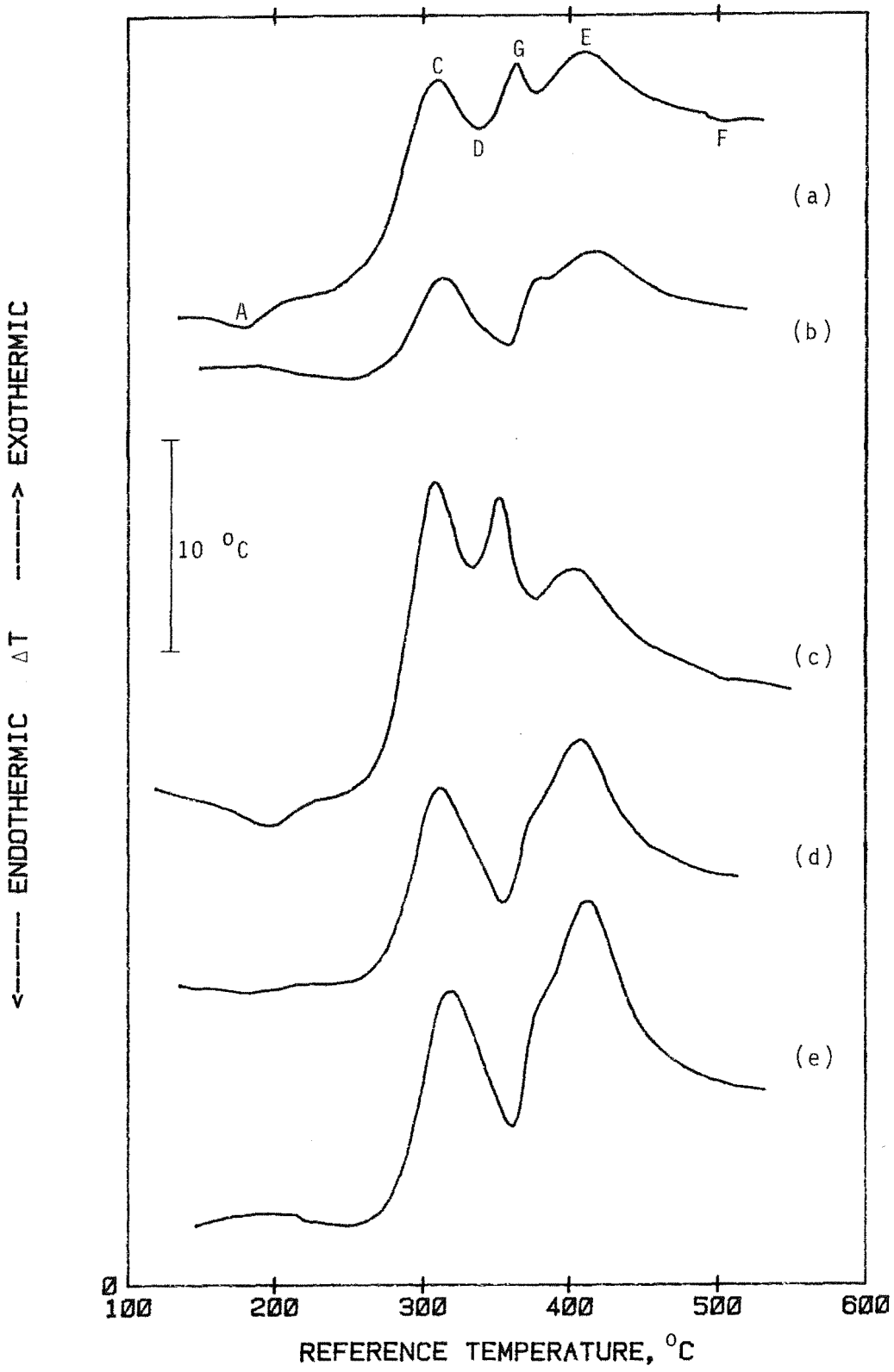

(a) 10 mm diam. pc.
(b) 10 mm diam. pc., boiled in water for 8 hours
(c) 19 mm diam. pc.
(d) 19 mm diam. pc., boiled in water for 14 hours
(e) 19 mm diam. pc., boiled in water for 4 days

Figure 41. DTA curves in N_2 of single test pieces with and without boiling in water

4.5 DTA Curves of Air-dry Wood

Figure 42 shows the DTA curves of two air-dry Rubber wood samples having a moisture content of around 8%. One sample was of particle size -10+18 mesh while the other consisted of a single test piece of diameter 19 mm and height 14 mm. The first sample weighed 3 gm and the second one around 2.5 gm. Each of the curves contained a relatively large endotherm (marked 'M'), attributed to evaporation of the free water from the wood. In Curve (a), this endotherm extended from around 30°C to 140°C while in Curve (b), it extended well beyond 200°C and swallowed up Endotherm A on the way. Had the samples been oven-dried before use, this drying curve would not be present to interfere with the other reactions peaks. This is one of the reasons why oven-dried samples were used in the present study. Except for the drying curve, the DTA curves of the air-dried wood were similar to those of the corresponding oven-dried wood. This shows that drying the samples in an oven at 105°C for 16-24 hours did not have a significant effect on the thermal behaviour of the wood.

4.4.6 Comparison between Wood from Different Trees

Up to now, only the wood of the **Tjir 1** tree was used in the experiments. Runs were also conducted using test samples obtained from the fresh wood of the other three trees to see if there was any difference in their thermal behaviours. Three particle sizes were used, namely -36+72 mesh fraction, 5 mm diameter pieces and 19 mm diameter single test piece of height 14-15 mm. In the case of the first two particle sizes, a sample size of 3 gm was used. The weights of the 19 mm diameter single test pieces varied from 2.4 gm to 2.7 gm.

The resultant DTA curves are presented in Figure 43 (-36+72 mesh fractions), Figure 44 (5 mm diameter pieces) and Figure 45 (19 mm diameter single pieces) together with those of **Tjir 1**. In Figure 43, there is hardly any difference in

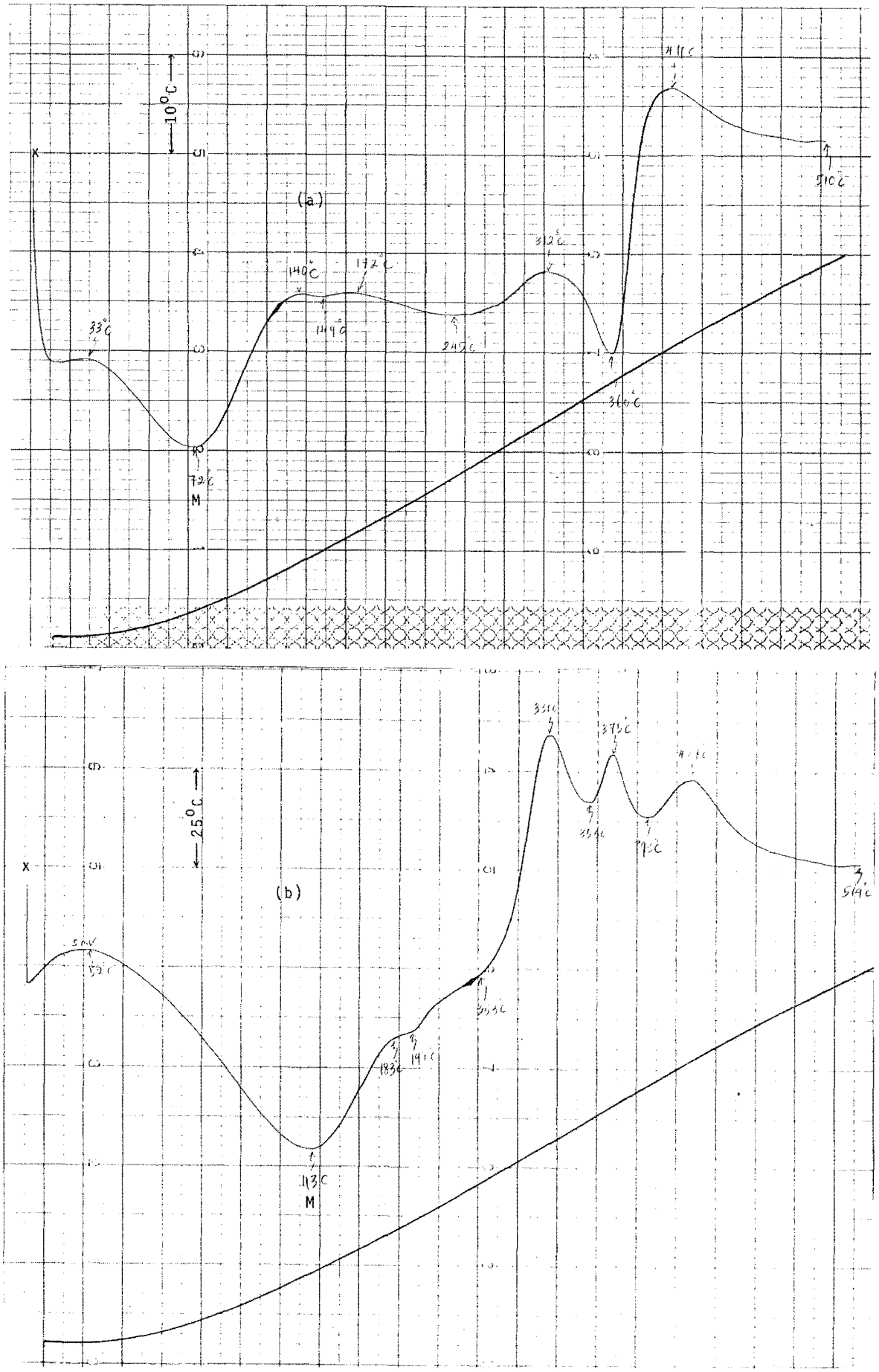

Figure 42. DTA curves in N_2 of air-dry Rubber wood: (a) -10+18 mesh particles and (b) 19 mm diam. pc.

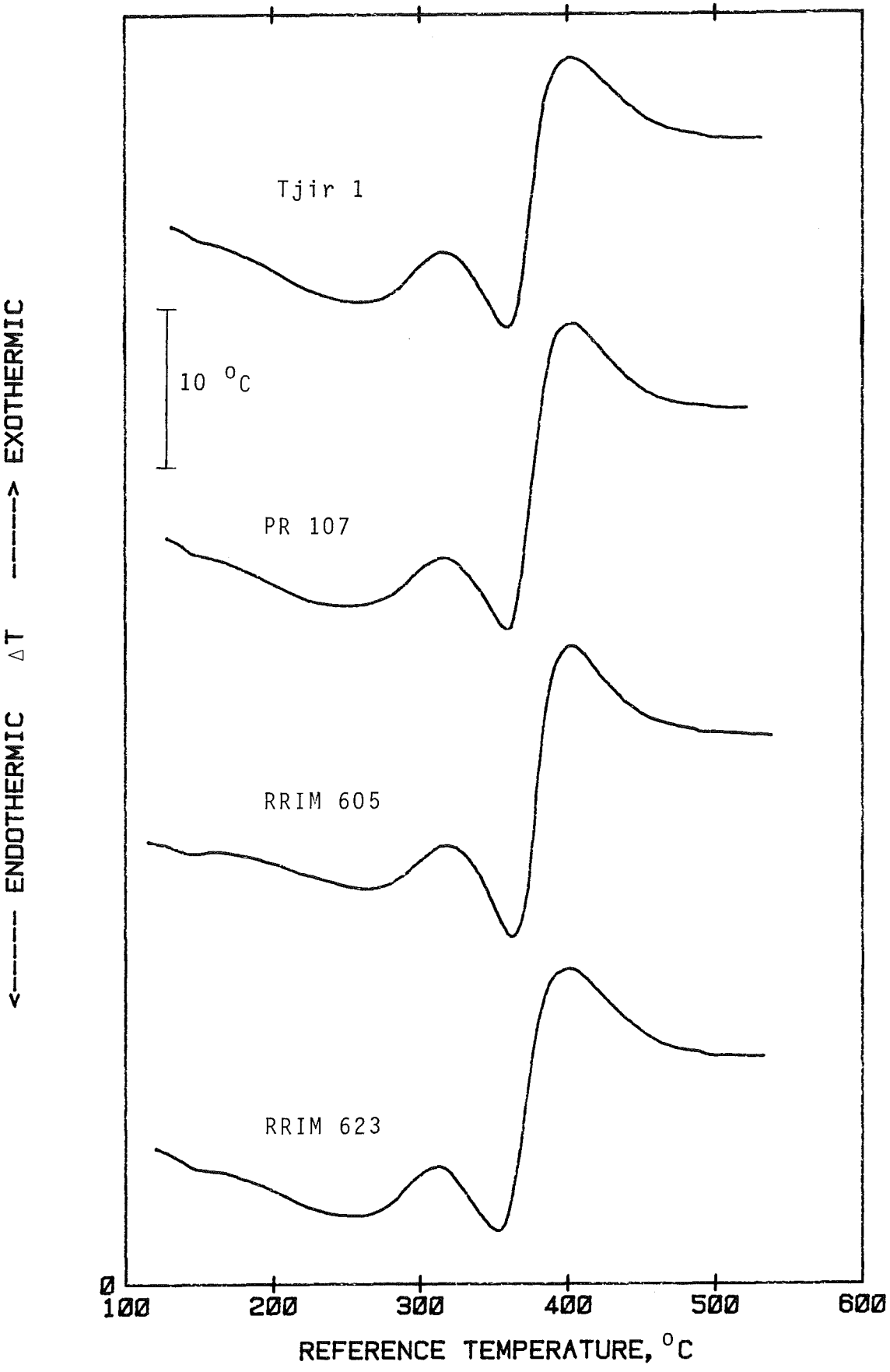

Figure 43. DTA curves in N_2 of Rubber wood from different trees (-36+72 mesh particles)

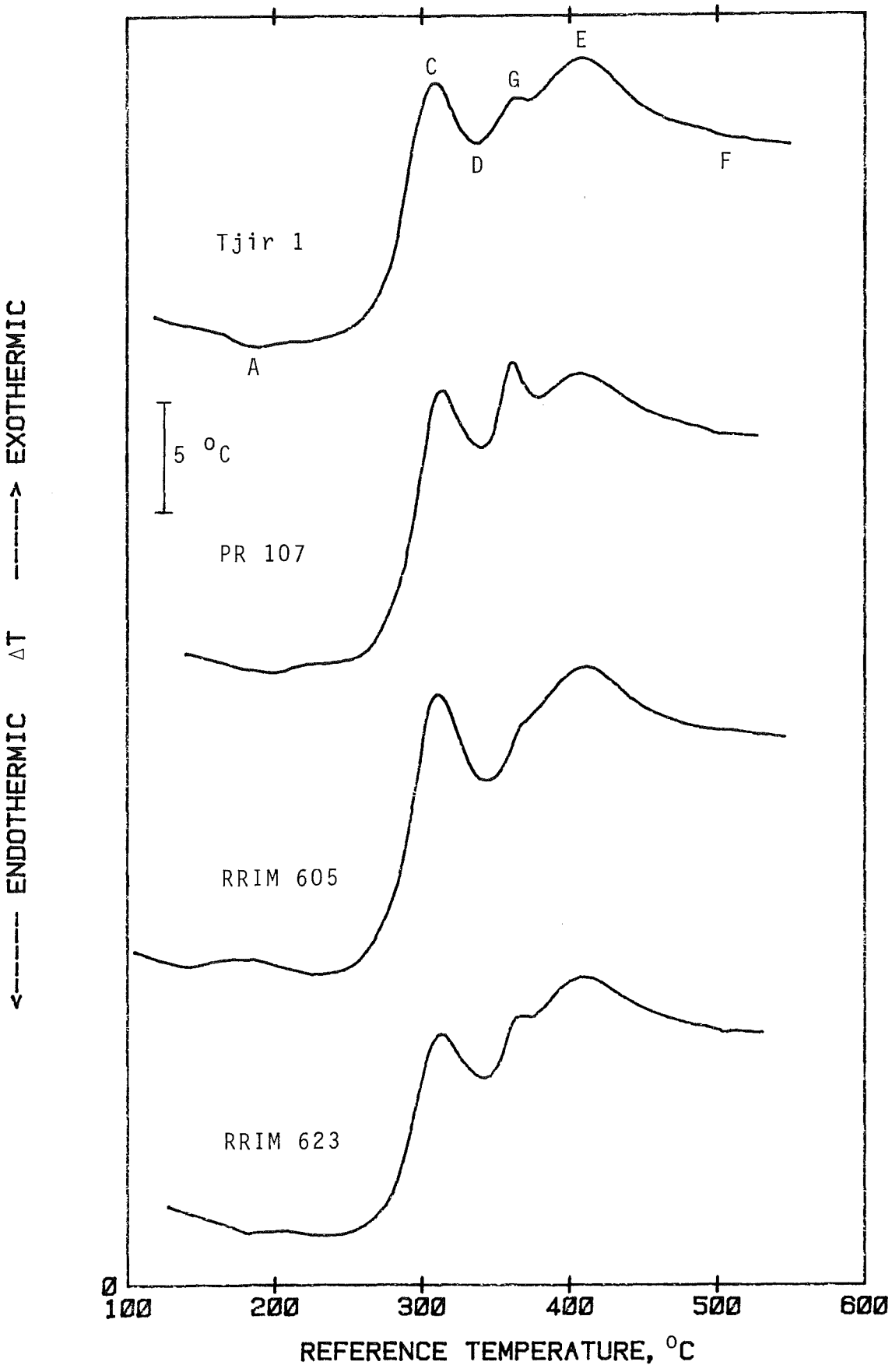

Figure 44. DTA curves in N_2 of Rubber wood from different trees (5 mm diam. pcs.)

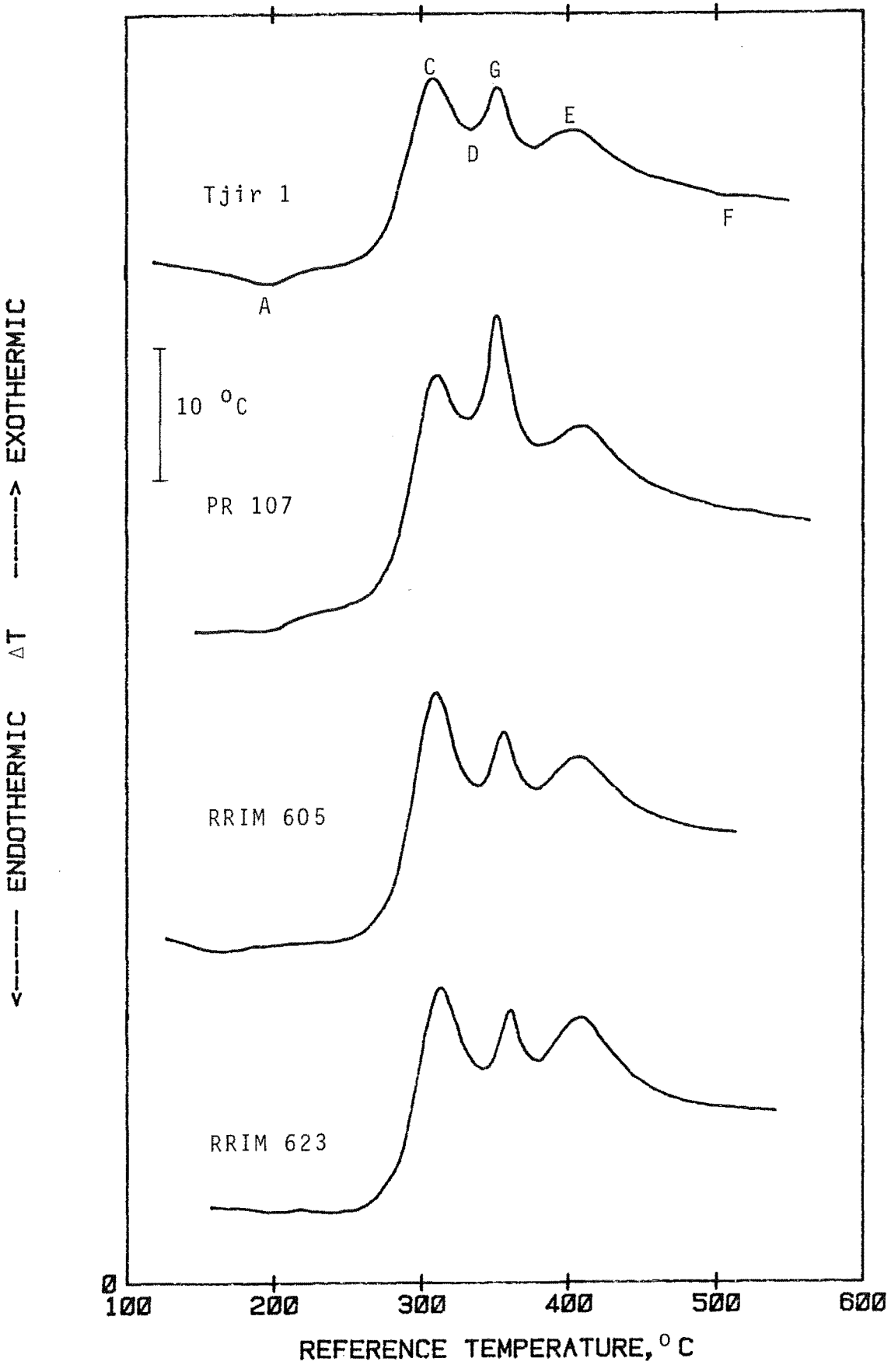

Figure 45. DTA curves in N_2 of Rubber wood from different trees (19 mm diam. pc.)

the shapes of the curves. A slight difference existed in Figure 44 and this lies in the relative size of the peak between 340°C and 380°C (Exotherm G). It will be seen that this peak is more prominent in the DTA curve of the **PR 107** sample than in those of the other three samples. The same observation was made in the DTA curves of the 19 mm diameter single pieces. The results obtained show that the two larger wood sizes of **Tjir 1, RRIM 605** and **RRIM 623** behaved similarly thermally while those of **PR 107** had a slightly different behaviour. As Exotherm G is due mainly to the extractives, it would appear that the **PR 107** test samples contained a higher percentage of these substances than those of the other samples. The fact that the density of the fresh wood of **PR 107** is 6-11% higher than those of the similar type of wood from the other trees is an indication of this. Repeat runs were carried out for the 19 mm diameter single pieces. The results obtained were similar to those obtained earlier.

4.4.7 Comparison between Fresh and Mouldy Wood

Runs were also carried out on the mouldy wood from each tree using single pieces of diameter 19 mm and height 14-15 mm. The DTA curves obtained from these runs are compared with those of the fresh wood in Figures 46(a) and 46(b). It will be seen that the DTA curve of the mouldy wood is slightly different from that of the fresh wood from the same tree, in that the relative size of Peak C is smaller while that of Peak G is larger in the former than in the latter. This could be due to a change in the chemical composition of the wood as a result of fungal infestation. The fact that the mouldy wood was 9-11% lower in density compared with the fresh wood (except for **Tjir 1**) made this a distinct possibility. However, there is also the possibility that the physical properties of the wood have been changed by fungal attack.

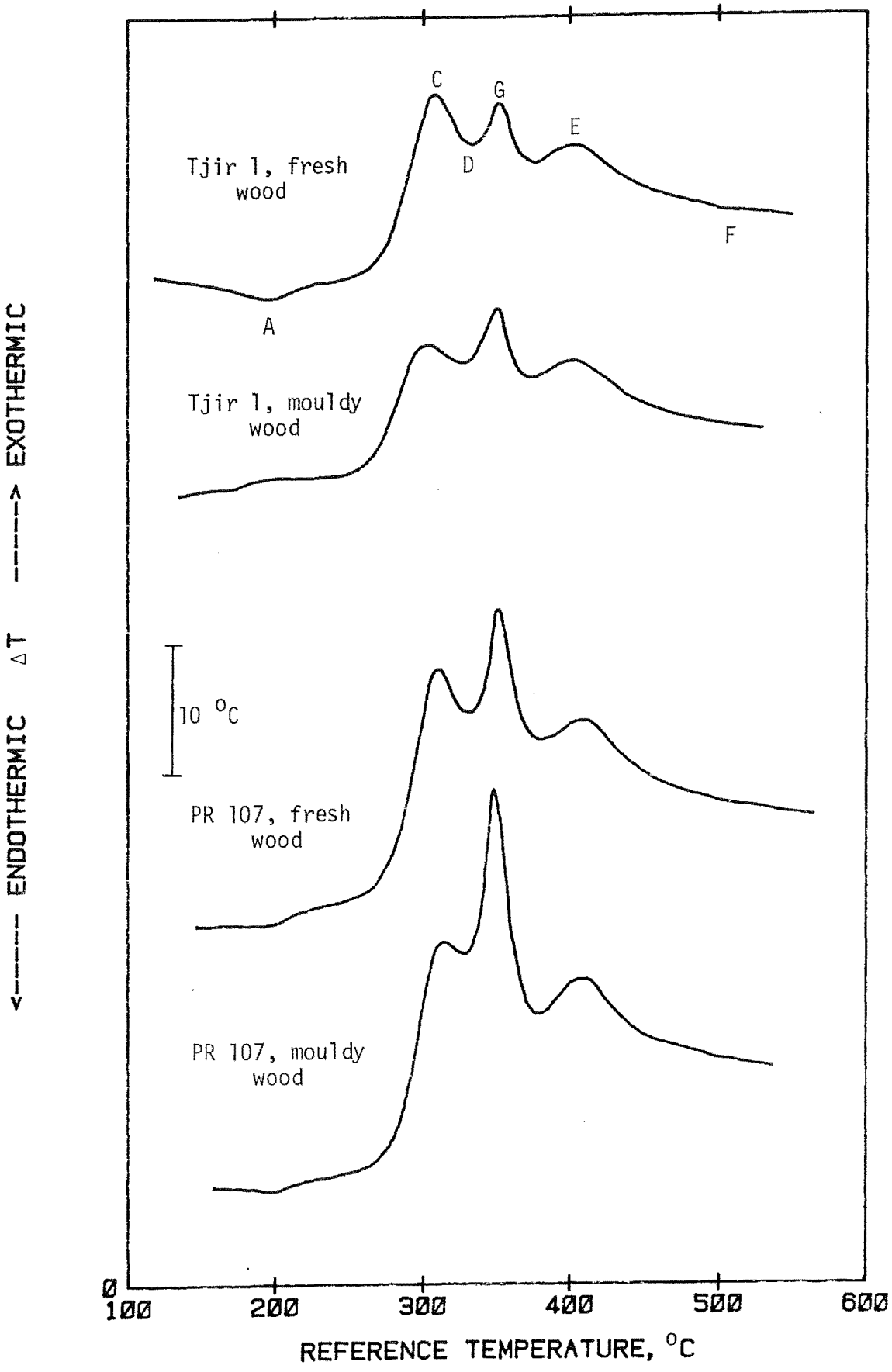

Figure 46(a). DTA curves in N_2 of fresh and mouldy wood (Tjir 1 and PR 107)

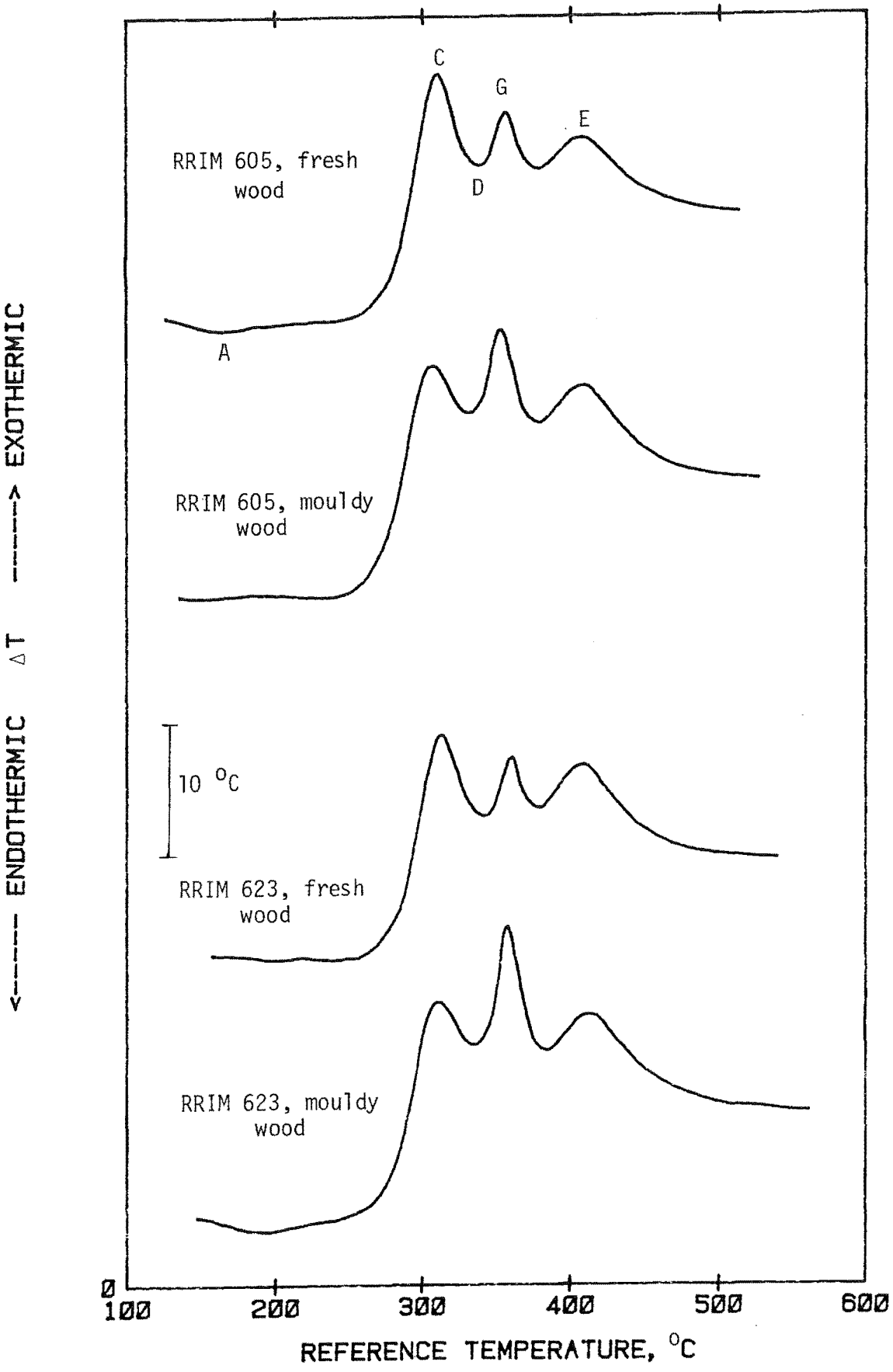

Figure 46(b). DTA curves in N_2 of fresh and mouldy wood (RRIM 605 and RRIM 623)

4.4.8 Comparison with other Wood Species

The comparison of the thermal behaviours of Rubber wood and other wood species was made using two particle sizes, viz (1) single piece of diameter 19 mm and height 14-15 mm and (2) sawdust. The sawdust samples were prepared from their respective wood pieces by drilling at a low speed. In runs using sawdust, a uniform sample size of 3 gm was used. The weights of the single test pieces varied from 1.1 gm to 3.6 gm.

Figure 47 shows the DTA curves obtained from the runs using the single test pieces. With the exception of Endotherms A and F, all the reaction peaks which are present in the DTA curve of Rubber wood are also present in those of the other wood species. There was only a slight variation in the individual peak temperatures, e.g. Peak C varied from 293°C to 316°C, Peak G from 351°C to 367°C and Peak E from 406°C to 429°C. The difference between the DTA curve of Rubber wood and those of the other species was greater in the relative sizes of the reaction peaks. By and large, Peaks G and E were more prominent in the DTA curves of the hardwood species than in that of Rubber wood. If they are also due to the extractives (Peak G) and lignin (Peak E), as in the case of Rubber wood, this would mean that the test pieces of the hardwood species contained a higher proportion of these two components than that of Rubber wood. The resolution of Peak C, however, was better in the DTA curve of Rubber wood than in those of the other wood species. The presence of Endotherms A and F in the DTA curve of Rubber wood but not in the other curves is a further indication that they are attributed to the extractives.

Besides tropical hardwoods, the thermal behaviour of Rubber wood was also compared with those of its bark, Coconut wood and Oil palm wood. Again single pieces of diameter 19 mm were used except for the bark whose test sample consisted of a

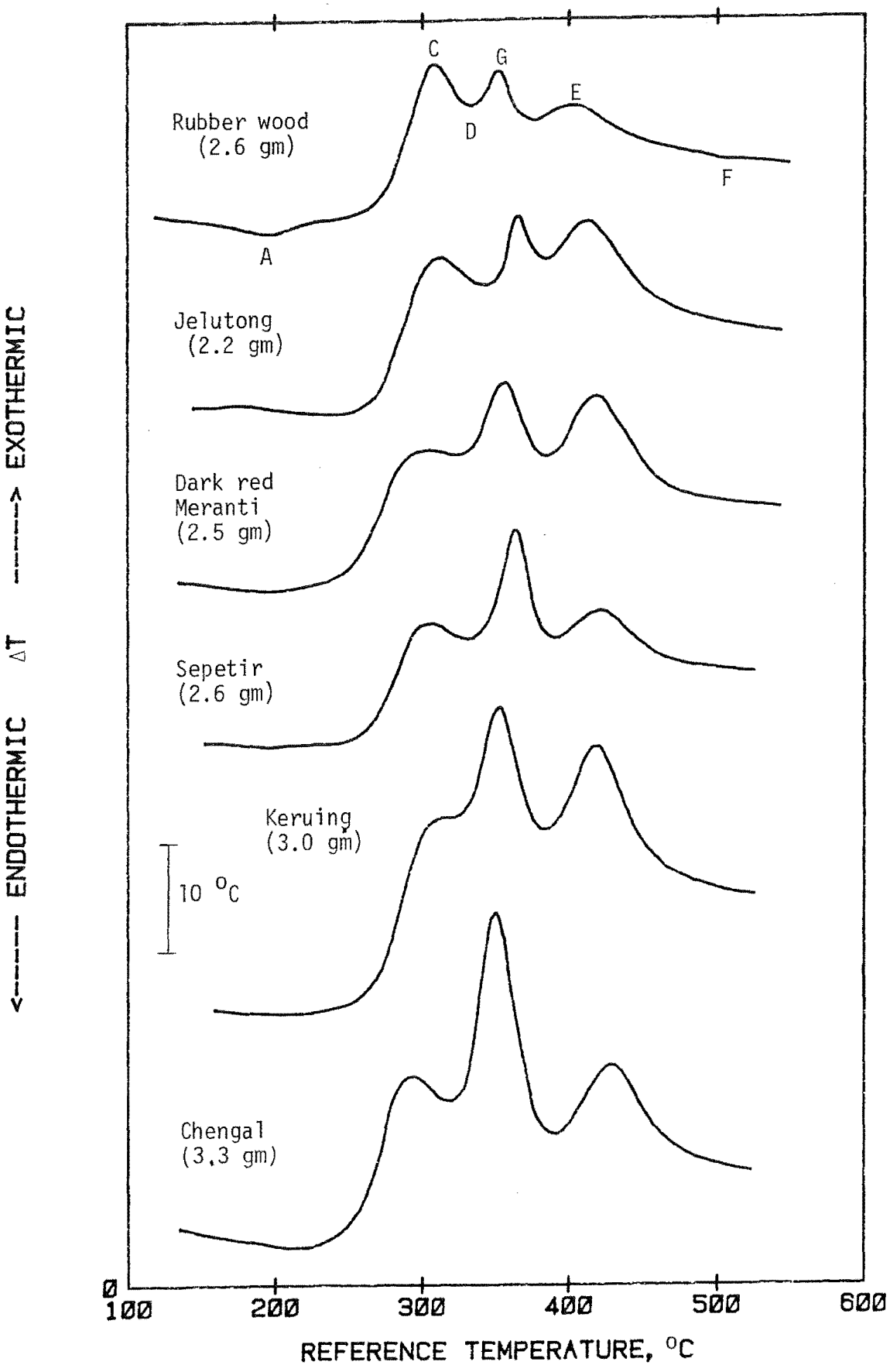

Figure 47. DTA curves in N_2 of some tropical wood species (19 mm diam. pc.)

square piece (16mmx16mm) of thickness 6 mm. As shown in Figure 48, the DTA curves of Coconut wood and Oil palm wood were fairly similar in shape. Each of them contained two strong and one weak exotherms, the first peaking at around 275°C, the second at around 340°C and the third at around 400°C. As the third exotherm is attributed to lignin, it appears that the lignin contents of the Coconut wood and Oil palm wood samples were lower than that of Rubber wood. The DTA curve of rubber tree bark was quite different from that of Rubber wood but both of them contained certain common features, namely an endotherm below 200°C (A), an exotherm which peaked at around 400°C (E) and a weak endotherm at about 500°C (F).

Figure 49 shows the DTA curves resulting from runs using sawdust. There is not a great deal of difference between these curves except that Endotherms A and F are only present in the DTA curve of Rubber wood. It is therefore fair to say that the thermal behaviours of the various sawdust samples were fairly similar. As a matter of fact, these curves were similar to that of Rubber wood of particle size -36+72 mesh (see Figure 30).

From the results obtained here and earlier (in Section 4.4.6), it is clear that in comparing the thermal behaviours of different wood species, it is desirable to use samples of greater particle sizes in order to bring out the difference, if any, more clearly.

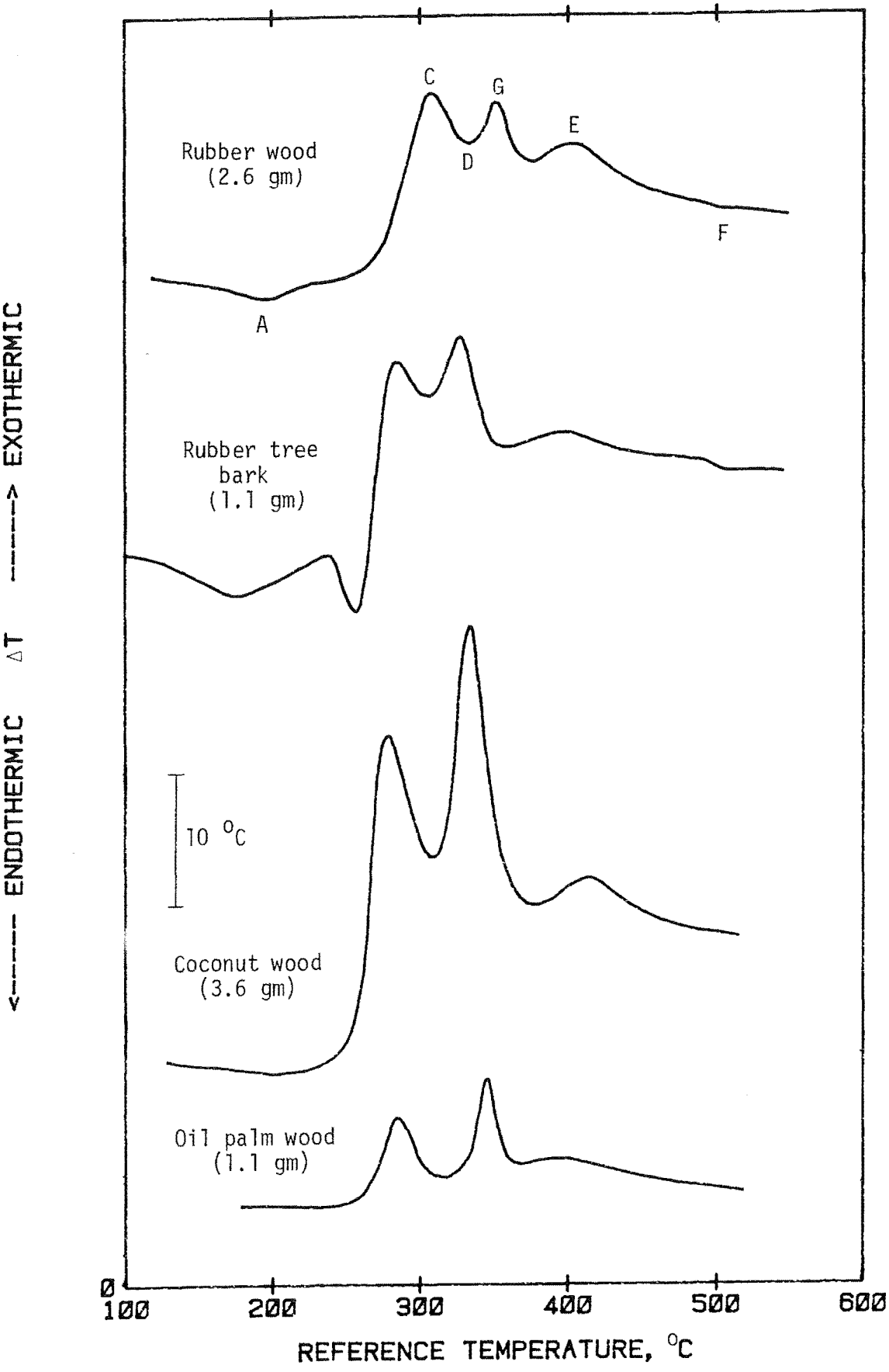

Figure 48. DTA curves in N_2 of some agricultural by-products (19 mm diam. pc.)

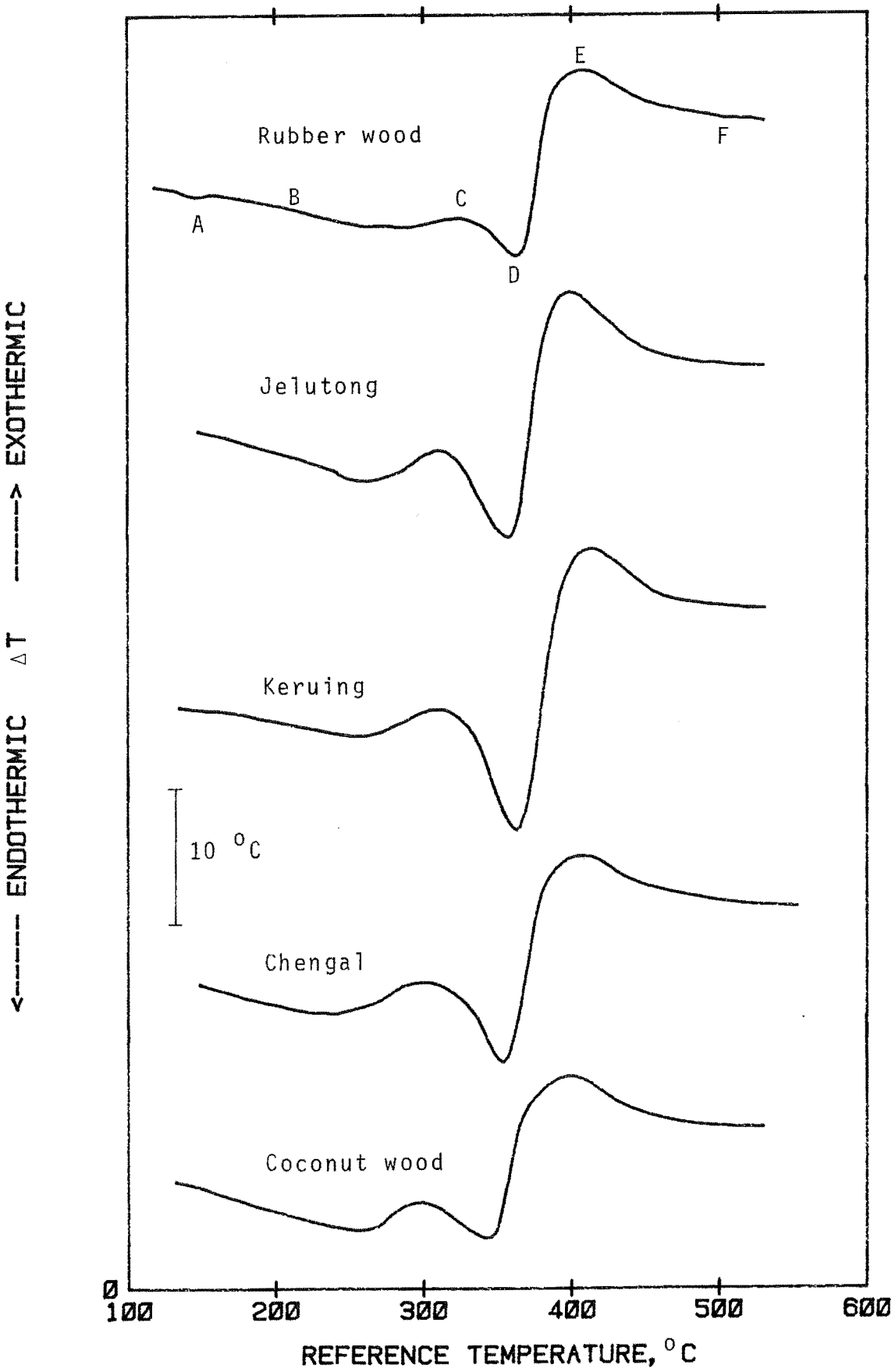

Figure 49. DTA curves in N_2 of some wood species (sawdust)

CHAPTER 5

ANALYSIS OF PYROLYSIS PRODUCTS

Several runs using Rubber wood as test materials were carried out in which the pyrolysis products were collected and their yields determined. The evolved gases and the liquid fractions were analysed, the former quantitatively and the latter qualitatively.

5.1 Collecting Device

In these runs, the steel frame in each bed was replaced by a stainless steel tube of height 60 mm, external diameter 25.4 mm and thickness 1 mm. Each tube contained a thin horizontal metal strip to enable it to be taken out of the bed. The one in the sample bed served as the sample holder. A piece of 'Kaowool' of thickness 7 mm was squeezed tightly into its lower end to hold the sample. After the sample had been put in, the sample holder was gently lowered into the sample bed using a long hook. Following this, a stainless steel connecting head was bolted to the top of the tube, as illustrated in Figure 50. A piece of PTFE tape was wrapped round the tapered end of the connecting head which was then inserted tightly into the side mouth of a double-necked round-bottomed flask of 100 ml capacity. This flask was connected by a thick rubber hose to a similar flask which was fitted with a condenser. The condenser was, in turn, connected by a rubber hose to a 30-litre polythene bag of thickness 0.125 mm. The connecting head was electrically heated and lagged with ceramic fibre to prevent the volatiles from condensing inside it. Both the flasks were ice-cooled. A block diagram of the collecting device is shown in Figure 51.

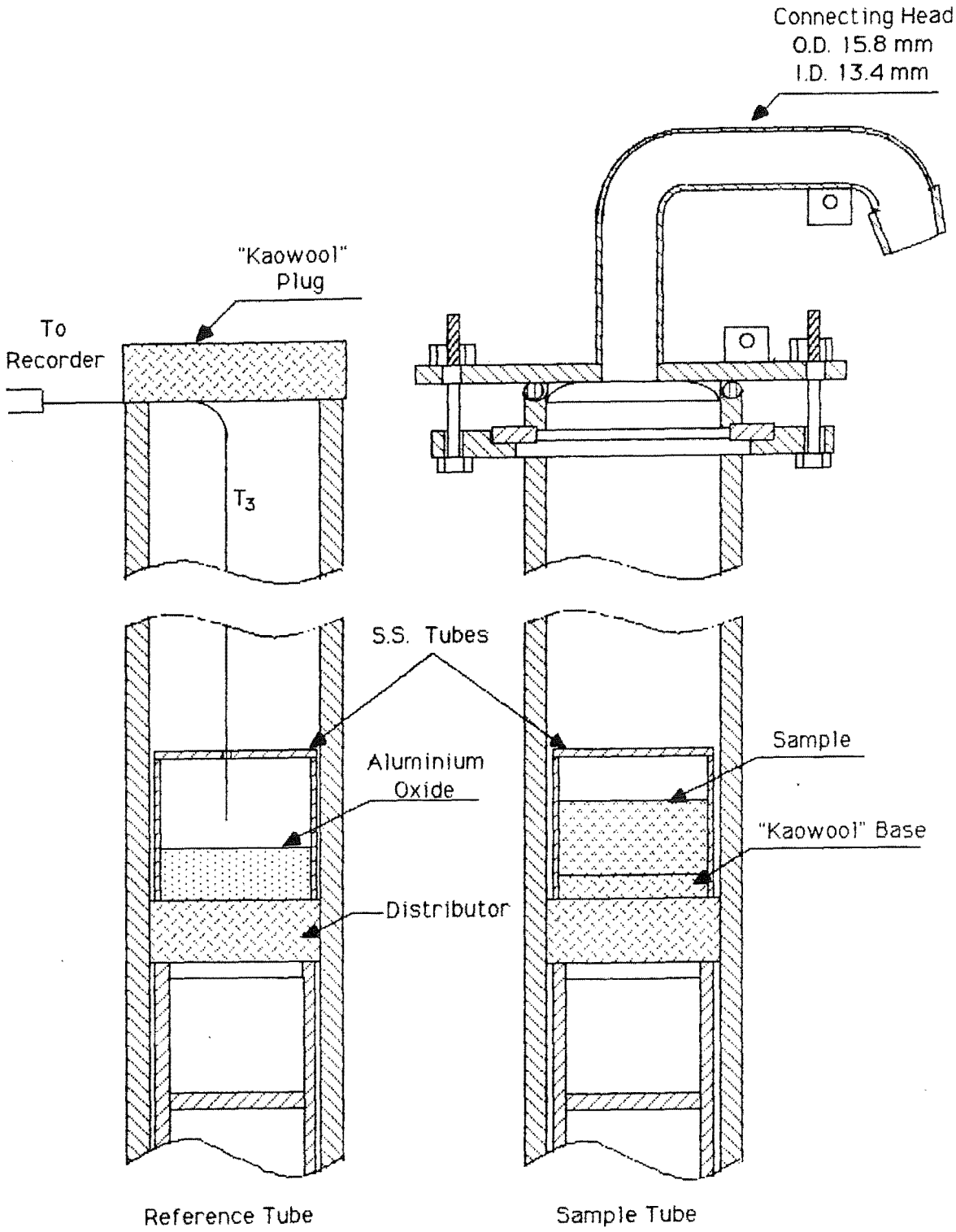

Figure 50. Experimental set-up for collection of pyrolysis products

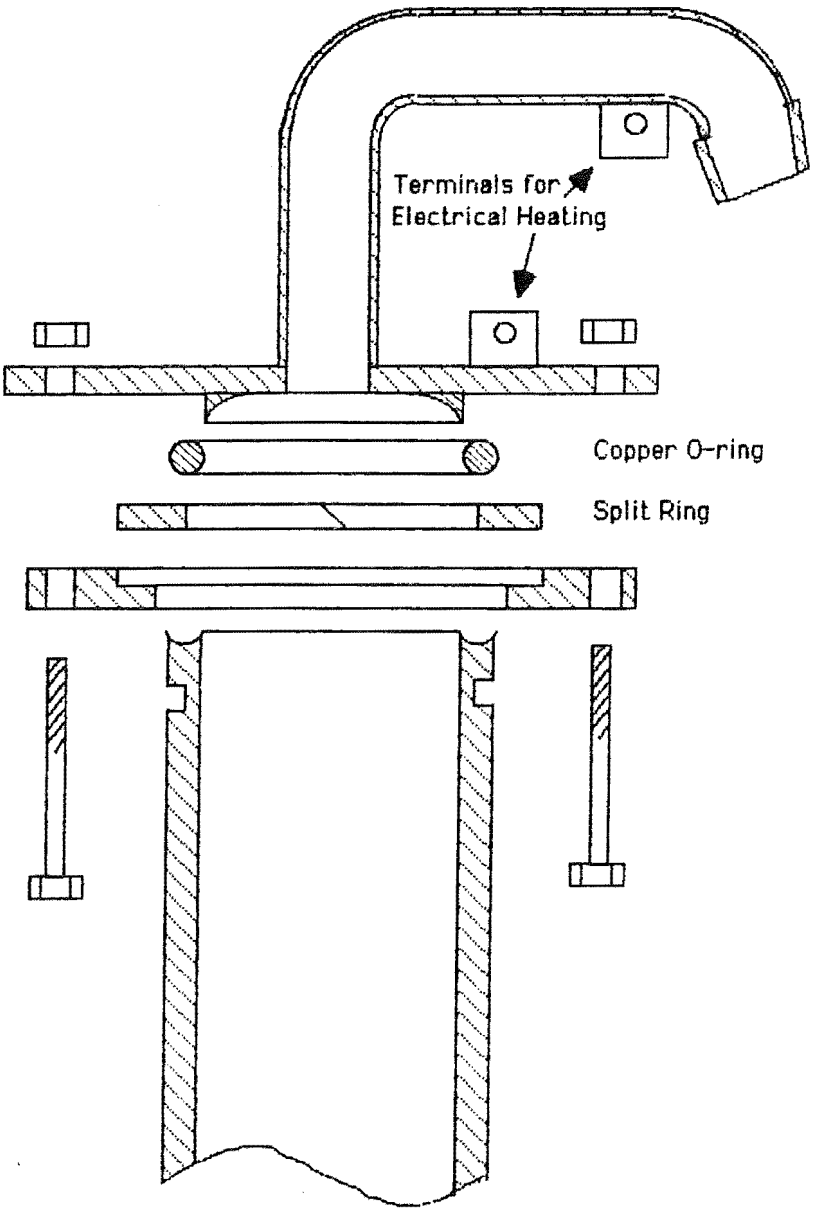

Details of connecting head

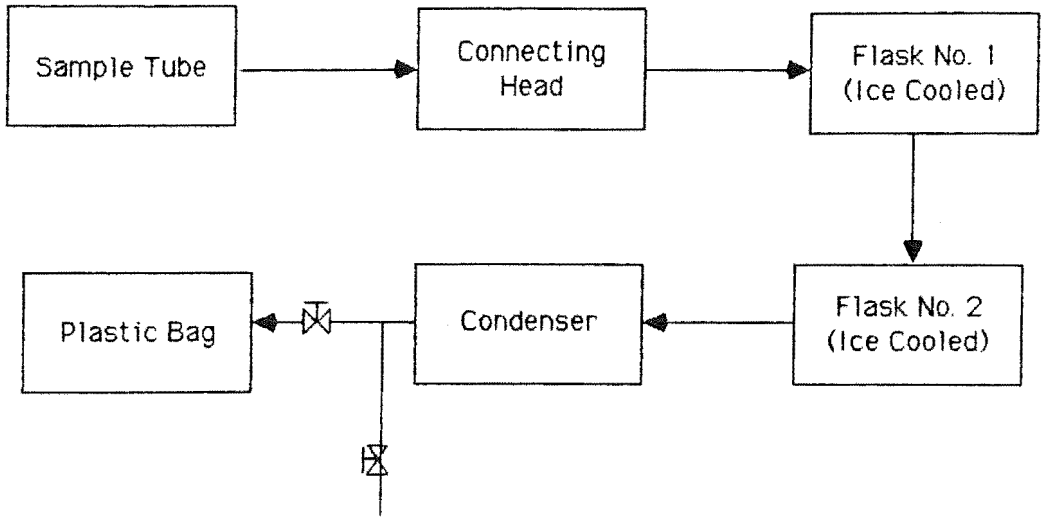

Figure 51. Block diagram of collecting device

5.2 Procedure

After the apparatus had been set up, nitrogen was passed through the reactor with a flowrate of 0.4 lit/min, which was only half of that used in the DTA runs. The reason for using a lower flowrate in these runs was two-fold. Firstly, with a gas flowrate of 0.8 lit/min, two polythene bags were required to collect the gases and the mixing of the contents of these two bags to give a uniform composition was quite a big problem. Secondly, using a lower gas flowrate resulted in the concentrations of the evolved gases in the gas stream being higher, making their detections easier. The reactor was heated at the usual rate, i.e. 5.5^{o}C/min. A chromel/alumel thermocouple was placed in the reference bed to measure its temperature which was continuously recorded on a chart recorder. The condensable volatiles were collected in the two flasks and the gases in the polythene bag. Collection of the gases started only after the reference bed temperature had reached 100^{o}C. The experiment was terminated at around 550^{o}C, after which the two flasks were removed and stoppered and the valve leading to the gas bag closed. Following this, the connecting head was disconnected and the reactor lifted up for

fan cooling. A piece of ceramic fibre was stuffed into the mouth of the sample tube to prevent air from entering into it and oxidising the residual char. In one of the runs, the experiment was allowed to continue until the reference bed temperature reached 635°C before it was stopped.

After the reactor had cooled down, the sample holder was taken out of the sample tube and its contents, i.e. the residual char, emptied out and weighed. The weight of the liquid fraction in each flask was obtained from the difference in weights of the flask with and without its contents. Determination of the amount of gases produced involved two steps, viz (1) measurement of the volume of all the gases in the polythene bag and (2) analysis of the gases. The volume of the gases in the polythene bag was determined by passing them through a gas meter with the help of a water pump. While the gases were being sucked out of the bag, samples were obtained for analysis using a gas chromatograph (Shimadzu GC-R1A) equipped with a processor (Shimadzu RPR-G1). The method by which a gas sample was obtained consisted in piercing the rubber hose connecting the polythene bag and the gas meter with the needle of a gas syringe and siphoning a portion out. CO_2, CH_4 and H_2 were analysed using a Porapak Q column of length 2 m while a molecular sieve column (10% 5A and 90% 13X) of length 6 m was employed for the analysis of CO and N_2.

5.3 Yields of Pyrolysis Products

A breakdown of the yields of the different pyrolysis products in each run is given in Table 3. It will be seen that there was very little variation in the yield of each product between the runs. The biggest component was the liquid fraction, whose yield amounted to slightly over half the weight of the sample. The yield of the gases was the lowest of the three products, making up only around 15% by weight of the sample. In each run, between 5% and 8% of the

Table 3. Yields of Pyrolysis Products

Run No.	Particle size	Sample size, gm	% by weight			Total
			Char	Liquid	Gases	
1	-18+36 mesh	5.4	25.49	53.40	14.68	93.57
2*	-18+36 mesh	5.5	24.62	53.89	14.38	92.89
3	-10+18 mesh	5.4	25.27	52.11	15.01	92.39
4	19 mm diam.	8.3	25.86	52.21	17.25	95.32

* Experiment stopped at 635 °C instead of 550 °C

sample's weight was unaccounted for, presumably lost to the surroundings or remained uncondensed in the case of the volatiles. Assuming that the loss of each product was proportional to its yield, the revised yields of the various products on the basis of 100% recovery are as follows : liquid fraction 57%, char 27% and gases 16%.

The evolved gases consisted mainly of CO_2, CO and CH_4 (Table 4). Their individual yields were fairly constant in all the runs - around 10% for CO_2, 4% for CO and 1% for CH_4, on a weight basis. The amount of CO produced in Run No.4 was about 25% higher than those produced in the other three runs, indicating that particle size of the sample might have an influence on its pyrolysis. H_2 was detected only towards the end of each run, but even then its yield was negligible compared with those of the other three gases. The retention times of the various gases in each column are shown in Figure 52 and Figure 53.

Table 4. Breakdown of Yields of Pyrolysis Gases

Run No.	% by weight			Total
	CO_2	CO	CH_4	
1	10.19	3.60	0.89	14.68
2	9.73	3.56	1.09	14.38
3	10.56	3.58	0.88	15.01
4	11.56	4.77	0.93	17.25

With the aim of finding out when are the pyrolysis gases formed, two additional runs were carried out in which gas samples were constantly drawn from the gas stream for analysis. The wood samples used in these runs were : (1) -10+18 mesh particles of weight 5.5 gm (Run No.5) and (2) 19 mm diameter pieces of weight 9.3 gm (Run No.6). The same gas flowrate was used here as in the earlier runs, i.e. 0.4 lit/min. The gas samples for analysis were obtained from the rubber hose connecting the condenser and the polythene bag. Analysis of CO_2 and CH_4 was carried out during the run, at about 5-minute intervals, while that of CO was performed after the run had ended from samples collected in gas sampling tubes. The reason for not doing CO analysis during the run was because of its long retention time - around 30 minutes. Results of the analyses are plotted in Figure 54 (for Run No.5) and Figure 55 (for Run No.6). In both the runs, CO_2 began to be released at about 170°C. Its concentration increased with increasing temperature, reaching a peak between 350°C and 370°C. It then dropped rather sharply and began to tail off at about 400°C. CO followed a similar pattern as CO_2, except that its concentration in the gas stream was lower. The evolution of methane followed a slightly different pattern. It did not make its presence felt until about 320°C.

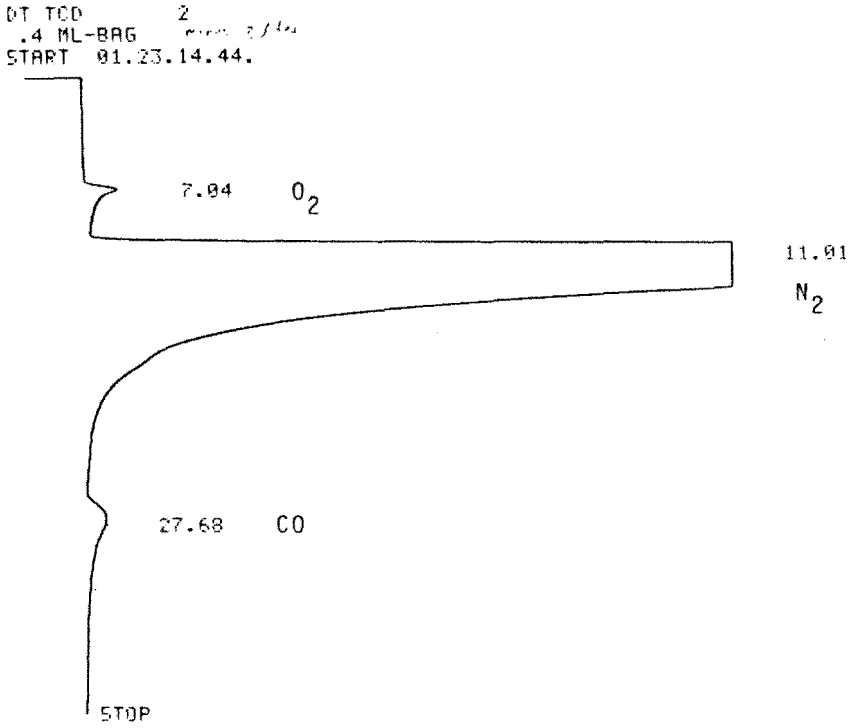

GC-R1A
SMPL # 00
FILE # 8
REPT # 1347
METHOD 41

#	NAME	TIME	CONC	MK	AREA
0		7.04	0.4144		8552
0		11.01	98.6818		2036237
0		27.68	0.9036		18646
	TOTAL		99.9999		2063435

Figure 53. Chromatogram resulting from gas analysis using molecular sieve column

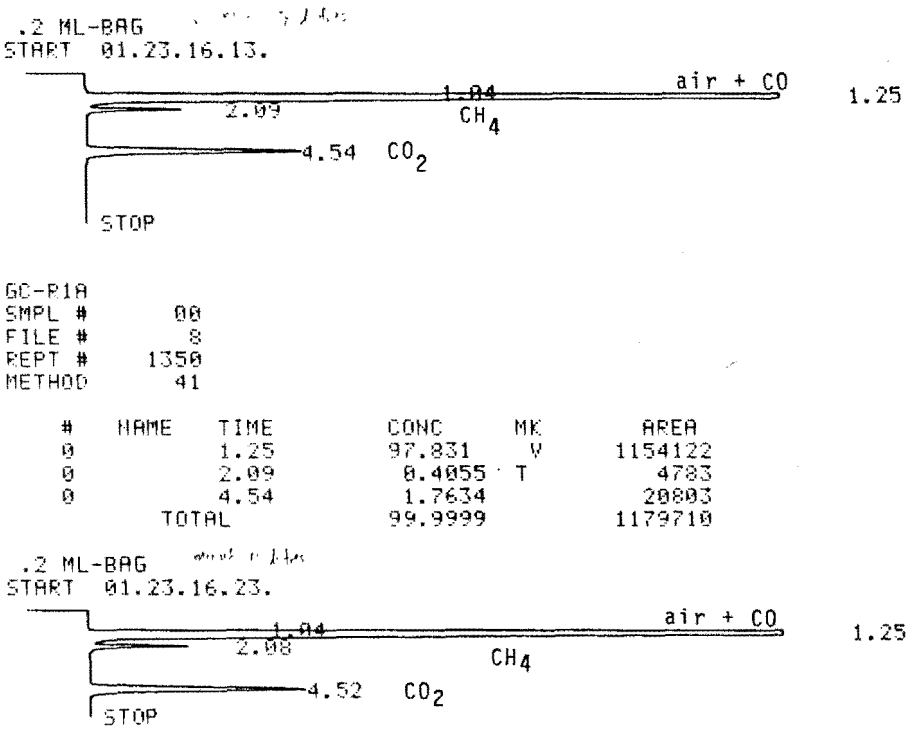

GC-R1A
SMPL # 00
FILE # 8
REPT # 1350
METHOD 41

#	NAME	TIME	CONC	MK	AREA
0		1.25	97.831	V	1154122
0		2.09	0.4055	T	4783
0		4.54	1.7634		20803
	TOTAL		99.9999		1179710

GC-R1A
SMPL # 00
FILE # 8
REPT # 1351
METHOD 41

#	NAME	TIME	CONC	MK	AREA
0		1.25	97.8542	V	1166686
0		2.08	0.4078	T	4862
0		4.52	1.7379		20721
	TOTAL		100.		1192270

Figure 52. Chromatogram resulting from gas analysis using Porapak Q column

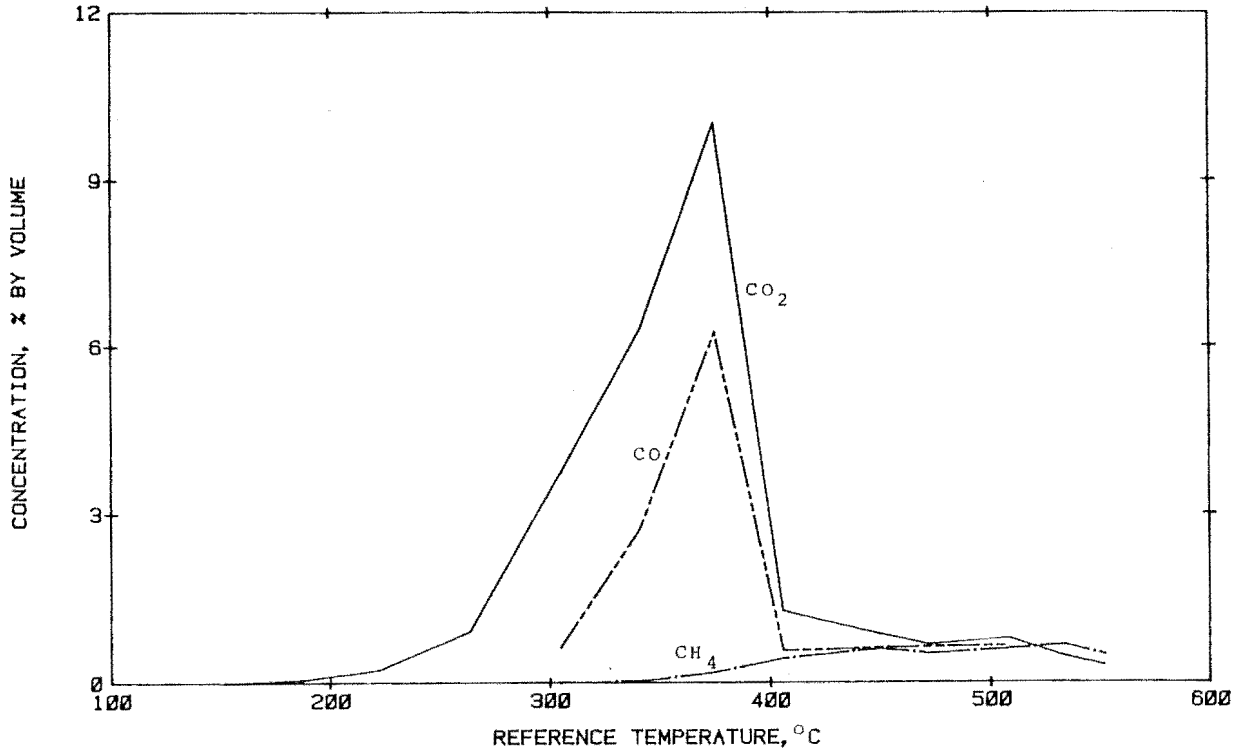

Figure 54. Concentration profiles of pyrolysis gases (Run No.5: -10+18 mesh particles)

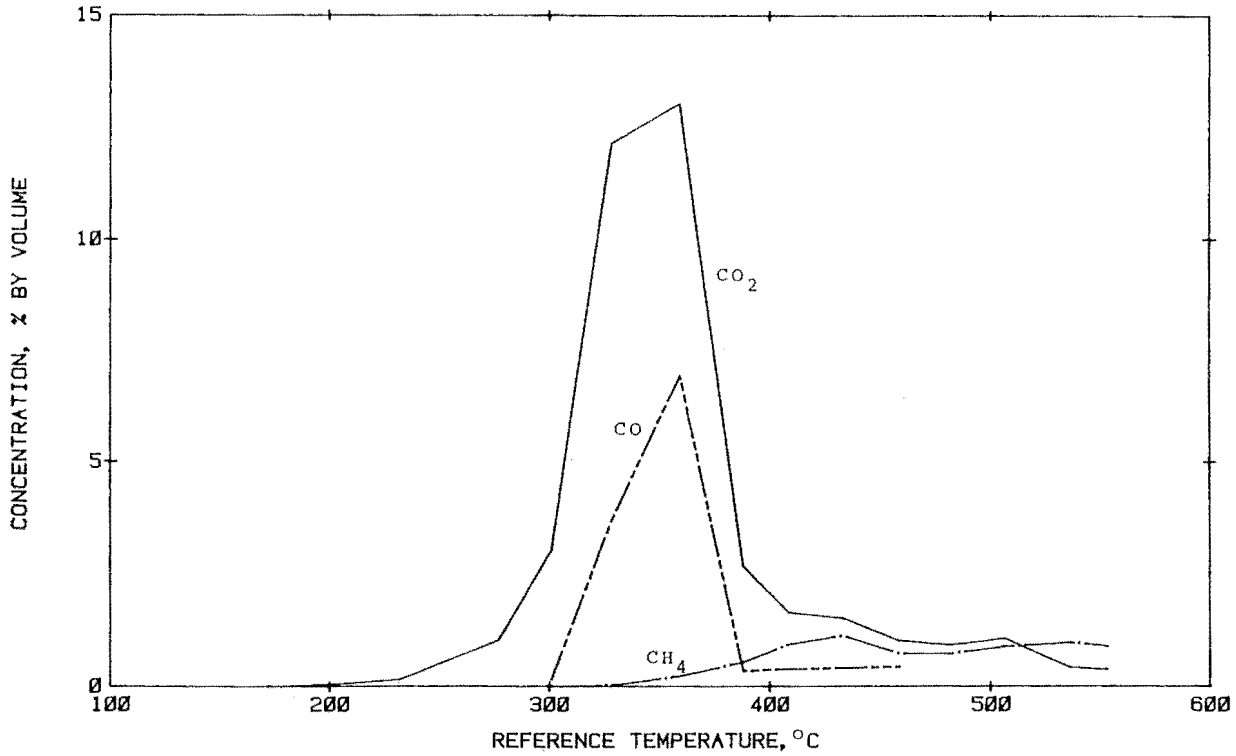

Figure 55. Concentration profiles of pyrolysis gases (Run No.6: 19 mm diam. pcs.)

Its concentration increased steadily and reached a peak at about 430°C. It then dropped gradually and began to level off at around 470°C. From around 520°C, the yield of CH_4 exceeded that of CO_2, on a volume basis. Most of the CH_4 is believed to be formed from the thermal degradation of lignin as this is the most stable of the wood components. This has been found to be the case in Spruce wood (Wenzl, 1970).

Another four runs were conducted, aimed at determining the temperature range within which most of the volatiles are liberated. In each of these runs, the reference bed temperatures corresponding to the collection of the first and the last drop of liquid in the first flask were noted. As shown in Table 5, the bulk of the volatiles are formed between 280°C and 400°C. This coincides with the temperature range within which most of the CO_2 and CO are liberated. It seems clear that the most 'active' part in the pyrolysis of Rubber wood lies between 280°C and 400°C. This is consistent with the findings from visual observation of the test sample in one of the DTA runs (see Section 4.1). It was noticed that the liquid fraction was light brown in colour and free-flowing initially but became darker and more viscous as the experiment progressed, indicating that the lighter fractions were formed first.

Table 5. Collection of Liquid Fraction

Run No.	Particle size	Sample size, gm	Temperature, °C	
			First drop collected	Last drop collected
7	-72+150 mesh	6.1	278	393
8	-36+72 mesh	6.3	293	403
9	-10+18 mesh	5.6	287	393
10	19 mm diam.	7.3	281	404

5.4 Examination of Liquid Fraction

The liquid fractions from six of the above runs were analysed qualitatively using NMR spectroscopy. Three of the fractions were examined using a Varian T-60 proton NMR spectrometer (at the Chemistry Department of the University) and the remaining three using a Varian FT-80A ^{13}C NMR spectrometer (at the Department of Scientific and Industrial Research, Lower Hutt). The fractions examined by the first instrument were obtained from Runs No.1, 4 and 7. The resultant spectra are shown in Figures 56-58. Only the signals of the lighter components appeared on each spectrum, among which were water (δ=5.2 ppm), acetic acid (δ=2.0 ppm), methanol (δ=3.3 ppm) and a few unidentified compounds. The liquid fractions examined by the second instrument were derived from Runs 2, 8 and 10. Each of the resultant spectra (Figures 59-61) contained numerous signals. The ones at δ=20.8 ppm and 176.4 ppm are attributed to acetic acid while that at δ=49.5 ppm to methanol. The strong signal at δ=56.4 ppm is believed to be due to the methoxyl groups on phenolic structures while their corresponding aromatic ring carbons are responsible for the band of signals between δ=105 ppm and δ=160 ppm. Signals within the range δ=20-40 ppm are characteristic of saturated hydrocarbon structures while those between δ=60-80 ppm are characteristic of carbohydrate-like structures. Water did not feature in the spectrum because it does not contain carbon. The signals which are attributed to the saturated-hydrocarbon structures appear to be slightly weaker in the spectrum of the liquid fraction obtained from the 19 mm diameter pieces than in those of the fractions obtained from the other two samples, again indicating that particle size of the wood has an effect on its pyrolysis. Other than that, there was very little difference between these three spectra.

According to Wenzl (1970), the heavier components of the pyrolysis liquid consist mainly of phenolic compounds,

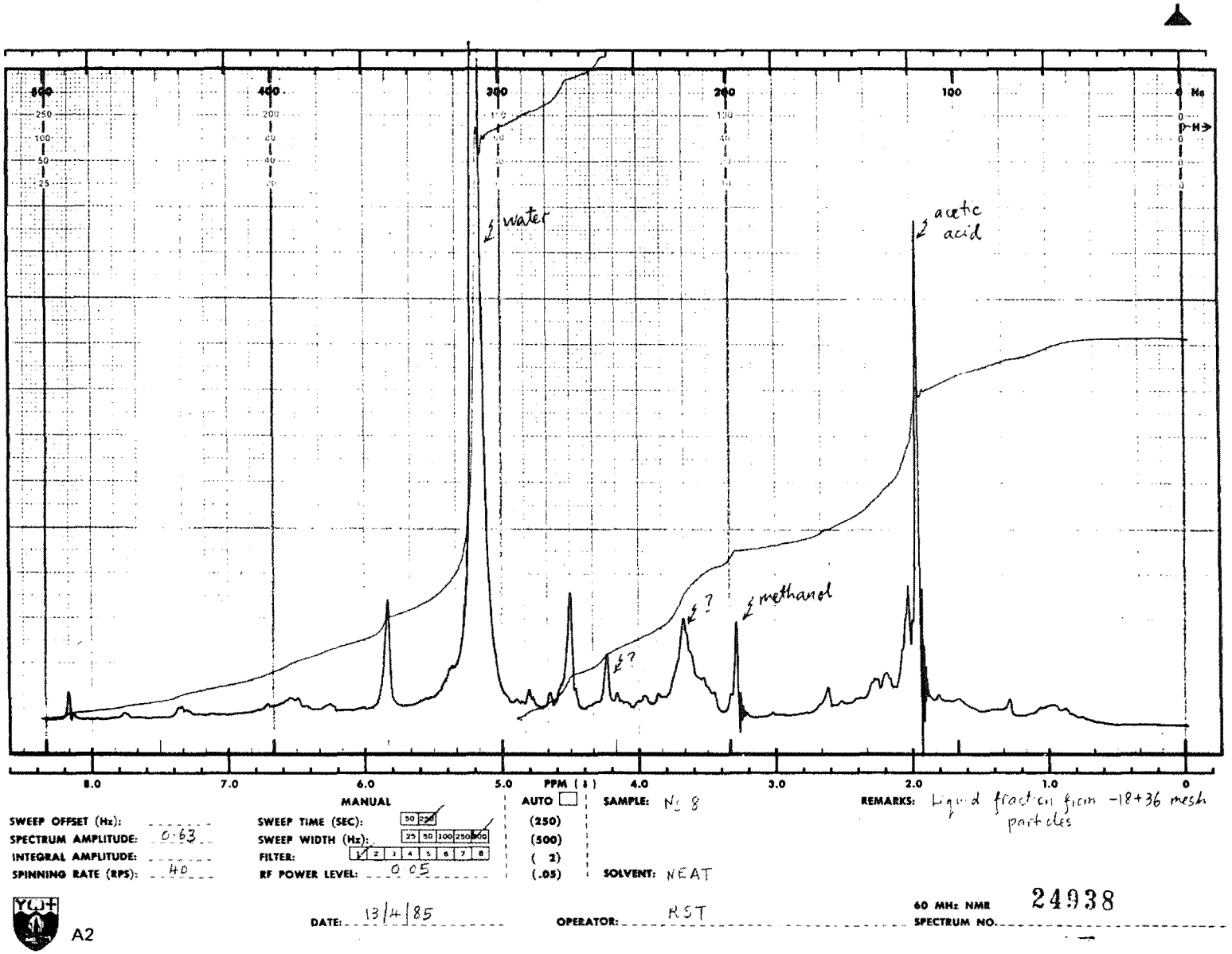

Figure 56. Proton NMR spectrum of liquid fraction from Run No.1 (-18+36 mesh particles)

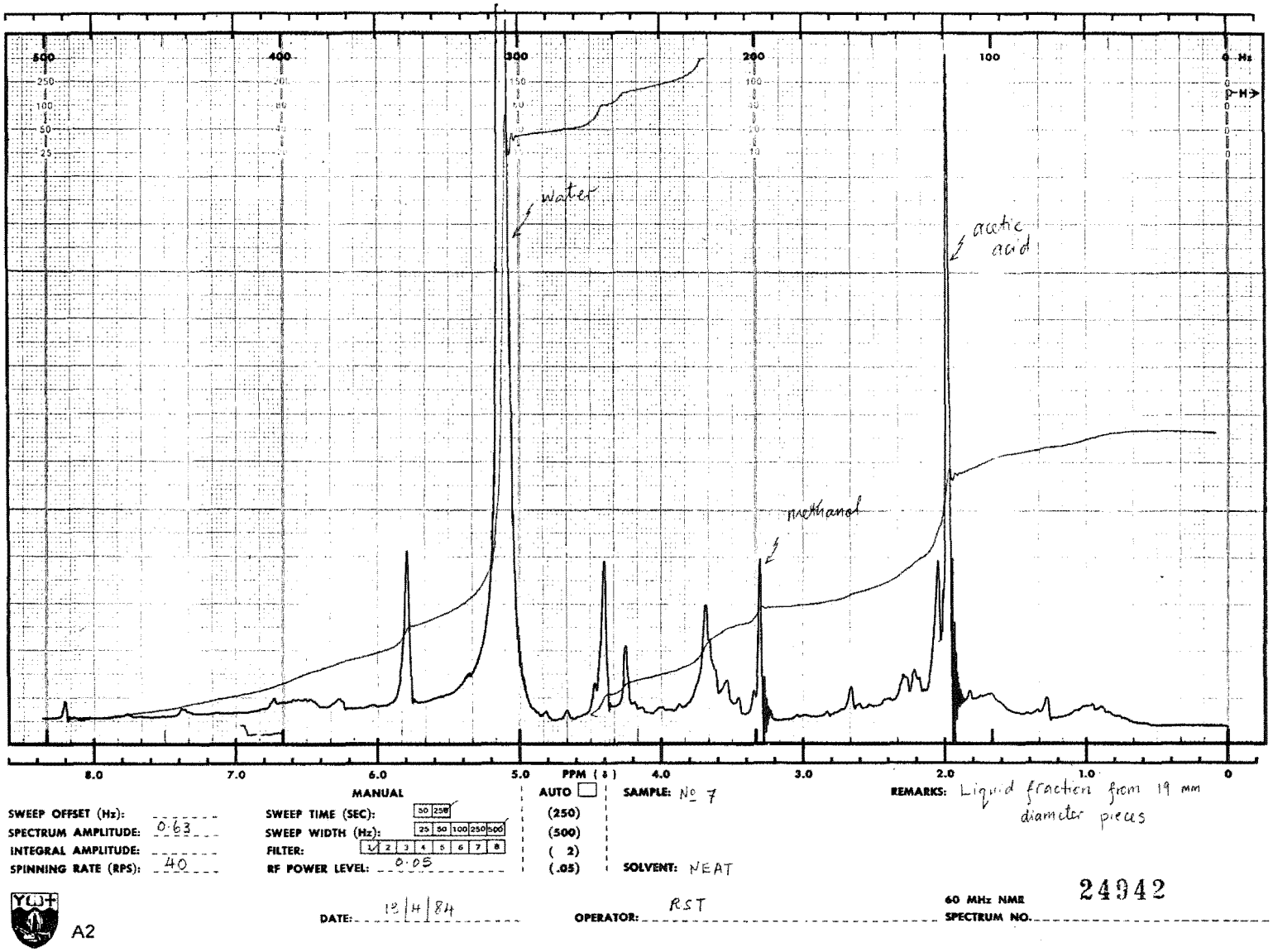

Figure 57. Proton NMR spectrum of liquid fraction from Run No.4 (19 mm diam. pcs.)

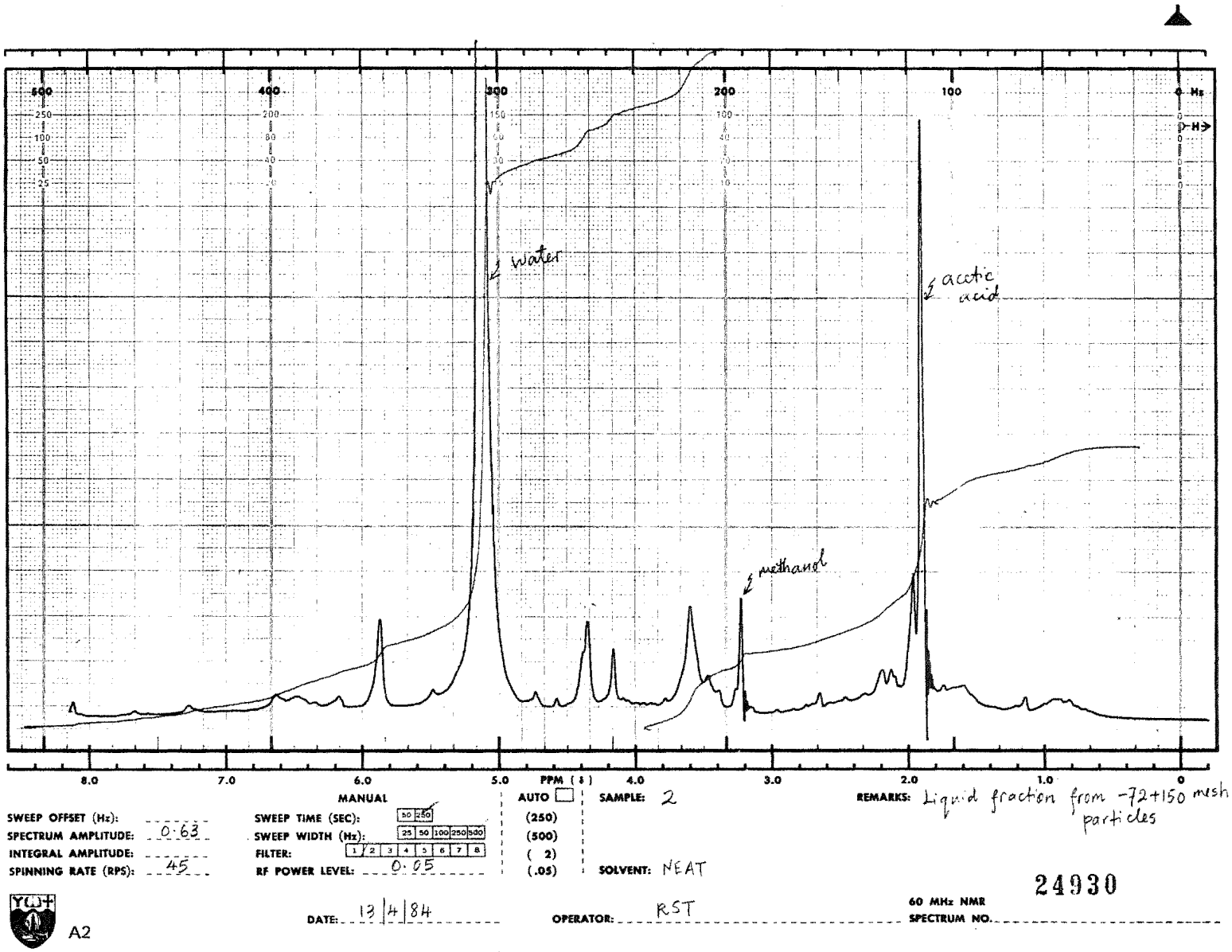

Figure 58. Proton NMR spectrum of liquid fraction from Run No.7 (-72+150 mesh particles)

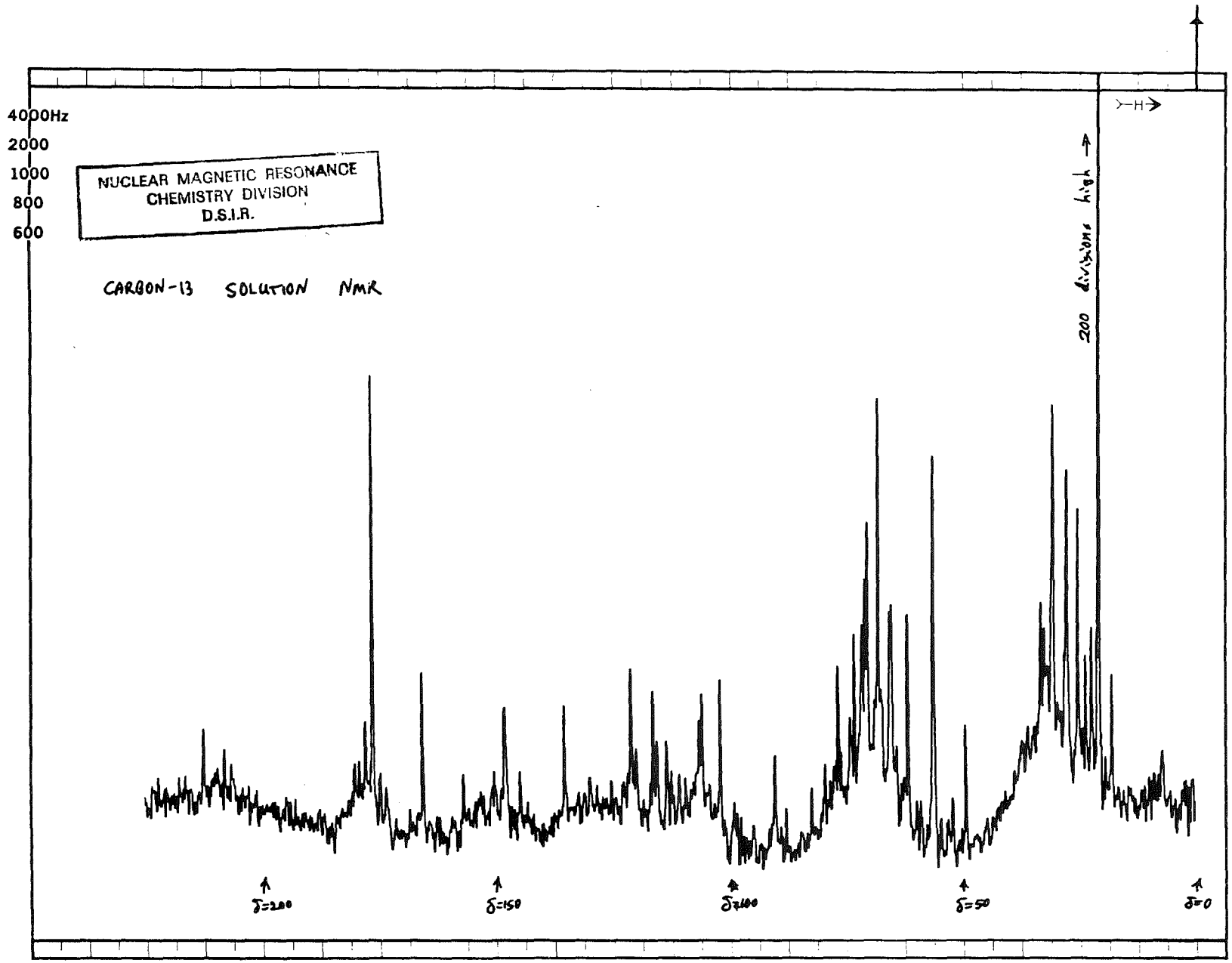

FT-80A SPECTRUM NO. 6422
OPERATOR RDR DATE 27/6/84
NUCLEUS ^{13}C FREQUENCY 20 MHz
SYNTHESIZER SETTING —
EXPERIMENT NAME 10 MM
FILE NAME RHN6422
SAMPLE

PYROLYSIS TAR #5
1.2 cm³
(+D_2O, 0.3 cm³)

LOCK ☑ INTERNAL ☐ EXTERNAL
LOCK SIGNAL D_2O
SPIN RATE ~20 rps. TEMP. 30 °C
INSERT C-13, 10 mm

ACQUISITION
SPECTRAL WIDTH (SW) 5000 Hz
NO. OF TRANSIENTS (NT) 21355
ACQUISITION TIME (AT) 0.2 sec.
PULSE WIDTH (PW) 7 μsec.
PULSE DELAY (PD) — sec.
DATA POINTS (DP) 2048

TRANSMITTER OFFSET (TO) 69
HIGH FIELD ✓ LOW FIELD —
RECEIVER GAIN (RG) 8

DECOUPLER MODE (DM) 1
DECOUPLER OFFSET (DO) 53
NOISE BANDWIDTH (NB) −2 kHz
ACQUISITION MODE (AM) —

DISPLAY
SENS. ENHANCEMENT (SE) −0.2 sec.
WIDTH OF PLOT (WP) 4500 Hz
END OF PLOT (EP) 0 Hz
WIDTH OF CHART (WC) 5000 Hz
END OF CHART (EC) 0 Hz
VERTICAL SCALE (VS) 200
REFERENCE LINE (RL) −216 Hz

varian PRINTED IN U.S.A.

Figure 59. ^{13}C NMR spectrum of liquid fraction from Run No.2 (-18+36 mesh particles)

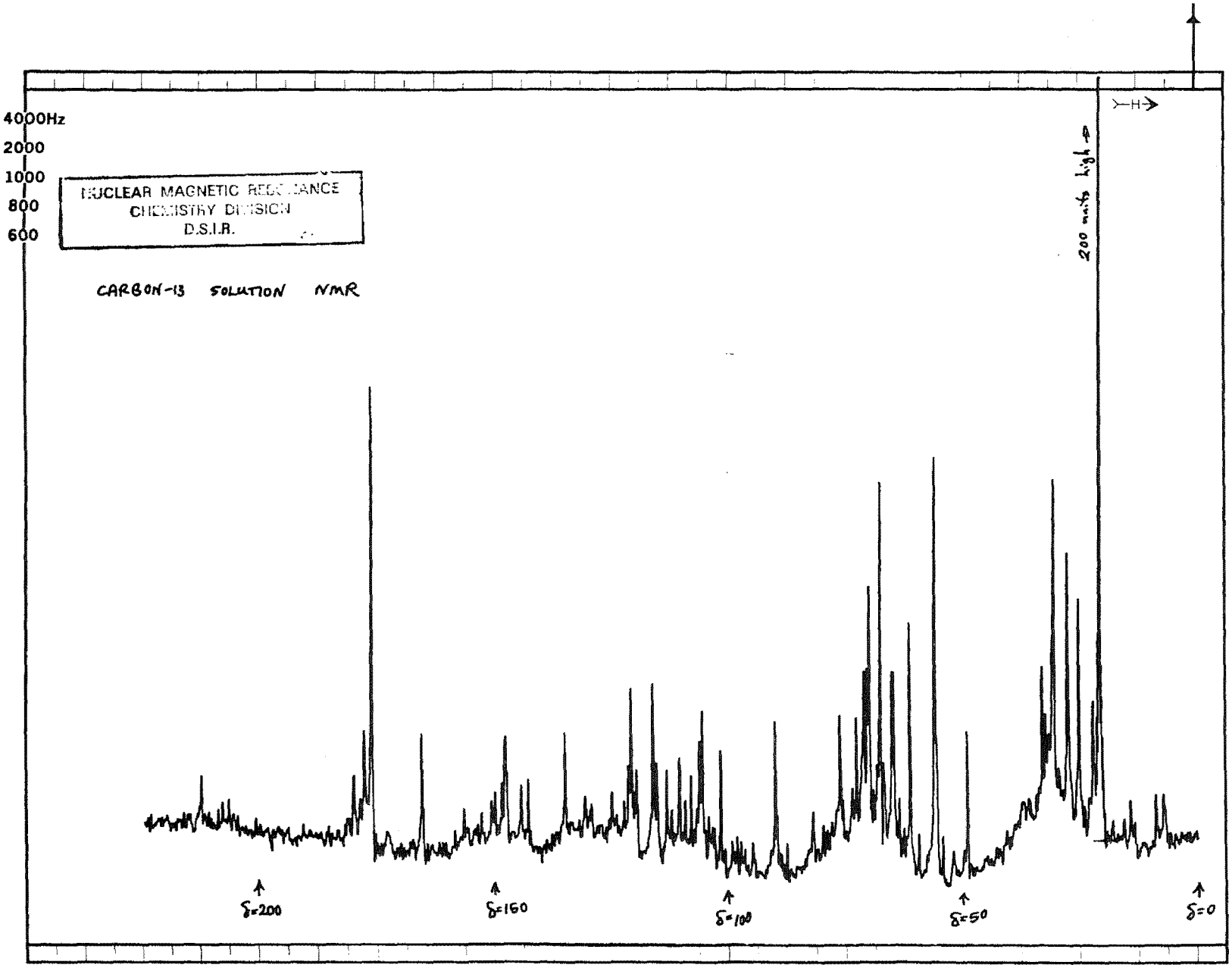

FT-80A SPECTRUM NO. 6280
OPERATOR RHN DATE 2/5/84
NUCLEUS ^{13}C FREQUENCY 20MHz
SYNTHESIZER SETTING —
EXPERIMENT NAME 10 mm
FILE NAME RHN6280
SAMPLE

Pyrolysis tar #3
1.2 cm³
+ D_2O, 0.3 cm³

LOCK ☑ INTERNAL ☐ EXTERNAL
LOCK SIGNAL D_2O
SPIN RATE ~20 rps. TEMP. 30 °C
INSERT c-13, 10 mm

ACQUISITION
SPECTRAL WIDTH (SW) 5000 Hz
NO. OF TRANSIENTS (NT) 24960
ACQUISITION TIME (AT) 0.2 sec.
PULSE WIDTH (PW) 7 μsec.
PULSE DELAY (PD) — sec.
DATA POINTS (DP) 2048

TRANSMITTER OFFSET (TO) 49
HIGH FIELD ✓ LOW FIELD —
RECEIVER GAIN (RG) 8

DECOUPLER MODE (DM) 1
DECOUPLER OFFSET (DO) 53
NOISE BANDWIDTH (NB) -2 kHz
ACQUISITION MODE (AM) —

DISPLAY
SENS. ENHANCEMENT (SE) 0.2 sec.
WIDTH OF PLOT (WP) 6500 Hz
END OF PLOT (EP) 0 Hz
WIDTH OF CHART (WC) 5000 Hz
END OF CHART (EC) 0 Hz
VERTICAL SCALE (VS) 200
REFERENCE LINE (RL) ~214 Hz

varian PRINTED IN U.S.A.

Figure 60. ^{13}C NMR spectrum of liquid fraction from Run No.8 (-36+72 mesh particles)

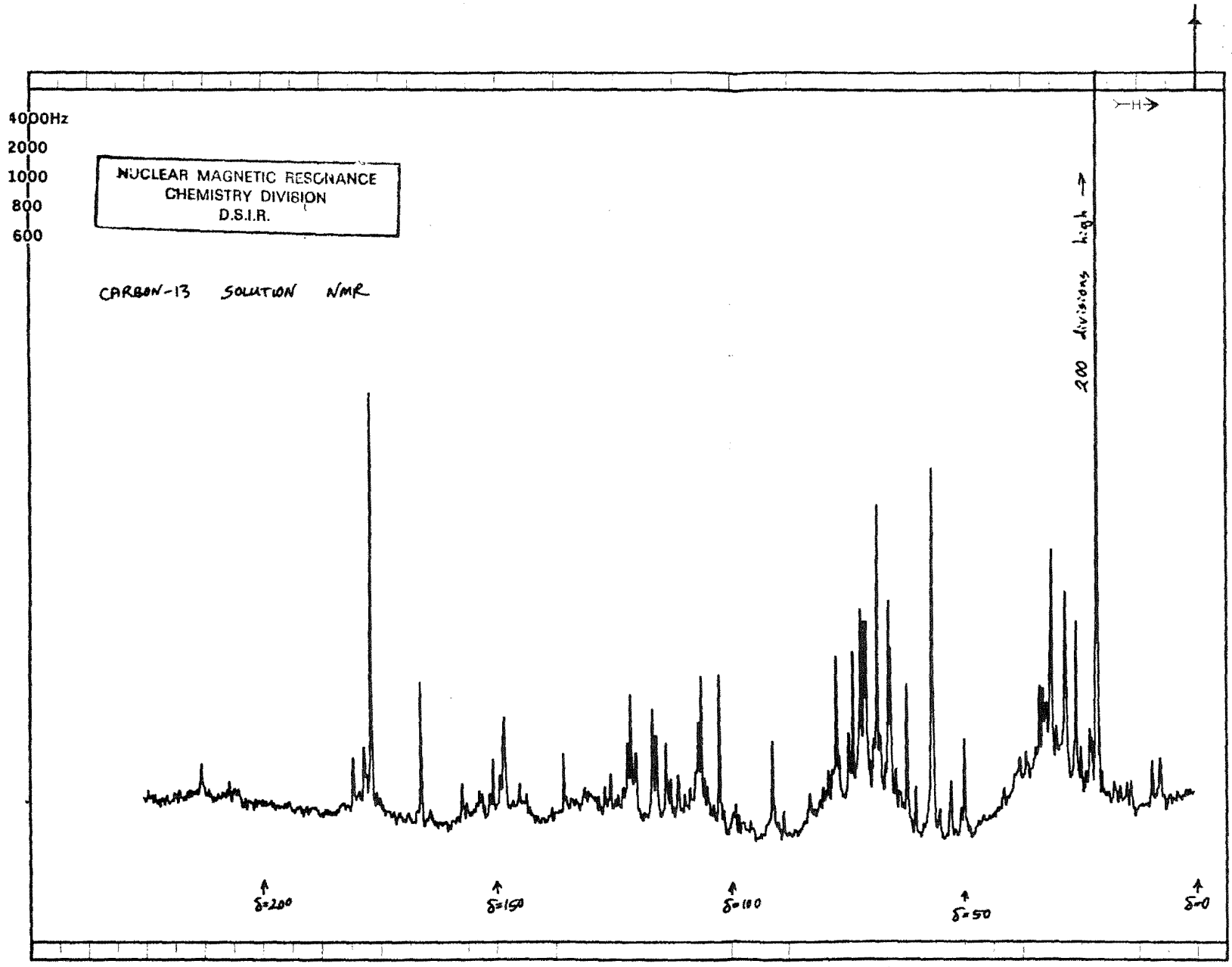

FT-80A SPECTRUM NO. 6421
OPERATOR RKR DATE 27/6/84
NUCLEUS ^{13}C FREQUENCY 20MHz
SYNTHESIZER SETTING —
EXPERIMENT NAME 10 MM
FILE NAME RHN6421
SAMPLE

PYROLYSIS TAR #6
1.2 cm³
+ D_2O, 0.3 cm³

LOCK ☑ INTERNAL ☐ EXTERNAL
LOCK SIGNAL D_2O
SPIN RATE ~20 rps. TEMP 30 °C
INSERT C-13, 10 mm

ACQUISITION
SPECTRAL WIDTH (SW) 5000 Hz
NO. OF TRANSIENTS (NT) 54652
ACQUISITION TIME (AT) 0.2 sec.
PULSE WIDTH (PW) 7 μsec.
PULSE DELAY (PD) — sec.
DATA POINTS (DP) 2048

TRANSMITTER OFFSET (TO) 49
HIGH FIELD ✓ LOW FIELD —
RECEIVER GAIN (RG) 8

DECOUPLER MODE (DM) 1
DECOUPLER OFFSET (DO) 53
NOISE BANDWIDTH (NB) ~2 kHz
ACQUISITION MODE (AM) —

DISPLAY
SENS. ENHANCEMENT (SE) -0.2 sec.
WIDTH OF PLOT (WP) 4500 Hz
END OF PLOT (EP) 0 Hz
WIDTH OF CHART (WC) 5000 Hz
END OF CHART (EC) 0 Hz
VERTICAL SCALE (VS) 200
REFERENCE LINE (RL) -216 Hz

varian PRINTED IN U.S.A.

Figure 61. ^{13}C NMR spectrum of liquid fraction from Run No.10 (19 mm diam. pcs.)

including guaiacols and cresols. They are formed chiefly from the decomposition of lignin. The main source of acetic acid is the hemicelluloses in which most of the acetyl groups are attached, although it is also formed from the pyrolysis of cellulose and lignin. Methanol is formed mainly from the pyrolysis of lignin which has a higher methoxyl content compared with the other components. A list of the pyrolysis products from cellulose and also xylan had been provided by Shafizadeh and DeGroot (1976).

Harris (1979) has studied the destructive distillation of Rubber wood in an iron retort and evaluated the products for a variety of applications. The yields of the products of interest from his experiments were as follows : charcoal 28%, acetic acid equivalent 5%, spirit (mainly methanol) 1.2% and tar 7%. About 25% of the tar collected consisted of phenols.

CHAPTER 6

DIFFERENTIAL THERMAL ANALYSIS IN AN OXIDATIVE ENVIRONMENT

In DTA runs in an oxidative environment, both the sample and the reference beds were fluidised. The inert material in each bed consisted of 30 gm of beach sand of particle size -85+100 mesh. A combined gas flowrate of 4 lit/min was used and this was chosen after trial runs showed it to be the most suitable. Details of the trial runs, including calculation of the minimum fluidising velocity, are given in Appendix 3.

6.1 Blank Runs

Blank runs were carried out to determine the temperature variation within a bed and also between the two beds as a function of temperature. If the variation is too great or erratic, it may lead to wrong conclusions being drawn in the experiments proper.

6.1.1 ΔT within Bed

Two runs were carried out in which both members of a differential thermocouple were placed in the reference bed while a temperature thermocouple was inserted into the sample bed, as illustrated in Figure 62. As a matter of fact, as the two beds contained only sand, it does not really matter in which bed was the differential thermocouple placed. The sensing tips of the differential thermocouple were placed 20 mm apart in one run and 30 mm apart in the other run. Air was used as the fluidising medium, with a flowrate of 4 lit/min. The reactor was heated at around 5.5^{o}C/min. As shown in the resultant DTA curves (Figure 63), which were recorded on the same scale as the actual runs in air, a slight temperature difference existed between the two thermocouple points in both the runs. The difference was less than 0.1^{o}C initially, but increased to around 1.5^{o}C at 550^{o}C, almost at a steady pace.

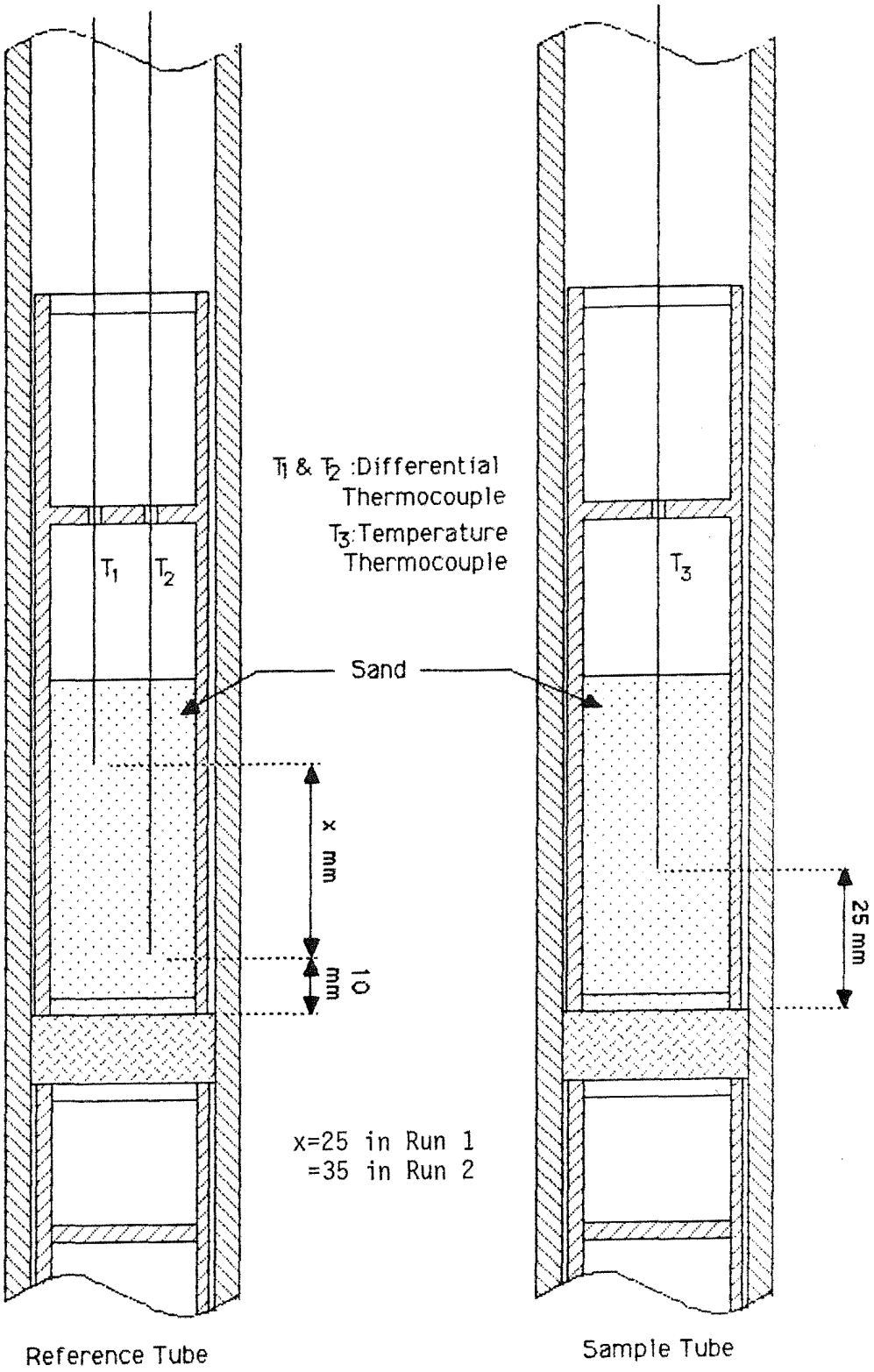

Figure 62. Experimental set-up for determining ΔT within a bed

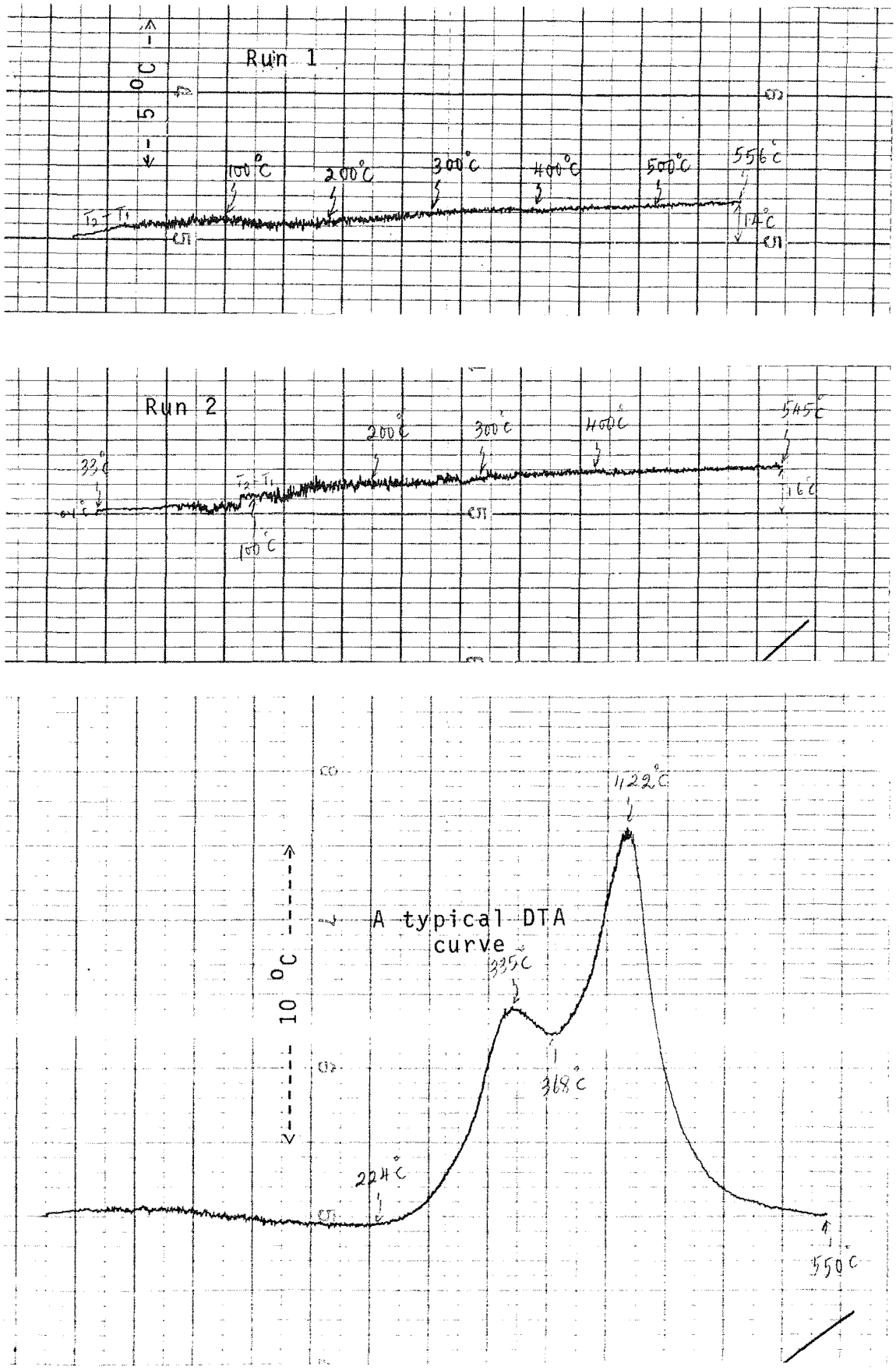

Figure 63. ΔT within a bed in comparison with the reaction peak heights

Even that, the difference is very small in comparison with the bed temperature. On the whole, the bed can be considered as having a uniform temperature which is characteristic of a fluidised-bed.

6.1.2 Δ T between Beds

The temperature variation between the two beds is more important as it can lead to wrong interpretation of the resultant curve. Blank runs were carried out from time to time to see if the variation was within the acceptable level. In these runs, one member of a differential thermocouple was placed in the sample bed while the other member as well as a temperature thermocouple were placed in the reference bed, as illustrated in Figure 64. The experimental conditions were the same as before. The DTA curves resulting from four of these runs are shown in Figure 65. In Run 1, there was almost no temperature variation between the two beds. In Run 2, there was an initial temperature difference of around $1^{o}C$ but this gradually disappeared as the experiment progressed. In Run 3, there was a slightly bigger temperature difference but as it remained almost constant throughout the run, it was not a problem. In Run 4, the temperature variation, although still small, was more erratic. When this happened, steps were taken to rectify the problem. Very often, it was overcome by putting in a new set of distributors.

In conclusion, the temperature variations within a bed and also between the two beds were rather small and did not pose a serious problem to the experiments being undertaken.

6.2 Experimental Procedure

The experimental set-up is shown in Figure 66. Unless otherwise stated, a sample size of 1-gm was used. All the test samples were oven-dried at $105^{o}C$ for 16-24 hours before use. The chosen fluidising gas was passed through the two

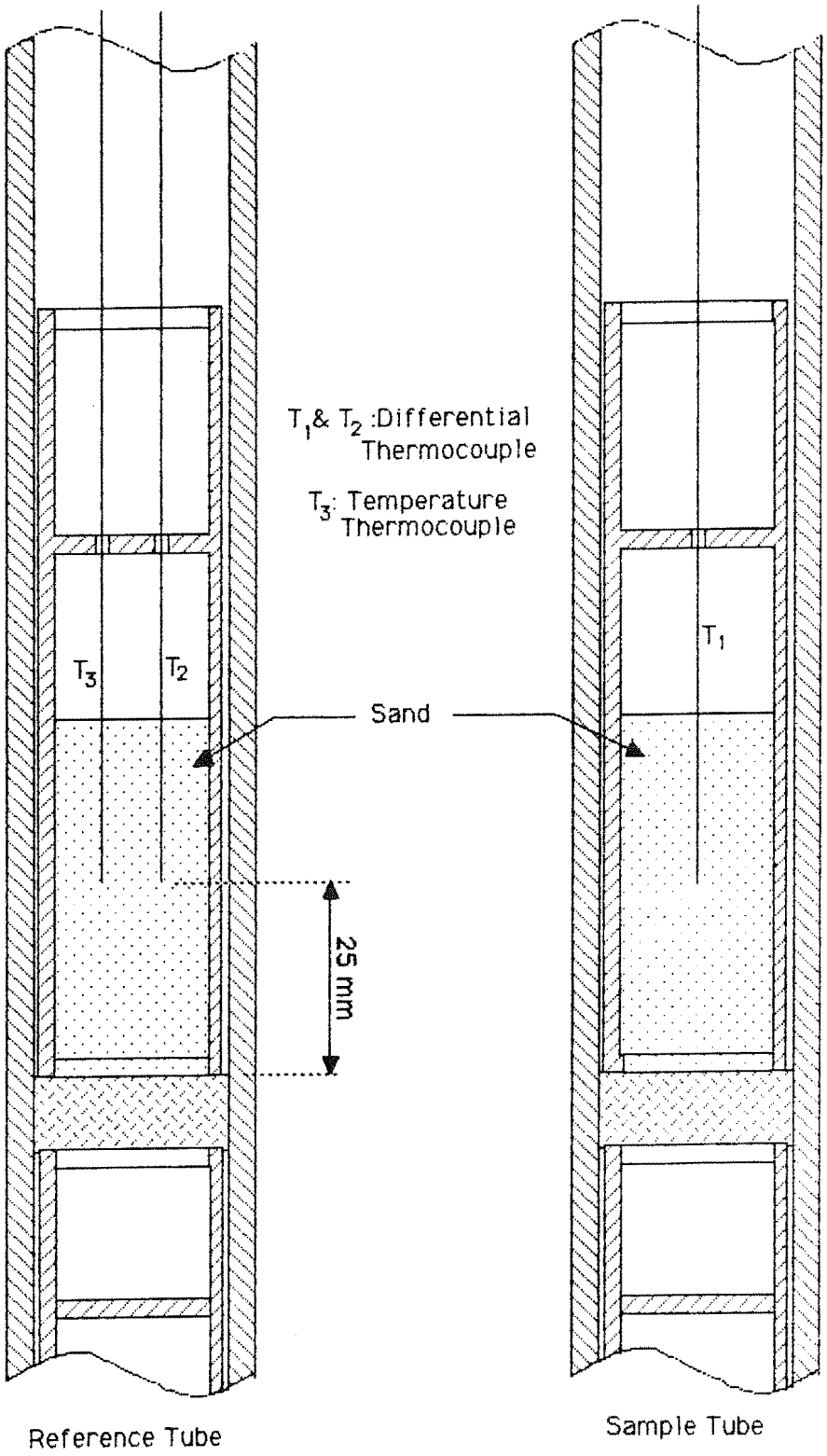

Figure 64. Experimental set-up for determining ΔT between beds

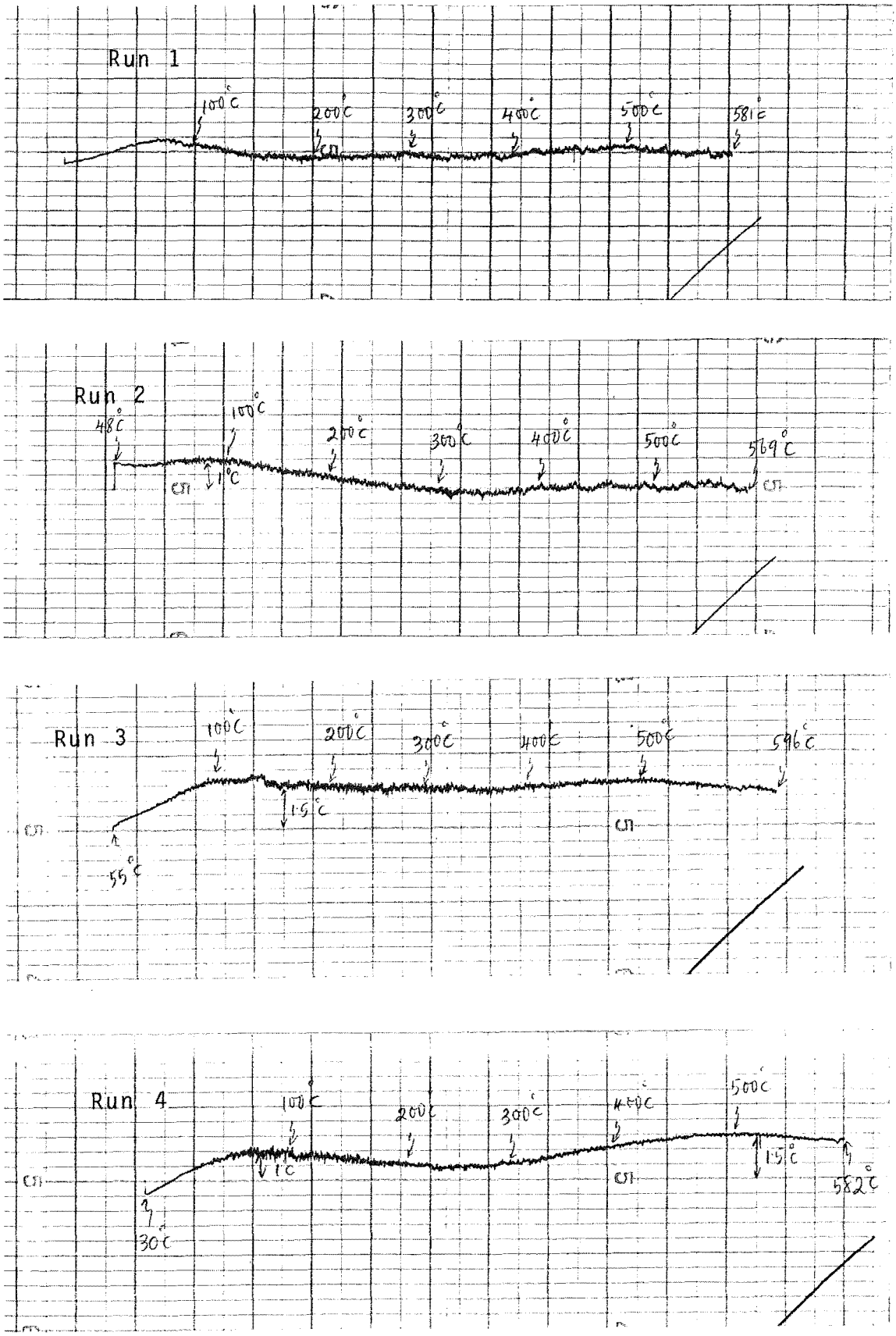

Figure 65. ΔT between beds

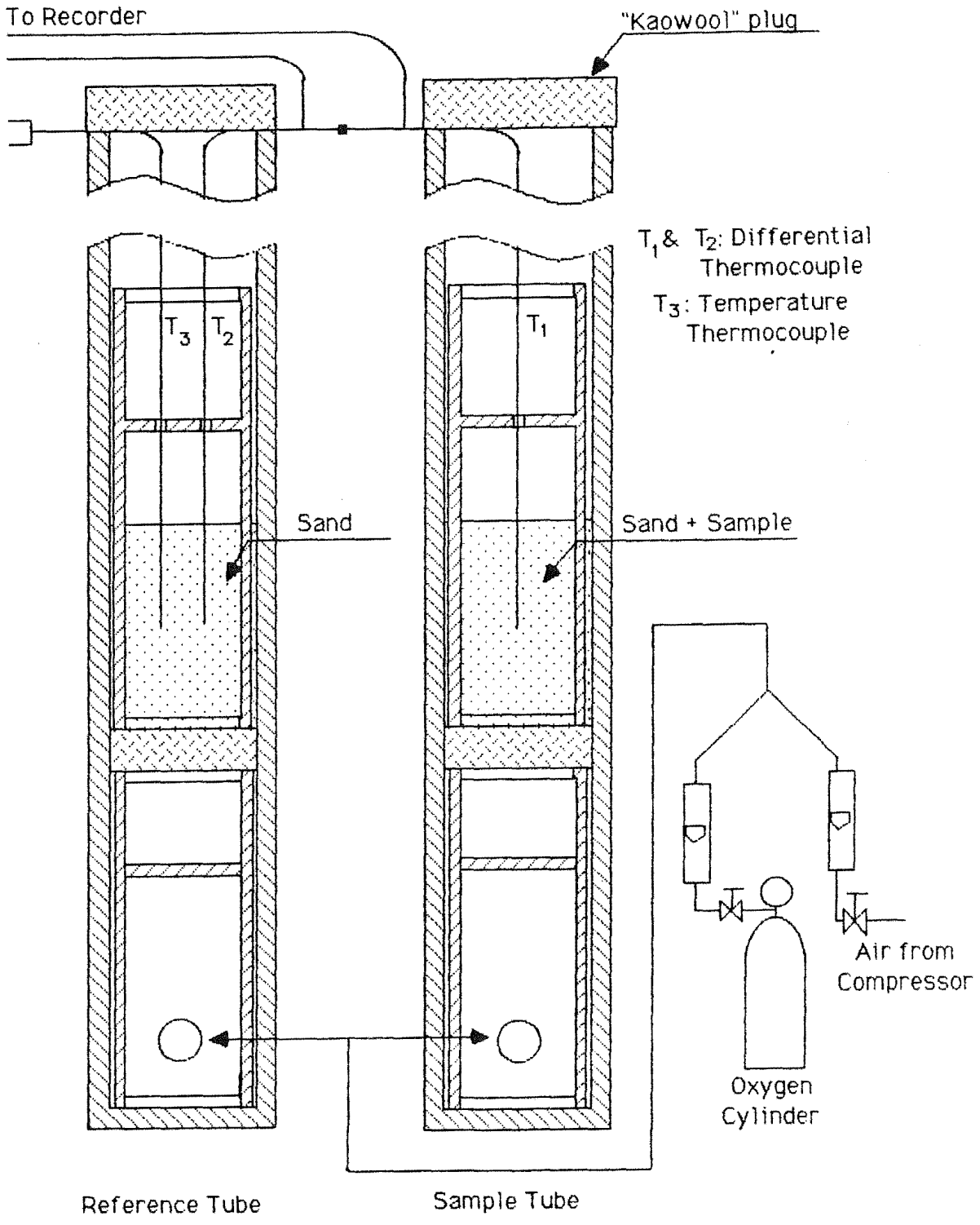

Figure 66. Experimental set-up for DTA in an oxidative environment

tubes with a combined flowrate of 4 lit/min. The desired oxygen concentration of the fluidising gas was obtained by blending oxygen from a cylinder and air from a compressor at the appropriate ratios. The reactor was heated at the usual rate, i.e. around 5.5°C/min. When there was no more sample left in the sample bed and the differential temperature curve had returned to the base line, the experiment was stopped and the reactor lifted up for fan cooling. In each run, visual observation of the sample was made regularly to see if there was flaming or glowing combustion which, if occurred, was clearly visible. This will be elaborated in the individual sections.

The sand in each bed was replaced by a new sample before the start of a new run.

6.3 Individual Wood Components

6.3.1 Cellulose

The DTA curve of cellulose in air, i.e. from the run in which air was used as the fluidising medium, is shown in Figure 67. Curve (a) is the differential temperature curve while Curve (b) is the reference temperature curve. Both were recorded as a function of time. Curve (a) contained two exothermic peaks with reasonably good resolution. The first exotherm resulted from thermal decomposition of the volatiles while the second exotherm resulted from that of the residual char. The curves were re-plotted so that the reference temperature formed the X-axis and the temperature differential between the two beds the Y-axis (Figure 68). It is seen that the first exotherm, which began at around 220°C, peaked at about 350°C while the second exotherm peaked at about 480°C. No flaming or glowing combustion occurred during the run. As the second peak is relatively small compared with the first one, it would appear that char forms only a small proportion of the pyrolysis products of cellulose. This was found to be true from thermogravimetric analysis of the material (Chapter

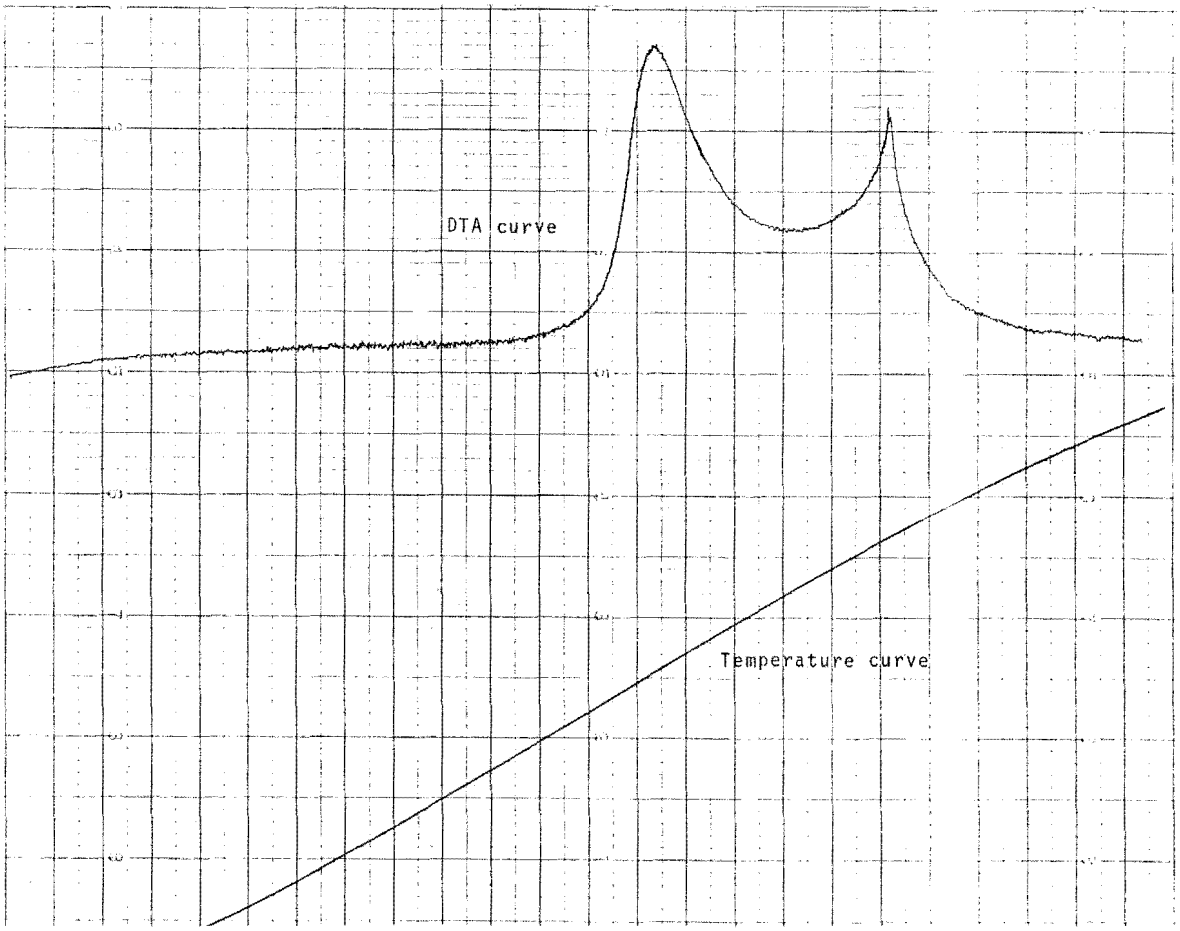

Figure 67. DTA curve in air of cellulose (original)

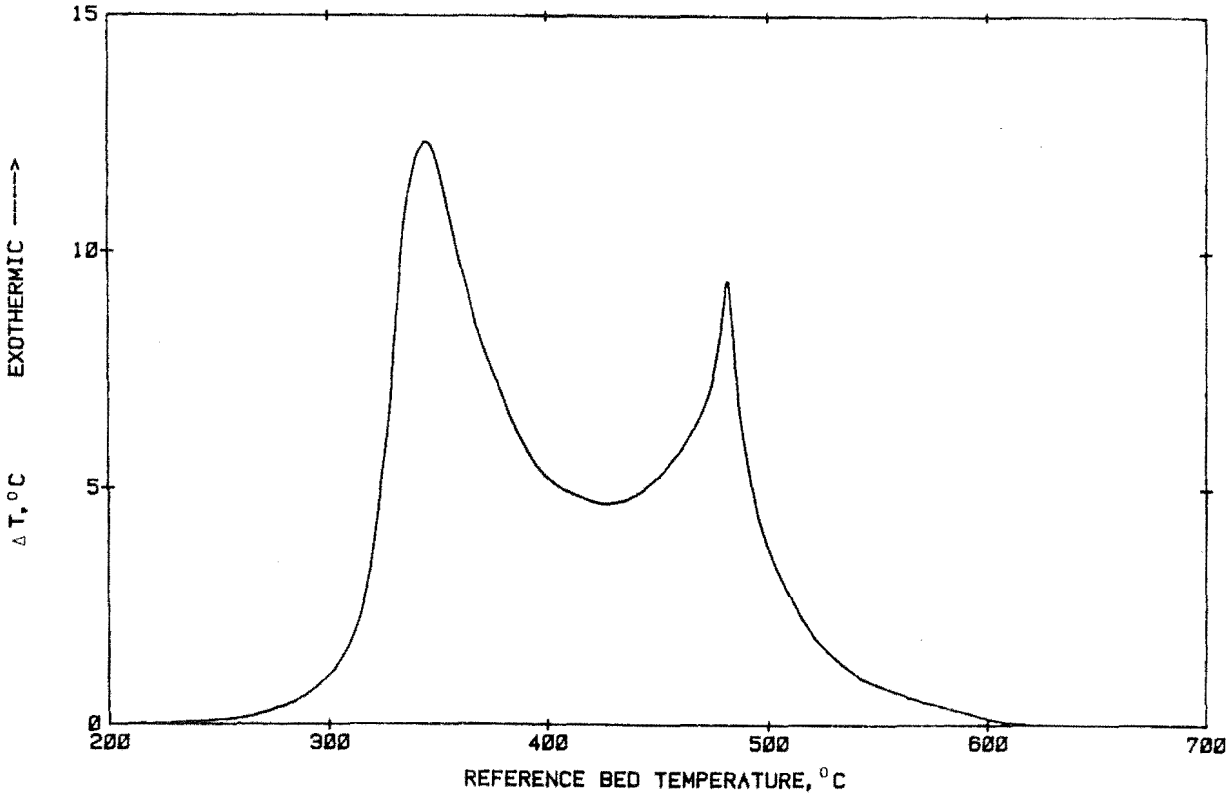

Figure 68. DTA in air of cellulose (re-plotted)

7). The underside of the 'Kaowool' plug in the sample tube was covered with tar droplets, indicating that not all the volatiles released were reacted or 'burnt'.

When the run was carried out using a gas mixture containing 80% O2 and 20% N_2 (v/v), the resultant DTA curve contained only one exotherm which peaked at about 315°C (Figure 69). What actually happened was the volatiles burst into flame by auto-ignition at about 310°C, resulting in the bed temperature rising sharply. As soon as the flaming combustion subsided but before the thermal trace made its way down, glowing combustion took place in the residual char, extending the height of the peak instead of forming a new one. So, in reality, the lone peak in this DTA curve was the result of two reaction peaks merging into one. Ignition of the combustibles was accompanied by quite a loud explosion in the sample tube. The 'Kaowool' plug on top of the tube was blown off by the explosion. Flaming combustion of the volatiles was rather noisy (like the noise of crackers from a distance) and occurred in the gas phase above the bed. In the repeat run, a second set of thermocouples was used. The sensing tip of the differential thermocouple in the sample tube was placed above the fluidised-bed, as illustrated in Figure 70. At the height of flaming combustion, a temperature of 850°C was recorded above the sample bed (Figure 71), as compared with 365°C within the bed. The same arrangement was made for the repeat of the run in air. The two resultant curves were similar, indicating that, in the absence of flaming combustion, the temperature above the bed was the same as that within the bed. Thus, the use of a second set of thermocouples helps confirm the occurrence of flaming combustion during a run.

The source of cellulose in the above runs was Whatman's extraction thimbles instead of filter paper. The reason for the switch was because cuttings from extraction thimbles are easier to fluidise and are less bulky for the same sample size than those from filter paper.

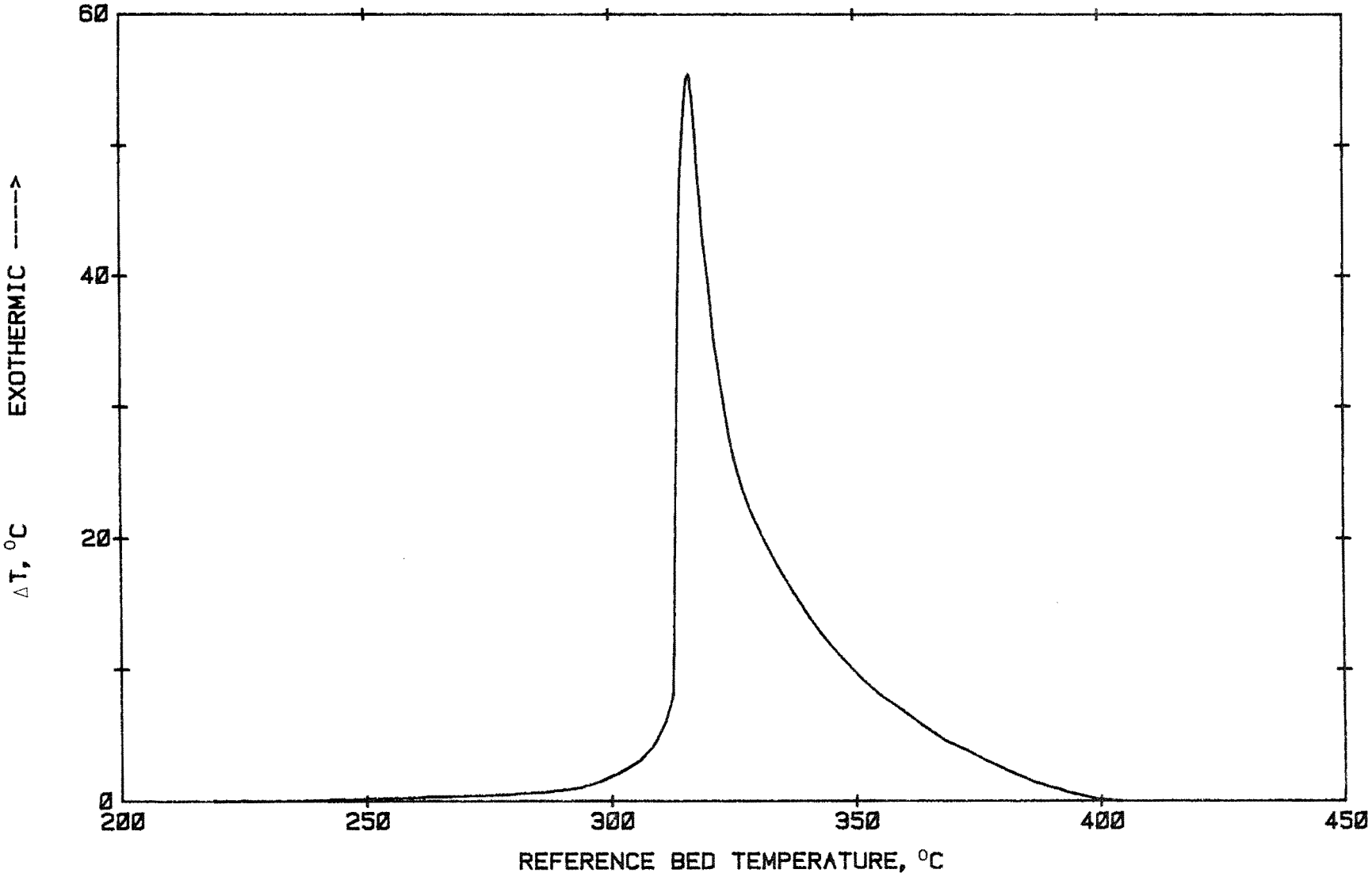

Figure 69. DTA curve in 80% O_2 of cellulose

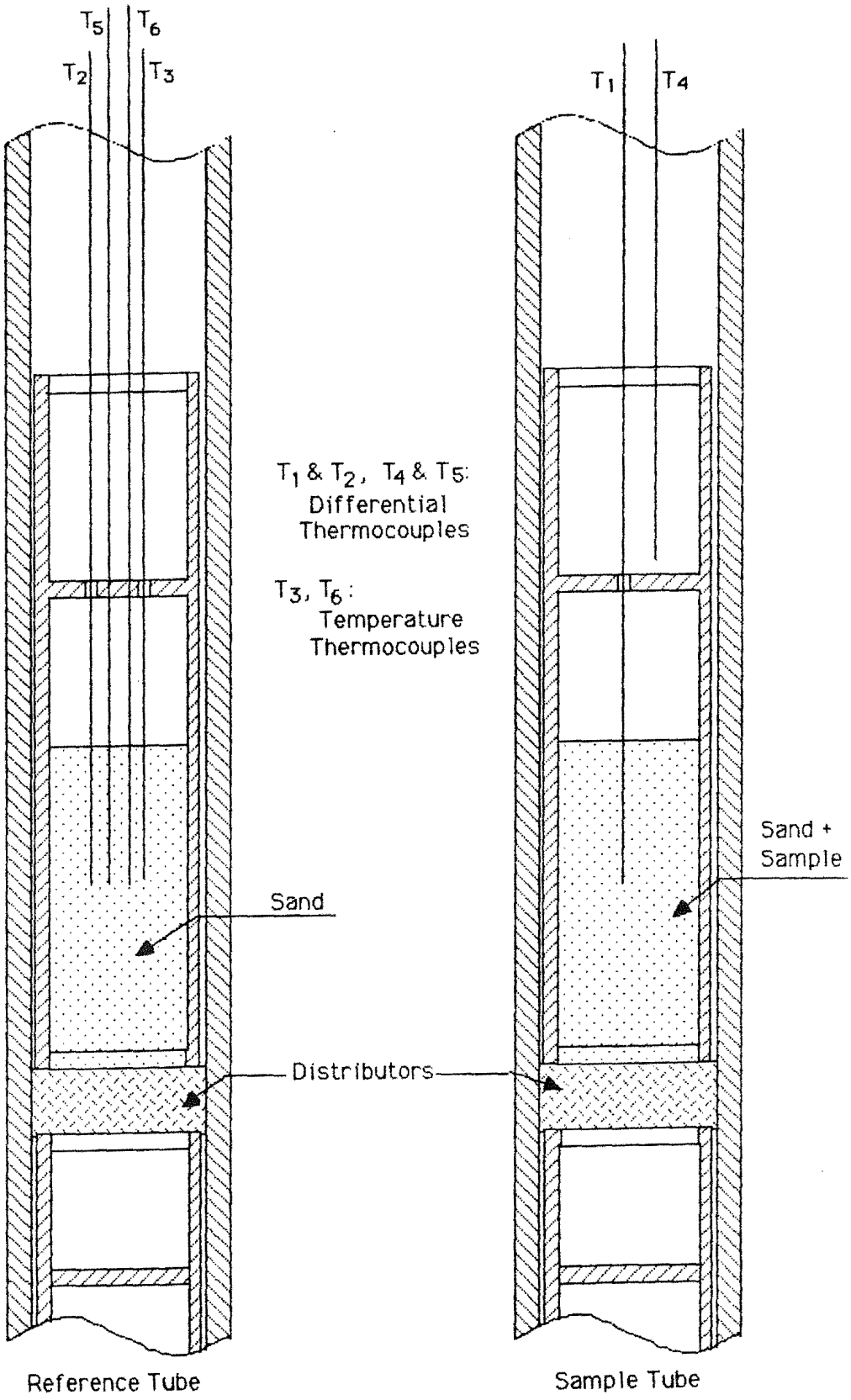

Figure 70. Experimental set-up for repeat run of cellulose in 80% O_2

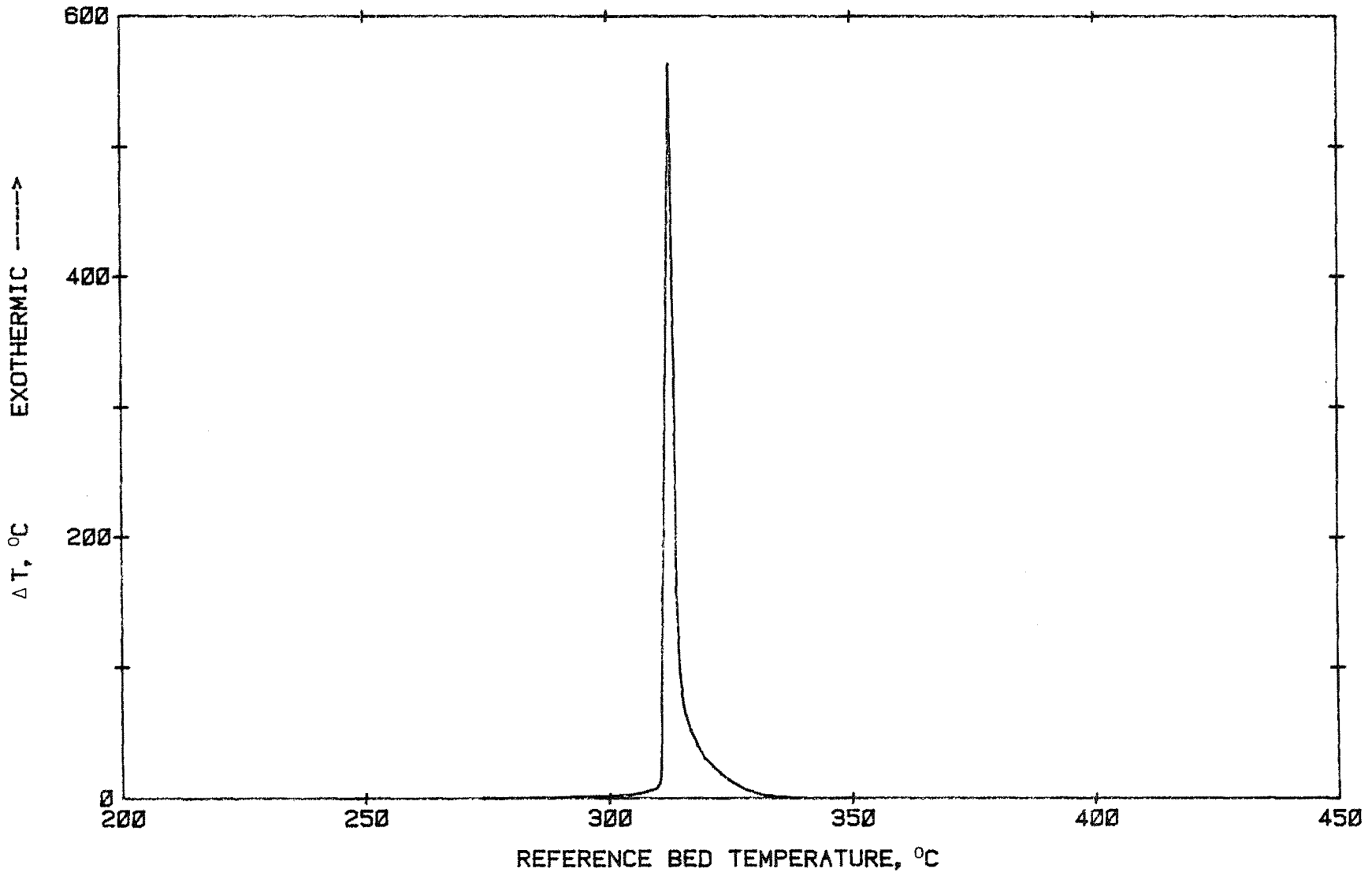

Figure 71. DTA curve of cellulose in 80% O_2 recorded by the second set of thermocouples

DTA of cellulose in an oxidative environment by other workers was carried out mainly in the conventional static bed apparatus. Using a sample size of 5 mg, a heating rate of 5.8°C/min and with the run conducted in air, Arseneau (1961) obtained a strong exotherm between 300°C and 390°C. However, his experiment was terminated around 420°C, as a result of which it is not possible to tell whether there was a second peak at higher temperatures. Tang (1972) used oxygen as the carrier gas and for a sample size of 50 mg and a heating rate of 12°C/min, obtained a strong and sharp exotherm between 300°C and 375°C, peaking at about 330°C. His results were quite similar to those obtained here.

6.3.2 Acid Lignin

DTA runs in air and in 80% O2 were carried out. Each of the resultant curves (Figure 72) contained two exotherms, with a considerable amount of overlapping between them. As in the case of cellulose, and indeed in the other wood components and wood, the first peak is attributed to the volatiles and the second one to the residual char. In these curves, the second peak is the dominant peak, indicating that lignin contributes more to char formation than cellulose. This was found to be true from thermogravimetric analysis (Chapter 7). No flaming or glowing combustion occurred in the run in air. The first exotherm peaked at about 345°C and the second one at about 490°C. In the run in 80% O2, there was again no flaming combustion but glowing combustion occurred in the char. The first peak was located at about 315°C while the second one at about 440°C. Thus increasing the oxygen concentration of the fluidising medium resulted in a shift of each peak nearer to the origin, i.e. to a lower temperature. Tang (1972) carried out similar studies using oxygen as the carrier gas in a static bed apparatus. The curve he obtained was similar to that obtained from the run in 80% O2, except that its second peak was of the same height as that of the first one.

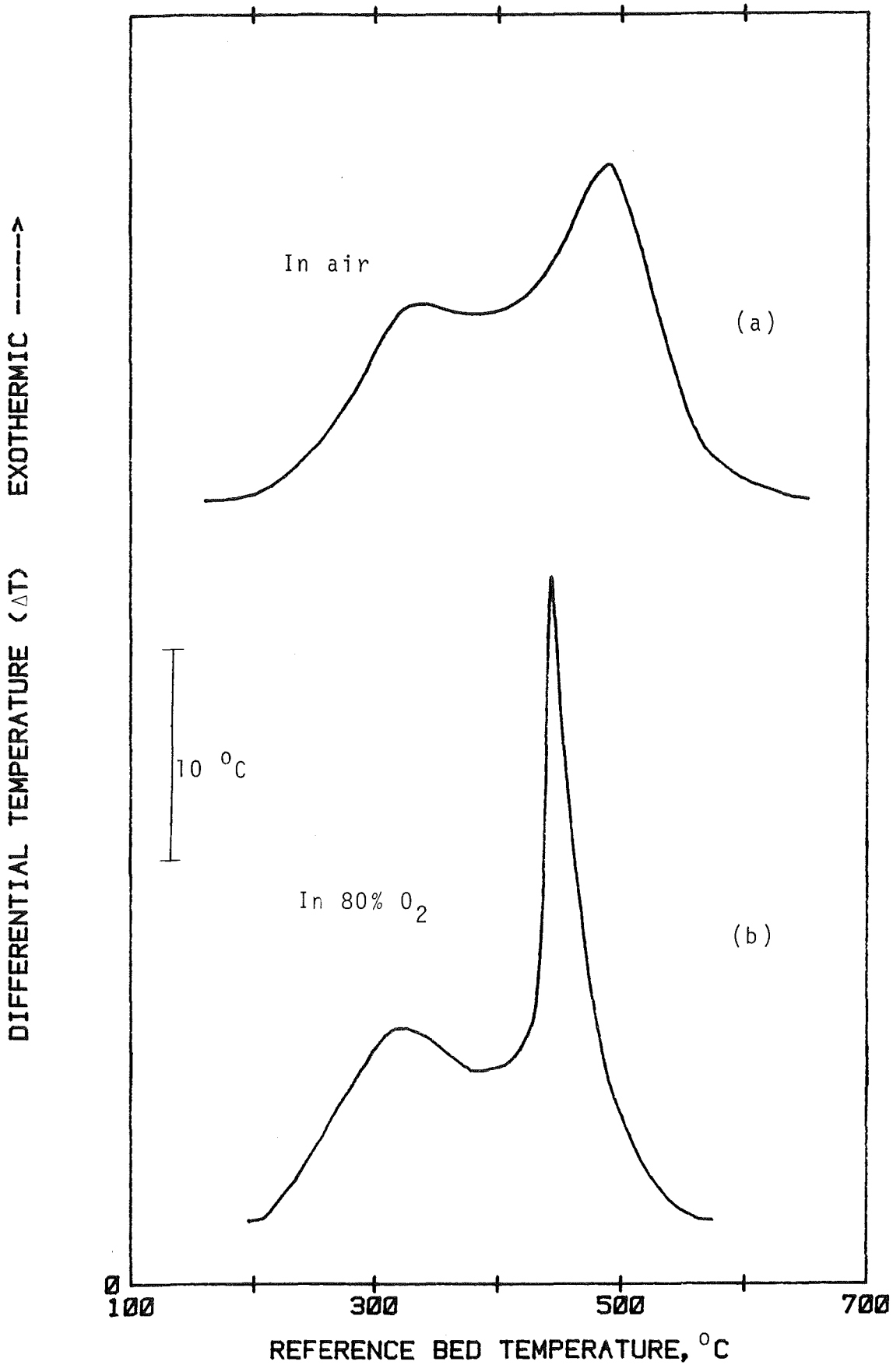

Figure 72. DTA curves of acid lignin

The heat of combustion of lignin is higher than that of cellulose - 26500 kJ/kg compared with 17000 kJ/kg (Susott et al.,1975). Ultimate analysis of acid lignin prepared from Rubber wood yielded the following results : C 65.9%, O 30.0%, H 3.9% and ash 0.3%, on a weight basis. The corresponding values for cellulose are : C 44.5%, O 49.4% and H 6.1%. Lignin thus contains around 20% more carbon than cellulose, which explains why it has a higher heat of combustion.

6.3.3 Extractives

The DTA curves of the water-solubles from Rubber wood in air and in 80% O2 are shown in Figure 73. Each of them contained two peaks, with the second one being much larger than the first. It therefore appears that the bulk of the extractives turned into char on pyrolysis. This is, however, not the case as their char yield at 530°C in a TG run in N_2 amounted to only 41% of the sample's weight (Chapter 7). In the same run, it was found that the sample began to lose weight at around 120°C and by 300°C, it had lost 35% of its weight. In the light of this finding, the relatively small size of the first peak can only mean that quite a large proportion of the volatiles formed were not reacted, especially those liberated at lower temperatures.

No flaming combustion occurred in either of the runs. Glowing combustion occurred in the residual char in the run in 80% O2 but not in that in air. The shift in the second peak temperature (from 457°C to 449°C) was not as great as that encountered in lignin. Ultimate analysis of a sample of the extractives yielded the following results : C 42.7%, O 43.3%, H 5.6% and ash 8.4%, on a weight basis. In view of its relatively low carbon content, its heat of combustion is expected to be lower than that of the other components.

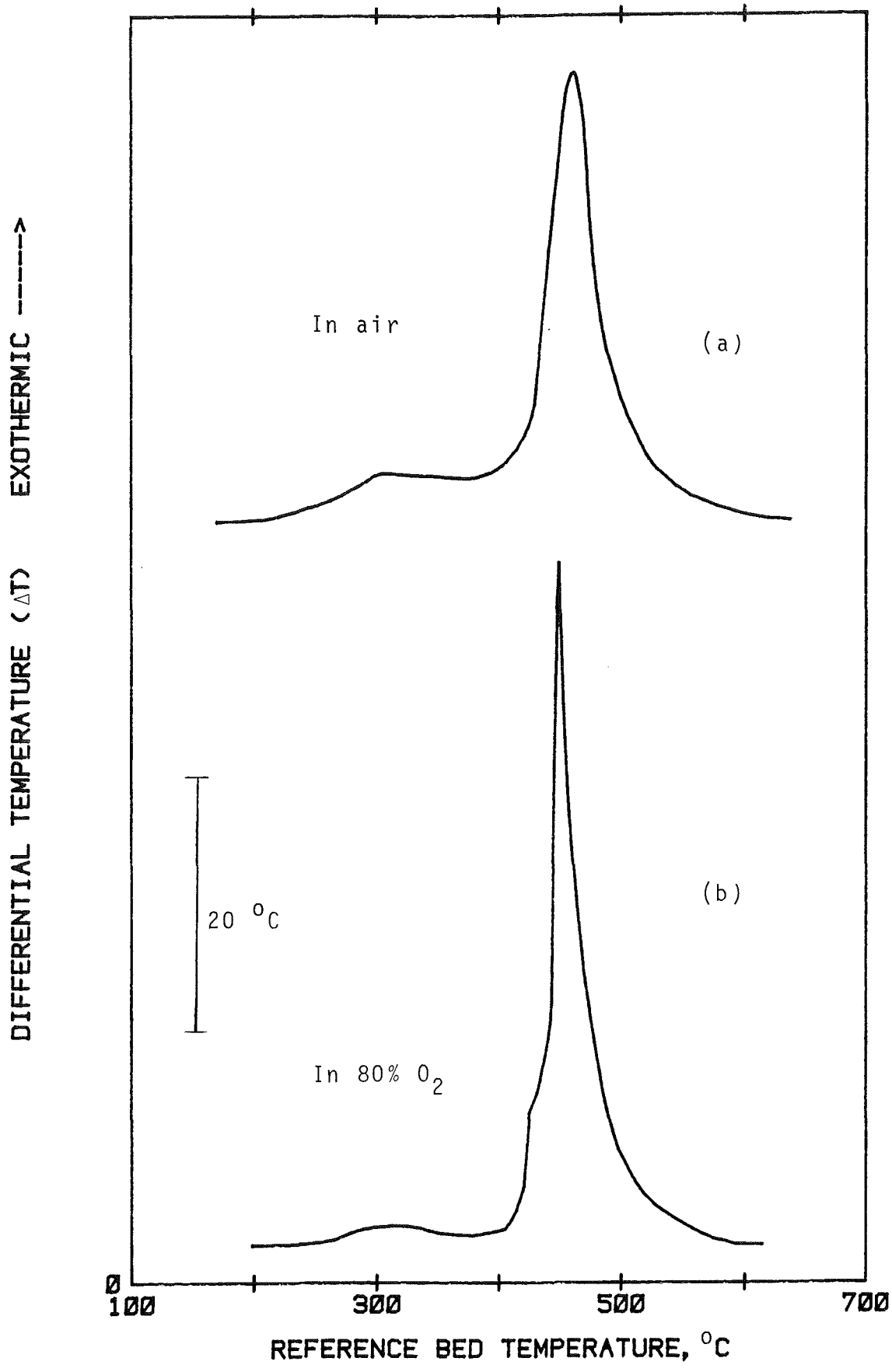

Figure 73. DTA curves of the water-soluble extractives

6.4 Rubber Wood

Unless otherwise stated, the test samples were obtained from the fresh wood sections of **Tjir 1** and were oven-dried before use.

6.4.1 Effect of Particle Size

The effect of particle size on the thermal behaviour of Rubber wood in air was investigated using the following wood samples : (1) -36+72 mesh particles, (2) -10+18 mesh particles, (3) -5+10 mesh particles, (4) 5 mm diameter pieces and (5) 10 mm diameter pieces. The height of the 5 mm diameter test pieces was 11-12 mm while that of the 10 mm diameter pieces was 10 mm. In a 1-gm sample, there were seven of the 5 mm diameter pieces and two of the 10 mm diameter pieces. No flaming or glowing combustion occurred in any of these runs. Each of the DTA curves (Figure 74) contained two overlapping peaks. The first one began its ascent at around 200^{o}C, indicating that those volatiles formed below this temperature were not reacted. In Curve (a), which is the DTA curve of the -36+72 mesh fraction, the first peak was centred at 336^{o}C and the second one at 445^{o}C, with the former being the larger of the two. Increasing the particle size resulted in : (1) the first peak becoming smaller and the second peak larger, (2) the resolution of the peaks becoming poorer and (3) a shift of the second peak to a lower temperature. Evidently part of the second peak is attributed to the volatiles whose share in it increases with increasing particle size. In other words, the evolution of the volatiles appears to be more spread out the larger the particle size of the wood.

Figure 75 shows the DTA curves in air of two Rubber wood char samples obtained from the runs in N_2. One was of particle size -10+18 mesh while the other consisted of cylindrical pieces of diameter 3.5-3.7 mm and height 9-10 mm

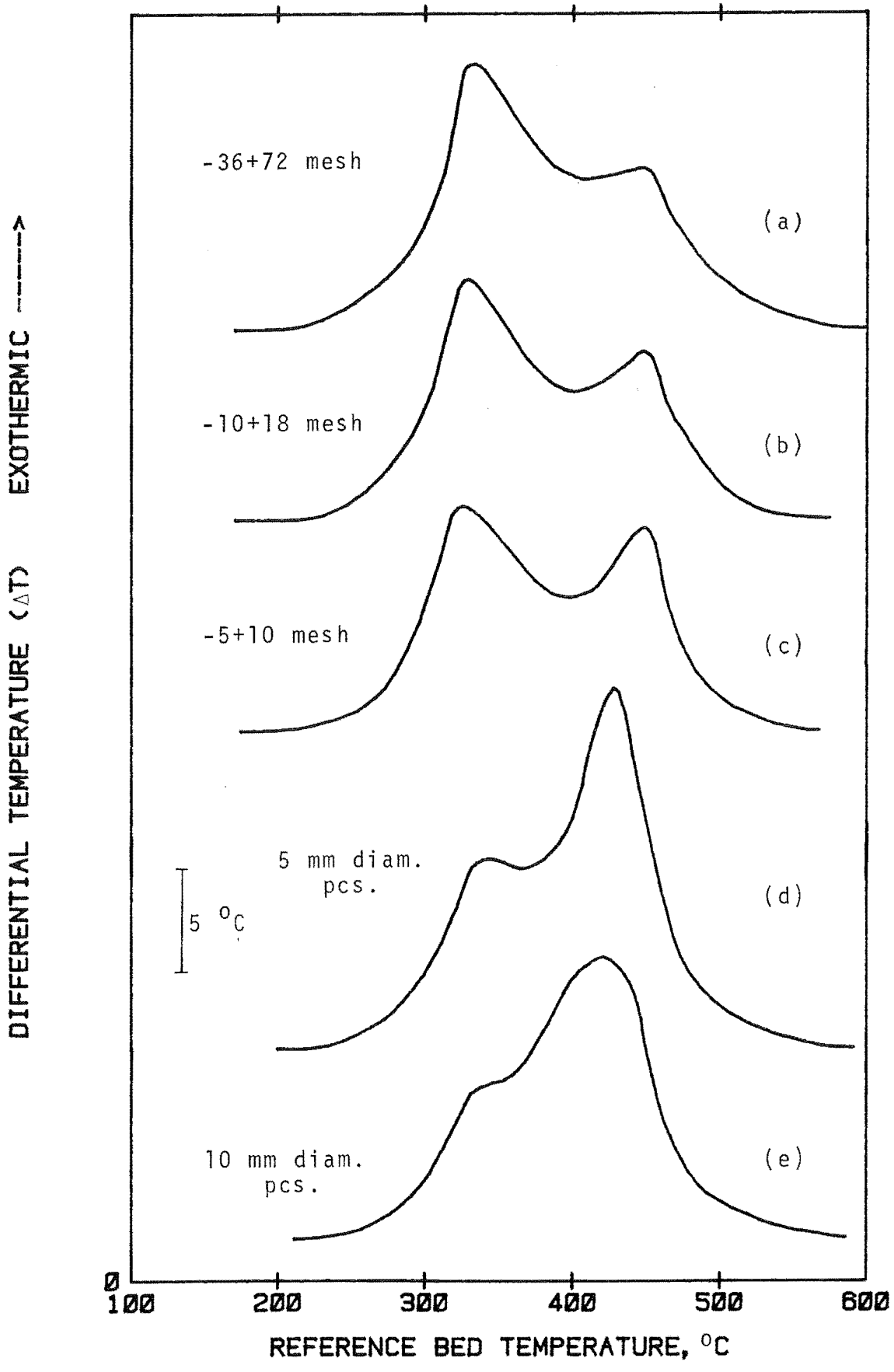

Figure 74. DTA curves in air of Rubber wood of different particle sizes

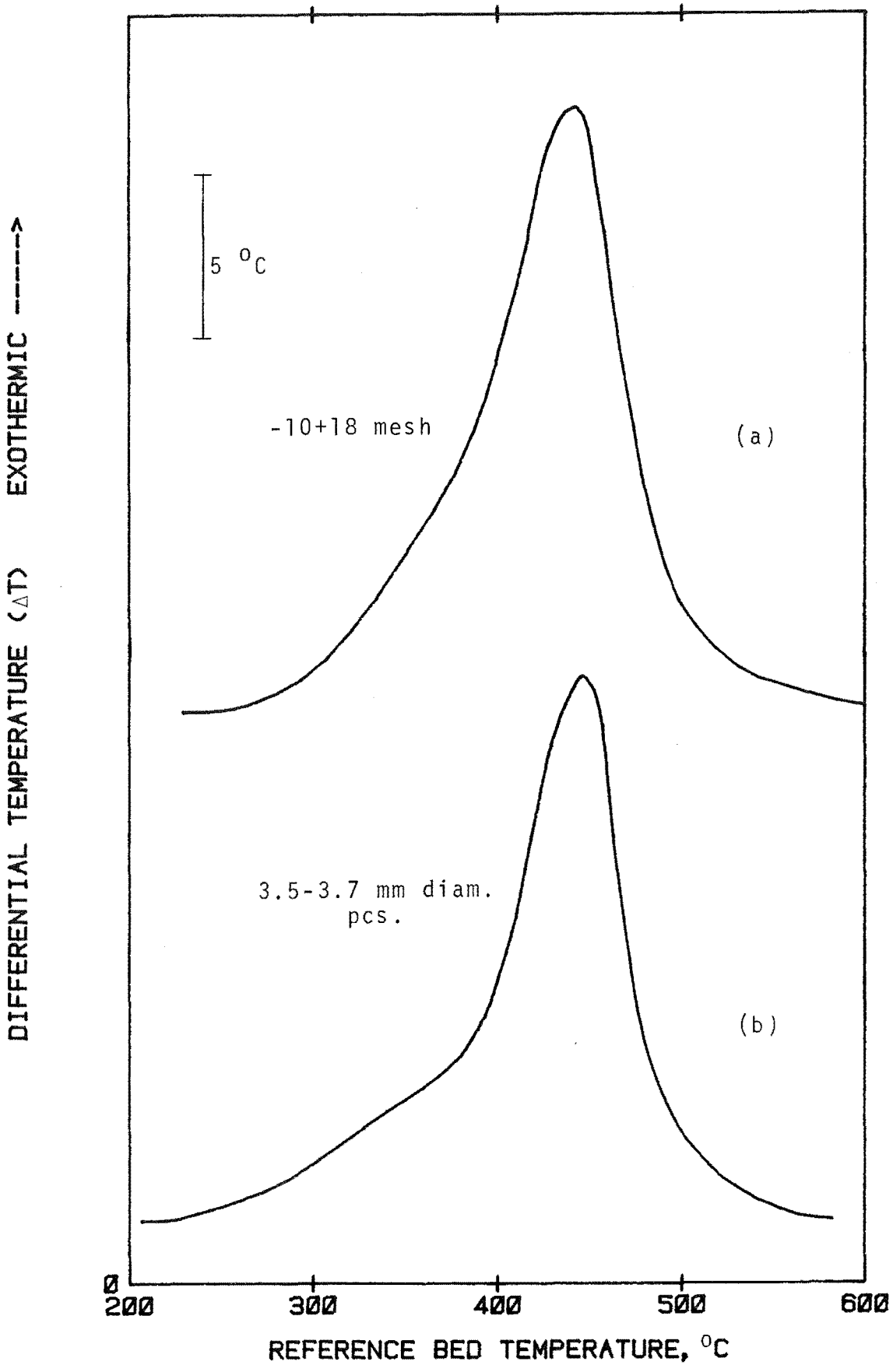

Figure 75. DTA curves in air of Rubber wood char

(derived from the 5 mm diameter wood pieces). Each of the samples weighed 0.5 gm. Both the curves contained only one peak which was centred at about 450°C. This serves to confirm that the second peak in the DTA curves of Rubber wood is indeed attributed to the residual char. The small bulge between 220°C and 390°C in each of the curves appears to be due to oxidation reactions involving the small amount of volatiles present in the char.

6.4.2 Effect of Oxygen Concentration of Fluidising Gas

The effect of oxygen concentration of the fluidising gas on the combustion of Rubber wood was investigated. Five particle sizes, ranging from -36+72 mesh to 10 mm diameter, were used. The results obtained are given below, in order of particle size.

(i) -36+72 Mesh Particles

The DTA curves resulting from the runs in air and in 100% O_2 are shown in Figure 76. Each of them contained two peaks. No flaming or glowing combustion occurred in both the runs. In the run in 100% O_2, the curve obtained from the second set of thermocouples was similar to that obtained from the first set, confirming the absence of flaming combustion during the run. Increasing the oxygen level of the fluidising medium from 21% to 100% merely resulted in a slight increase in the height of the first peak and a shift of each peak to a lower temperature - the first from 336°C to 322°C and the second from 445°C to 411°C.

(ii) -10+18 Mesh Particles

Runs were carried out in air and in 60% and 100% O_2. Again no flaming or glowing combustion occurred in any of the runs. Each of the DTA curves contained two peaks (Figure 77). As in the case of the -36+72 mesh fraction, increasing the

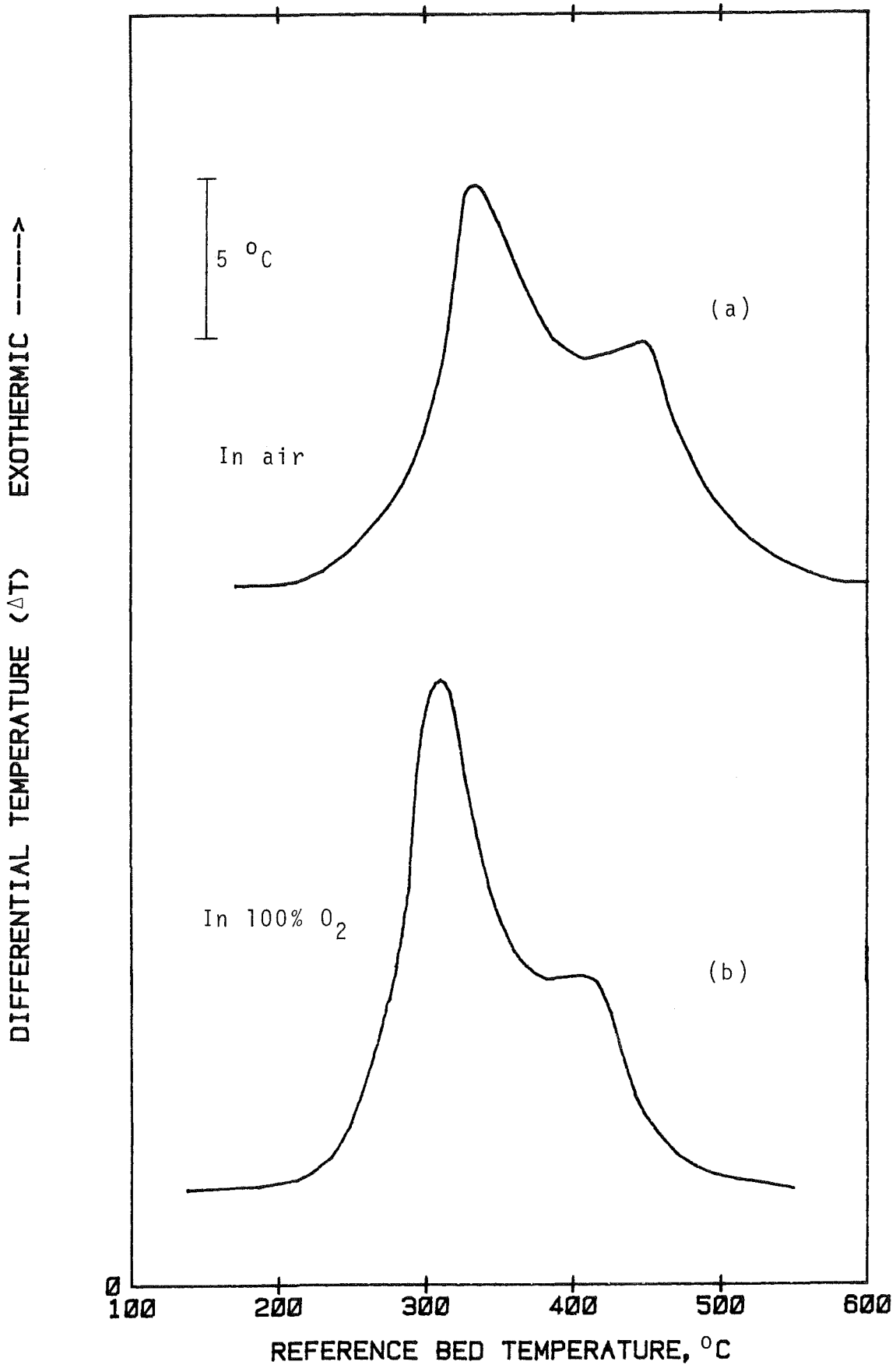

Figure 76. DTA curves of -36+72 mesh particles

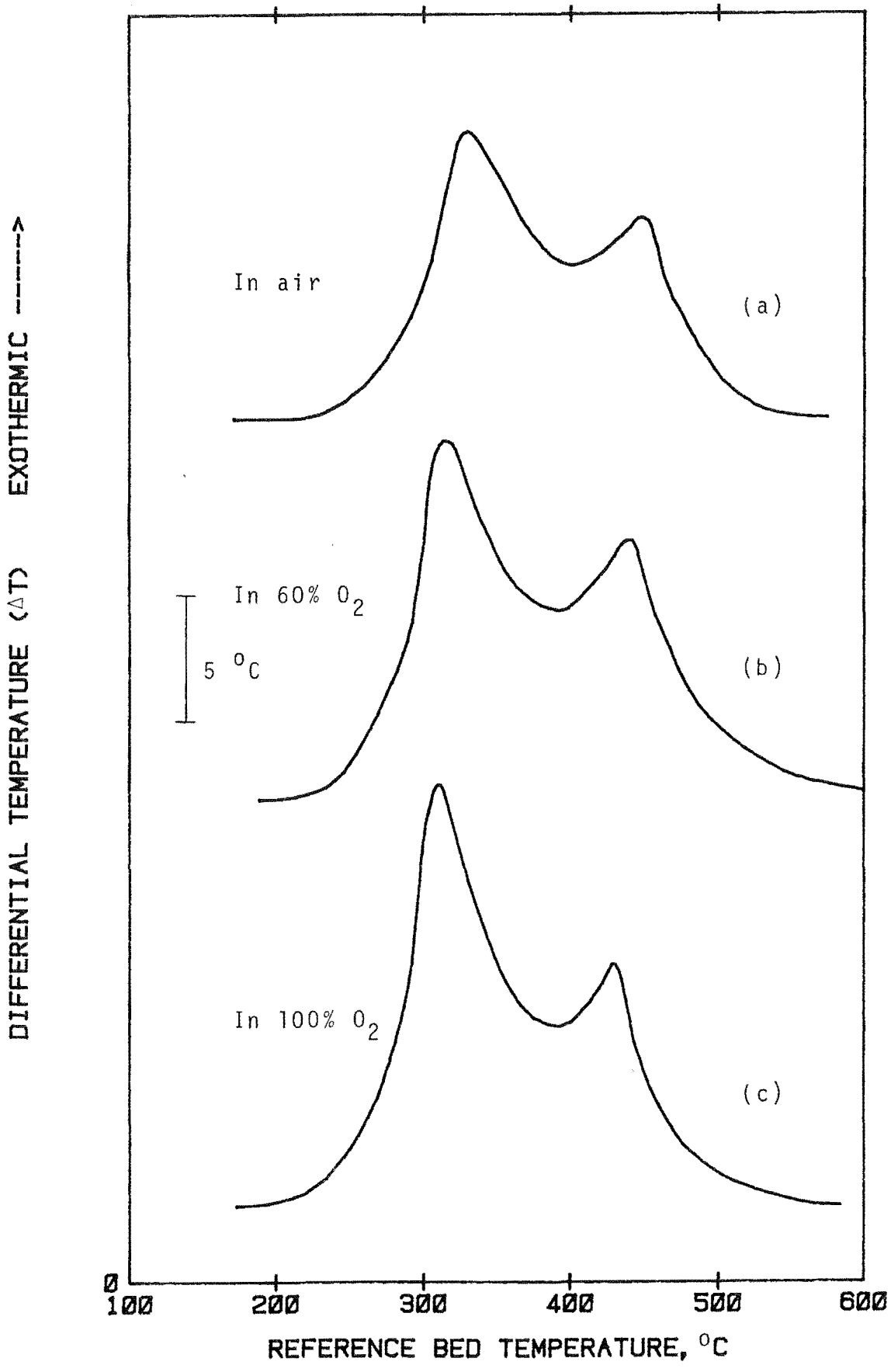

Figure 77. DTA curves of -10+18 mesh particles

oxygen concentration of the fluidising medium resulted in the first peak becoming higher and a shift of each peak to a lower temperature.

(iii) -5+10 Mesh Particles

Figure 78 shows the DTA curves obtained from the runs in air and in 60% and 100% O_2. No flaming or glowing combustion occurred in the run in air. In the run in 60% O_2, there was again no flaming combustion but glowing combustion occurred in some of the char pieces. Flaming combustion occurred in the run in 100% O_2, beginning at 287°C and lasted for less than a minute. However, only some of the wood pieces burst into flame. Ignition of the combustibles was accompanied by an explosion which caused the 'Kaowool' plug to be blown away, as in the case of the run of cellulose in 80% O_2. Glowing combustion took place in some of the char particles as soon as flaming combustion subsided. Thus the first peak in the DTA curve of this run, which was centred at 292°C, was partly attributed to glowing combustion of some of the char particles.

(iv) 5 mm Diameter Pieces

Runs were carried out in air and in 40%, 60% and 80% O_2. The DTA curves resulting from these runs are shown in Figure 79. No flaming or glowing combustion occurred in the run in air. In the run in 40% O_2, there was no flaming combustion but glowing combustion occurred in the char from about 380°C, giving rise to the second peak. However, it was only confined to the ends of each piece, i.e. only the ends turned red hot. In the run in 60% O_2, there was again no flaming combustion. All the char pieces burnt by glowing combustion which extended to the whole piece instead of just at the ends, as in the case of the run in 40% O_2. However, they did not burn at the same time and this explains why there were more than two peaks in the DTA curve of this run. In the repeat run, there was again

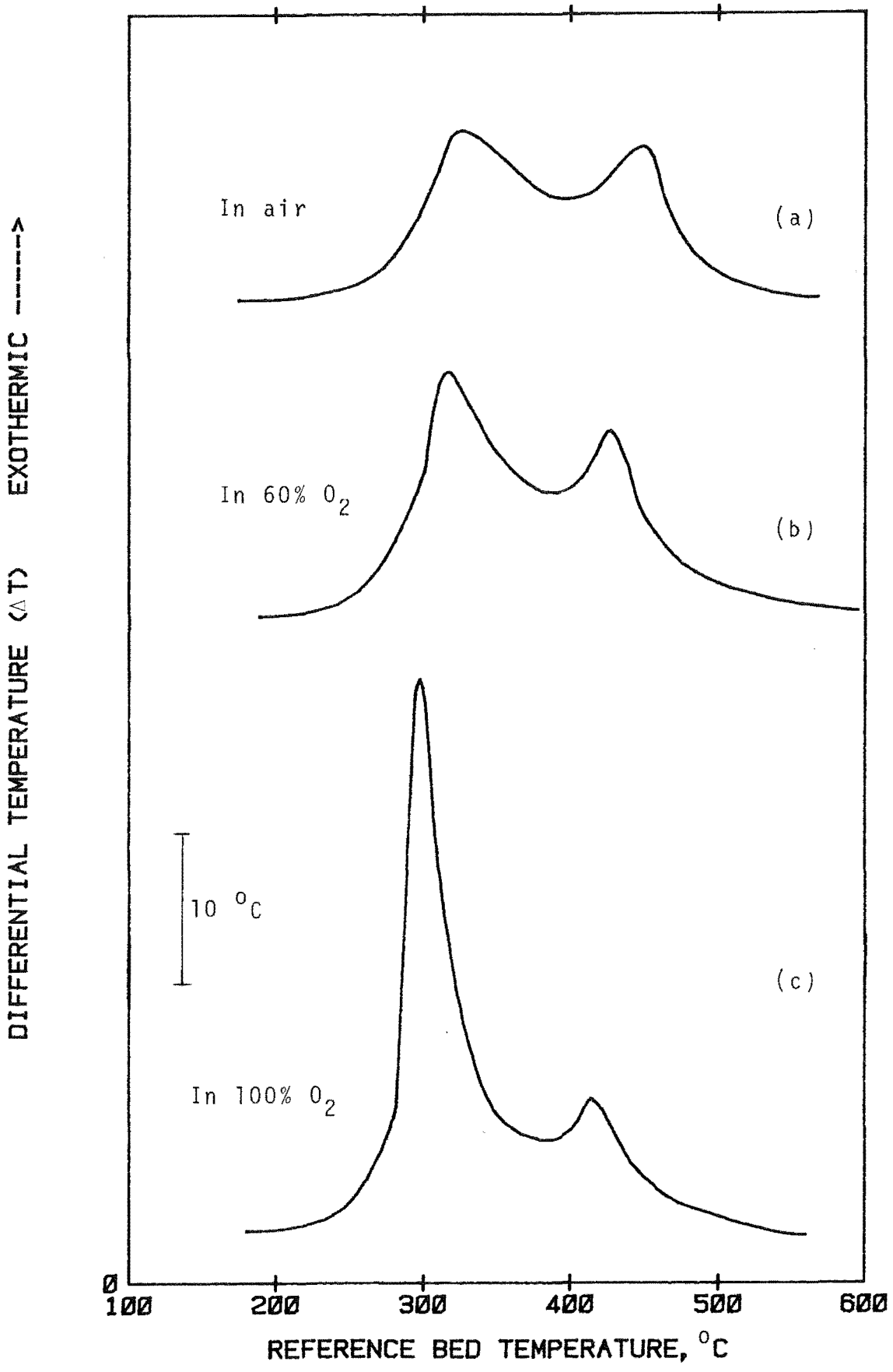

Figure 78. DTA curves of -5+10 mesh particles

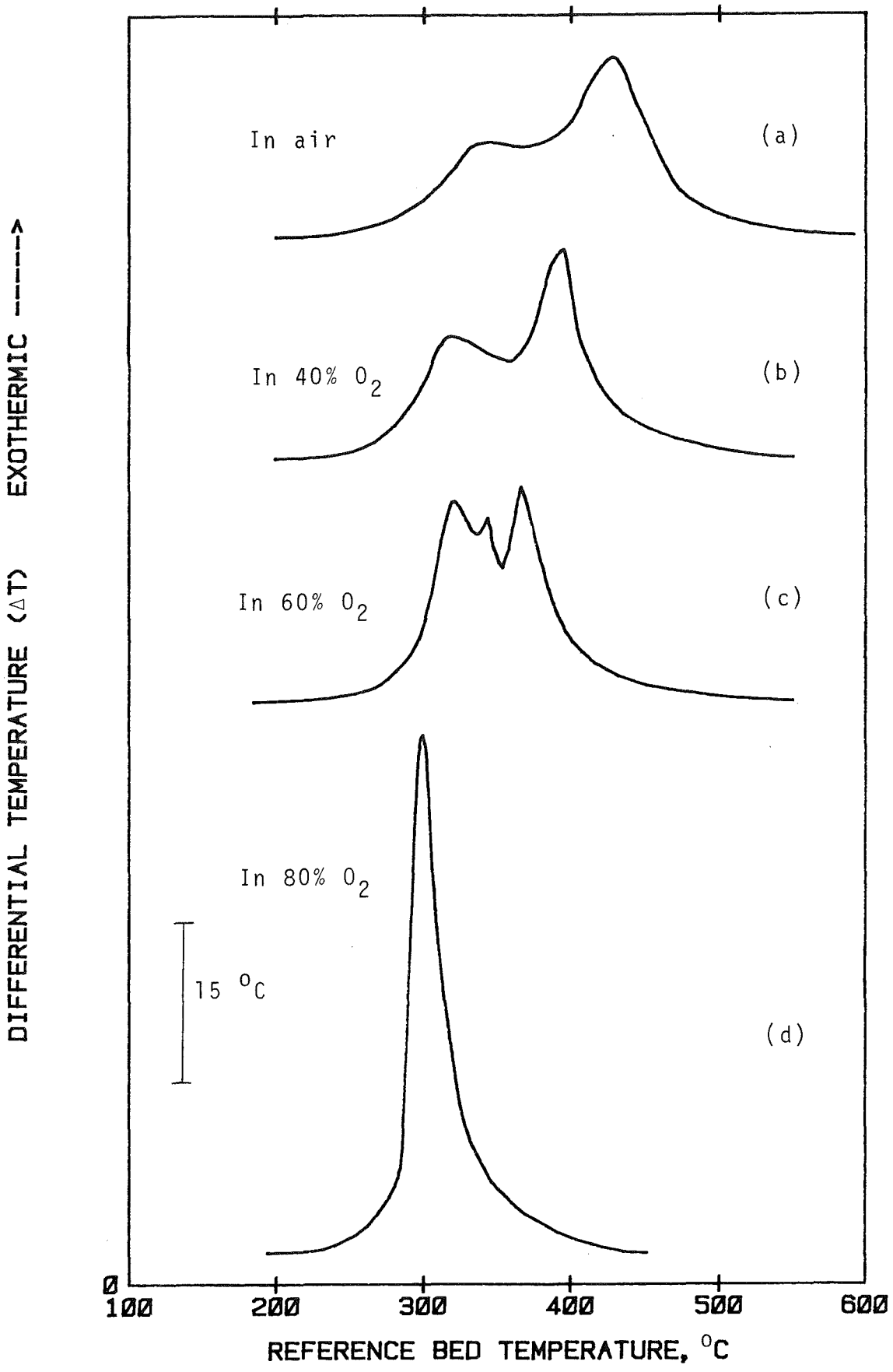

Figure 79. DTA curves of 5 mm diameter pieces

no flaming combustion but this time all the char pieces burnt at about the same time, giving rise to essentially only one peak which was centred at 310-320°C. In the run in 80% O_2, ignition occurred at about 285°C. It was observed that the wood pieces burnt individually and rather noisily. Flaming combustion of the volatiles was followed by glowing combustion of the residual char, resulting in only one peak being formed which was centred at about 300°C. Similar results were obtained in the repeat run.

(v) 10 mm Diameter Pieces

Runs in air and in 40%, 60% and 80% O_2 were conducted. Figure 80 shows the resultant DTA curves. No flaming or glowing combustion occurred in the run in air. In the runs in 40% and 60% O_2, there was no flaming combustion but their char pieces began to burn by glowing combustion at a relatively low temperature (330°C). As a result, only one peak was formed in each of their DTA curves. Glowing combustion of the char was more intense in the run in 60% O_2 than in that in 40% O_2. In the run in 80% O_2, both flaming and glowing combustions took place. Burning of the combustibles occurred at 270°C, as compared with 284°C in the case of the 5 mm diameter pieces. The resultant peak was centred at 284°C, again lower than that of the 5 mm diameter pieces - by about 15°C.

The results of the above runs are summarised in Table 6. In these runs, flaming combustion occurred in only three of them, namely in the -5+10 mesh particles in 100% O_2 and in the 5 mm and 10 mm diameter pieces in 80% O_2. Glowing combustion took place in all of these runs and also in those of the 5 mm and 10 mm diameter pieces in 40% and 60% O_2. No flaming or glowing combustion occurred in any of the runs involving the -36+72 mesh and -10+18 mesh particles. The results obtained are rather interesting, in that under similar circumstances, the larger wood particles have a greater tendency to burst into flame in fluidised-bed combustion than the smaller ones.

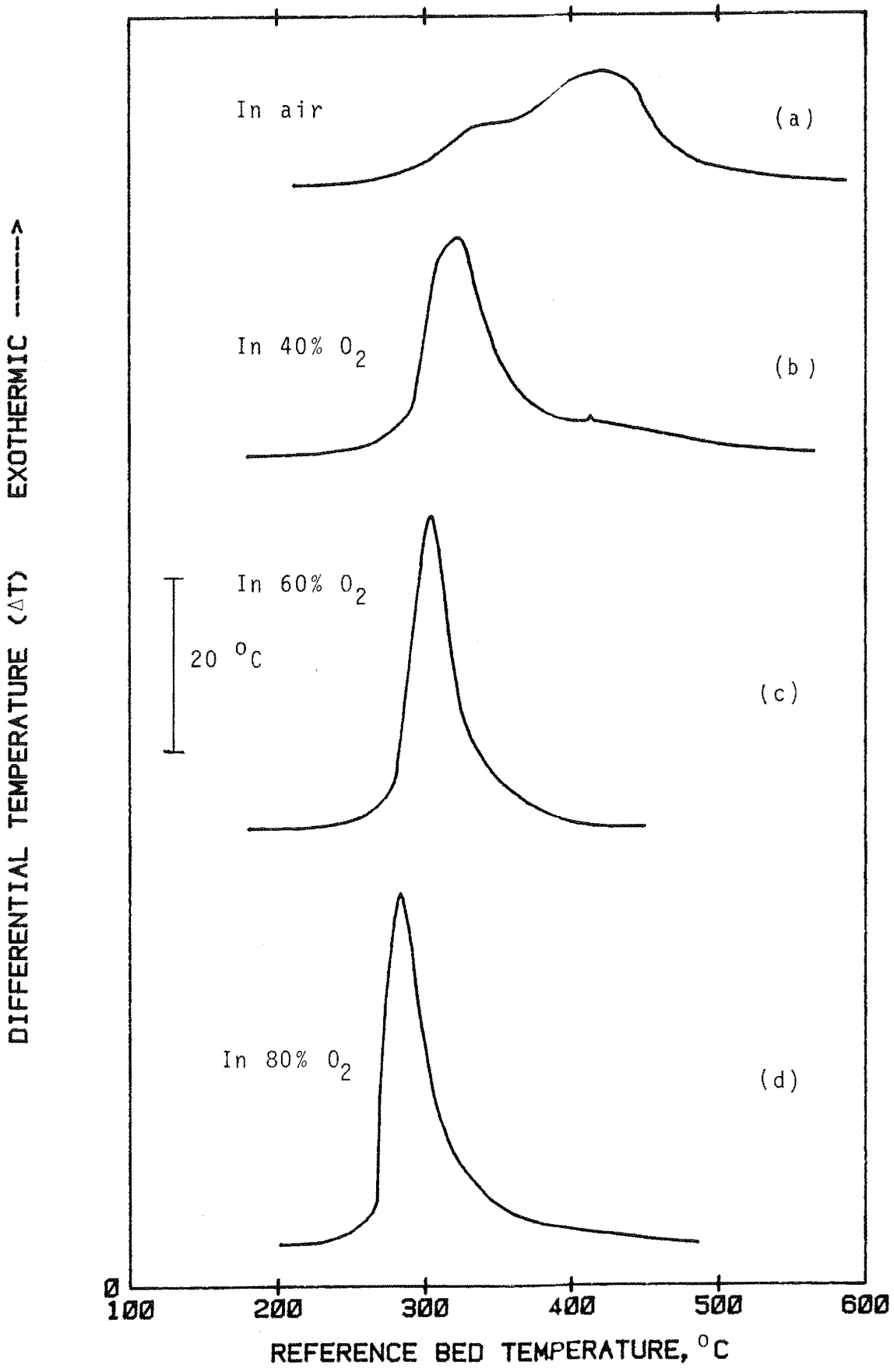

Figure 80. DTA curves of 10 mm diameter pieces

Table 6. Summary of DTA Runs

Particle size	O_2 conc. of fluidising gas, %(v/v)				
	21	40	60	80	100
-36+72 mesh	-				-
-10+18 mesh	-		-		-
-5+10 mesh	-		-		**F+G**
5 mm diam. pcs	-	G	G	**F+G**	
10 mm diam. pcs	-	G	G	**F+G**	

\- : no flaming or glowing combustion occurred
G : glowing combustion occured but not flaming combustion
F+G : both flaming and glowing combustions occurred

One would have thought that it is the other way round since the smaller wood particles give out the volatile products more easily than the larger pieces.

To help explain why ignition occurred in the larger wood pieces and not the smaller ones, two additional sets of runs were carried out. In the first set, the effect of sample size on the combustion of the 5 mm diameter wood pieces in 80% O_2 was investigated. Four sample sizes were used, viz 0.15 gm (1 pc), 0.46 gm (3 pc), 0.77 gm (5 pc) and 1.0 gm (7 pc). Flaming combustion occurred only in the last run. The resultant DTA curves are shown in Figure 81. The results obtained show that besides particle size, flaming combustion is also dependent on sample size. In the second set of runs, the effect of particle size on the combustibility of Rubber wood char in 80% O_2 was studied. Three particle sizes were used, namely -10+18 mesh fraction, 3.6 mm diameter pieces

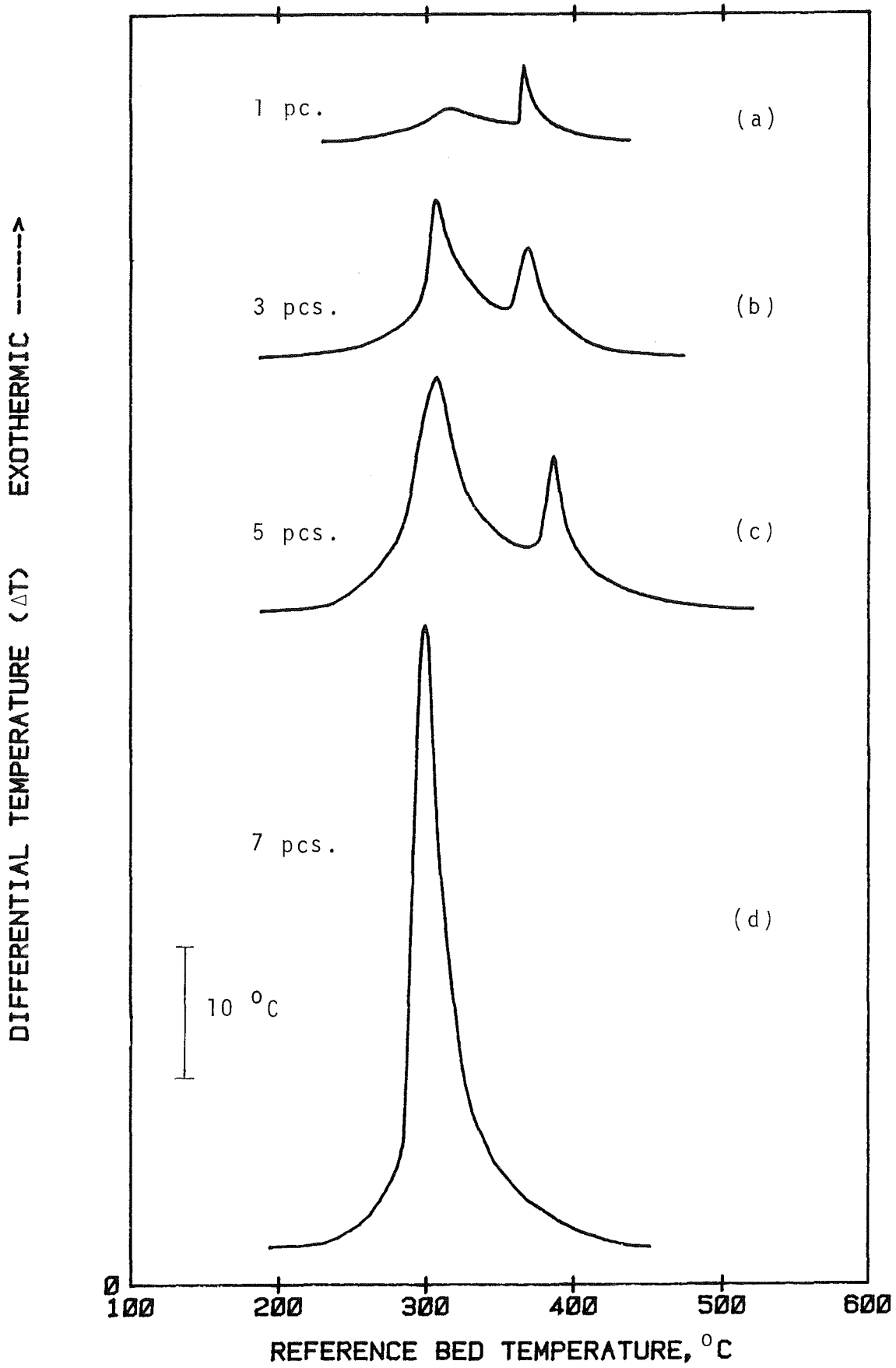

Figure 81. DTA curves in 80% O_2 of 5 mm diameter pieces (different sample sizes)

(derived from 5 mm diameter wood pieces) and 7 mm diameter pieces (derived from 10 mm diameter wood pieces). A uniform sample size of 0.3 gm, which corresponds to the char yield from 1 gm of wood, was used. The resultant DTA curves are shown in Figure 82. No glowing combustion occurred in the first run. The peak in the its DTA curve was centred at about 420°C. In the second run, glowing combustion occurred at about 370°C, resulting in the bed temperature rising sharply. The resultant exotherm peaked at about 390°C. In the third run, glowing combustion again occurred but this time it began at a much lower temperature (270°C). The resultant peak was the tallest of the three and was centred at about 280°C. The results obtained from these runs show that (1) the larger the char particles, the greater is the tendency for glowing combustion to occur and (2) glowing combustion occurs independently of flaming combustion, although the latter usually takes place first.

From the results obtained from the various experiments, it is clear that for ignition to occur, the concentration of the combustible mixture above the bed must exceed the flammability limit. In the case of the larger wood pieces, the combustible products are concentrated around them and if the fuel is sufficiently rich and the right conditions prevail, are capable of ignition. In the case of the smaller wood particles, they are dispersed over a bigger area. As a consequence, the combustibles released are more evenly distributed above the bed surface and are thus denied the opportunity to form a mixture capable of ignition. This seems to be the most logical explanation. It is suggested that the phenomenon may be due to a difference in the gas flowrates, resulted from the use of wood of different particle sizes. The difference, if any, if any, was not very great since the base line was practically unaffected by a change in the particle size of the sample. The fact that flaming combustion occurred in the 5 mm diameter pieces in 80% O_2 but not in the -36+72 and -10+18 mesh fractions even in 100% O_2 seems to rule

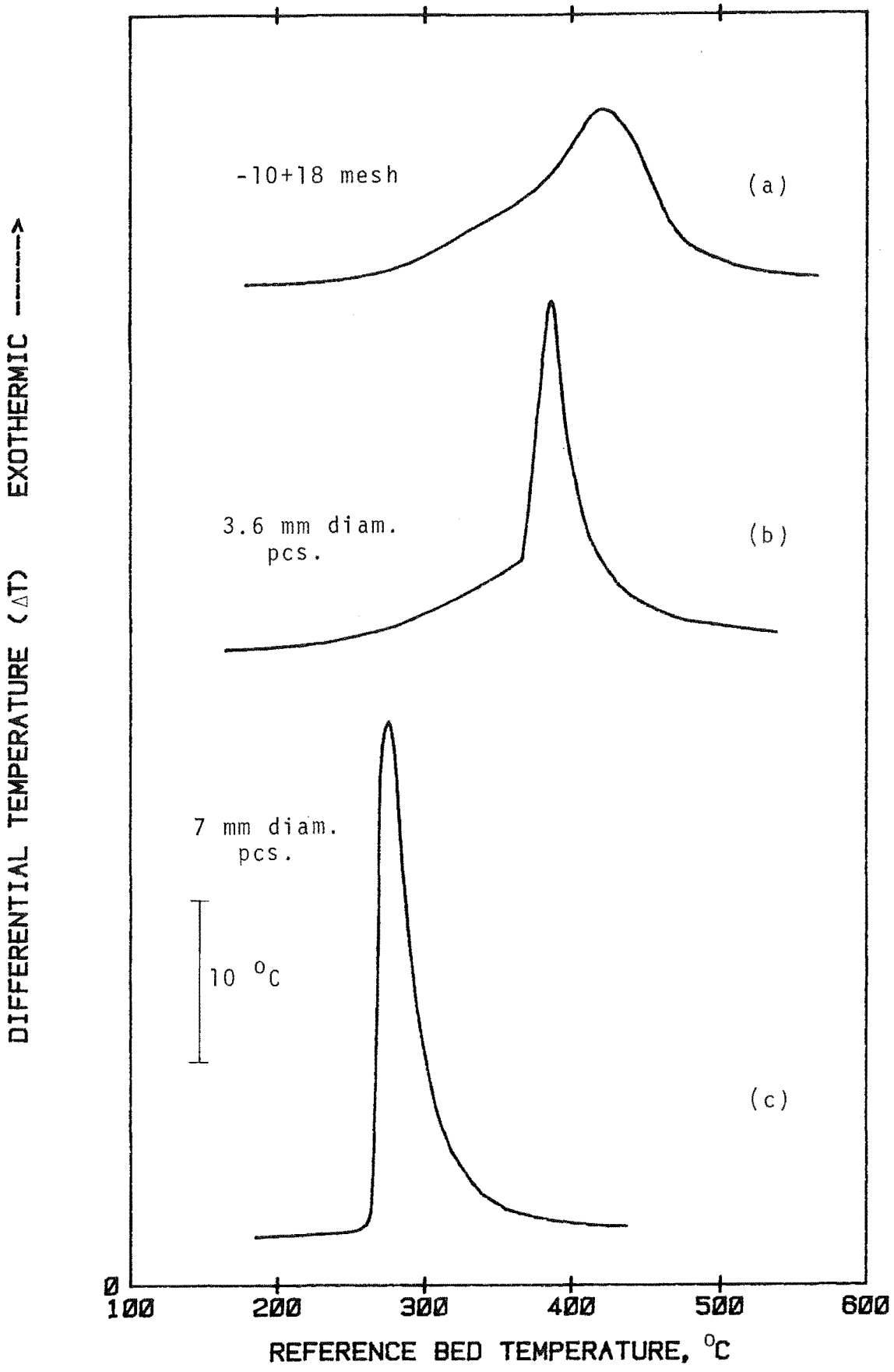

Figure 82. DTA curves in 80% O_2 of char samples

out this as the cause.

6.4.3 Heat of Reaction

It would be interesting to know how much heat was generated by each sample in the combustion runs carried out so far. This can be determined by first performing an internal calibration involving the insertion of a suitable heating coil into one of the beds and noting the area of the resultant peak for a particular power input.

The experimental set-up for the internal calibration is illustrated in Figure 83. The heating coil was made from Nichrome wire and had a resistance of 9.8 ohms. Thin copper wires were used as leads and were enclosed within a ceramic thermocouple sheath of length 675 mm and diameter 4 mm. Two series of runs were carried out, one with the bed temperature maintained at a constant value of 330^{o}C and the other with it rising at the rate of 5.5^{o}C/min. Air was used as the fluidising medium with a flowrate of 4 lit/min, i.e. the same as in the combustion runs. The DTA curves resulting from the first series of runs are shown in Figure 84 and those from the second series in Figure 85. Figure 84 contains four peaks which correspond to power inputs of 5.63 W for durations of 1, 3 ,5 and 10 minutes. The three curves in Figure 85 resulted from power inputs of 5.74 W for 48 min, 7.92 W for 52 min and 14.4 W for 61 min. For ease of reference, the curves are numbered 1 to 4 in Figure 84 and 5 to 7 in Figure 85. The area under curve of each peak was computed with the aid of a computer and the results obtained are given in Table 7. It will be seen that although the power input varied considerably, the area under curve per kilojoules of power input was fairly constant. The mean of the seven values was 32.54 deg min/kJ and this was used as the basis for determining the heat of reaction (or combustion) in each run. It must be pointed out that the heat of reaction so calculated was the amount of heat transmitted to the bed. In those runs

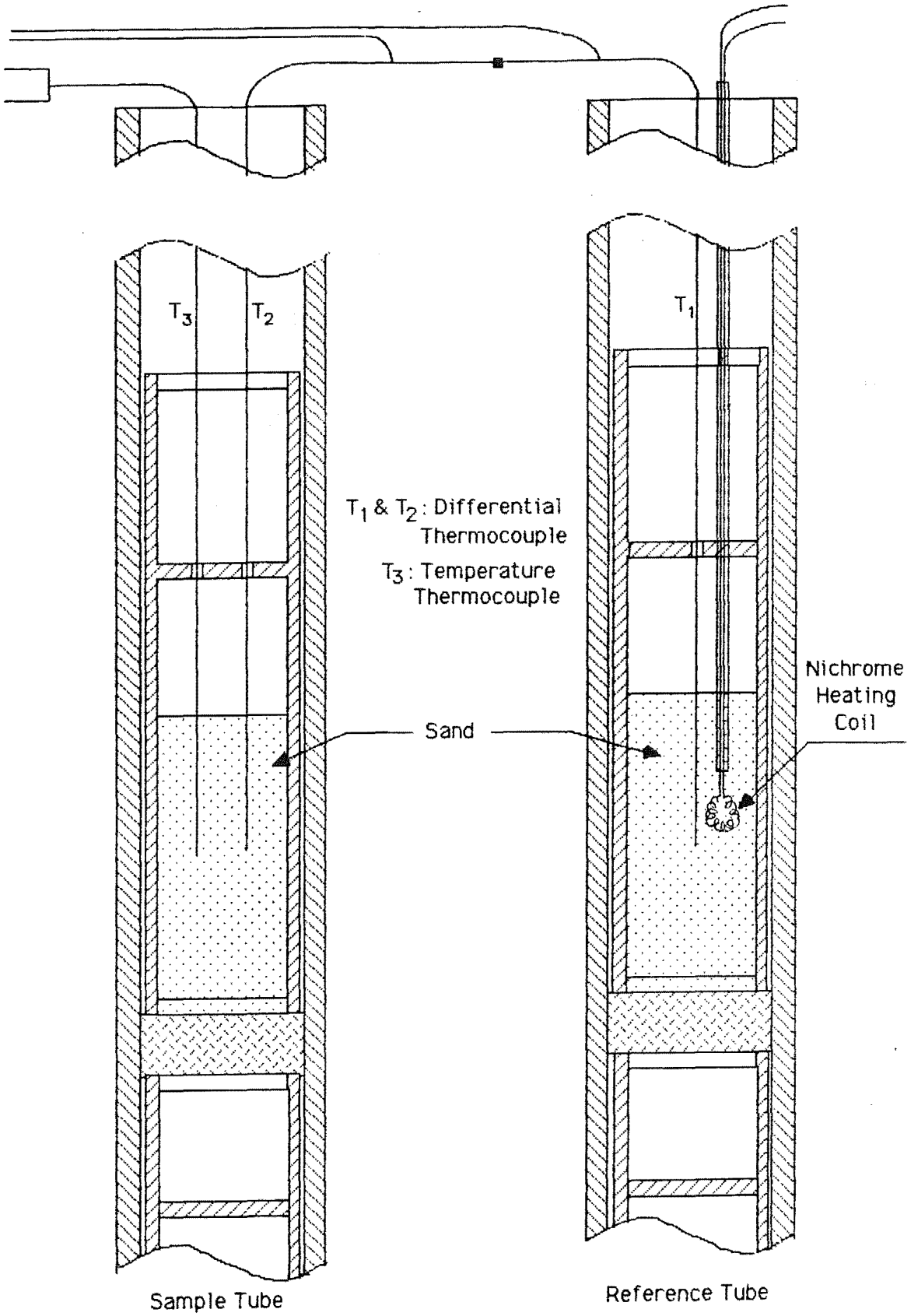

Figure 83. Experimental set-up for internal calibration

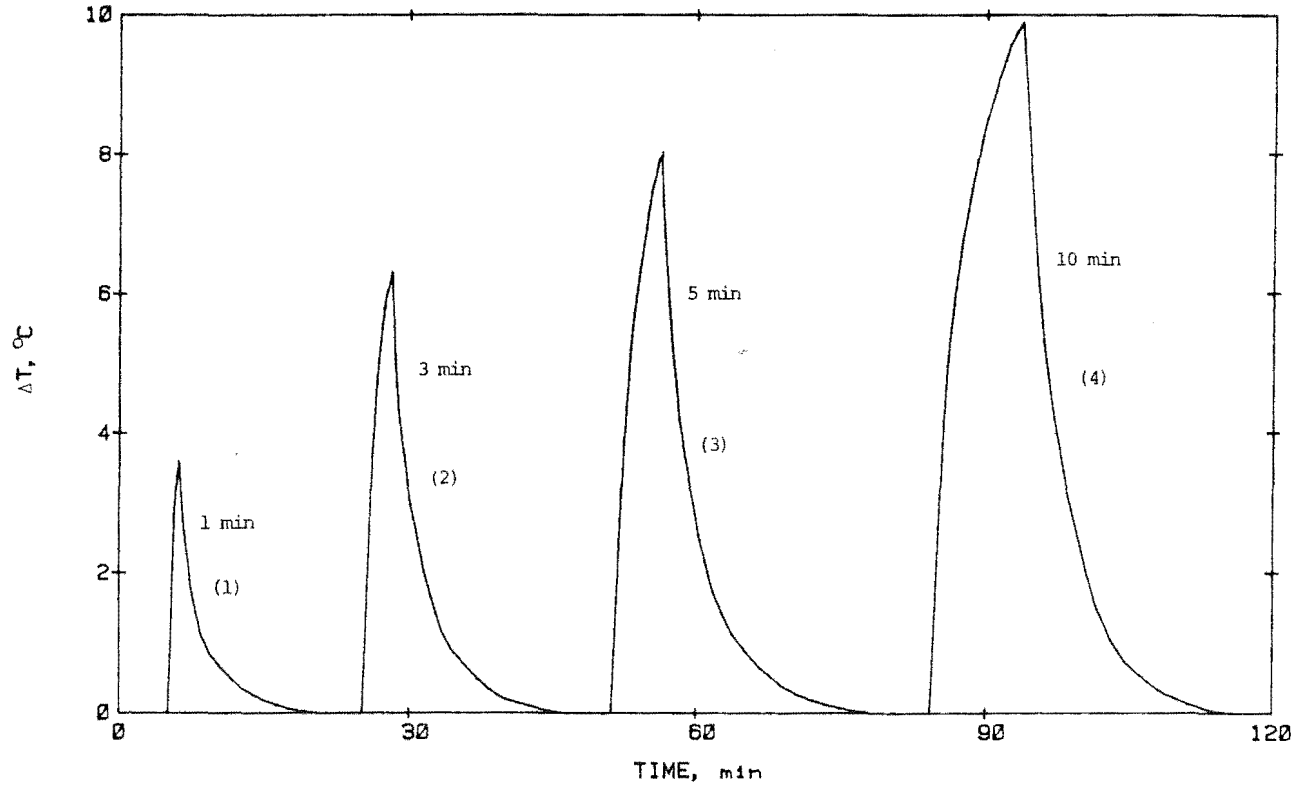

Figure 84. DTA curves resulting from calibration runs with a fixed bed temperature

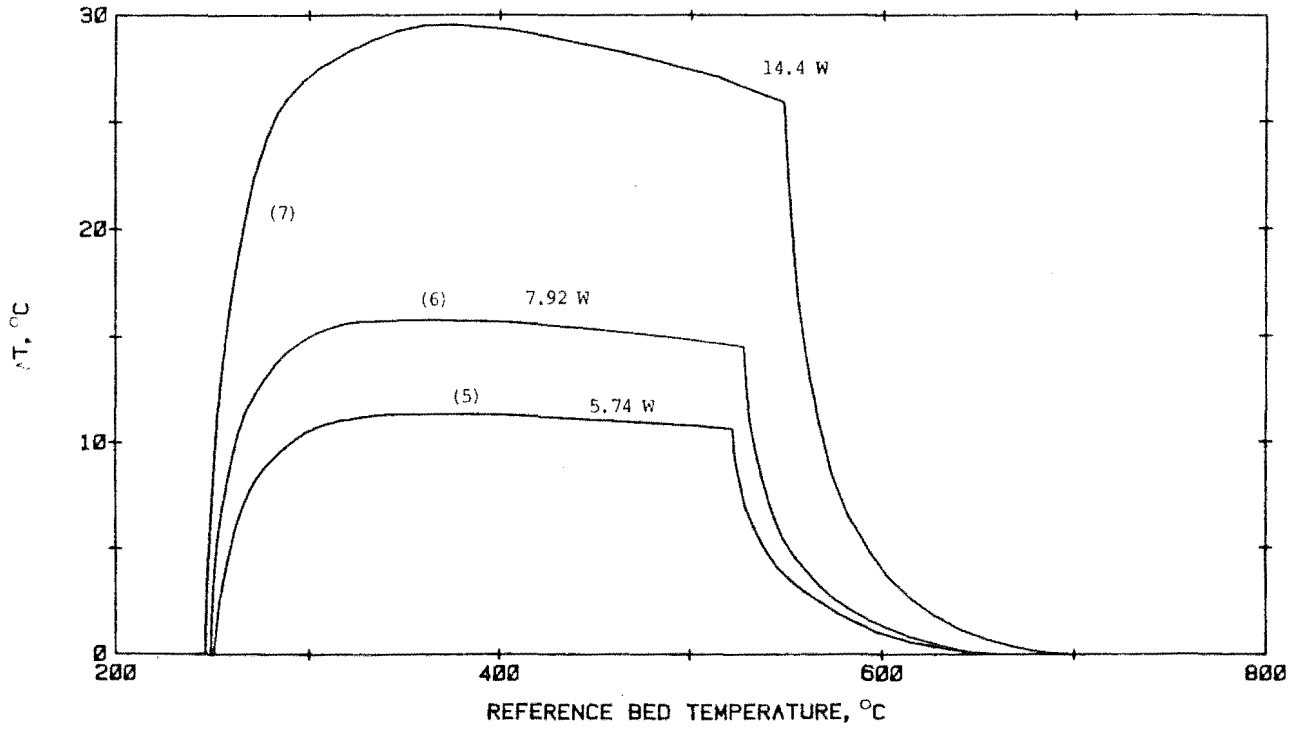

Figure 85. DTA curves resulting from calibration runs with the bed temperature rising at a steady rate

Table 7. Internal Calibration

Curve No.	Power input, kJ	Area under curve, deg min	Area per kJ, deg min
1	0.34	11.06	32.72
2	1.01	32.10	31.72
3	1.69	55.85	33.09
4	3.38	107.59	31.88
5	16.53	568.55	34.40
6	24.71	806.91	32.66
7	52.88	1656.91	31.32

where no flaming combustion occurred, this is the actual heat of reaction. However, in those runs where flaming combustion occurred, some of the heat released was not transmitted to the bed and therefore the computed heat of reaction was lower than the actual value.

As shown in Table 8, the heat released by the various substances per unit weight increased in the order : cellulose, wood, extractives, lignin and char. This is almost in the same order as their carbon contents. For the same substance, there was not a great deal of difference between the computed heats of reaction in air and in an oxygen-rich environment. Taking the heat of combustion of Rubber wood to be 18500 kJ/kg, the same as its calorific value (Leong, 1983), it is noted that only between 50% and 70% of the heating value of the wood was transmitted to the bed in the various combustion runs. The rest were either locked in the unreacted pyrolysis products or escaped to the surroundings. The heats of combustion of cellulose, acid lignin and char are about 16000 kJ/kg, 24000 kJ/kg and 29000 kJ/kg respectively (Susott et al., 1975). From these figures, the heat recovery rates for these substances were estimated at 40-50% for cellulose, around 65% for acid lignin and 60-80% for the char.

Table 8. Heats of Reaction

Sample	Heat of reaction (kJ/kg) in run in				
	21% O_2	40% O_2	60% O_2	80% O_2	100% O_2
cellulose	7800	-	-	6500	-
acid lignin	15900	-	-	15400	-
extractives	12900	-	-	12400	-
char					
-10+18 mesh	21600	-	-	22700	-
3.6 mm diam pcs	17800	-	-	23600	-
7.0 mm diam pcs	-	-	-	21300	-
Rubber wood					
-5+10 mesh	9100	-	11400	-	12600
5 mm diam pcs	10700	9900	10000	9500	-
10 mm diam pcs	9500	10300	8500	10200	-

6.4.4 Comparison with Other Wood Species

Runs in air and in 80% O_2 were also carried out for the other wood species, including the bark of the Rubber tree. The test samples consisted of 5 mm diameter pieces of height 11 mm. A uniform sample size of 1 gm was used. Particulars of the resultant DTA curves are presented in Tables 9 and 10 while the curves themselves can be found in Appendix 4.

No flaming or glowing combustion occurred in any of the runs in air. Each of the DTA curves contained two exotherms, as in the case of Rubber wood. The first exotherm, however, appeared more like a shoulder in some of them, as shown in Figure 86. The location of the first peak varied from 302°C (Oil palm wood) to 364°C (Nyatoh, Tembusu and Chengal) and that of the second peak from 401°C (Oil palm wood) to 501°C (Chengal). The height of the first peak, measured on a

Table 9. Locations and Heights of Reaction Peaks (DTA in Air)

Species	First peak		Second peak	
	Centre, °C	Height, °C	Centre, °C	Height, °C
Oil palm wood	302	12.5	401	14.2
Jelutong	338	10.7	432	16.5
Mengkulang	353	6.3	435	22.5
Pulai	347	9.8	436	16.5
Mersawa	351	4.6	458	21.0
Meranti, light red	348	6.0	463	13.9
Meranti, dark red	363	5.0	472	13.3
Sepetir	339	8.9	428	18.0
RUBBER WOOD	343	8.9	426	16.3
Nyatoh	364	4.7	449	24.0
Keruing	356	4.7	478	17.5
Tualang	359	5.7	464	19.0
Ramin	341 ?	7.1 ?	426	18.5
BARK	339	4.8	451	22.5
Tembusu	364	4.6	490	13.4
Merbau	356	5.9	451	19.5
Kempas	356	5.0	480	14.8
Chengal	364	4.0	501	15.7
Coconut wood	360	4.9	474	18.8
Balau	361	3.9	498	16.0

Table 10. Locations and Heights of Reaction Peaks (DTA in 80% O_2)

Species	First peak		Second peak	
	Centre, °C	Height, °C	Centre, °C	Height, °C
Oil palm wood	263	85.0	-	-
Jelutong	284	64.0	-	-
Mengkulang	310	8.3	362	54.0
Pulai	287	65.0	-	-
Mersawa	322	7.9	385	48.0
Meranti, light red	321	8.5	406	27.0
Meranti, dark red	338	7.6	409	36.0
Sepetir	295	59.5	-	-
RUBBER WOOD	295	49.5	-	-
Nyatoh	350	6.5	393	55.0
Keruing	354	6.2	425	37.0
Tualang	340	9.0	408	36.0
Ramin	316	42.0	-	-
BARK	308	8.4	378	36.0
Tembusu	360	5.5	449	28.0
Merbau	325	9.5	375	44.0
Kempas	335	9.3	411	28.5
Chengal	357	5.2	438	39.5
Coconut wood	330	5.7	402	37.0
Balau	358	4.5	449	39.0

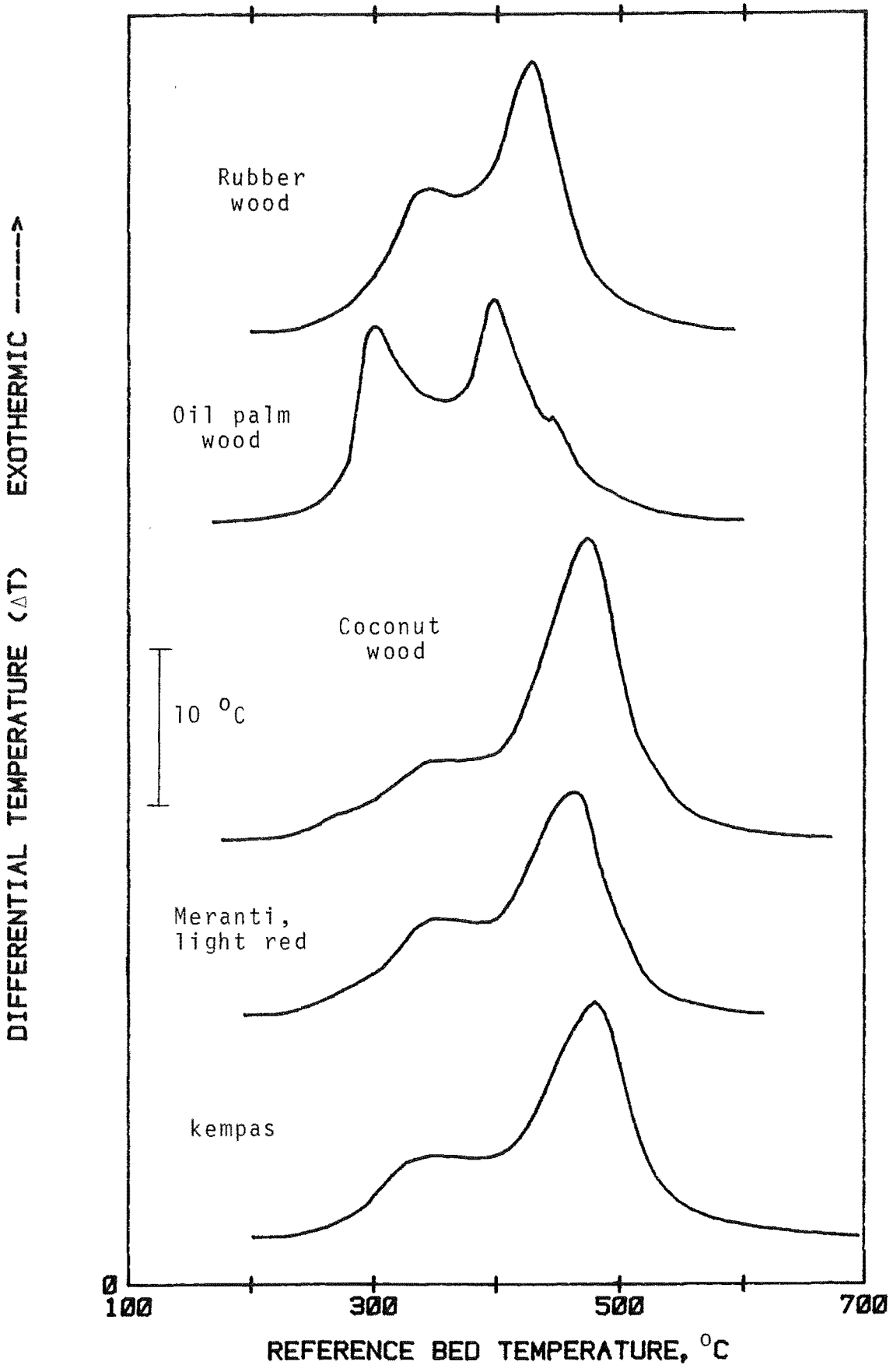

Figure 86. DTA curves in air of some wood species

temperature scale for convenience, varied from 3.9°C (Balau) to 12.5°C (Oil palm wood) and that of the second peak from 13.3°C (dark red Meranti) to 24°C (Nyatoh). In the case of Ramin, the location and height of the first peak could not be ascertained because of poor resolution. In all of the curves, the second peak was the taller of the two and, in general, the lower the density of the wood, the higher was its first peak. Of the twenty wood species tested, Rubber wood ranked fourth, together with Sepetir, in terms of height of first peak - after Oil palm wood, Jelutong and Pulai. As this peak resulted from thermal degradation of the volatiles, either the yield of these products is higher in Rubber wood than in most of the other species under study or Rubber wood gives out these products more readily than the other species. The location of the second exotherm, which resulted from burning of the residual char, provides an indication of the burning time of a wood sample and the farther away it is from the origin, the longer is its burning time. It follows that since the second peak temperature of Oil palm wood was the lowest of the various wood species, its burning time was the shortest. The difference between the second peak temperatures of two wood samples divided by the heating rate gives approximately the difference in their burning times. Based on this criterion, the burning times of the other wood samples relative to that of Oil palm wood were calculated. As shown in Table 11, the other wood species took between 4.5 minutes and 18.2 minutes longer to burn to completion compared with Oil palm wood. With a few exceptions, the greater the density of a wood species, the longer was its burning time. Rubber wood ranked second, along with Ramin, in terms of fastness of burning.

Of the runs conducted in 80% O_2, flaming combustion occurred in only four of them, namely in those involving Oil palm wood, Jelutong, Pulai and Sepetir. Each of their DTA curves contained only one peak, as a result of glowing combustion occurring in the residual char almost immediately

Table 11. Burning Times Relative to that of Oil Palm Wood (DTA in Air)

Species	Ranking in density	Extra burning time, min
Oil palm wood	20	0
RUBBER WOOD	12	4.5
Ramin	8	4.5
Sepetir	13	4.9
Jelutong	19	5.1
Mengkulang	18	6.2
Pulai	17	6.4
Nyatoh	11	8.7
BARK	7	9.1
Merbau	5	9.1
Mersawa	16	10.4
Meranti, light red	15	11.3
Tualang	8	11.5
Meranti, dark red	14	12.9
Coconut wood	2	13.3
Keruing	10	14.0
Kempas	4	14.4
Tembusu	6	16.2
Balau	1	17.6
Chengal	3	18.2

after flaming combustion subsided. In the case of Ramin, although no flaming combustion occurred during the run, its char began to burn by glowing combustion at a relatively low temperature - around 300°C. That is why there was only one peak in its DTA curve. All the DTA curves of the other samples contained two peaks. A few of these curves are shown in Figure 87. Thus, including Rubber wood, flaming combustion occurred in only five of the twenty wood species tested. Again the burning time of Oil palm wood was the shortest. The burning times of the other wood species relative to that of Oil palm wood were calculated in the same way as for the runs in air. As shown in Table 12, the other wood species took between 4 minutes and 34 minutes longer to burn to completion compared with Oil palm wood. Again, with a few exceptions, the lighter species were easier to burn. This time, Rubber wood ranked fourth - after Oil palm wood, Jelutong and Pulai.

For the same wood species, it took a shorter time to burn to completion in 80% O_2 than in air. As shown in Table 13, the time difference varied from around 8 minutes (Tembusu) to 27 minutes (Pulai). As expected, the difference was greater in those species which burnt with a flame in 80% O_2 than in those which did not. In Table 14, the various wood species were listed in descending order of height of the first peak from their DTA runs in air. It is interesting to note that the five species which burnt with a flame in 80% O_2 occupied the first five slots. Evidently the height of this peak has some bearing on the combustibility of the wood and also on its burning time (see Tables 11 and 12). It appears that the higher the peak, the easier it is for flaming combustion to take place in the wood and the shorter is its burning time. In short, the wood burns more easily.

To carry the comparison a step further, two additional sets of runs were conducted, viz (1) in 60% O_2 for those species which burnt with a flame in 80% O_2 using a sample size of 1 gm and (2) in 80% O_2 for the remaining ones using a

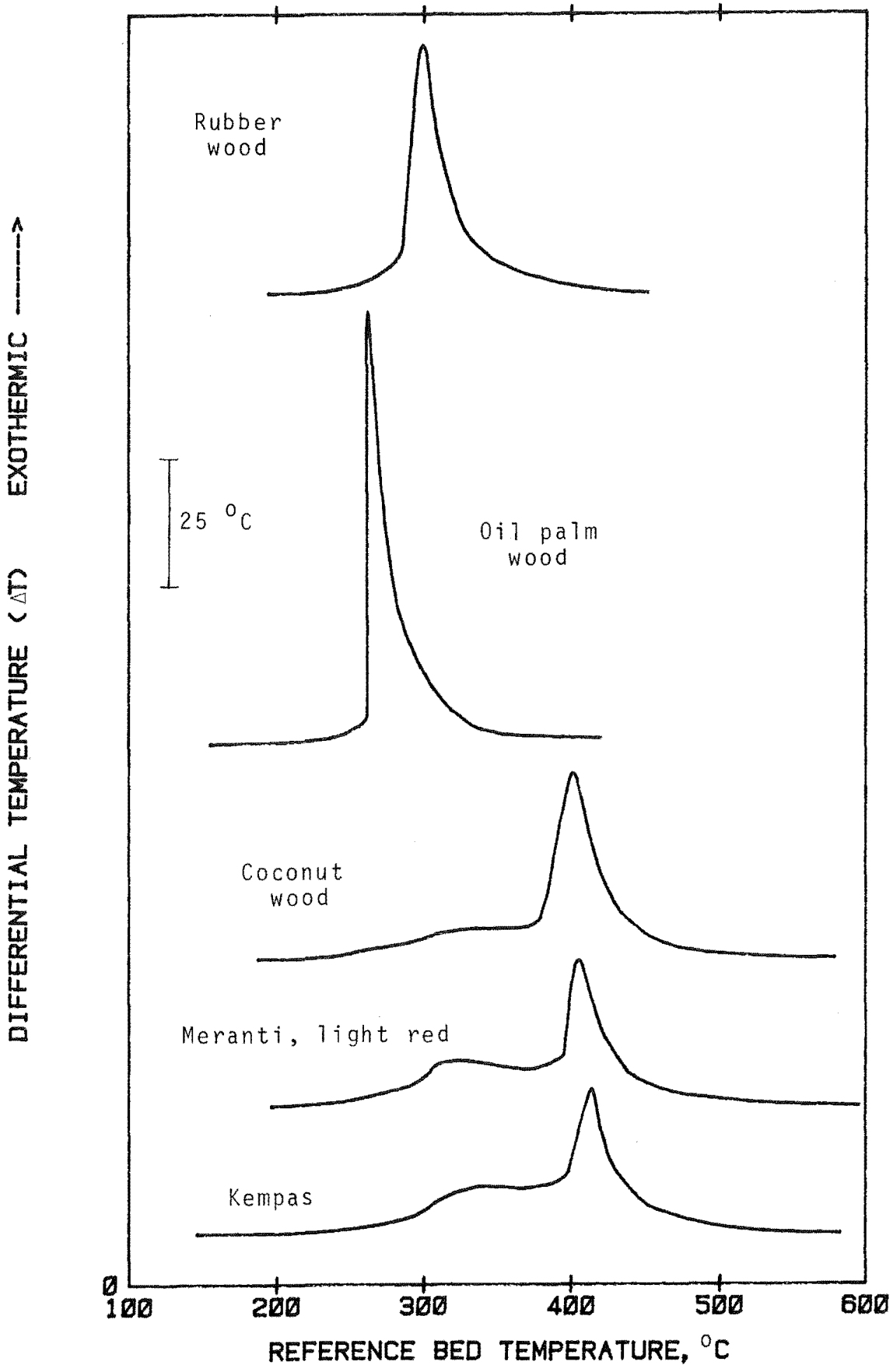

Figure 87. DTA curves in 80% O_2 of some wood species

Table 12. Burning Times Relative to that of Oil Palm Wood (DTA in 80% O_2)

Species	Ranking in density	Extra burning time, min
Oil palm wood	20	0
Jelutong	19	3.8
Pulai	17	4.4
RUBBER WOOD	12	5.8
Sepetir	13	5.8
Ramin	8	9.6
Mengkulang	18	18.0
Merbau	5	20.4
BARK	7	20.9
Mersawa	16	22.2
Nyatoh	11	23.6
Coconut wood	2	25.3
Meranti, light red	15	26.0
Tualang	9	26.4
Meranti, dark red	14	26.5
Kempas	4	26.9
Keruing	10	29.5
Chengal	3	31.8
Tembusu	6	33.8
Balau	1	33.8

Table 13. Difference in Burning Times between Runs in Air and in 80% O_2

Species	Ranking in density	Time difference min
Pulai	17	27.1
Jelutong	19	26.9
Oil palm wood	20	25.1
Sepetir	13	24.2
RUBBER WOOD	12	23.8
Ramin	8	20.0
Merbau	5	13.8
Mersawa	16	13.3
Mengkulang	18	13.3
BARK	7	13.3
Coconut wood	2	13.1
Kempas	4	12.5
Chengal	3	11.5
Meranti, dark red	14	11.5
Meranti light red	15	10.4
Nyatoh	11	10.2
Tualang	9	10.2
Keruing	10	9.6
Balau	1	8.9
Tembusu	6	7.5

Table 14. Heights of First Peaks from DTA Runs in Air

Species	Ranking in density	Height of first peak, ^{o}C
Oil palm wood	20	12.5
Jelutong	19	10.7
Pulai	17	9.8
Sepetir	13	8.9
Ramin	8	7.1 ?
Mengkulang	18	6.3
Meranti, light red	15	6.0
Merbau	5	5.9
Tualang	9	5.7
Kempas	4	5.0
Meranti, dark red	14	5.0
Coconut wood	2	4.9
BARK	7	4.8
Keruing	10	4.7
Nyatoh	11	4.7
Mersawa	16	4.6
Tembusu	6	4.6
Chengal	3	4.0
Balau	1	3.9

sample size of 1.5 gm instead of the usual 1 gm. The test samples consisted of 5 mm diameter pieces, i.e. the same as before. In the first set of runs, flaming combustion occurred in Oil palm wood, Jelutong and Pulai but not in Rubber wood and Sepetir. In the second set, it took place only in Ramin, Mengkulang and light red Meranti which came as no surprise as these three species were listed just below the above five in Table 14 on first peak height. The results obtained enabled the various wood species under study to be divided into four groups in terms of combustibility. These are :-

Group 1 : Oil palm wood, Jelutong and Pulai
Group 2 : RUBBER WOOD and Sepetir
Group 3 : Ramin, Mengkulang and light red Meranti
Group 4 : Merbau, BARK, Mersawa, Tualang, Nyatoh, Kempas, Coconut wood, dark red Meranti, Keruing, Chengal, Balau and Tembusu

In the above listing, the combustibility of the wood decreases from Group 1 to Group 4. Group 4 may be sub-divided by carrying out further runs using other experimental conditions, such as using a larger sample size or increasing the particle size.

6.4.5 Comparison between Wood from Different Trees

The source of Rubber wood in the experiments conducted so far was the fresh wood of **Tjir 1**. Runs in air and in 60% and 80% O_2 were also carried out for the wood of **PR 107, RRIM 605** and **RRIM 623.** The test samples consisted of 5 mm diameter wood pieces and, as usual, a sample size of 1 gm was used. The DTA curves resulting from the runs in air are shown in Figure 88 together with that of **Tjir 1.** Particulars of the curves are provided in Table 15. There was very little variation in the location and height of the first peak. The variation was greater in the second peak, especially between the wood of **PR 107** and **RRIM 605.** The second peak of **PR 107**

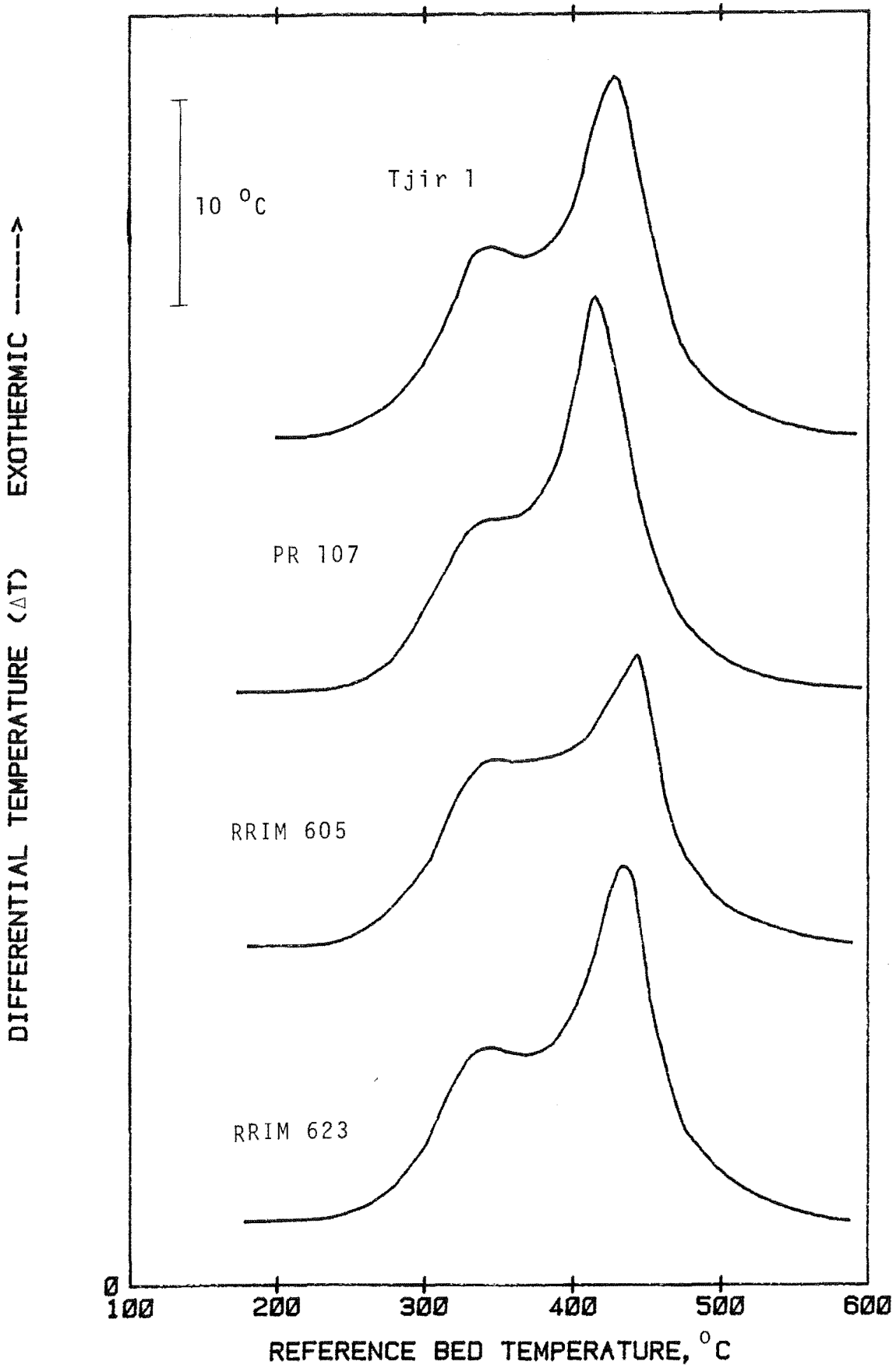

Figure 88. DTA curves in air of Rubber wood from different trees

Table 15. Locations and Heights of Reaction Peaks (Wood from Different Trees)*

Source of wood	First peak		Second peak	
	Centre, °C	Height, °C	Centre, °C	Height, °C
Tjir 1	345	8.5	428	16.2
PR 107	345	7.9	419	17.3
RRIM 605	344	8.3	443	13.3
RRIM 623	340	8.3	435	14.9

*mean values of duplicate runs.

was the highest of the four, besides being centred at the lowest temperature. It will be remembered that the thermal behaviour of the wood of **PR 107** in N_2 was slightly different from those of the other three trees (see Figure 45). On the whole, the variation in the reaction peak temperatures of the wood from the four trees was very small compared with that between Rubber wood and the other tropical hardwoods. No flaming combustion occurred in any of the runs in 60% O_2. In the runs in 80% O_2, flaming combustion took place in all of them. As expected, there was only one peak in each of the resultant DTA curves (Figure 89). The four peaks were located at about the same temperature, i.e around 300°C. It may therefore be concluded that there is no significant difference in the combustion characteristics of the wood obtained from the four trees.

6.4.6 Comparison between Fresh and Mouldy Wood

The combustion characteristics of the fresh and the mouldy wood from two of the trees (**PR 107** and **RRIM 623**) in air and in 60% and 80% O_2 were compared. As usual, the comparison was made using 5 mm diameter wood pieces with a

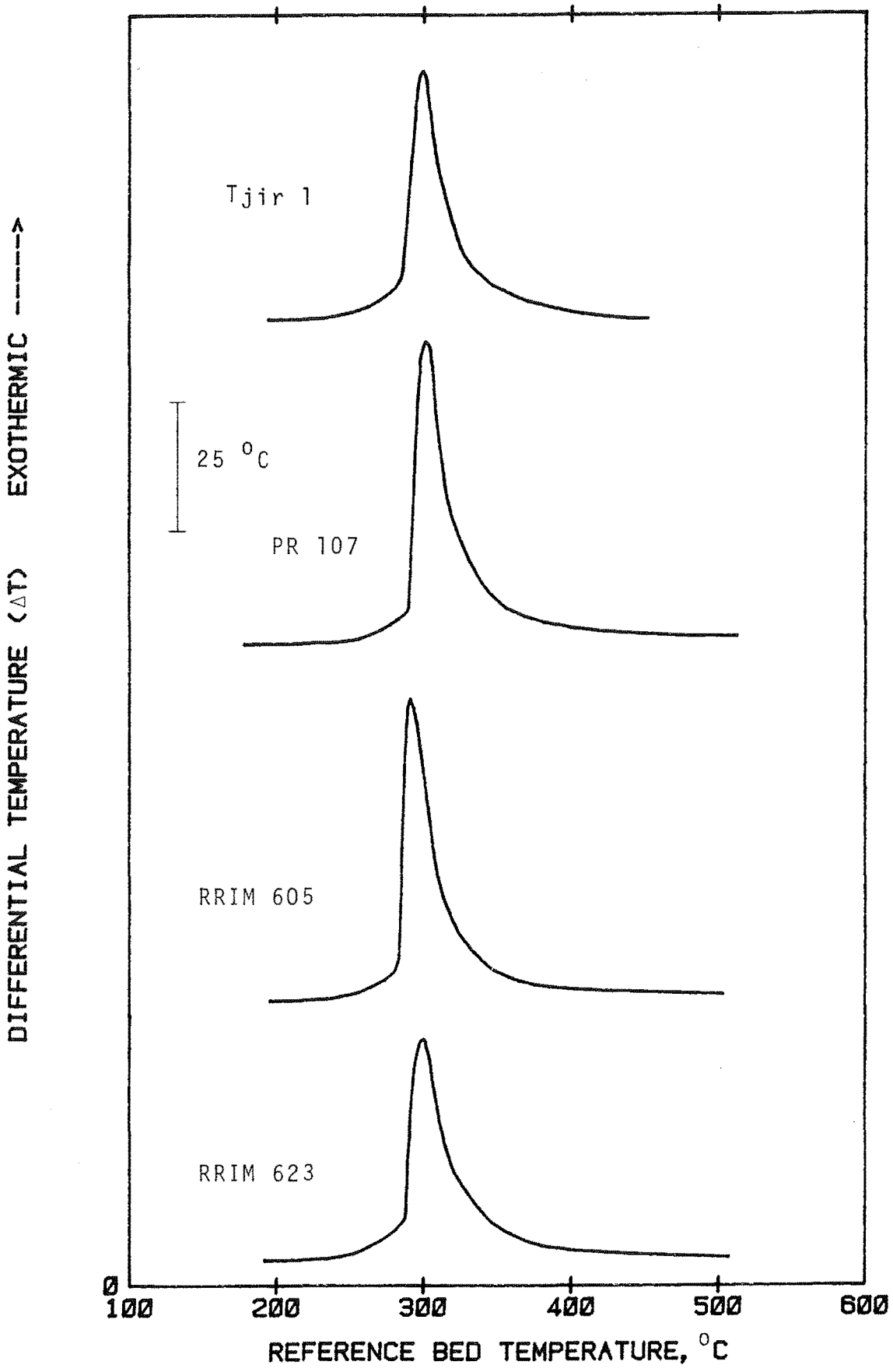

Figure 89. DTA curves in 80% O_2 of Rubber wood from different trees

sample size of 1 gm. Particulars of the resultant DTA curves in air are given in Table 16. There was very little difference in the locations of the two peaks between the two types of wood from each tree. The difference was greater in the height of the first peak, with that of the mouldy wood being higher by 11-16%. No flaming or glowing combustion occurred in any of these runs. In the runs in 60% O_2, there was again no flaming combustion. Both flaming and glowing combustions occurred in the runs in 80% O_2. Thus, the difference in the combustion characteristics of the fresh and the mouldy wood, if any, is very small compared with that between Rubber wood and other wood species.

Table 16. Locations and Heights of Reaction Peaks (Fresh and Mouldy Wood)*

Type of wood	First peak		Second peak	
	Centre, °C	Height, °C	Centre, °C	Height, °C
PR 107				
Fresh	345	7.9	419	17.3
Mouldy	336	9.4	426	15.3
RRIM 623				
Fresh	340	8.3	435	14.9
Mouldy	337	9.3	429	15.9

*mean values of duplicate runs.

6.4.7 Effect of Chemical Treatment

DTA has often been used to study the effect of chemical treatment on the pyrolysis and combustion of wood. It provides a useful means of evaluating a chemical compound for its potential value as a fire retardant. Using a fixed bed apparatus, Tang (1972) has investigated the fire retarding potentialities of a variety of chemicals, including sodium

tetraborate decahydrate (borax), sodium chloride, potassium bicarbonate and ammonium dihydrogen phosphate.

As a side interest, the effect of treatment of Rubber wood with borax on its combustibility was examined. The test samples (5 mm diameter pieces) were treated by immersing in 20% (w/w) borax solution for 3½ hours. The solution was maintained at around 85°C during treatment and the treated pieces were oven-dried before use. The chemical retention in the wood was not determined but is expected to be quite substantial in view of the strong solution used. Runs in air and in 80% O_2 were carried out using 1 gm samples. The resultant DTA curves are compared with those of the untreated wood in Figure 90. No flaming or glowing combustion occurred in the run in air. The DTA curve of this run was distinctly different from that of the untreated wood. It contained three reaction peaks (marked 'A', 'B' and 'C') instead of the usual two, with the last one being the largest and the most well-defined of the three. Peak A, which is attributed to the volatiles, was located at about the same temperature as that of the untreated wood but its height was slightly over half that of the latter (5.0°C compared with 8.9°C). Peak C, which was centred at 521°C, is attributed to degradation of the residual char. It is not known whether Peak B, which was centred at 424°C, is due to the volatiles or char. It took the treated wood a longer time to burn to completion compared with any of the twenty wood species tested, the time difference being 21.8 minutes relative to that of Oil palm wood.

No flaming combustion occurred in the run in 80% O_2. The residual char burnt by glowing combustion, giving rise to two peaks - one located at 369°C and the other at 481°C. Another run was carried out in 80% O_2, this time using a 2 gm sample. Again no flaming combustion occurred during the run. The chemical treatment had undoubtedly drastically reduced the combustibility of the wood, from one which ranked highly of

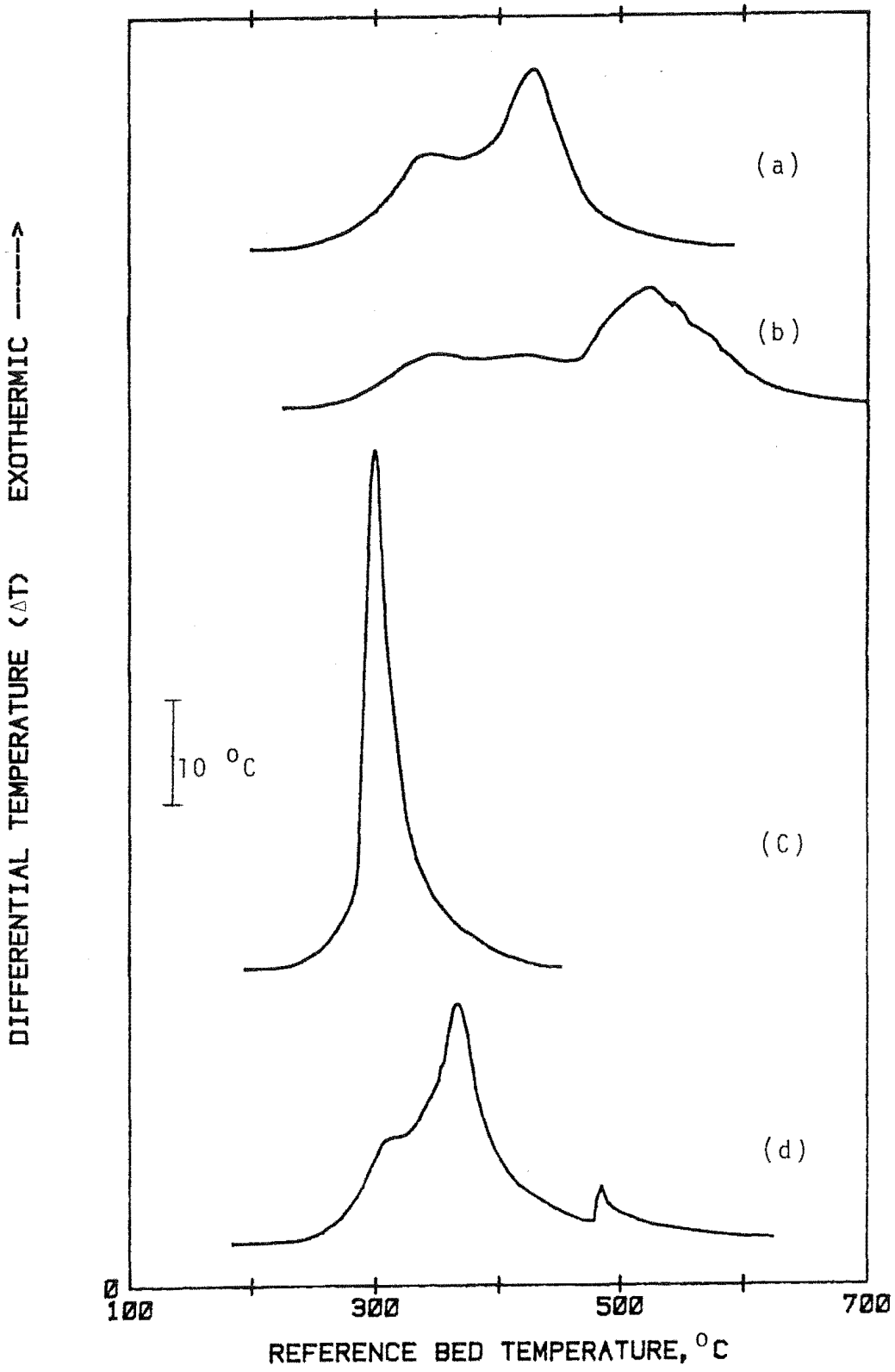

(a) DTA curve in air of untreated wood
(b) DTA curve in air of treated wood
(c) DTA curve in 80% O_2 of untreated wood
(d) DTA curve in 80% O_2 of treated wood

Figure 90. DTA curves of treated and untreated Rubber wood

the wood species being tested to among those in the bottom rung, if not the bottom-most. It achieved this by reducing the rate of production of the volatile products, as indicated in the DTA curves. In fact, most of the flame retardants are formulated to produce this effect (Shafizadeh et al., 1982). Incidentally, besides being a potential fire retardant, borax is a well-established wood preservative (Findly, 1960).

Other prospective fire retardants may be tested in a similar manner. The main advantage of this apparatus, as mentioned before, is that it enables larger wood pieces or a larger sample size to be used, which is not normally possible with the conventional fixed-bed apparatus.

6.5 Temperature Drop across Reactor

In all the DTA runs, heat is transferred from the furnace to the bed via the heat sink, magnesia, the reactor tube and a wall-to-bed boundary layer. The temperature drop across each of them for a bed temperature of 400^{o}C was calculated. This was done for one side of the reactor and for a section of length 70 mm, corresponding to the height of the expanded bed at this temperature (Figure 91). The calculations were based on conditions of a blank run, i.e. with only sand in each bed, a heating rate of 5.5^{o}C /min and an air flowrate of 4 lit/min. As a first approximation, it was assumed that the rate of temperature rise was the same in all the regions, and this was used to determine the heat flux into each region. The calculated temperature drops across the four regions, assuming steady state heat transfer, are as follows :

Region	Temp. drop, ^{o}C
wall-to-bed	2.79
reactor tube	0.21
magnesia	8.04
heat sink	7.80

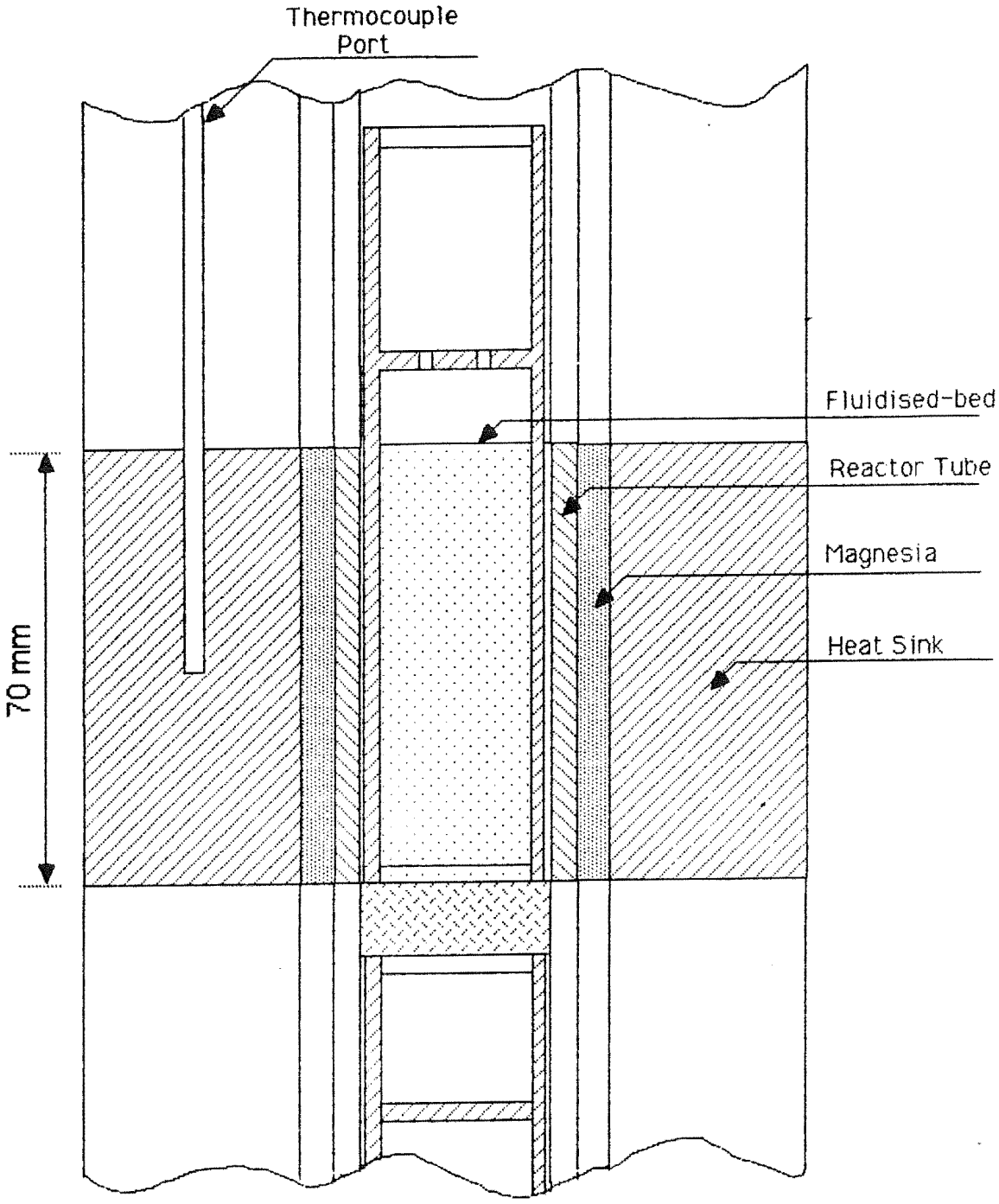

Figure 91. Cross-section of reactor showing the various regions

It is seen that the temperature drop is highest across the magnesia layer and lowest across the reactor tube. The total temperature drop across the reactor is 18.84°C. Details of the calculations are provided in Appendix 5.

The actual temperature drop from the heat sink to the bed was recorded as a function of the bed temperature in a separate blank run. In this run, a differential thermocouple was placed across the bed and a thermocouple port in the middle of the heat sink and a temperature thermocouple was inserted in the bed. As shown in the resultant DTA curve (Figure 92), the temperature drop from the middle of the heat sink to the bed (above 150°C) was fairly constant, varying only from 11°C to 12°C. Assuming that the temperature drop across the heat sink is linear, the temperature drop from the middle of the heat sink to the bed is calculated at 14.94°C , which is not very far off from the experimental value.

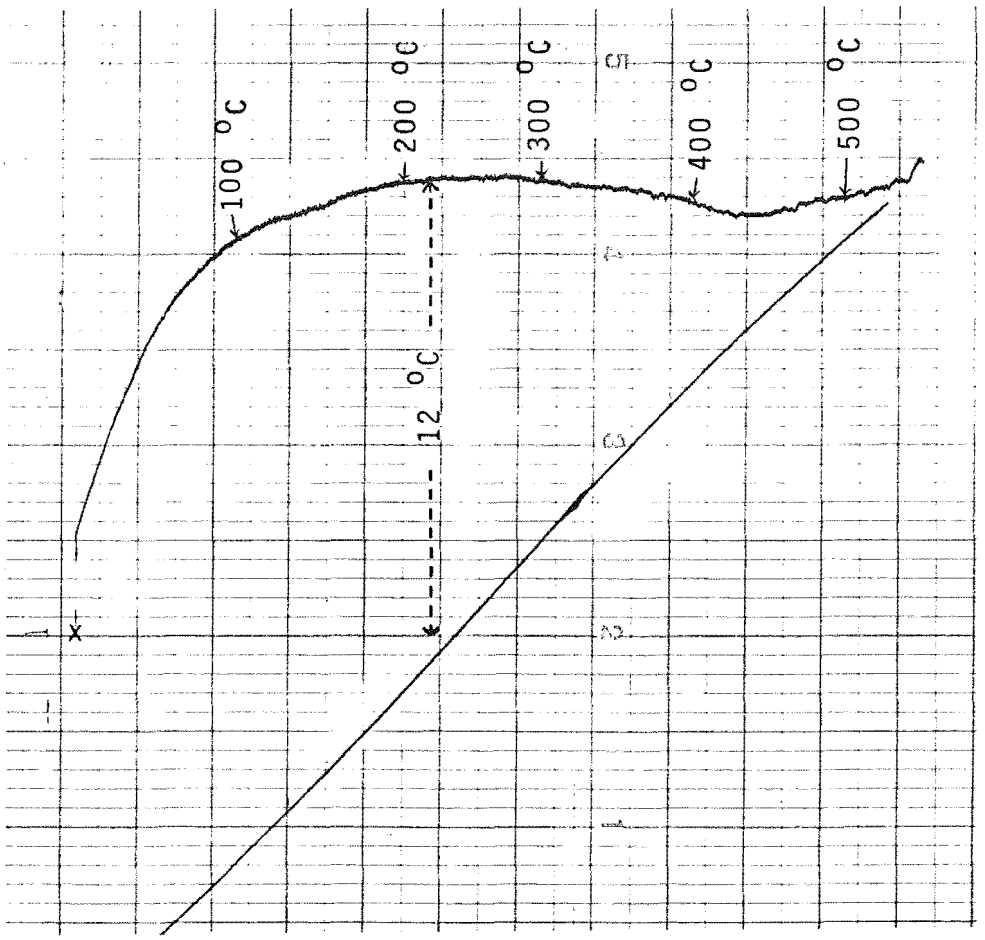

Figure 92. ΔT between the middle of the heat sink and a fluidised bed as a function of the bed temperature

SECTION II

THEMOGRAVIMETRY

CHAPTER 7

THERMOGRAVIMETRY

7.1 Brief Introduction

Thermogravimetry (TG) is one of the most widely used methods of thermal analysis, especially for the study of the thermal stabilities of substances. It plays a complementary role to differential thermal analysis (DTA) in that the information obtained from the use of one of them is often enhanced by the application of the other. For example, in the case of wood, it can be used to determine the temperatures and the rates of pyrolysis while DTA provides information concerning the endothermic or exothermic nature of the reactions taking place. In addition, it gives the yields of the different pyrolysis products at various temperatures. Among those who have used it to study the thermal behaviour of wood and related products are Tang (1972), Fang et al.(1975), Shafizadeh and DeGroot (1975) and Beall et al.(1976). A recent review of the application of TG in this area of research has been provided by Nguyen et al.(1981).

A common TG instrument, or thermobalance, consists of the following items: (1) a sample holder, (2) a recording balance, (3) a furnace, (4) a temperature programmer, (5) a recorder and (6) an atmospheric controlling system. This is shown schematically in Figure 93. A variety of thermobalances are available in the market.

Very often in the course of a TG run, the rate of weight loss of the sample as a function of time is simultaneously recorded on the chart recorder along with the TG curve. This is known as derivative thermogravimetry, or DTG, and the curve resulting from it is called a DTG curve. In DTG curves, weight changes are represented as peaks as opposed to steps in the case of TG curves.

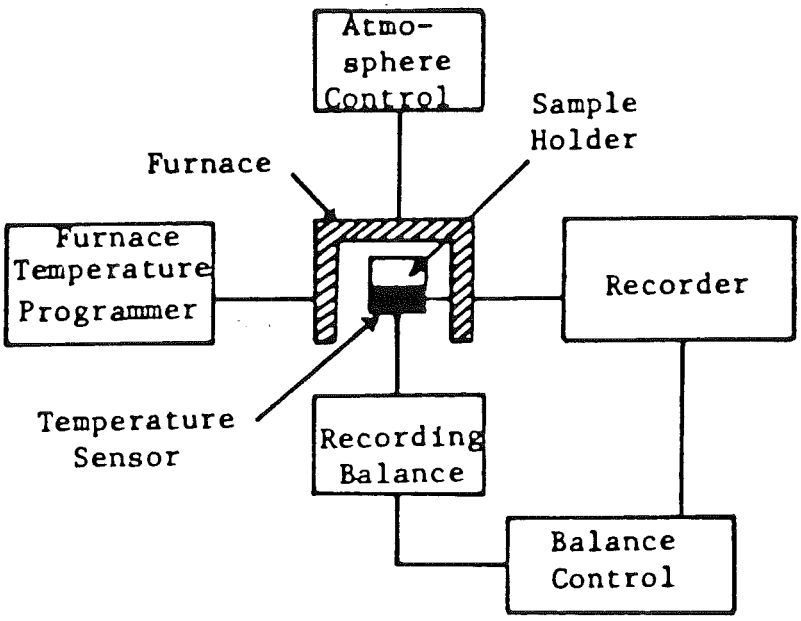

Figure 93. Schematic diagram of a modern thermobalance. After Wendlandt (1974)

7.2 Analysis using Stanton Redcroft TG-750 Thermobalance

Thermogravimetric analysis of Rubber wood was at first performed on a Stanton Redcroft TG-750 thermobalance in the Chemistry Division of the Department of Scientific and Industrial Research, Lower Hutt. This is a sensitive and automated apparatus and has an operating temperature range of between 20°C and 1000°C. It is designed mainly for thermal studies of substances involving small sample sizes, in the order of a few milligrams in the case of wood. A diagrammatic representation of the instrument is provided in Figure 94. The sample pan is 6 mm in diameter and is made of 5% rhodium-platinum. The sample temperature is measured by a plate-type platinum versus 0.3% rhodium-platinum thermocouple positioned approximately 1.5 mm from the sample pan.

Two particle sizes were used, namely (1) -36+72 mesh fraction and (2) single piece, in the shape of a cube of sides approximately 2.5 mm. The sample size varied between 6 mg and 8 mg. Runs were carried out in nitrogen and in air using a

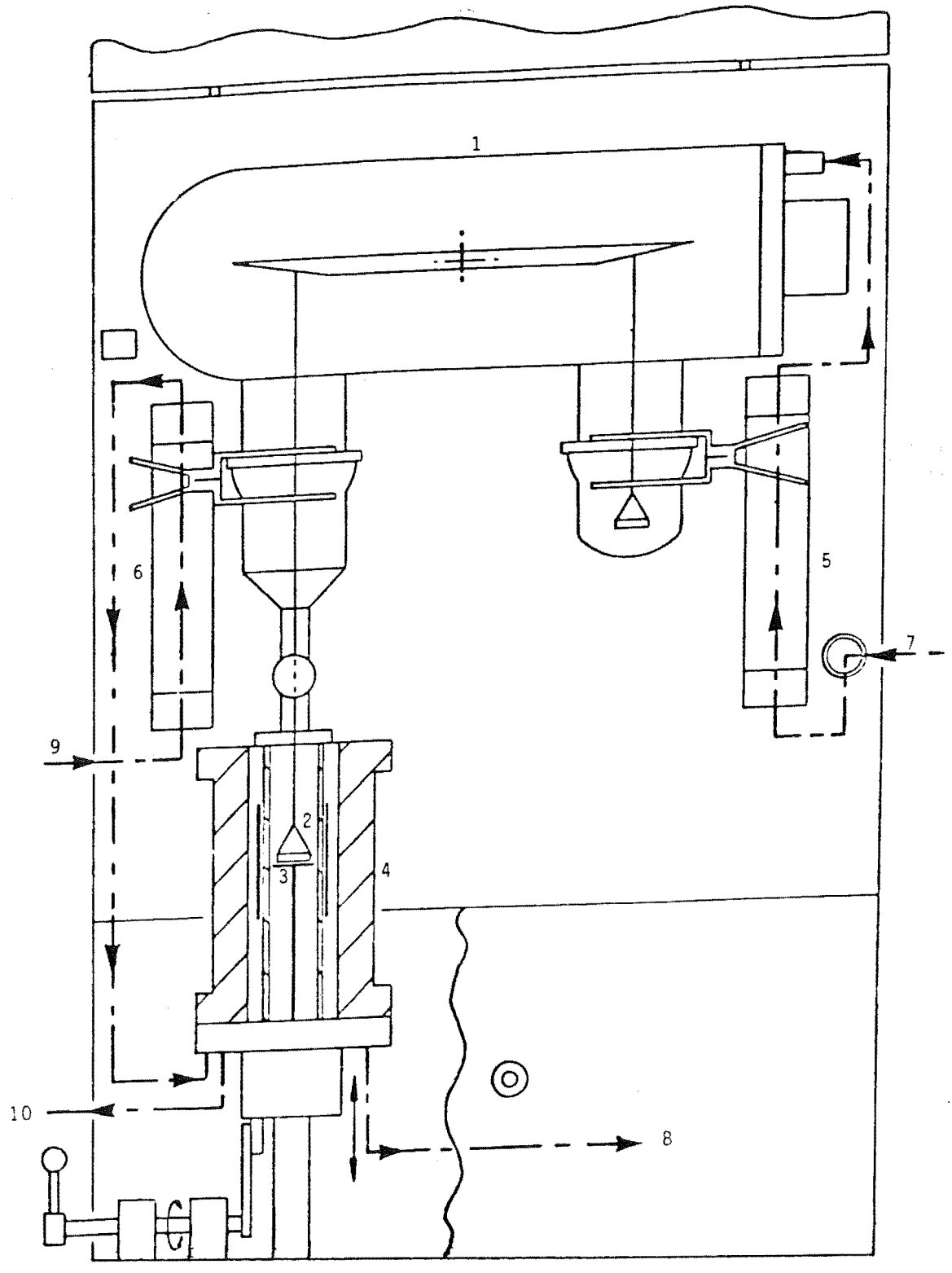

1. Electronic microbalance and glass vacuum assembly
2. Sample holder
3. Thermocouple
4. Furnace
5. Gas-flow meter
6. Water-flow meter
7. Gas inlet
8. Gas outlet
9. Water inlet
10. Water outlet

Figure 94. Main features of a Stanton Redcroft TG-650 thermobalance

flowrate of 50 ml/min. The sample was heated at a constant rate of 10°C/min. A Stanton Redcroft TG-770 differentiator connected to the thermobalance enabled the DTG curve to be plotted simultaneously on the chart recorder along with the TG curve.

7.2.1 In Nitrogen

Figure 95 shows the TG and DTG curves of the -36+72 mesh particles in N_2 while Figure 96 shows those of the single test piece. As shown in the figures, both the samples began to lose weight at around 150°C but it was only after 200°C that the weight loss began to gain momentum. The rate of weight loss continued to increase and reached a peak at about 370°C, after which it dropped sharply and began to level off at about 390°C. As shown in the DTG curves, it in fact slowed down between 310°C and 340°C before picking up again. The first peak was more well-defined in the DTG curve of the single test piece than in that of the -36+72 mesh particles. At the height of pyrolysis, each sample was losing weight at the rate of close to 10% of its original weight per minute. More char was produced by the single test piece than by the -36+72 mesh particles at the same temperature. At 550°C, for example, the char yield of the single test piece was 22% compared with 18% for that -36+72 mesh particles. This is consistent with the findings of Shafizadeh and DeGroot (1976) that the yield of char from wood increases with particle size.

With the aim of identifying the wood components responsible for each of the two peaks in the DTG curve of Rubber wood, two additional runs were carried out. The following samples were used : (1) -36+72 mesh particles, minus extractives and (2) -36+72 mesh particles, minus extractives and hemicelluloses. The DTG curves obtained were compared with that of the sample with all the components intact in Figure 97. It will be seen that removal of the extractives from the wood resulted in a reduction in the size of the first

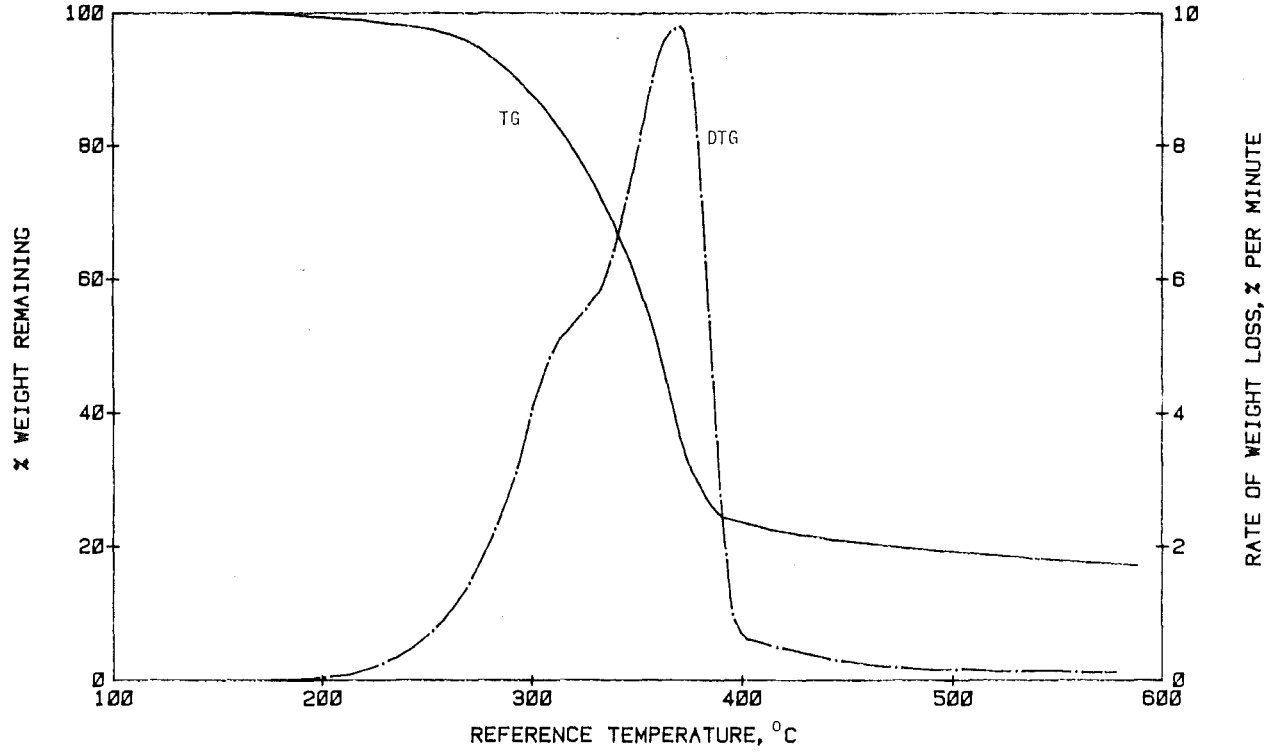

Figure 95. TG and DTG curves in N_2 of -36+72 mesh particles

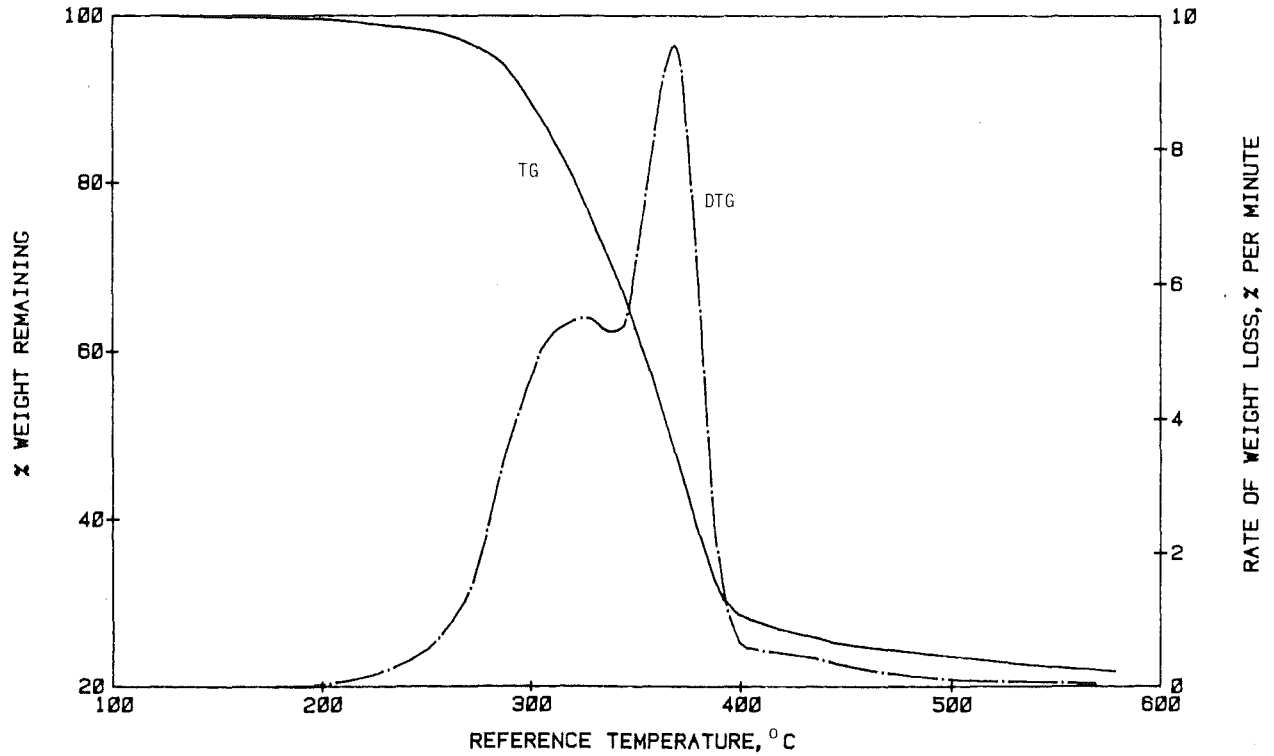

Figure 96. TG and DTG curves in N_2 of single test piece

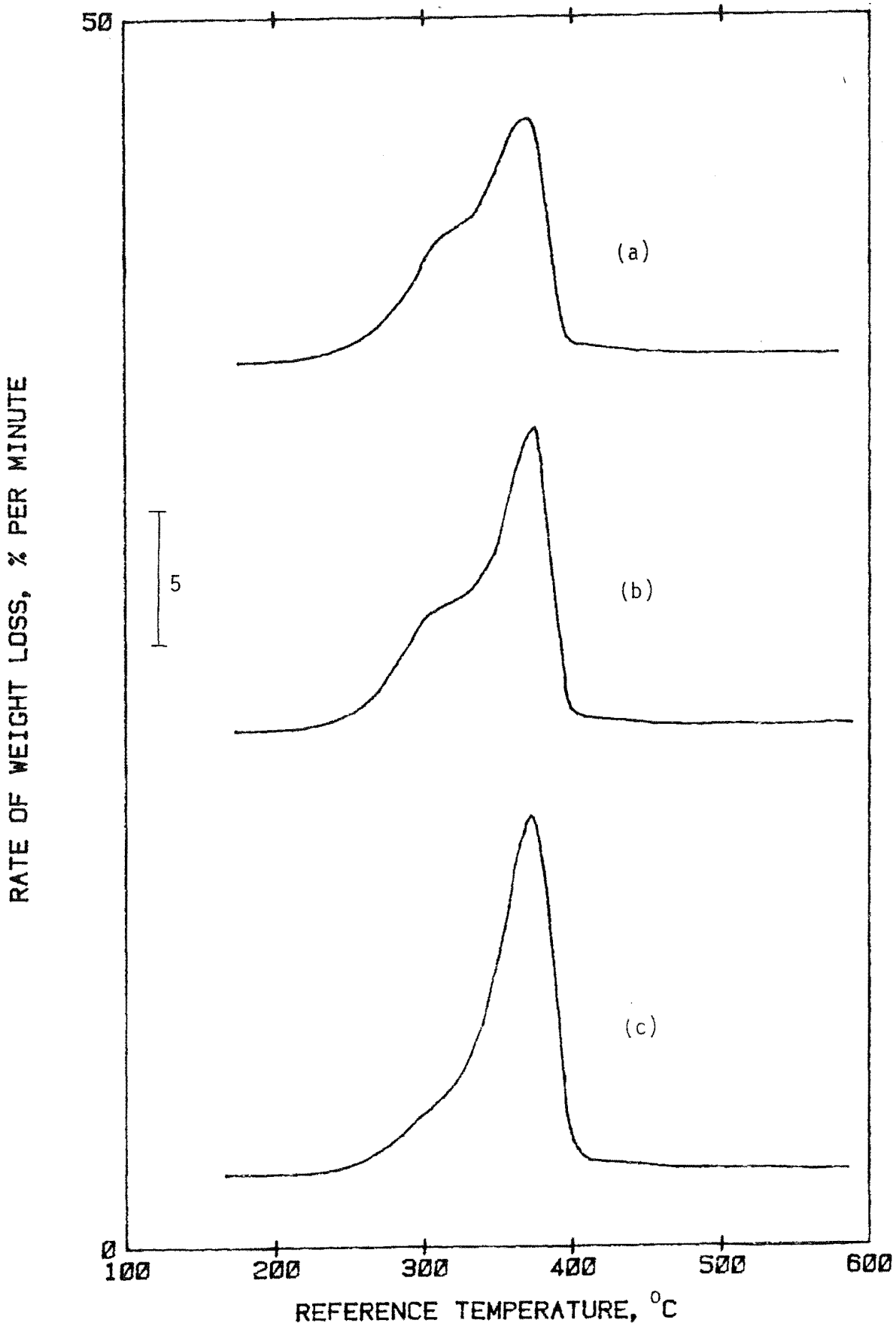

Figure 97. DTG curves in N_2 of -36+72 mesh particles (a) all components intact, (b) minus extractives and (c) minus extractives and hemicelluloses

peak relative to that of the second one. By removing the hemicelluloses from the wood, in addition to the extractives, the first peak was reduced to just a small bulge, while there was a corresponding increase in the height of the second peak. This indicates that the first peak in the DTG curve of Rubber wood is attributed mainly to the extractives and the hemicelluloses. The results obtained here serve to confirm that the exotherm preceeding the cellulose endotherm in the DTA curve of Rubber wood is indeed mainly due to these two components (see Figure 40). The second peak, which is centred at about 370°C, is evidently attributed to the remaining two components, i.e. cellulose and lignin.

7.2.2 In Air

The TG and DTG curves resulting from the runs in air were compared with those obtained earlier in N_2 in Figures 98-101. The sudden dip at around 440°C in each TG curve is due to degradation of the char. This appears as a third peak in the corresponding DTG curve. The reaction peaks from the runs in air were higher and nearer to the origin than those resulted from the runs in N_2. This means that pyrolysis of the wood not only occurred at a lower temperature but also at a faster rate in an oxidative environment than in an inert atmosphere. At the height of pyrolysis, the rate of weight loss of the single test piece was around 30% per minute as compared with around 23% per minute for the -36+72 mesh particles. As shown in the figures, the char of the single test piece burnt at a faster rate than that of the -36+72 mesh sample.

7.3 Analysis using DTA Apparatus

TG runs involving larger particle or sample sizes were carried out in the DTA apparatus incorporated with the necessary means for the weight of the sample to be read in the course of the experiment. The experimental set-up is shown in Figure 102. A 'Dexion' steel platform was built at a height

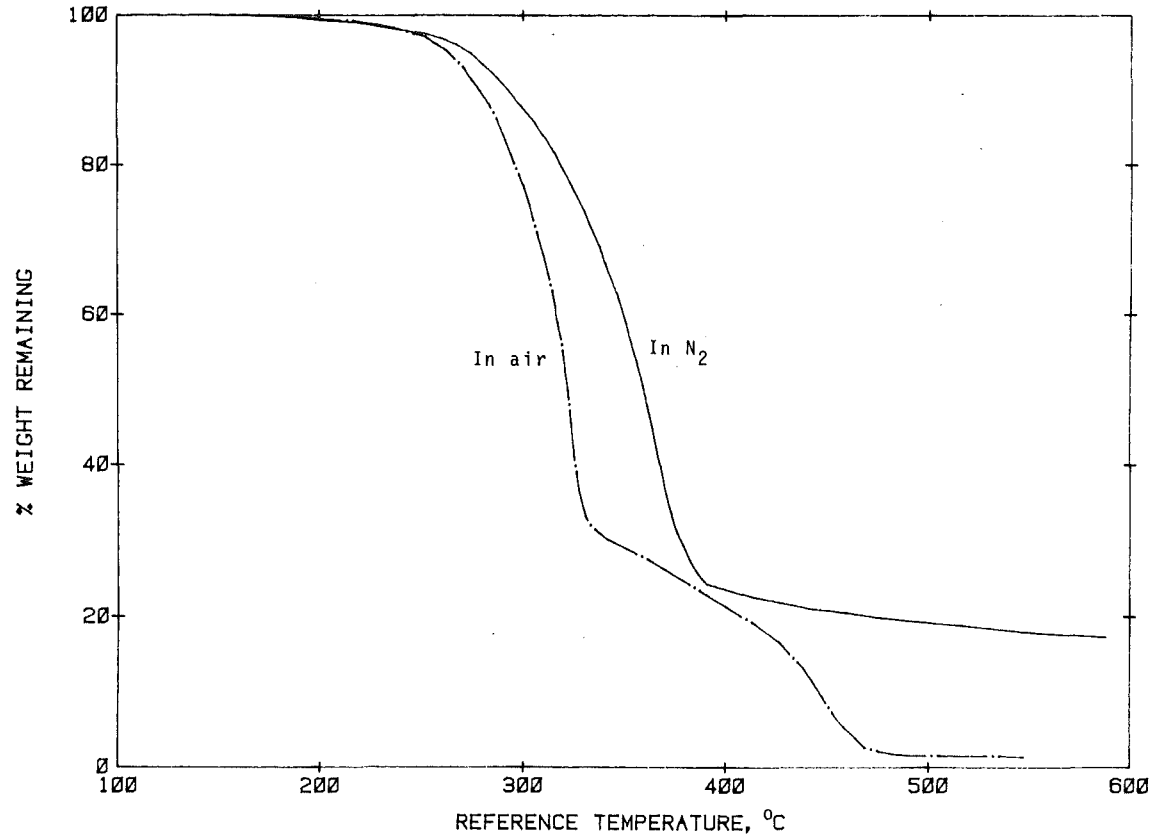

Figure 98. TG curves in N_2 and in air of -36+72 mesh particles

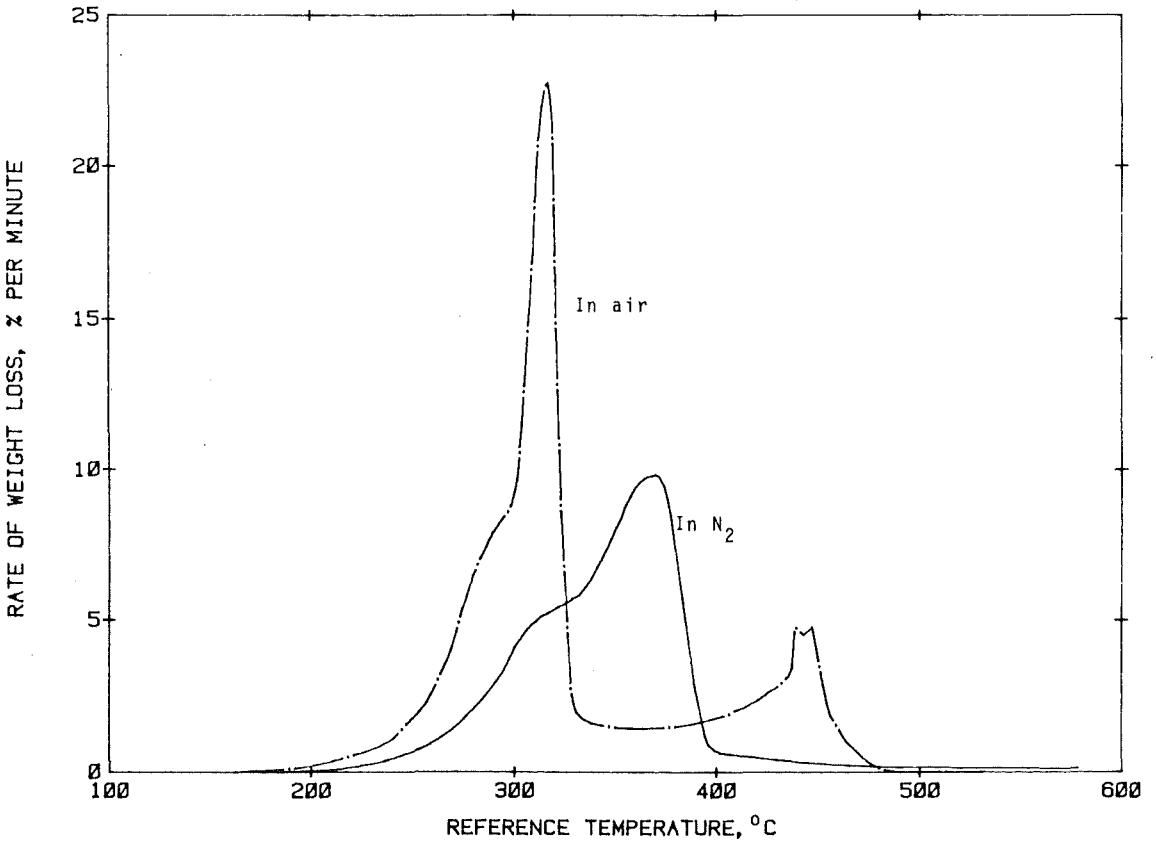

Figure 99. DTG curves in N_2 and in air of -36+72 mesh particles

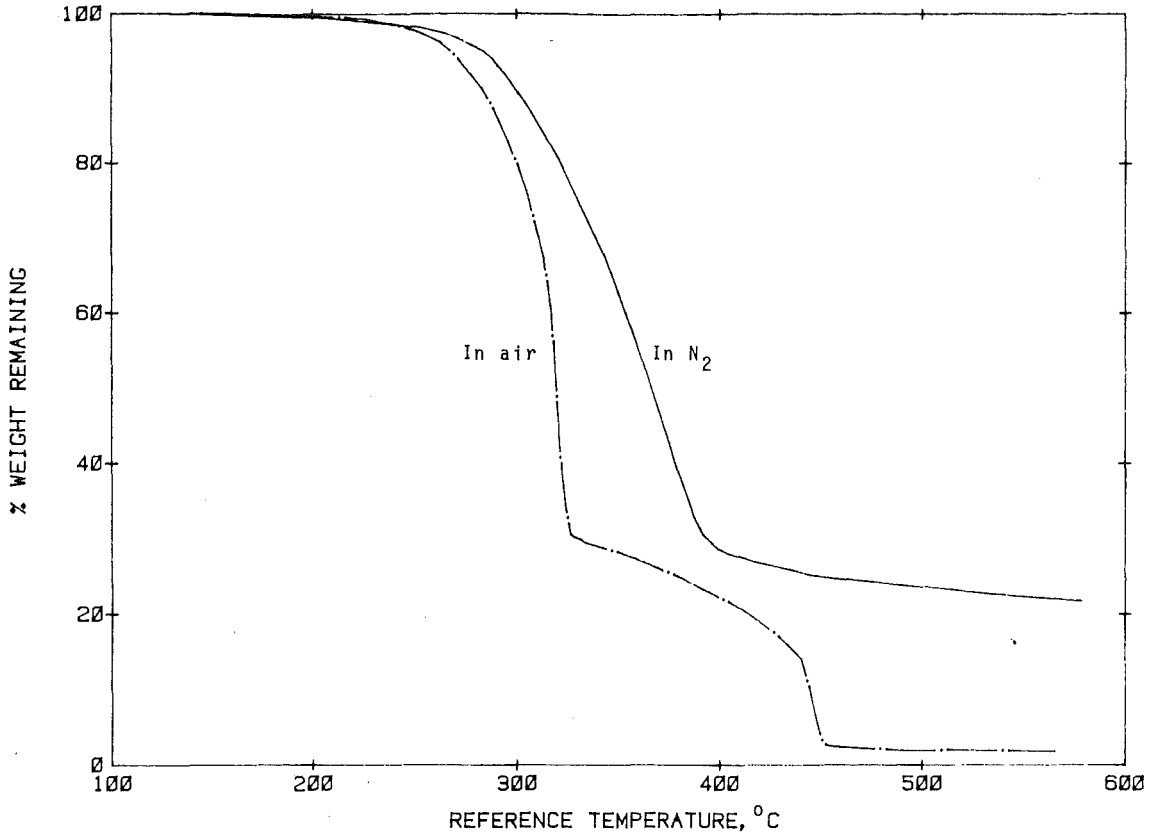

Figure 100. TG curves in N_2 and in air of single test piece

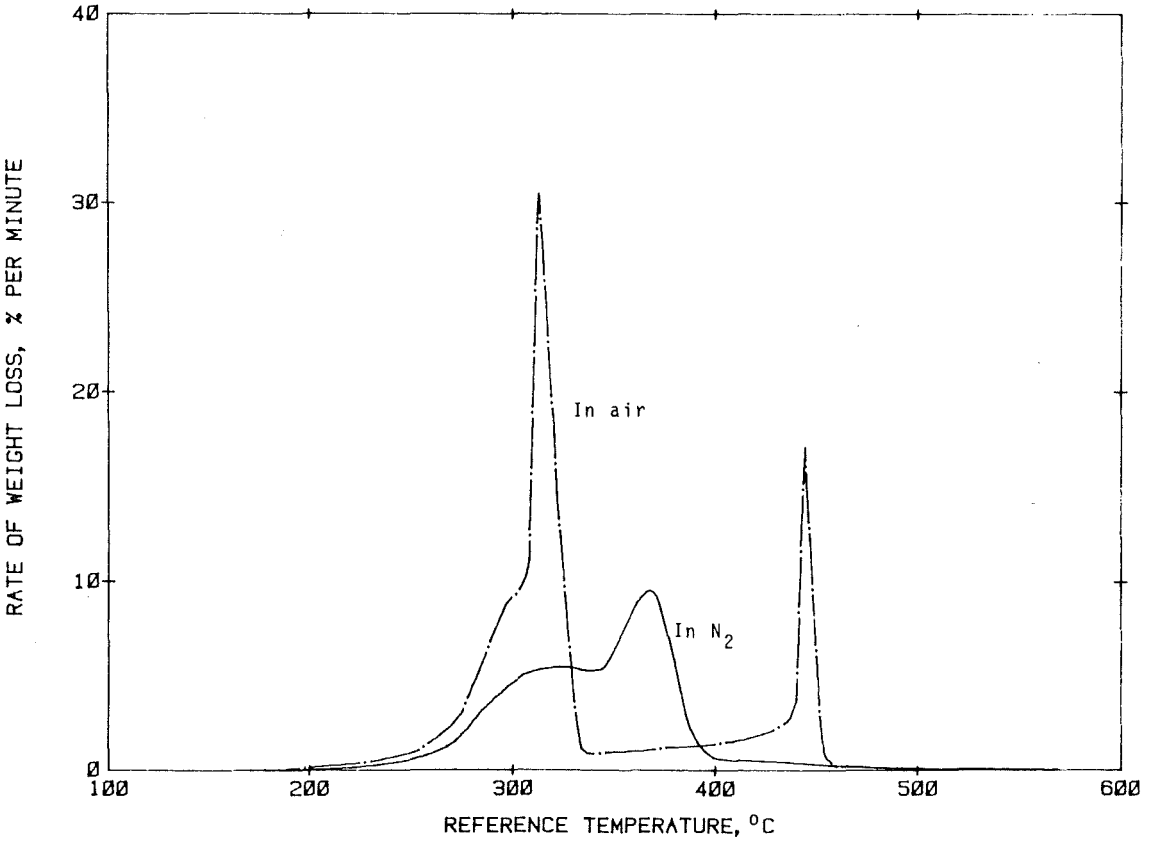

Figure 101. DTG curves in N_2 and in air of single test piece

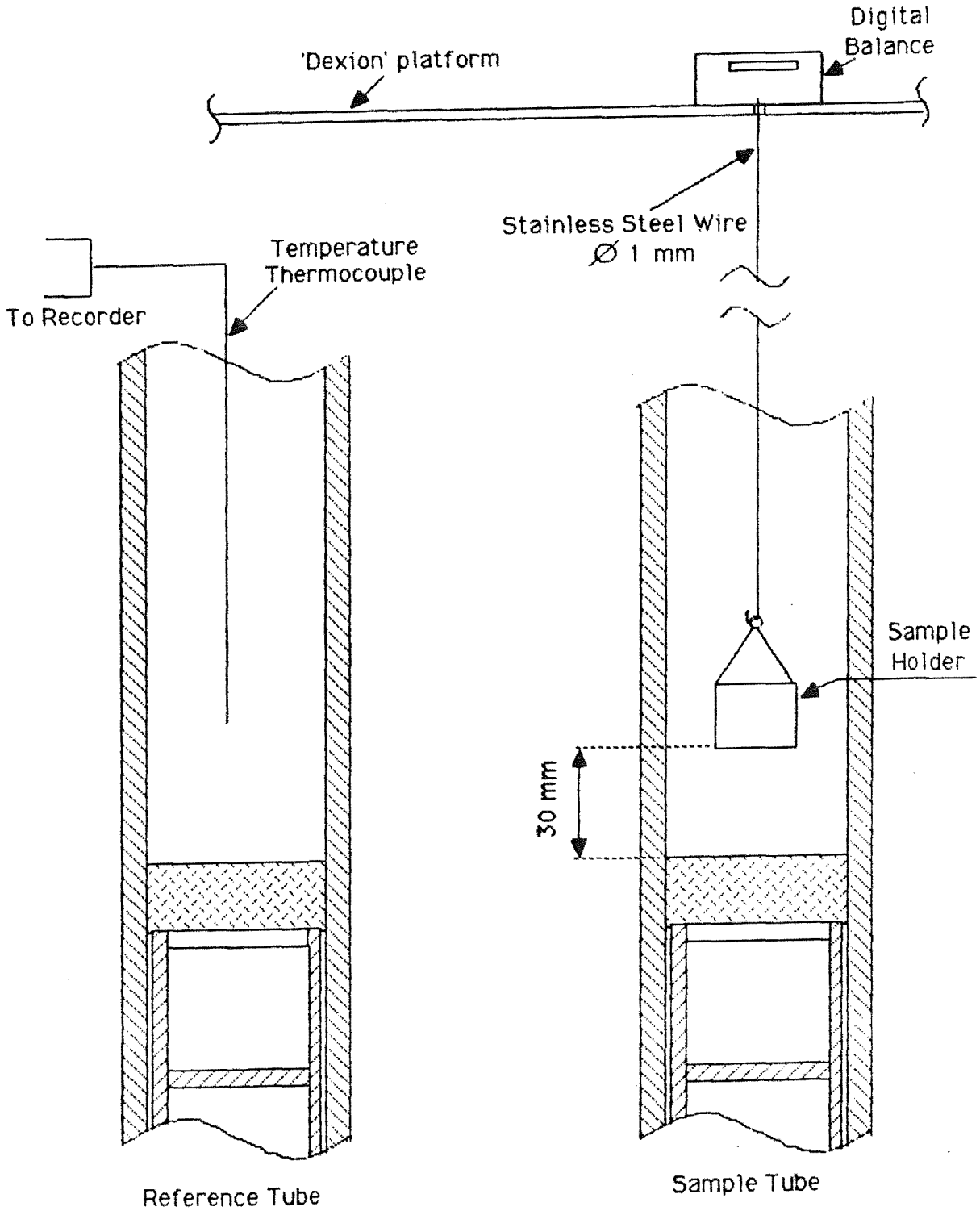

Figure 102. Experimental set-up for thermogravimetric analysis in DTA apparatus

of approximately 40 cm above the lid of the furnace. Sitting on the platform, directly above the sample tube, is a Mettler digital balance (PE 360) which reads down to one-thousandth of a gram for a load not exceeding 60 gm. This balance can be loaded either from the top or bottom. The sample holder consists of a cylindrical basket made from 100-mesh stainless steel screen. It has a diameter as well as a depth of 16 mm. After the test sample, which was oven-dried and weighed, had been placed in it, it was hung from the hooked end of a stainless steel wire of diameter 1 mm and length 66 cm. It was then lowered into the sample tube, following which the other end of the wire was hooked to the bottom of the balance. If the sample holder was in contact with the tube wall, the balance was shifted slightly and gently until it was well clear of it. The base of the sample holder was about 30 mm above the distributor. A chromel/alumel thermocouple was placed in the reference tube, at about the same level as the sample holder. No steel frame or inert material was placed in either tube.

The carrier gas was passed through the two tubes with a combined flowrate of 0.8 lit/min in the case of nitrogen and 0.4 lit/min in the case of air. The reactor was heated at the usual rate of around 5.5^{o}C/min. Readings on the balance were taken from the time the sample began to lose weight (at around 120^{o}C for most samples), at intervals varying from 1/2 minute (at the height of pyrolysis) to 5 minutes. The volatile products were sucked away by a suction hose placed near the mouth of the sample tube to ensure that they did not land on the delicate parts of the balance and affect its performance. The experiment was ended when the reference tube temperature exceeded 500^{o}C in runs in N_2 and when the sample had been completely burnt away in runs in air. The actual heating rate was determined from the temperature curve. Subsequently, the TG curve was plotted as a function of temperature. Although this method of analysis is not expected to have the same level of accuracy as the Stanton Redcroft thermobalance, it

nevertheless provided a useful means of comparing the thermal stabilities and char yields of the various wood species under study.

7.3.1 Wood components

Runs in N_2 were carried out for cellulose, acid lignin and the water-soluble extractives using sample sizes of 0.5 gm, 0.7 gm and 0.8 gm respectively. The resultant TG curves are shown in Figure 103, together with that of xylan obtained by Shafizadeh and DeGroot (1976). It can be seen that the extractives are the least stable of the wood components, beginning to lose weight at around 120°C, compared with around 180°C for acid lignin, 200°C for xylan and 260°C for cellulose. This serves as a further confirmation that the extractives are mainly responsible for the endothermic reactions in Rubber wood below 200°C. As shown in Figure 104, the temperature range within which the greatest weight loss occurred was 240-310°C for the extractives, 310-390°C for cellulose and 320-460°C for acid lignin. In the case of xylan, this was between 250°C and 320°C. This would mean that lignin has the highest overall thermal stability, followed by cellulose and then by the other two components. The results obtained show that the pyrolysis reactions in Rubber wood below 300°C involve mainly the hemicelluloses and the extractives, which are in agreement with the findings of DTA. It should, however, be realised that the extractives consist of a great number of components, some of which are even more stable than lignin. The rates of weight loss of xylan and cellulose at the height of pyrolysis were considerably higher than those of the other two components.

As indicated in the TG curves, the char yield increased in the order : xylan, cellulose, extractives and acid lignin. At 500°C for example, the amounts of char produced by the various components were : acid lignin 64%, extractives 42%, cellulose 15% and xylan, negligible. Thus lignin and the

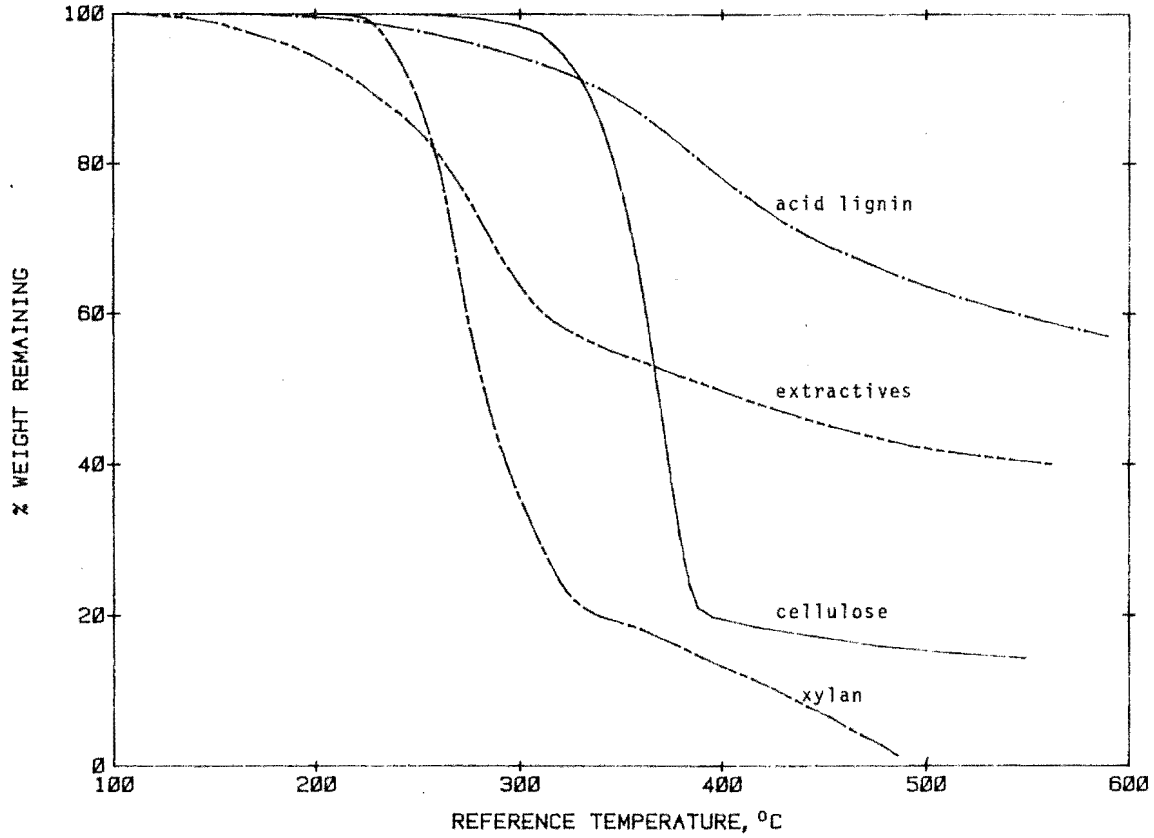

Figure 103. TG curves in N_2 of wood components

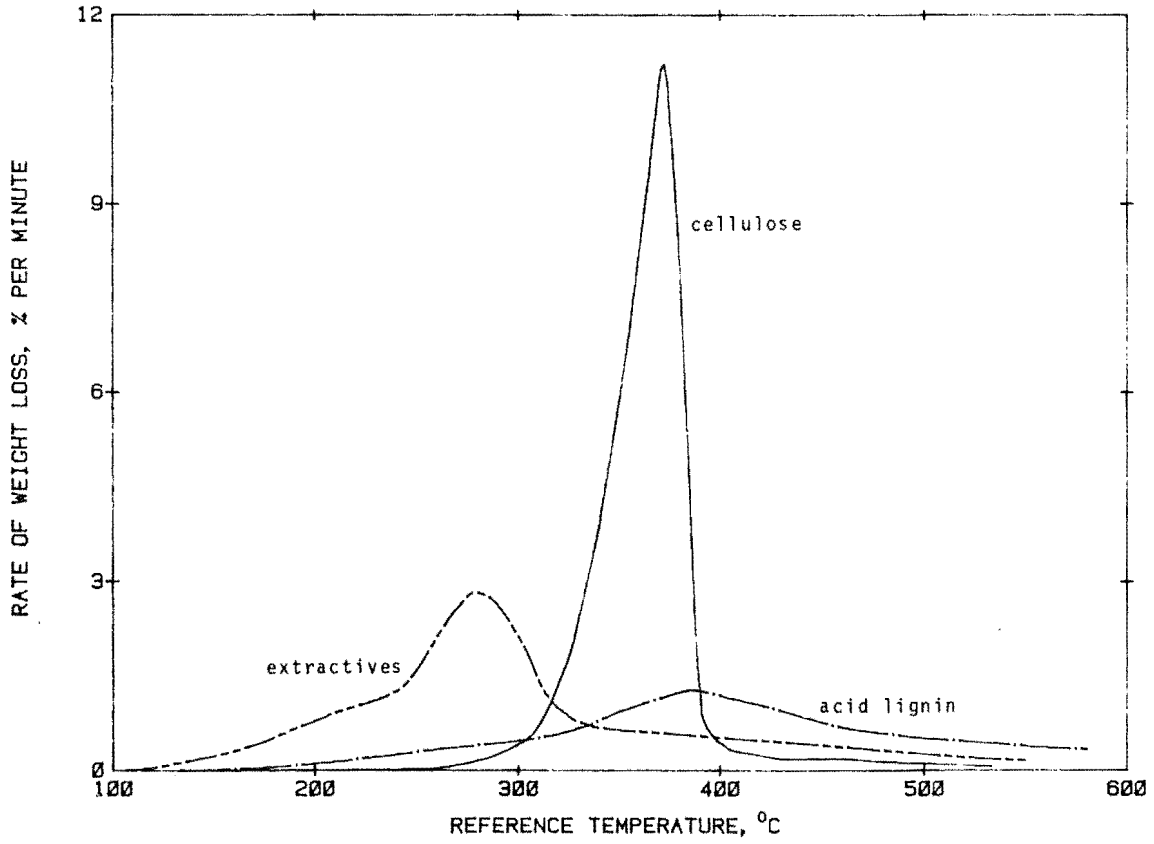

Figure 104. DTG curves in N_2 of cellulose, acid lignin and the water-solubles

extractives contribute more to char formation than cellulose and the hemicelluloses. The low char yields of the last two components means that they produce more volatile products which promote flaming combustion. This explains why in DTA runs in 80% O_2, cellulose burnt with a flame but not acid lignin or the extractives. The char yield of Rubber wood falls in between those of cellulose and its extractives.

7.3.2 Rubber Wood and other Wood species

Runs in N_2 and in air were carried out for Rubber wood of the following particle sizes : (1) -36+72 mesh fraction and (2) 5 mm diameter pieces of height 11-12 mm. The test samples were obtained from the fresh wood sections of **Tjir 1.** A sample size of approximately 0.6 gm was used except for the run in N_2 of the 5 mm diameter pieces in which a 1-gm sample was used. The TG curves resulting from the runs in N_2 are shown in Figure 105, and it can be seen that there is not a great difference in the pyrolysis temperatures of the two wood samples. The char yield of the 5 mm diameter pieces was higher than that of the -36+72 mesh particles - by between 4% and 5%. It was also noted that the char yield of the -36+72 mesh particles was slightly higher than that obtained using the Stanton Redcroft thermobalance.

No flaming combustion occurred in either of the runs in air. As shown in the resultant TG curves (Figure 106), the -36+72 mesh particles pyrolysed sooner and took a shorter time to burn to completion compared with the 5 mm diameter pieces. There was no sudden dip in these curves, unlike those obtained using the Stanton Redcroft thermobalance. It is therefore quite difficult to tell when the char began to burn in these runs. The slight difference in the results obtained from the two methods may be explained by the fact that the experimental conditions were not the same. For the same reason, it would not be fair to compare the pyrolysis temperatures of the wood in one instrument with those in the other instrument.

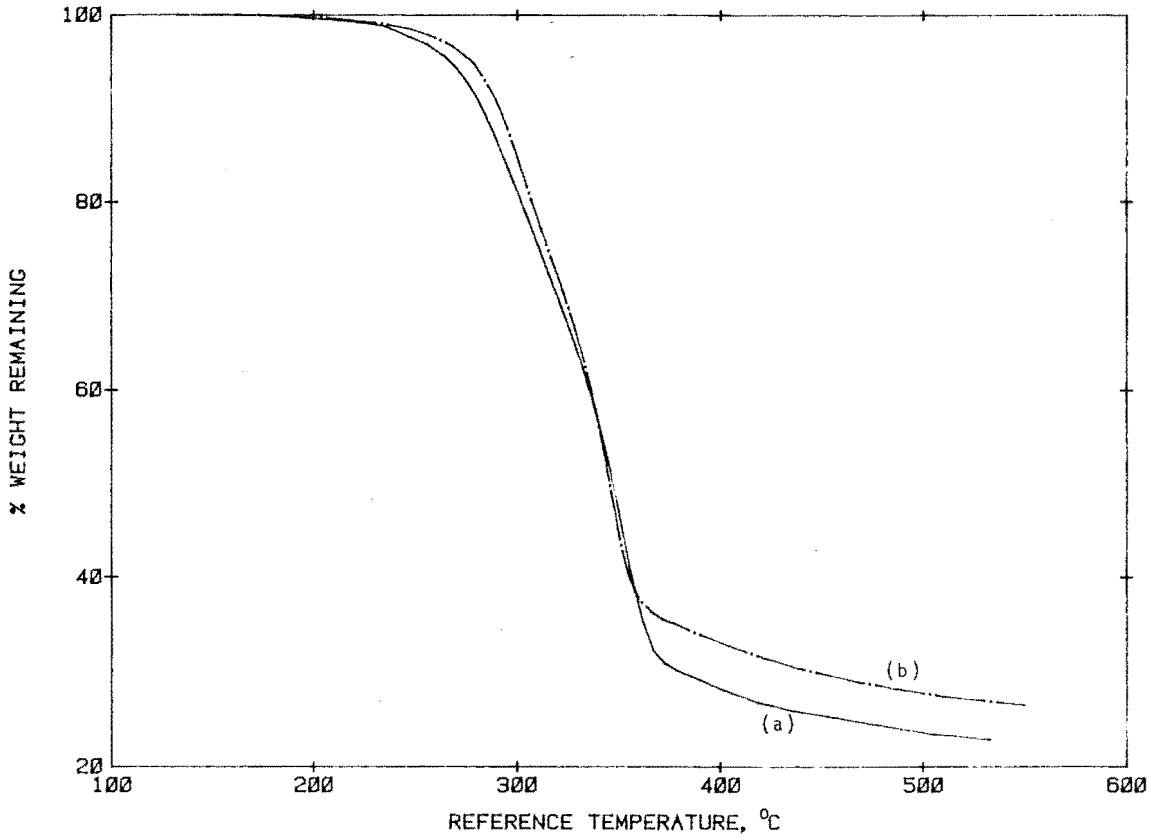

Figure 105. TG curves in N_2 : (a) -36+72 mesh particles and (b) 5 mm diam. pcs.

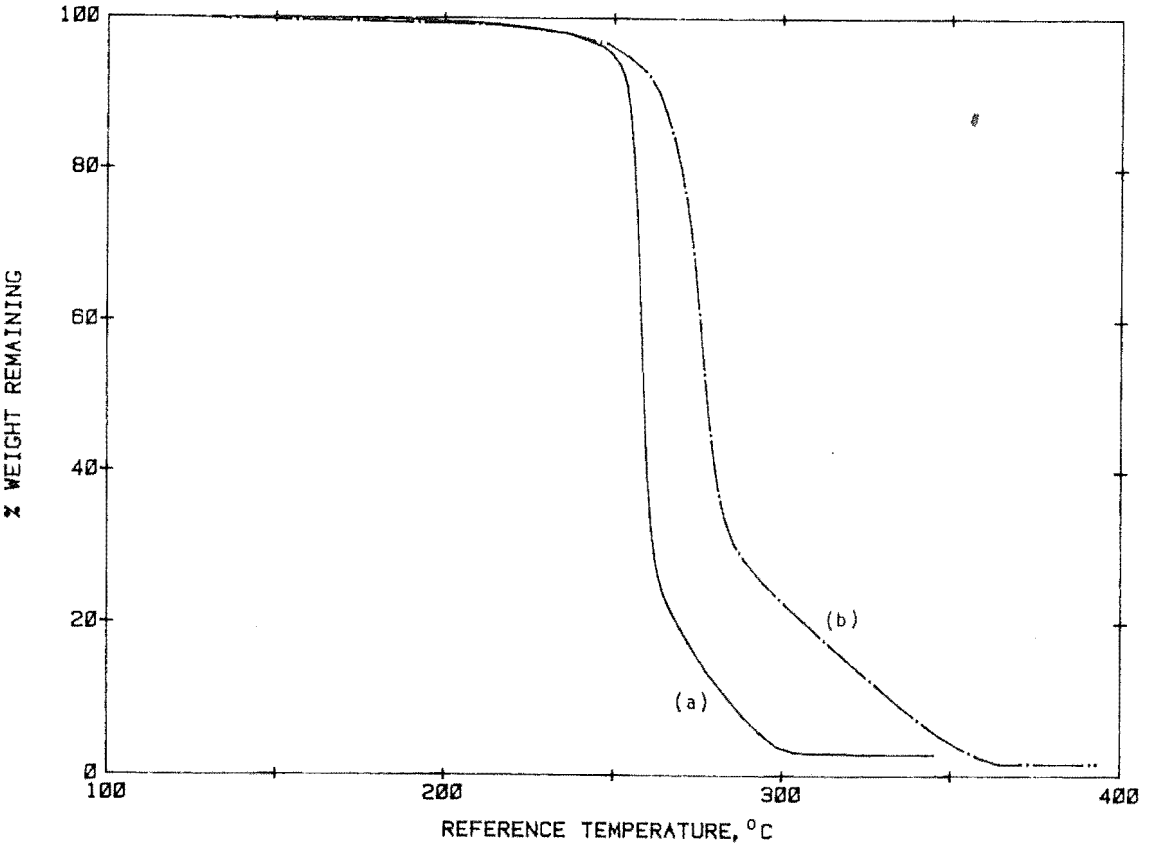

Figure 106. TG curves in air : (a) -36+72 mesh particles and (b) 5 mm diam. pcs.

Before proceeding further, a clarification needs to be made regarding the comparison of TG results. In runs in N_2, the sample temperature is not very much different from that of the reference temperature. As such, comparison of the results from different runs may be made on the basis of temperature or time. This is, however, not the case in runs conducted in an oxidative environment in which the sample temperature can be substantially higher than that of the reference temperature. This is illustrated in the DTA curve in air of a 2-gm Rubber wood sample of particle size -18+36 mesh (Figure 107). The experimental set-up of the run from which this curve was obtained is the same as that for DTA runs in N_2 (see Figure 19). It can be seen that the sample temperature reached a high of around 600°C, which was more than 300°C higher than that of the reference temperature. In the light of this observation, in TG runs conducted in an oxidative environment, it is perhaps more meaningful to compare the results obtained on the basis of time difference rather than temperature difference, although the resultant curves could still be plotted on a temperature scale for ease of reference or consistency.

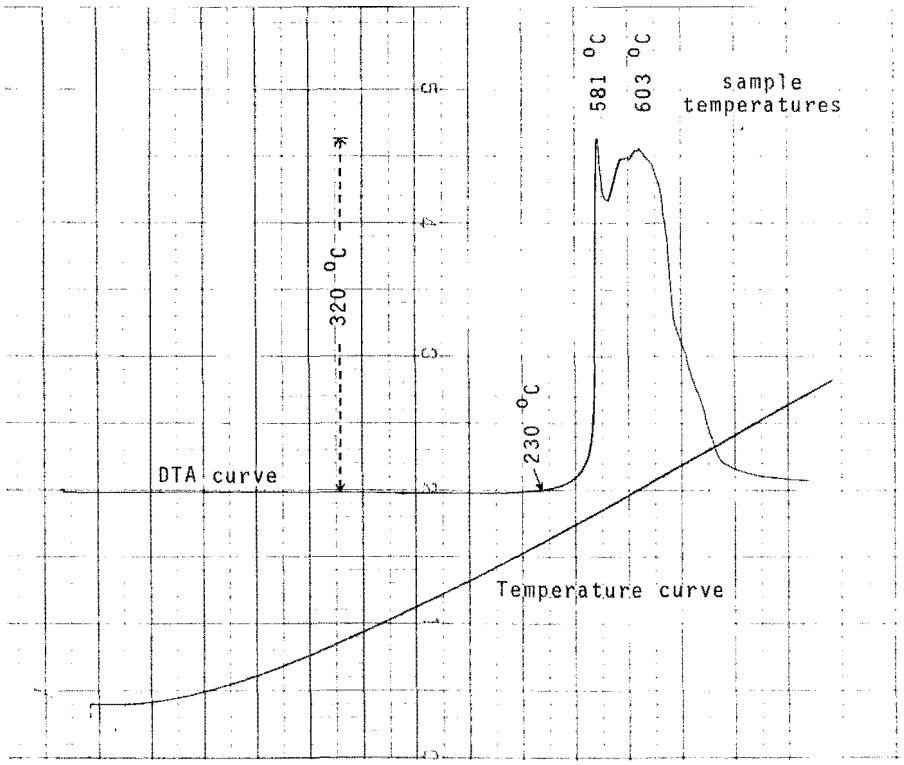

Figure 107. DTA curve in air of -18+36 mesh particles (no inert material in sample bed)

TG runs in N_2 and in air were carried out for the other wood species, including the bark of the rubber tree, using 5 mm diameter test pieces. The sample size used was around 1 gm for runs in N_2 and 0.6 gm for runs in air. Particulars of the resultant curves are provided here while the curves themselves can be found in Appendix 9.

The TG curves in N_2 of the various wood species differed slightly in shape but not in the basic characteristics, as shown in Figure 108. The char yield at a particular temperature varied from species to species. At 500°C, for example, it ranged from for Oil palm wood to 40.5% for rubber tree bark and appeared to be unrelated to the density of the wood (Table 17). The char yields of those species which burnt with a flame in DTA runs in 80% O_2, except for sepetir, were the lowest. This is not at all unexpected since a lower char production means more volatiles were liberated and the greater was the likelihood of flaming combustion taking place. The char yield of Rubber wood was the third lowest of the wood species being tested - after Oil palm wood and Jelutong.

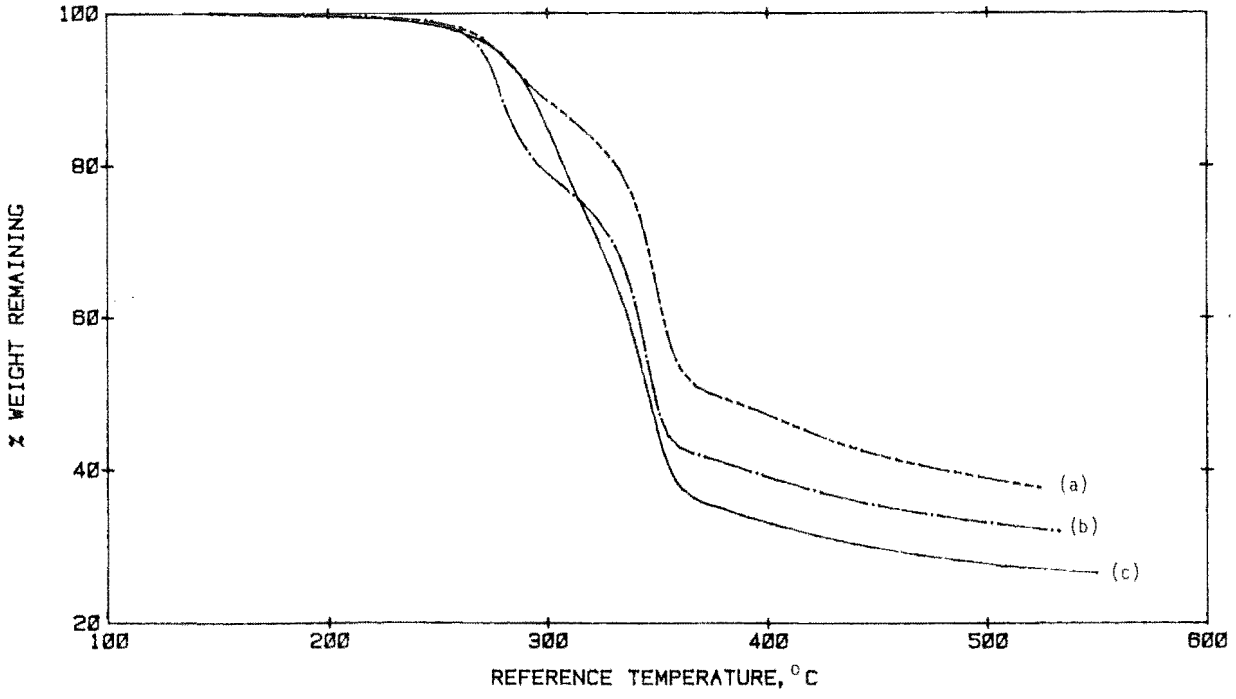

Figure 108. TG curves in N_2: (a) Rubber wood, (b) Coconut wood and (c) Chengal

Table 17. Char Yields at 500°C of Various Wood Species

Species	Ranking in density	Char yield, %
Oil palm wood	20	26.6
Jelutong	19	27.1
RUBBER WOOD	12	27.8
Pulai	17	28.4
Ramin	8	30.2
Tembusu	6	30.2
Keruing	10	31.0
Meranti, light red	15	31.2
Kempas	4	32.6
Sepetir	13	32.9
Coconut wood	2	33.2
Mengkulang	18	33.2
Mersawa	16	33.7
Tualang	9	34.2
Nyatoh	11	35.2
Balau	1	36.1
Meranti, dark red	14	36.7
Chengal	3	38.8
Merbau	5	39.5
BARK	7	40.5

Figure 109 shows the TG curves in air of three of the wood species, namely Rubber wood, Coconut wood and Chengal. Point A in Curves (b) and (c) corresponds to the outset of degradation of the residual char. In Curve (a), it is more difficult to tell at which point the char began to burn due to the absence of a sudden dip. In any case, it can be seen that the outset of char combustion and also the overall burning time varied from species to species. As in the case of DTA runs in an oxidative environment, the burning time of each of the wood species relative to that of Oil palm wood was determined. As the exact time a sample had just completely burnt out was rather difficult to pinpoint, it was decided to use the 5% weight mark as the end-point. As shown in Table 18, it took the other wood species between 4 minutes and 35 minutes longer to burn to completion compared with Oil palm wood. Only three of the 19 species listed burnt quicker than Rubber wood and these were Oil palm wood, Jelutong and Sepetir. The five species which burnt with a flame in DTA runs in 80% O_2 occupied the first five spots, indicating that these species burnt just as well in a fixed bed as in a fluidised-bed. It will be noticed that the rubber tree bark

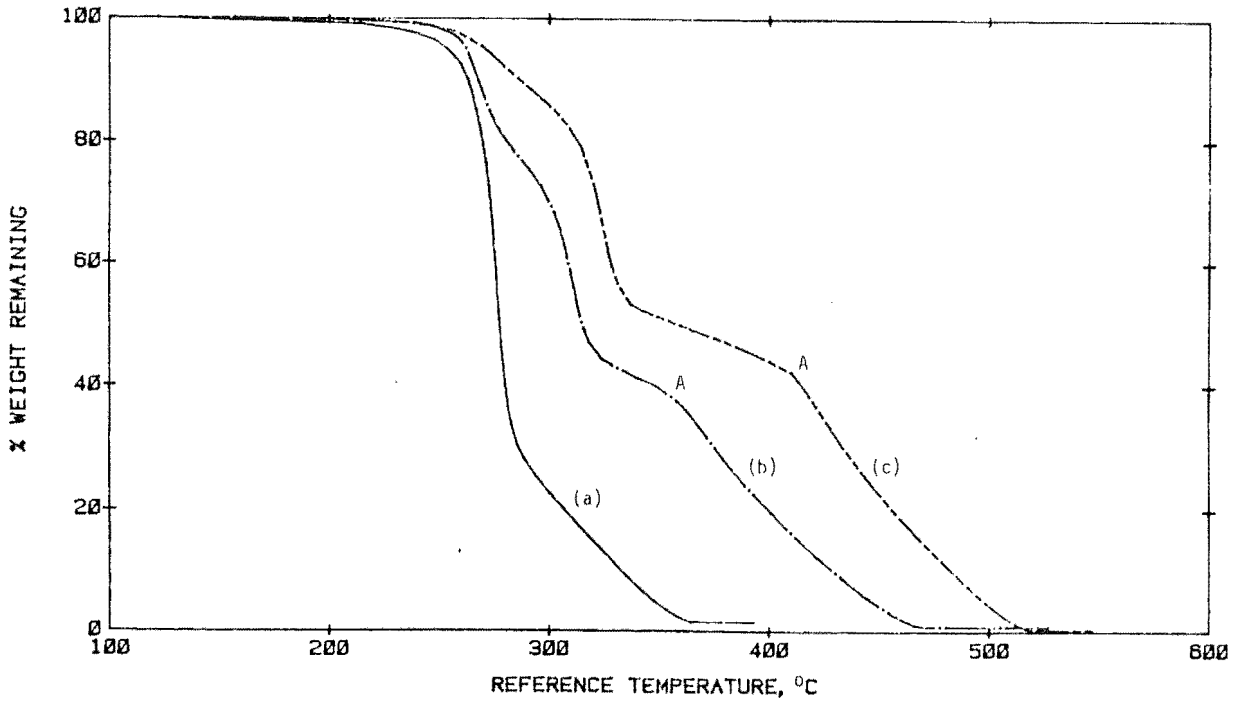

Figure 109. TG curves in air: (a) Rubber wood, (b) Coconut wood and (c) Chengal

Table 18. Burning Times Relative to that of Oil Palm Wood (TG in Air)

Species	Temp. with 5% of sample remaining, °C	Extra burning time, min
Oil palm wood	319	0
Jelutong	339	3.7
Sepetir	345	4.7
RUBBER WOOD	348	5.3
Pulai	355	6.5
Ramin	364	8.2
Mengkulang	380	11.1
Tualang	384	11.8
Merbau	389	12.7
Mersawa	398	14.4
Nyatoh	408	16.2
Meranti, light red	413	17.1
Meranti, dark red	415	17.4
Kempas	415	17.4
Tembusu	424	19.1
Coconut wood	447	23.3
Keruing	455	24.7
Chengal	497	32.4
Balau	500	32.9

was not listed in the table. This is because its TG curve did not come down to the 5% weight mark due to its high ash content - around 12%. Except for one or two species, the order of the wood species in terms of burning time was about the same as that obtained from the DTA runs (see Tables 11 and 12).

The average rate of burning of each of the wood samples was determined from its TG curve. Again, as the exact temperatures a sample began to lose weight and when it had just burnt out were difficult to pinpoint, it was decided to use the 95% weight mark as the starting point and the 5% weight mark as the end point. The results obtained are provided in Table 19. It will be seen that the average burning rate of Rubber wood was similar to those of Pulai, Sepetir and Ramin. Only two species burnt faster than Rubber wood, viz Oil palm wood and Jelutong. The burning rates of the top three species in the table were 2 to 3 times those of the bottom three species. The top spots were again occupied by those species which burst into flame in DTA runs in 80% O_2.

7.4 Char Yields from Flash Pyrolysis

In the TG runs, the samples were heated gradually at the rate of 5.5°C/min. It would be interesting to compare the char yields under these conditions and those from flash pyrolysis in which the samples are pyrolysed in a preheated chamber. In a way, flash pyrolysis can be likened to heating a sample at a high heating rate. The experimental procedure was the same as that for the TG runs in N_2 except that the reactor was heated to around 530°C and maintained at this temperature before the sample was introduced into the sample tube. Eight of the wood species under study were pyrolysed in this way using 5 mm diameter pieces with a sample size of approximately 1 gm. Their char yields were compared with those from TG runs at the same temperature in Table 20. It can be seen that for each species, the char yield from flash

Table 19. Average Rates of Burning

Species	Ranking in density	Rate of burning, mg/min
Oil palm wood	20	49
Jelutong	19	38
RUBBER WOOD	12	35
Pulai	17	35
Sepetir	13	35
Ramin	8	35
Mengkulang	18	28
Tualang	9	28
Mersawa	16	26
Merbau	5	25
Nyatoh	11	24
Meranti, light red	15	23
Kempas	4	23
Meranti, dark red	14	22
Tembusu	6	21
Keruing	10	19
Coconut wood	2	18
Chengal	3	15
Balau	1	14

Table 20. Comparison of Char Yields at 530 C from TG Run and Flash Pyrolysis

Species	Char yield from TG run, %	Char yield from flash pyrolysis, %
BARK	38.9	33.6
Chengal	37.4	27.7
Jelutong	26.2	20.2
Meranti, dark red	35.2	27.0
Mersawa	32.7	24.3
Pulai	27.5	21.5
Ramin	29.2	22.9
RUBBER WOOD	27.0	20.8

pyrolysis was lower than that from TG run - by between 5.3% and 9.7%. This shows that a faster heating rate promotes gasification of the wood, resulting in a lower char production.

7.5 Ash Determination

Ash is defined as the incombustible material which remains when a fuel is burnt. In the case of wood, it originates mainly from the inorganic compounds in its tissues. The major components of wood ashes are calcium, potassium, sodium, magnesium, iron, silica, phosphate, sulphate, chloride and carbonate (Browning, 1967). If not removed, it can adversely affect combustion by forming a barrier between the fuel bed and the surrounding air. Hence, it is useful to know the ash content of a wood species before using it for fuel so that the necessary measures can be taken to ensure that burning of the wood proceeds without hindrance.

The ash contents of the wood species under study were determined as follows : A sample (5 mm diameter pieces, 1-2 gm) was weighed into a porcelain crucible and incinerated around 650°C until all the carbonaceous material had been burnt away. The crucible was allowed to cool down slightly before being weighed. The ash content was expressed as a percentage of the oven-dried wood. Two or more determinations were made for each wood species, except for light red Meranti which had only one because it had run out of material. The mean ash contents of the various wood species are given in Table 21 while the individual ash contents of the test samples are provided in Appendix 11.

It will be seen that the ash content of rubber tree bark is considerably higher than that of its wood. The ash contents of the various tropical hardwoods ranged from less than 0.1% to slightly over 2%. Rubber wood has an ash content of around 1% which is relatively high compared with those of the other wood species. Most of it comes from its water-soluble extractives which have an ash content of 8-12% (see Sections 6.3.3 and 7.3). There was very little difference in the ash contents of wood from the four Rubber trees. Incidentally, those species which took the shortest time to burn to completion (Oil palm wood, Sepetir, Rubber wood, Pulai and Jelutong) have a comparatively high ash content. The ash content of Radiata pine, which is a softwood, was also determined and included in the table for comparison. It will be seen that it amounted to only a fifth of Rubber wood's.

The ash contents of the various wood species can also be obtained from their respective TG curves in air but these are only approximate values.

Table 21. Ash Contents of Wood Species Under Study

Species	Mean ash content, % of oven-dried wood
BARK	7.12
Ramin	2.13
Oil palm wood	1.52
Sepetir	1.27
Tualang	1.24
RUBBER WOOD	1.08
Mersawa	0.91
Pulai	0.74
Coconut wood	0.65
Jelutong	0.52
Mengkulang	0.51
Merbau	0.51
Nyatoh	0.44
Keruing	0.34
Pine, radiata	0.22
Tembusu	0.19
Kempas	0.13
Balau	0.10
Meranti, dark red	0.09
Meranti, light red	0.09
Chengal	0.08

SECTION III

BURNING OF WOOD BLOCKS IN AN INCINERATOR

CHAPTER 8

BURNING OF WOOD BLOCKS IN AN INCINERATOR

This investigation of the combustion characteristics of Rubber wood has so far been confined to laboratory scale. In this section, a semi-laboratory scale study, involving the burning of 5 cm thick blocks in a down-draught incinerator, is described.

8.1 Method of Study

8.1.1 Apparatus

The apparatus consists essentially of a fuel drum and a burner head (Figure 110). It was designed to burn solid fuels by down-draught combustion with secondary combustion occuring at more than 700°C so that less pollutants are produced. The fuel drum, which was constructed from 1 mm thick stainless steel plate, is 500 mm in diameter and 890 mm in height and weighs 22 kg. The burner head consists of a primary combustion chamber, a secondary combustion chamber, a flue duct, a heat exchanger and twelve air inlet tubes (Figures 111 and 112). It was also made of stainless steel and weighs 25 kg. The two combustion chambers were lined with a layer of 'Kaowool' insulator of thickness 25 mm to reduce heat loss. The lower end of the flue duct contains a side tube to allow gas samples to be drawn out of the secondary combustion chamber for analysis. A cross section of the heat exchanger is shown in Figure 113. Both the flue duct and the outer tube are finned to provide a more efficient transfer of heat from the flue gas to the inlet air which flows downwards. Six of the air inlet tubes are located around the periphery of the primary combustion chamber and the remaining six around that of the secondary combustion chamber. Each air inlet tube contains a valve to enable the air flowrate to be regulated. Thermocouple ports were built in the secondary combustion chamber, in one of the air inlet tubes and in the flue duct to facilitate measurement of temperatures using chromel/alumel

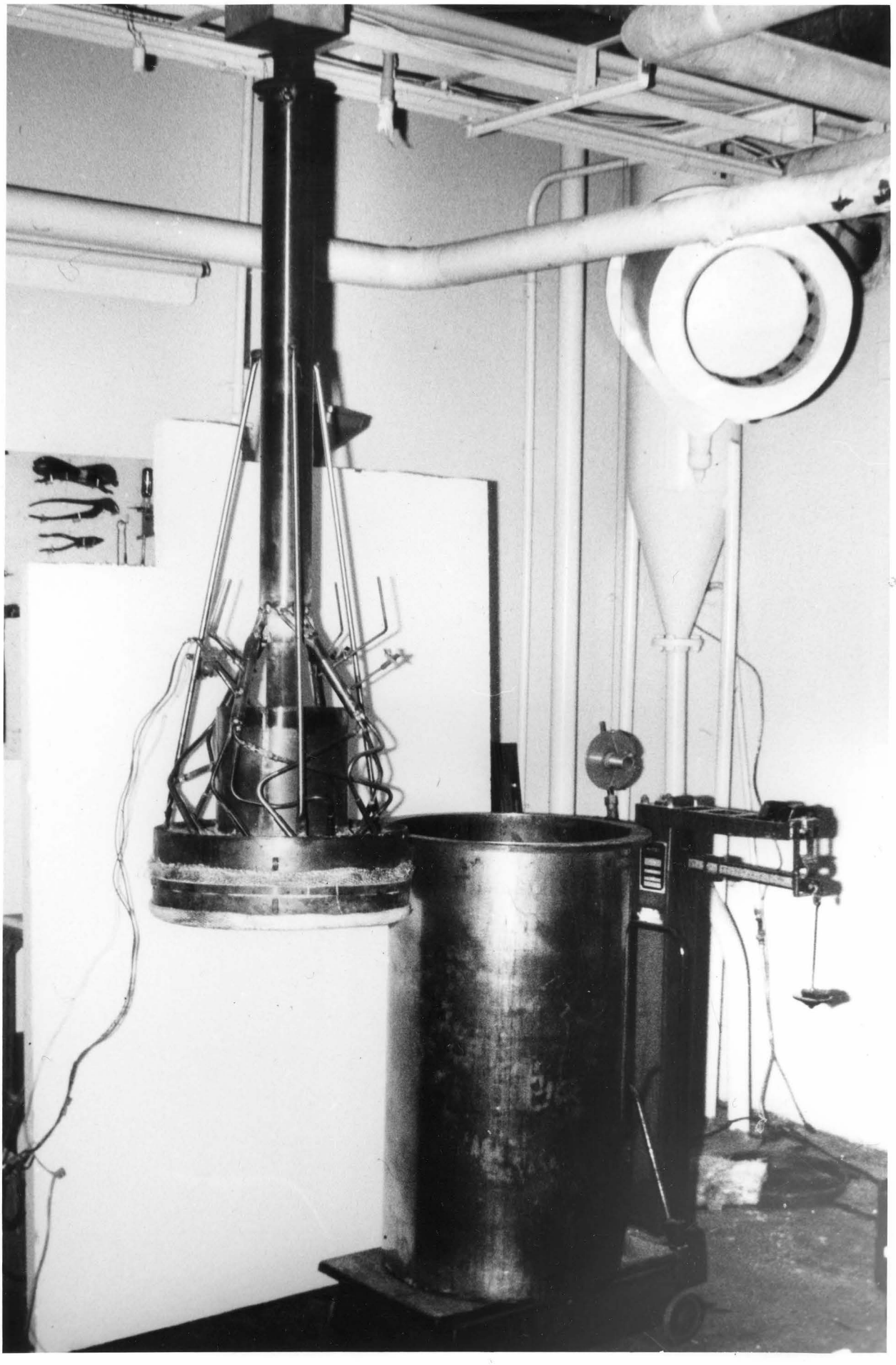

Figure 110. Down-draught incinerator.

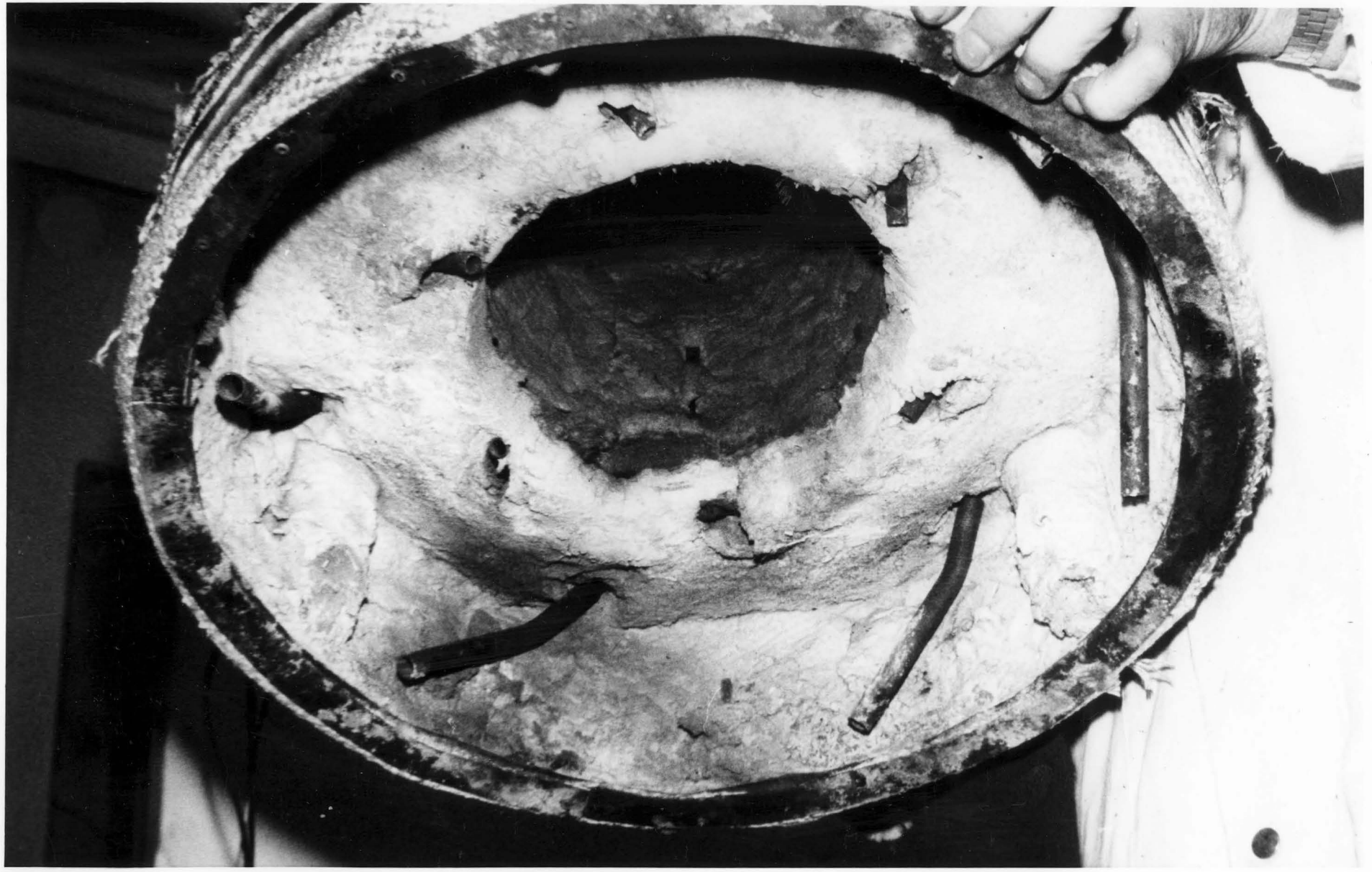

Figure 111. Burner head showing the combustion chambers.

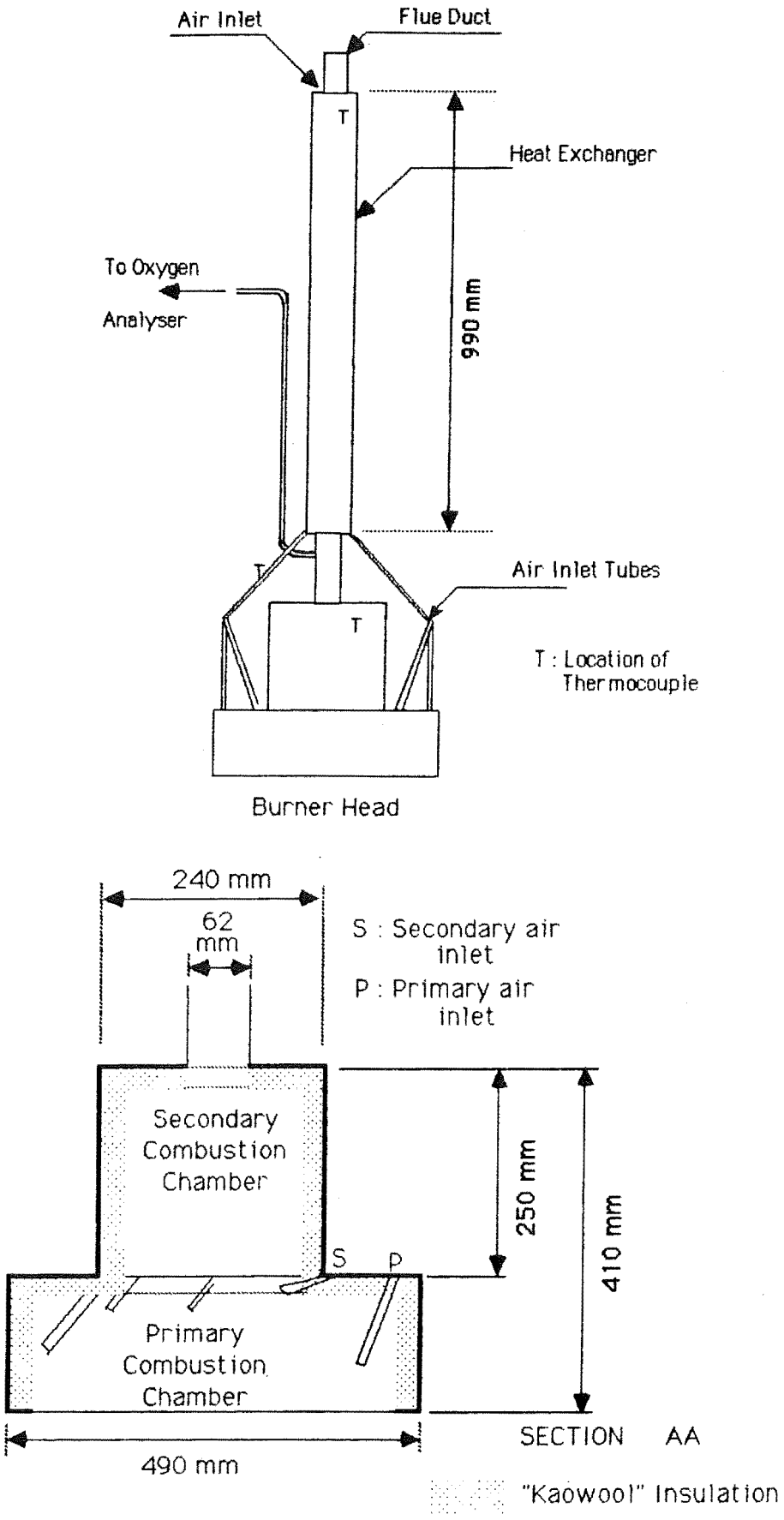

Figure 112b. Schematic representation of burner head

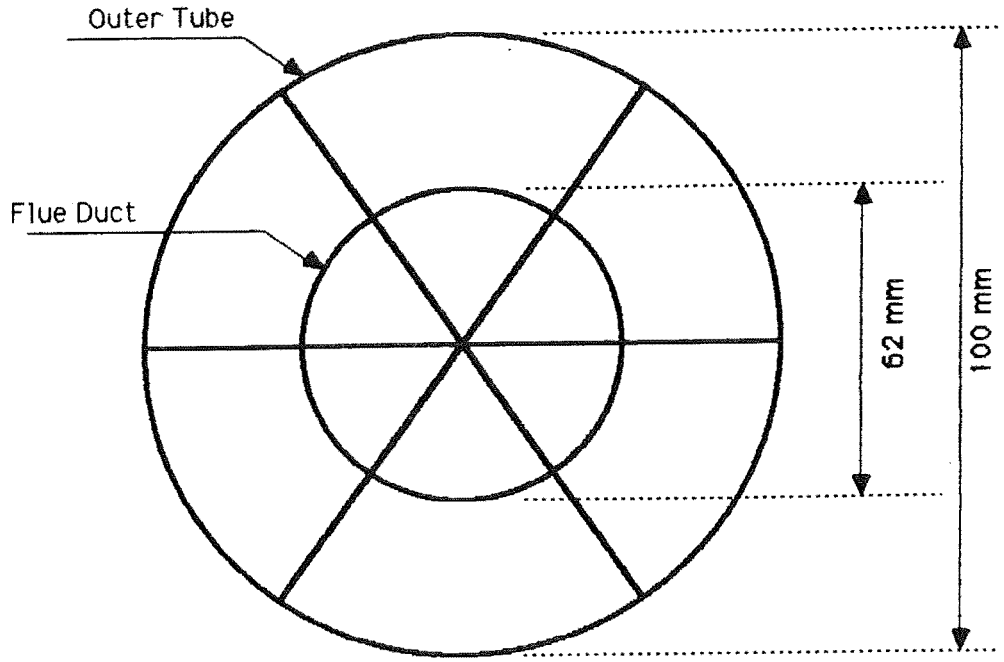

Figure 113. Cross-section of heat exchanger

thermocouples. Two glass fibre tapes, each of width 50 mm, were wrapped round and fastened to the outside of the primary combustion chamber to serve as seals between the burner head and the fuel drum.

8.1.2 Test Materials

Besides Rubber wood, three other wood species were used in the combustion experiments. These were Balau, Jelutong and Radiata Pine. Rubber wood was provided by the Rubber Research Institute of Malaysia while the other three species were purchased from a local timber merchant. All of them were in the form of 5 cm by 10 cm boards and air-dried. Incidentally, Balau and Jelutong were the only Malaysian hardwoods available in Christchurch at the time the study was conducted. All the wood pieces were untreated except for Rubber wood which was dip-treated when first converted in the sawmill with a preservative solution containing 1-2% by weight each of gamma benzenehexachloride (26% WP), borax decahydrate and sodium pentachlorophenate. As this is basically a surface treatment, penetration of the chemicals into the wood was only skin deep.

In any case, in order to ensure that the chemicals did not play a part in the combustion of the wood, a surface layer of thickness 2 to 3 mm was planed off from each of its test pieces all round. Having done this, they were cross-cut into 5 cm lengths to give test blocks measuring approximately 5cmx5cmx10cm. The test pieces of the other species were cut in a similar manner. Subsequently all the test blocks were conditioned in a hot room of temperature around 30°C for about two weeks to ensure that their moisture contents were about the same when used.

Like Jelutong, Radiata pine burnt with a flame in 60% and 80% O_2 in DTA experiments using 5 mm diameter pieces and a sample size of 1 gm.

8.1.3 Experimental Procedure

The fuel drum was placed on a platform scale and its weight noted. Following this, the test blocks were loaded into it to a height of 50-55 cm and their weight determined. Several sheets of newspaper were placed over them to form a partition. Around 4 kg of air-dried Radiata pine sawdust was put on top of the newspapers and evenly spread out, as illustrated in Figure 114. The actual weight of the sawdust, which was used primarily as a fire starter, was determined after which around 100 ml of kerosene was poured over it, covering as wide an area as possible and set alight. This took place usually in the late afternoon. Burning of the kerosene and sawdust was allowed to continue for a few minutes before the burner head was lowered into the fuel drum. The top end of the flue duct was inserted into a fume extraction line by means of a 'telescopic' extension tube. In this way, an artificial draught was created in the burner, enabling combustion of the fuel to continue. The initial weight of the assembled unit was recorded. The amount of draught in the burner, i.e. the pressure difference between the inside of the burner and the outside atmosphere, was measured using a Dwyer

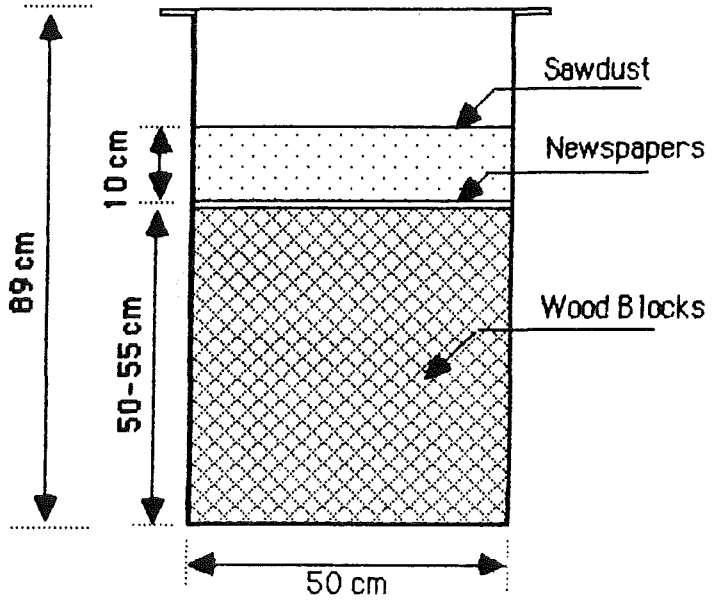

Figure 114. Fuel drum and its contents

gauge which is basically an inclined manometer. One side of the gauge was open to the atmosphere while the other side was connected by a rubber hose to a steel tube projecting out of the secondary combustion chamber. The sawdust was allowed to burn for around 25 minutes before the draught, which was set at around 3.3 mm H_2O, was cut off. Flaming combustion immediately ceased but the heat generated in the burner and the small amount of draught present in it due to natural convection enabled the sawdust to continue burning overnight by smoldering combustion.

On the next morning, draught was re-introduced into the burner which resulted in the sawdust burning again. From now on, it was always maintained at 3.3 mm H_2O. At this time, usually only around 2 kg of sawdust remained in the fuel drum. The experiment proper began when all the sawdust had been burnt away. The flue gas emerging from the side tube of the flue duct was passed through an oxygen analyser (Figure 115) with the aid of a metering pump after cleaning. The oxygen concentration of the flue gas and the temperatures of the

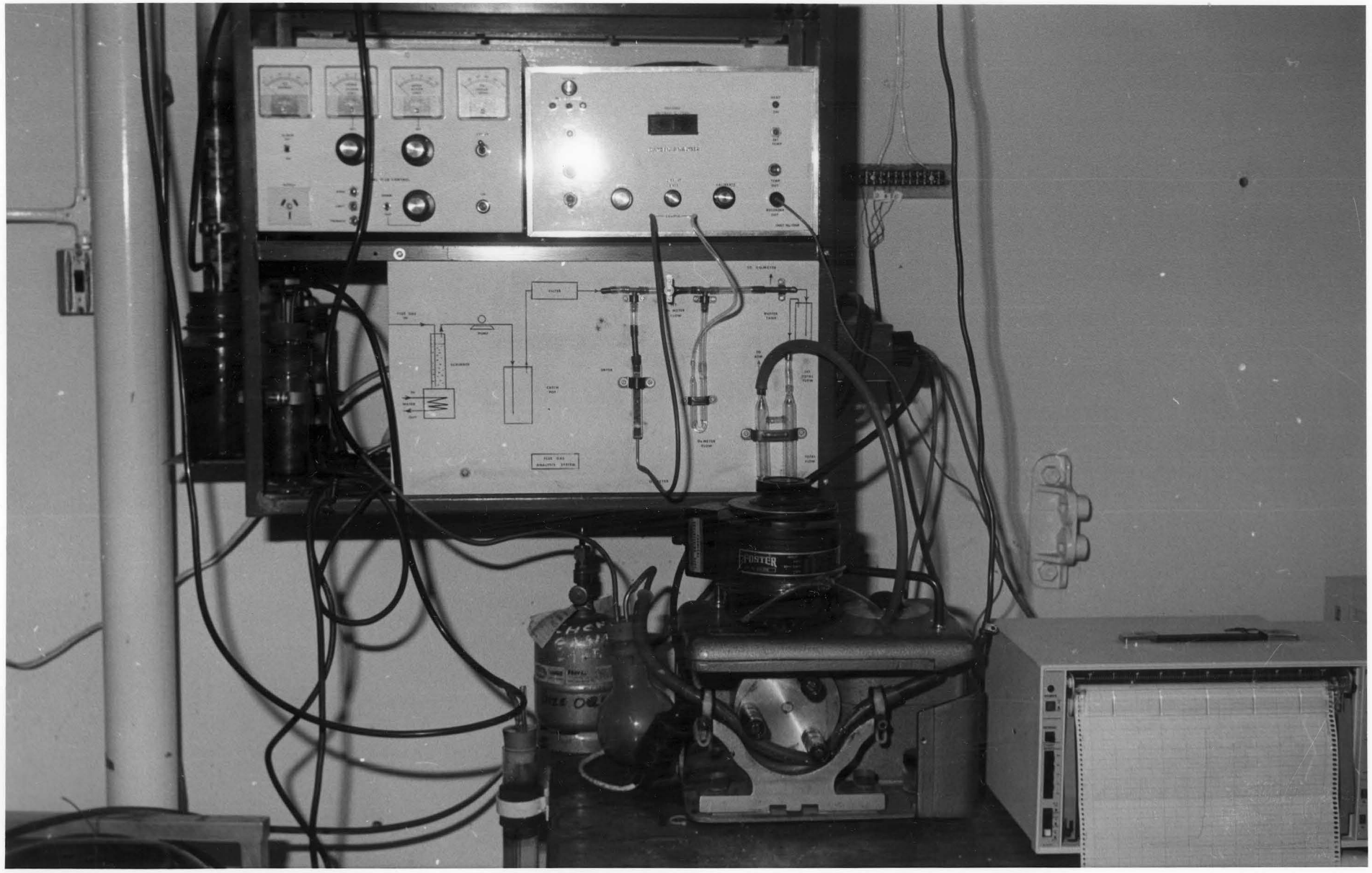

Figure 115. Oxygen analyser.

secondary combustion chamber, the inlet air and the flue gas were recorded on two hot-pen recorders as a function of time. The weight of the burner and its contents was read from the scale on an hourly basis. After taking each reading, the burner head was pushed down the fuel drum to be in contact with the fuel bed, care being exercised not to damage the seal. Any leaks around the seal were plugged using glass fibre tapes. The burner head was originally designed to descend on its own by incorporating rollers on the outside of the primary combustion chamber, but this did not materialise because of the uneven surface of the fuel drum. Gas samples were taken at regular intervals for analysis of CO_2, CO and CH_4 using gas chromatography. After the last reading of the day had been taken, the draught was cut off and the wood allowed to continue burning by smoldering combustion. In five of the six runs carried out (two each for Rubber wood and Radiata pine and one each for Jelutong and Balau), the experiment was continued on the second day and in one of them, it was carried on to the third day. The procedure for re-starting a run on the second or third day was the same as that for the first day. In terminating a run, the draught was cut off and the inlet air valves closed. The contents of the fuel drum were allowed to cool down overnight before the burner head was lifted up.

8.2 Results

8.2.1 Rate of Burning

Particulars of the six combustion runs are given in Table 22. Each test load consisted of around 200 blocks. There was very little difference in the moisture contents of the various test blocks. Balau is the densest of the four wood species and Jelutong the lightest.

The rate of burning of each test load was highest in the beginning (around 2 kg/h) and decreased with time, as shown in Figures 116-119. The rate of decrease was slightly higher in

Table 22. Particulars of Combustion Runs

Run No.	Species	Weight of wood, kg	Av. MC %	Density kg/m^3	Duration of run, days
1	Rubber wood	30.90	11.55	670	2
2	"	32.00	10.30	670	2
3	Radiata pine	25.40	11.47	474	2
4	"	26.70	10.64	474	1
5	Jelutong	25.25	11.43	424	2
6	Balau	50.55	11.48	975	3

Rubber wood than in the other three species in the first day of burning, which lasted 12 hours. This is reflected in their test loads losing less than 1 kg/h towards the end of the day as compared with over 1 kg/h for the other three species. There was very little difference in the average rates of burning in the first day of Rubber wood, Jelutong and Radiata pine, which varied between 1.27 kg/h and 1.38 kg/h (Table 23). The average rate of burning of Balau was around 15% higher than those of the other wood species, although its test load was 60% heavier than those of Rubber wood and nearly twice as heavy as those of the other two species. The rate of burning continued to drop in the second or third day.

Following is a brief description of the events taking place in the burner. First of all, the heat released from the combustion of the sawdust was radiated to the top layer of the test blocks, causing them to be pyrolysed. The volatile products formed burnt in the secondary combustion chamber and the heat released resulted in the burning of the char and pyrolysis of the wood blocks immediately below them. More volatiles were evolved to sustain the flaming combustion. In this way, a chain reaction was established which kept the

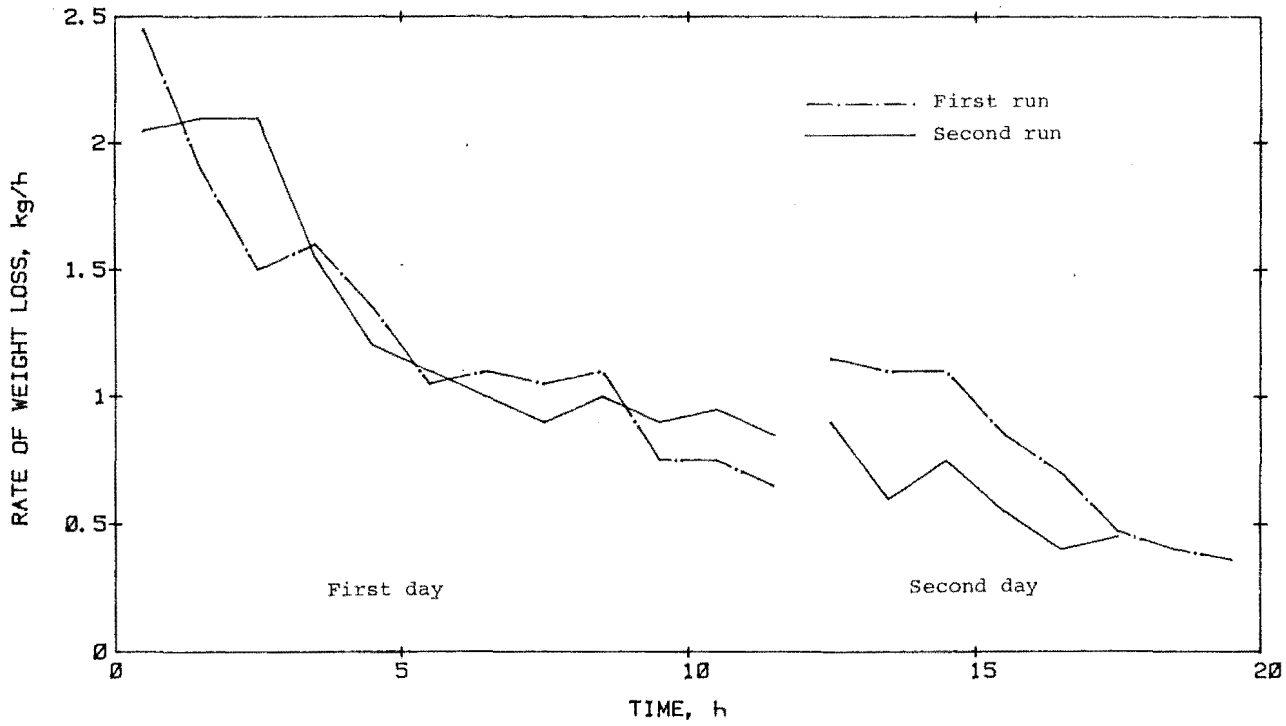

Figure 116. Burning rates of Rubber wood

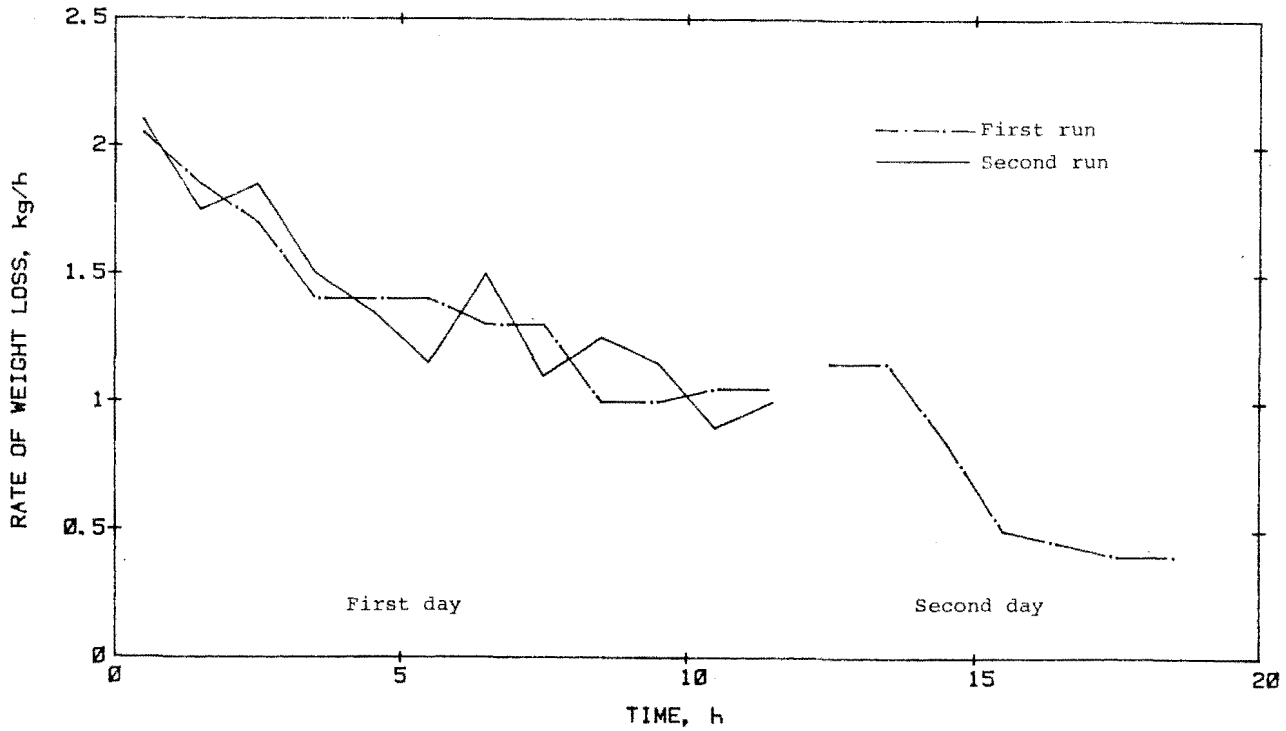

Figure 117. Burning rates of radiata Pine

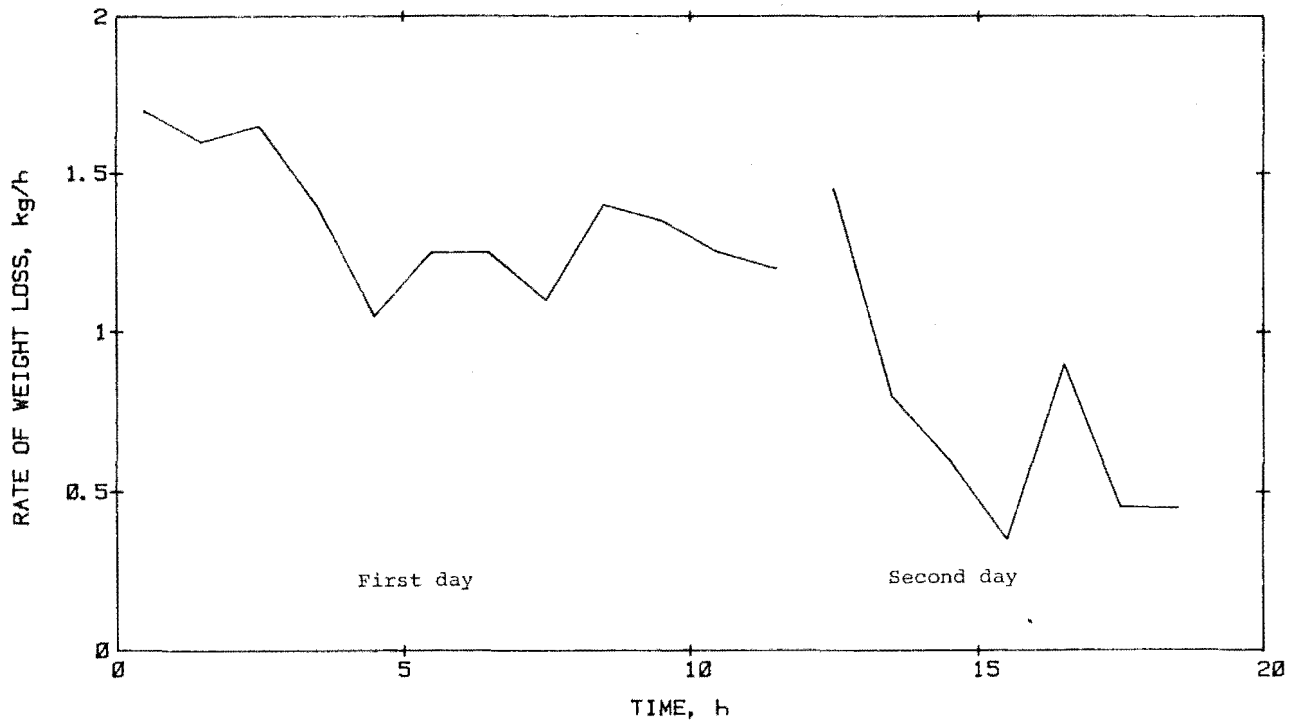

Figure 118. Burning rate of Jelutong

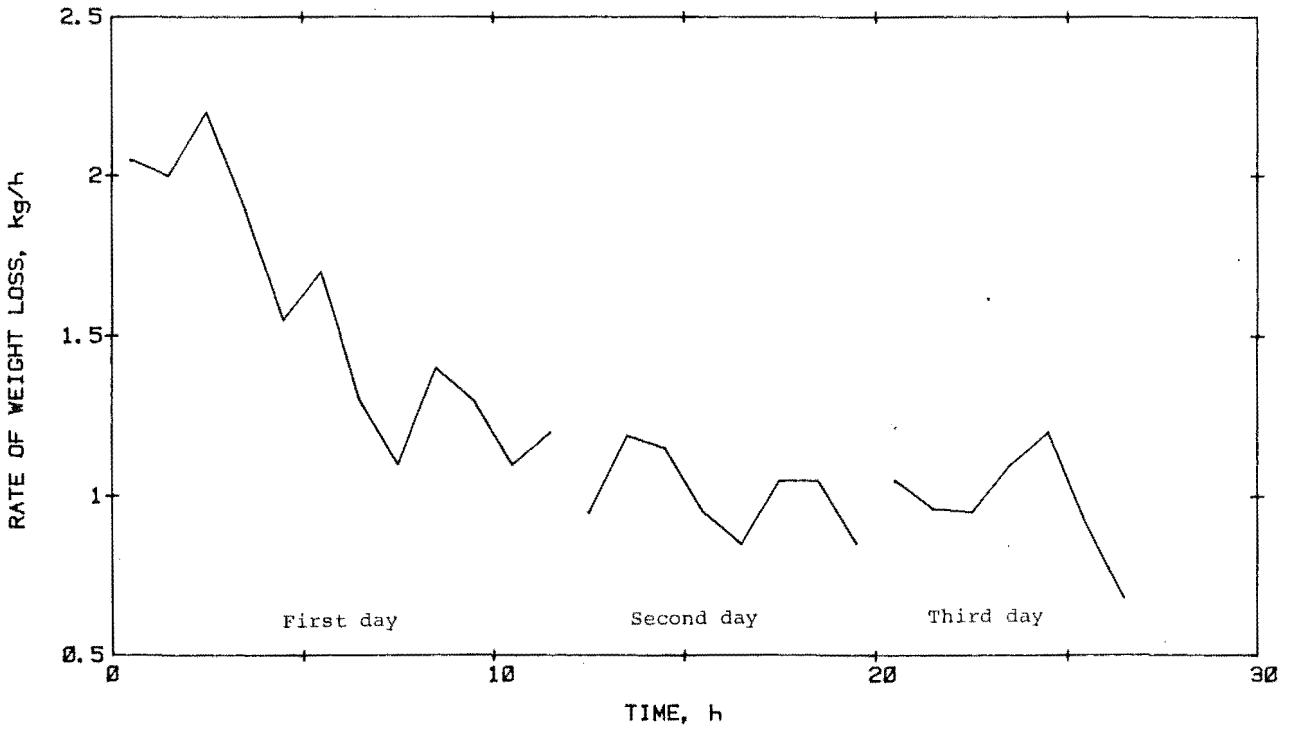

Figure 119. Burning rate of Balau

Table 23. Results of Combustion Experiments

Run No.	Species	Av. rate of burning in day 1, kg/h	% test load left at end of		
			Day 1	Day 2	Day 3
1	Rubber wood	1.27	51	19	-
2	"	1.31	51	31	-
3	Radiata Pine	1.38	35	7	-
4	"	1.38	38	-	-
5	Jelutong	1.35	36	7	-
6	Balau	1.56	63	41	21

combustion going. The heat of combustion of the char also contributed to burning of the wood. The weight loss at any moment is thus the result of a combination of pyrolysis of wood blocks and burning of char. Initially, pyrolysis played a more dominant role and this explains why the initial rate of weight loss was higher. It will be recalled that in the pyrolysis of Rubber wood, the volatile products constitute around 70% of its weight (see Section 5.3). At steady state, one would have expected the rate of weight loss to remain constant but this was not the case because of ash formation. A layer of ash was formed on top of the fuel bed, making it difficult for air to reach into the pieces down below. As the experiment progressed, more ash was formed and the burning rate dropped further. As shown in Figure 120, the left-over of the Rubber wood test load in Run No.2 was almost completely covered by ash. The situation was not as bad in the case of Radiata pine (Figure 121) and the other two wood species. This is not surprising in view of the fact that the ash content of Rubber wood is considerably higher than those of the other four species (see Table 21).

Figure 120. Left-over of Run No.2 (Rubber wood).

Figure 121. Left-over of Run No.3 (Radiata Pine).

8.2.2 Burner Temperatures

Figures 122-125 show the temperature curves of four of the runs, one for each species. It will be seen that in each of these runs, and in fact in the other two as well, the secondary combustion chamber temperature hovered around 600°C in the first day of burning. In Runs No. 1 and 3 (Rubber wood and Radiata pine respectively), it remained at around this value for some time in the second day of experiment before gradually dropping to 400-450°C, as a result of ash formation or depletion of test material. The secondary combustion temperature, too, dropped on the second day of burning in Run No.5 (Jelutong), except for a momentary rise to around 700°C a few hours after start-up. In Run No.6 (Balau), except for a slight drop now and then, it remained fairly constant in the three days of burning. The effect of ash on the combustion of the wood appeared to be minimal, which is not surprising since it has a relatively low ash content - around 0.1%.

In all of these runs, the inlet air was heated up to around 100°C by the flue heat exchanger before entering the combustion chambers. In this way, less energy was spent in heating it up to the combustion temperature than if it had been admitted cold. Had the heat exchanger been insulated, the inlet air temperature would have been higher. The flue gas temperature remained fairly constant, at slightly more than 200°C. A drop in the secondary combustion chamber temperature resulted in a corresponding drop in the flue gas and inlet air temperatures.

8.2.3 Flue Gas Analysis

The flue gas consisted of N_2, CO_2, CO, CH_4, C_2H_6 and O_2. The concentration of each component (except for N_2) was plotted against time for each of the runs in Figures 126-131. It can be seen that in the first day of burning, the levels of CO_2 and O_2 in the flue gas remained almost constant in each of

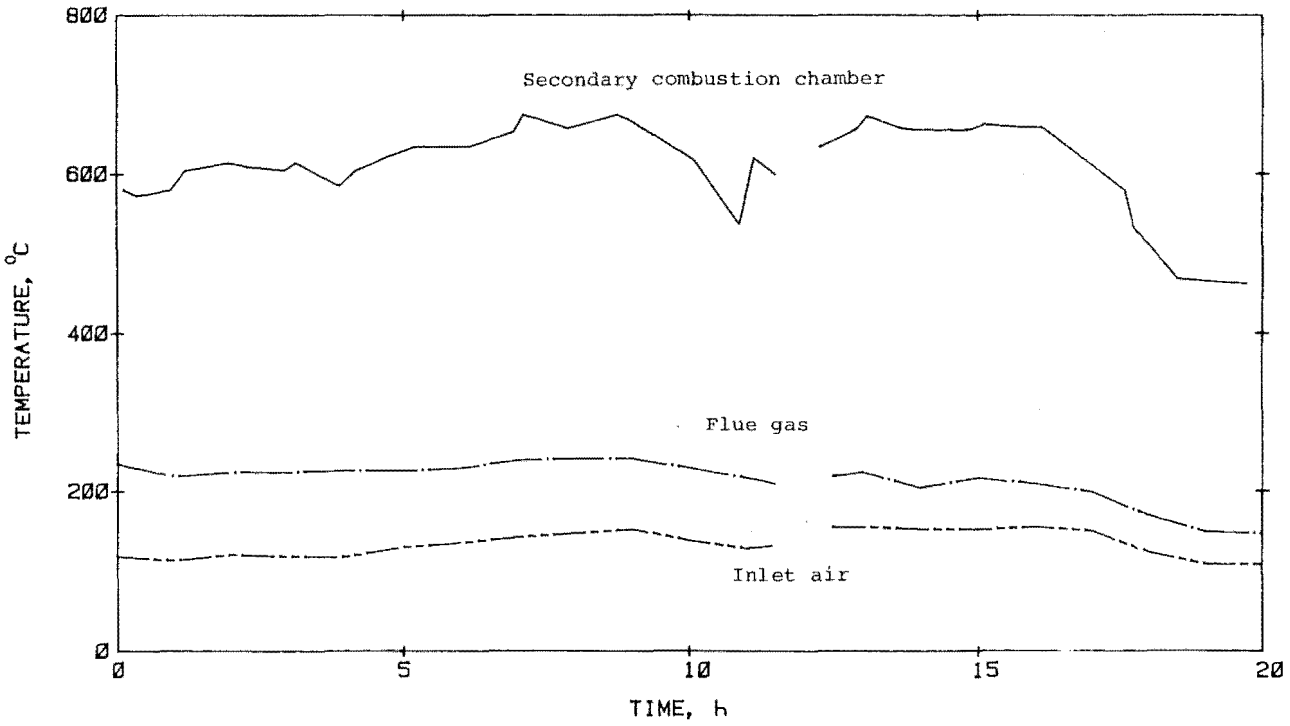

Figure 122. Temperature curves of Run No.1 (Rubber wood)

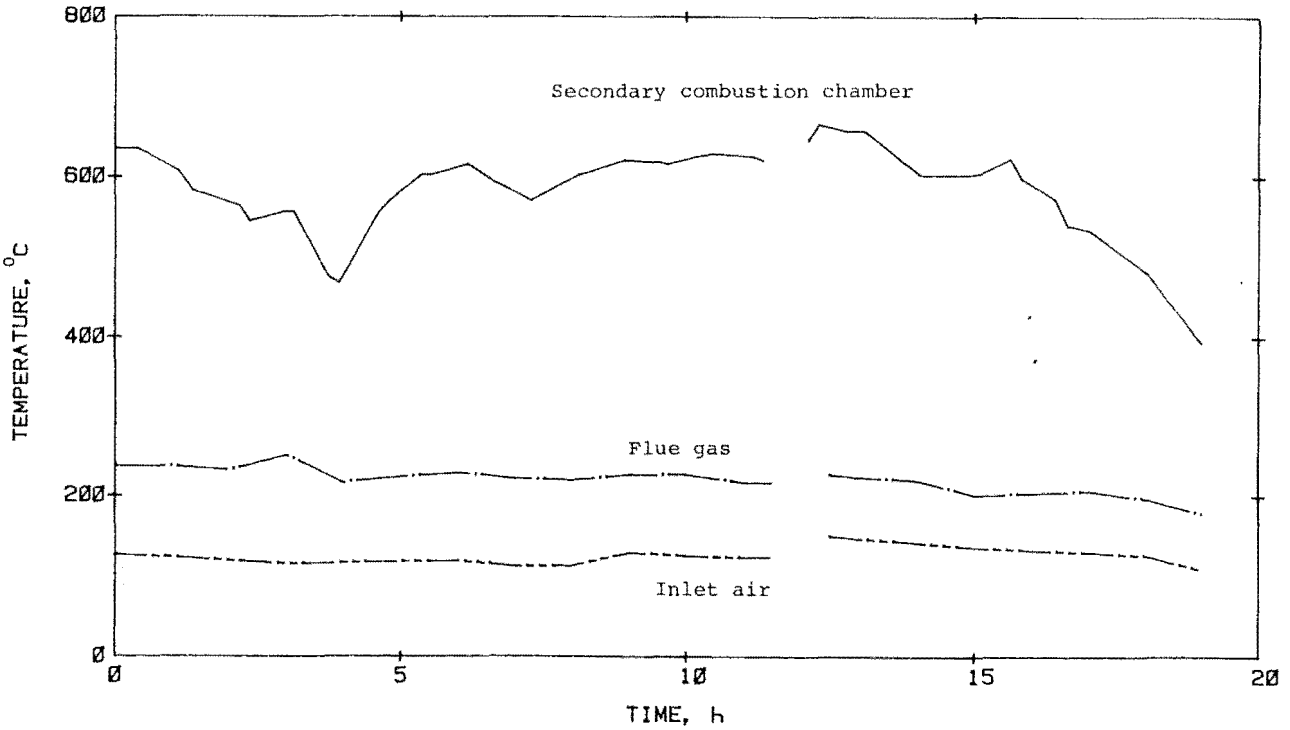

Figure 123. Temperature curves of Run No.3 (radiata Pine)

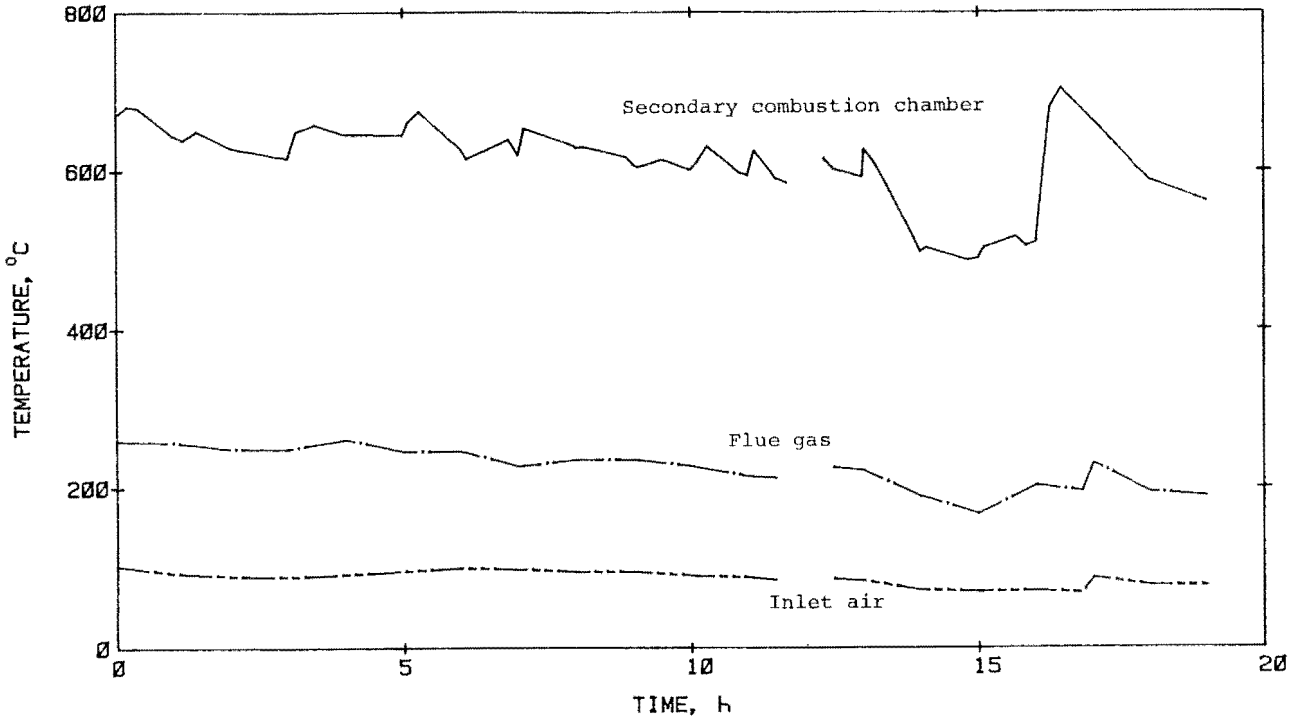

Figure 124. Temperature curves of Run No.5 (Jelutong)

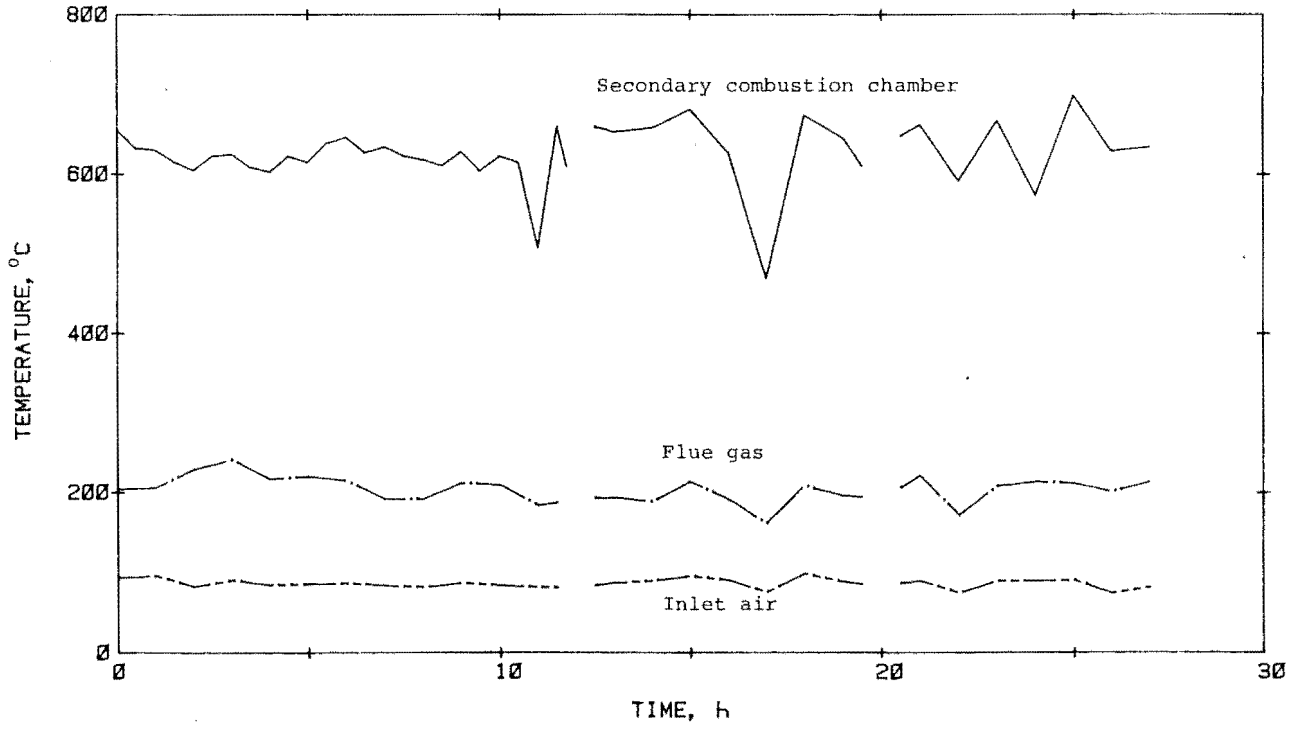

Figure 125. Temperature curves of Run No.6 (Balau)

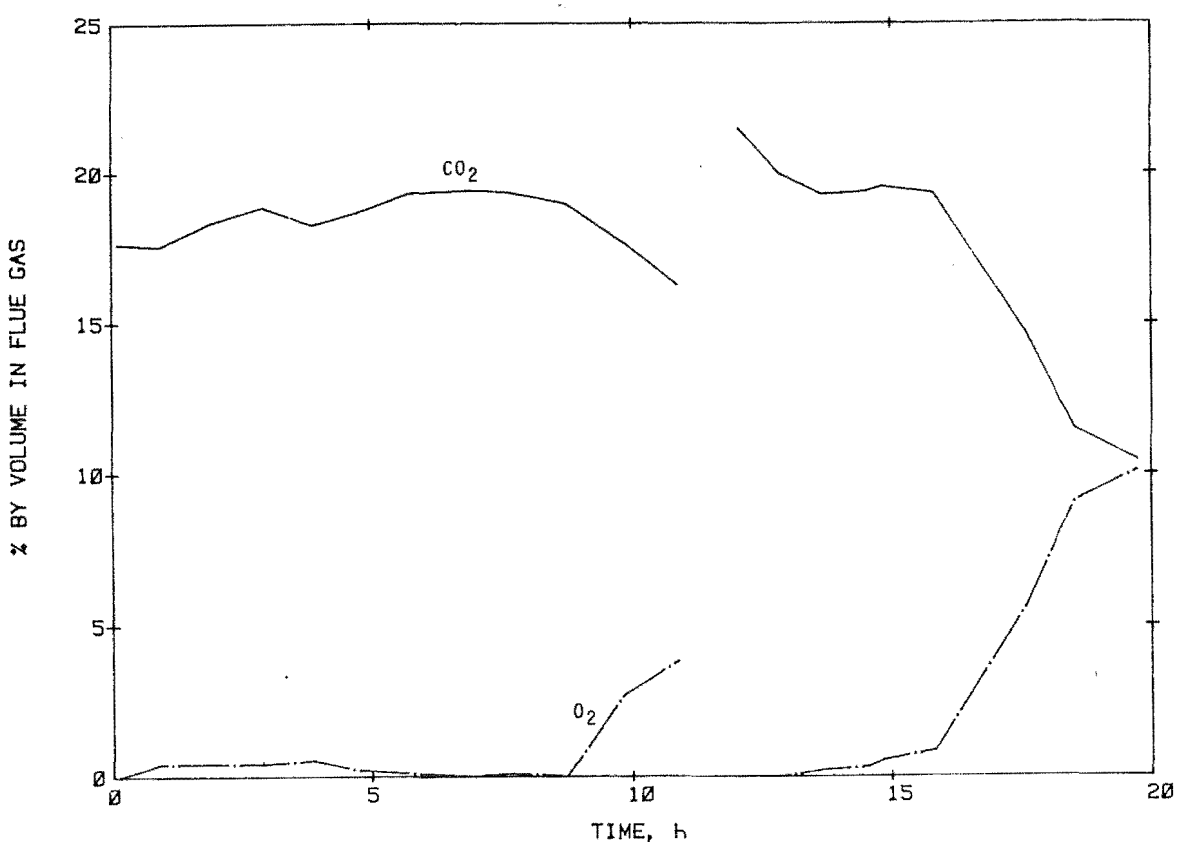

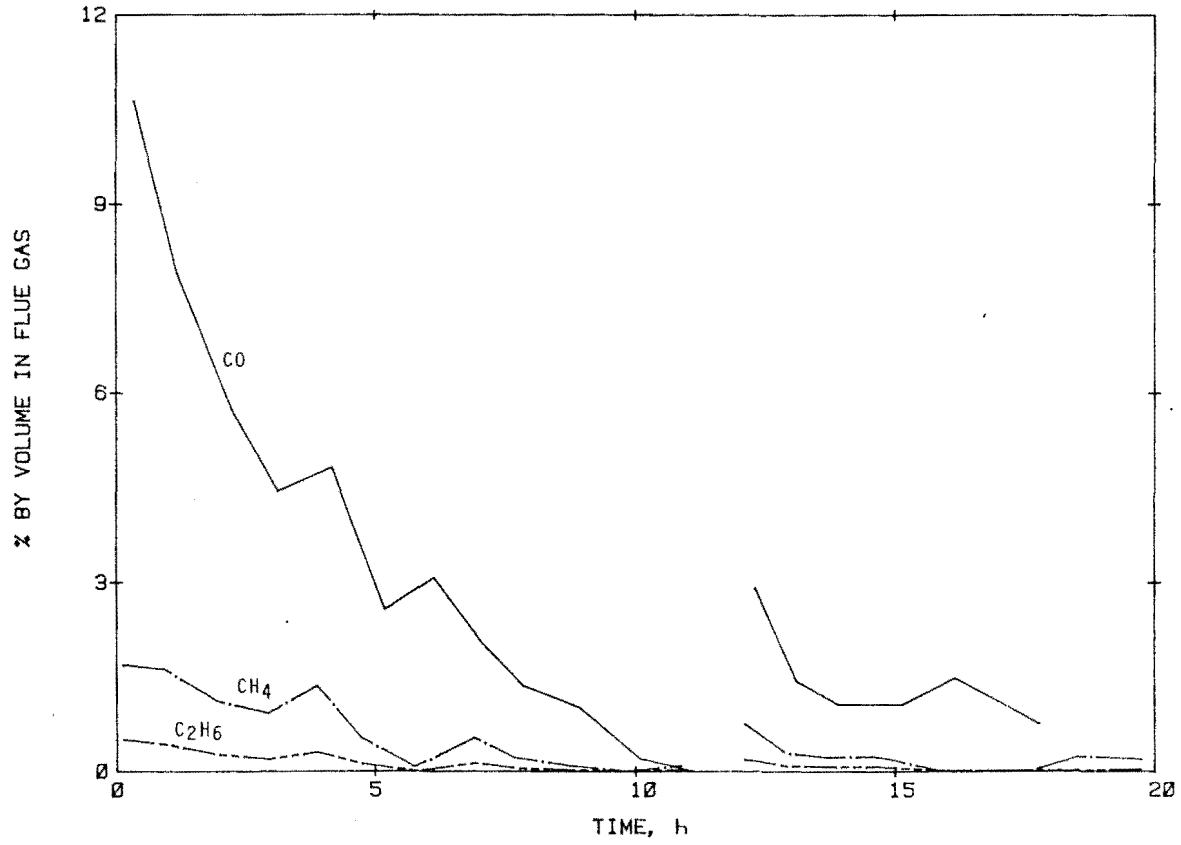

Figure 126. Flue gas analysis - Run No.1 (Rubber wood)

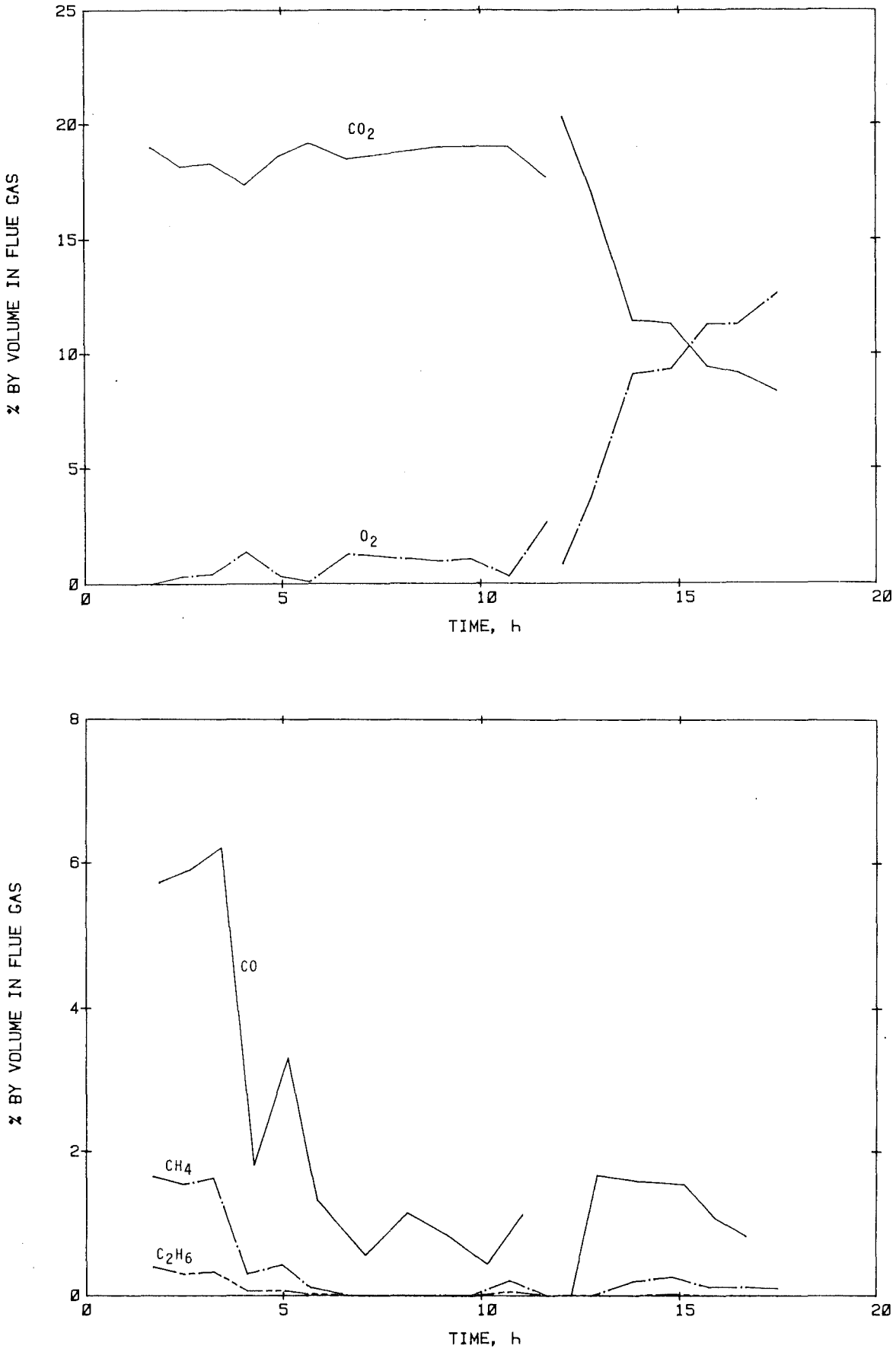

Figure 127. Flue gas analysis - Run No.2 (Rubber wood)

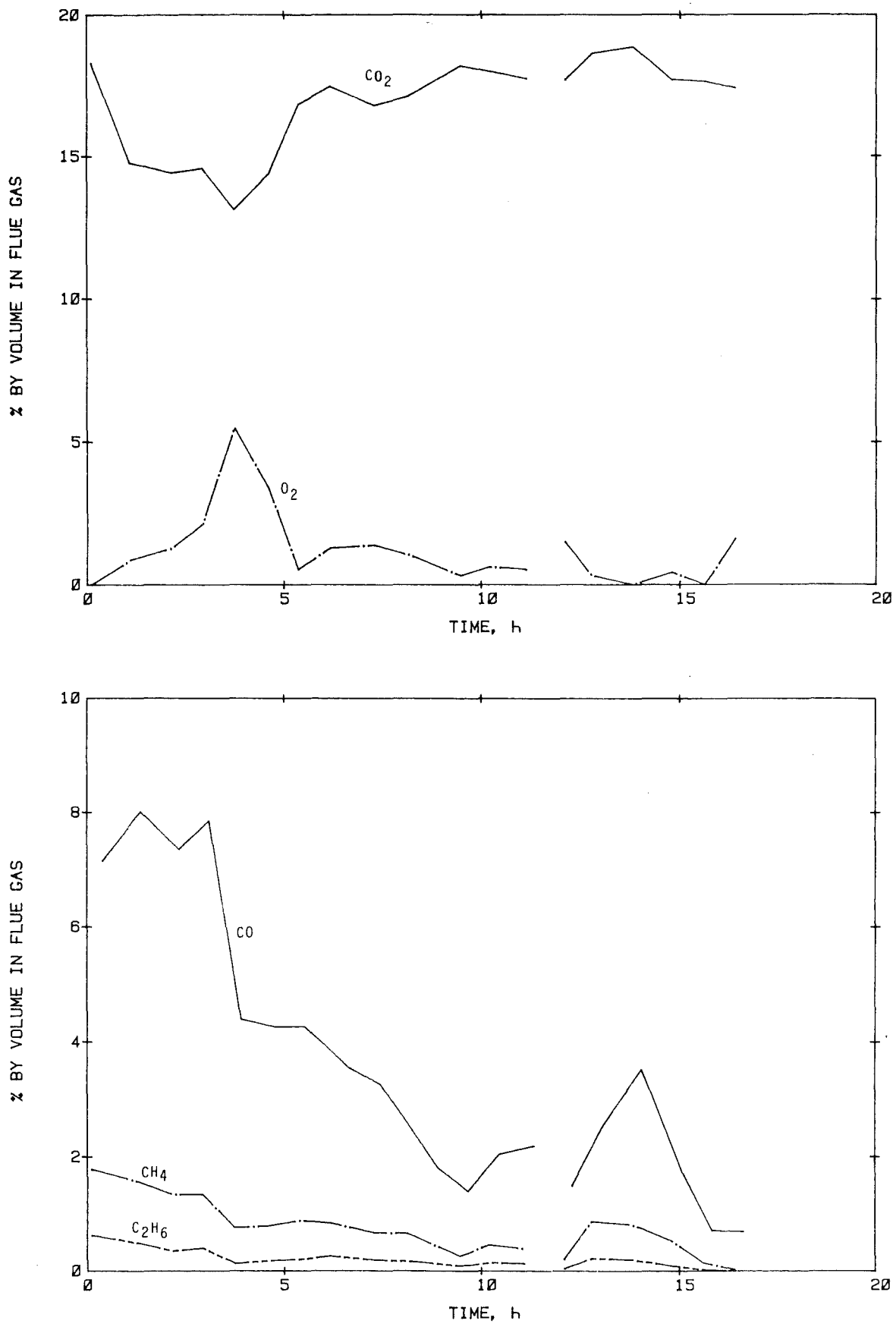

Figure 128. Flue gas analysis - Run No.3 (radiata Pine)

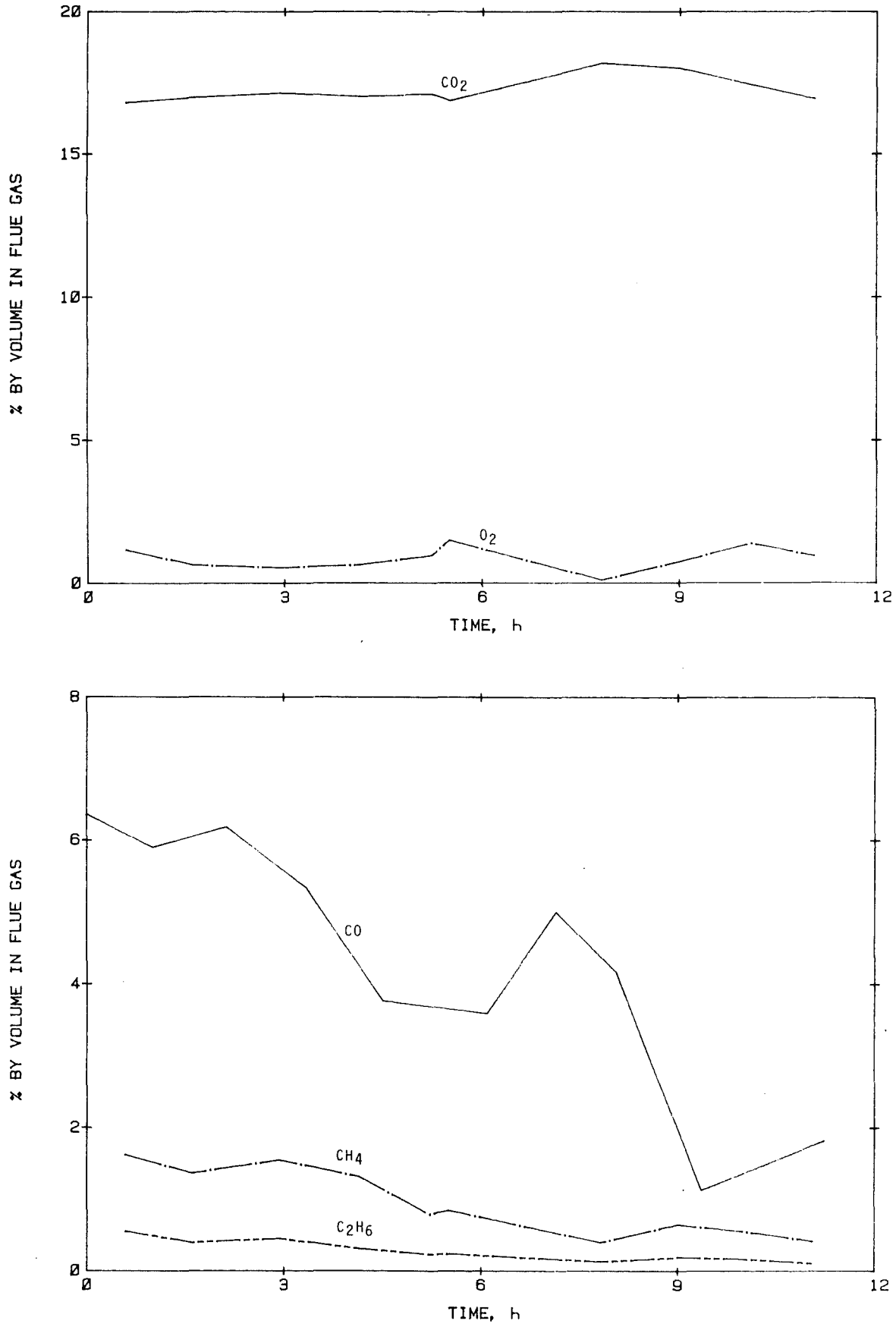

Figure 129. Flue gas analysis - Run No.4 (radiata Pine)

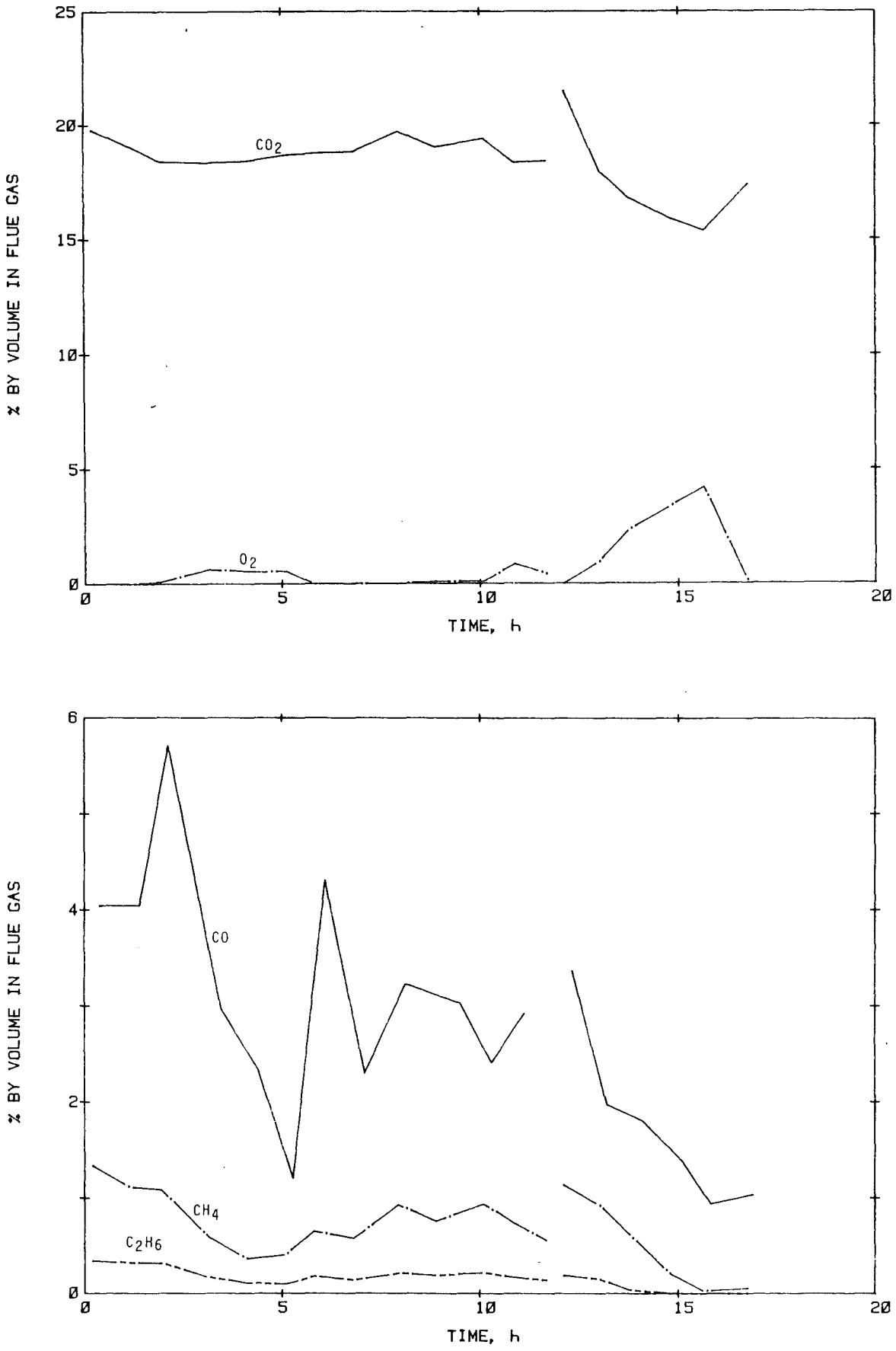

Figure 130. Flue gas analysis - Run No.5 (Jelutong)

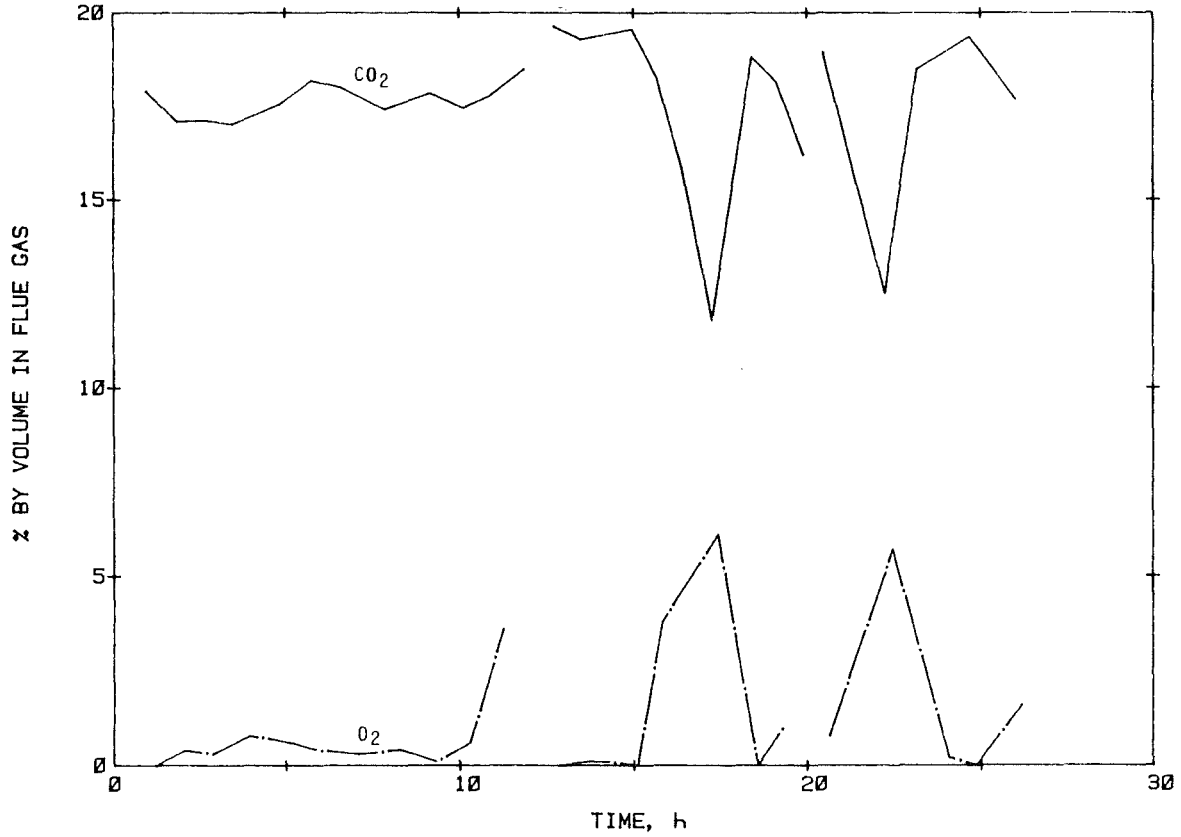

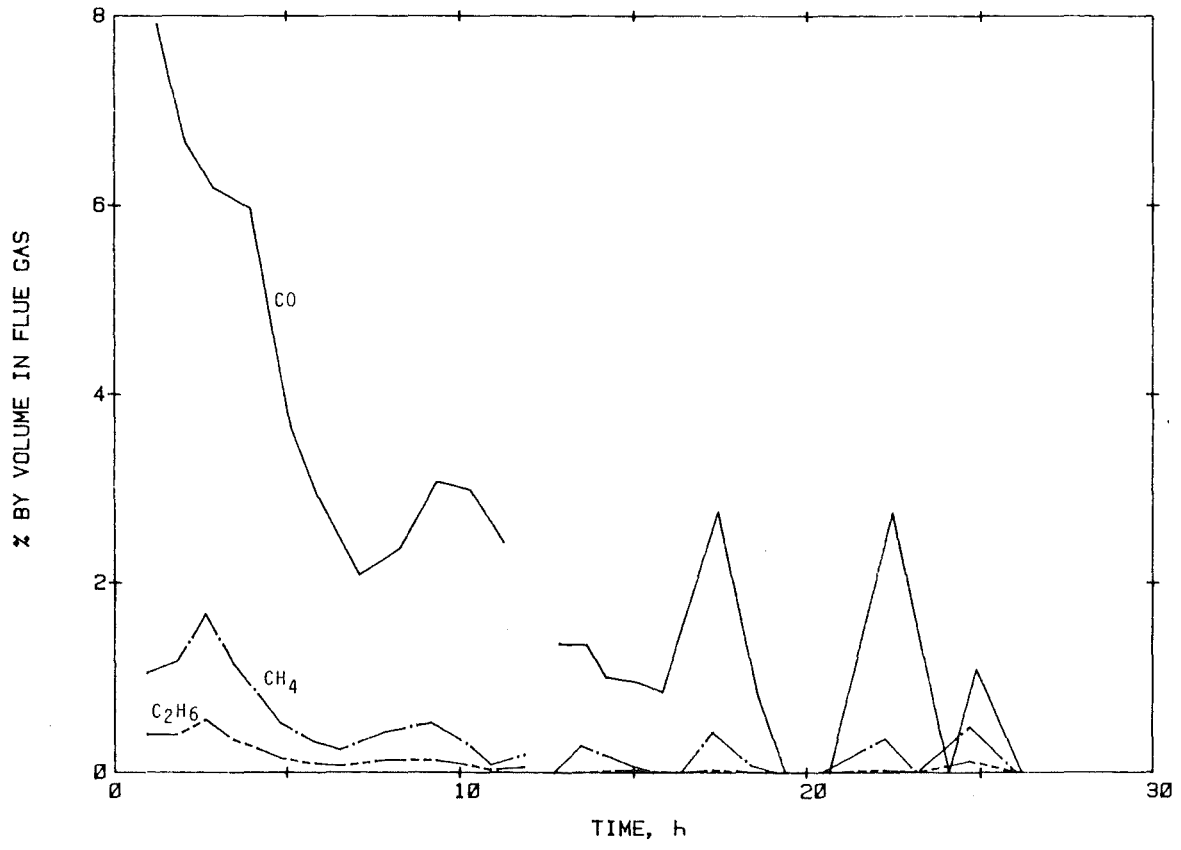

Figure 131. Flue gas analysis - Run No.6 (Balau)

the runs, the former at 17-18% v/v and the latter at 0-1% v/v. The concentrations of CO, CH_4 and C_2H_6, however, decreased with time except in Run No.5 (Jelutong) where they seemed to level off a few hours after start-up. CO was present in a greater quantity than the other two gases and its initial concentration varied from about 4% v/v (Run No.5) to more than 10% v/v (Run No.1). The presence of these gases in the flue gas indicates that combustion was incomplete. As the experiment progressed, less of these gases were produced. In Run No.3, the oxygen content of the flue gas increased to around 5% v/v between the fourth and fifth hours of burning before dropping down again. This appears to be due to a drop in the temperature of the combustion chamber for unknown reasons (see Figure 128), resulting in some of the reactions not being able to take place. An increase in the O_2 concentration of the flue gas was accompanied by a drop in the concentration of CO_2, and vice versa. On balance, burning of each test load proceeded quite well in the first day and could have been better if more air was available.

Combustion of the two Rubber wood test loads in the second day did not proceed as smoothly as in the first day. In the first run, the oxygen level in the flue gas began to rise a few hours after the run was re-started and continued doing so until the experiment was terminated. This was a corresponding drop in the rate of burning and in the combustion chamber temperature. This has earlier been found to be due to the formation of ash on top of the fuel bed. The same thing happened in the second run in which the O_2 concentration even exceeded that of CO_2 at some stage. In contrast, burning of Radiata pine and Jelutong test blocks in the second day proceeded quite well. The only significant increase in the O_2 concentration was in Jelutong (to about 5% v/v) but this lasted only for a short time. The drop in their rates of burning was perhaps due more to the depletion of material than ash formation. In the case of Balau, burning on the second and third days on the whole proceeded

satisfactorily. A certain amount of the CO, CH_4 and C_2H_6 produced on the second day remained unreacted.

The adverse effect of ash on the combustion of wood is clearly demonstrated in these experiments. Thus, in the use of wood for fuel, there is a need to remove the ash formed regularly to ensure that burning of the fuel remains unhindered. In most of the conventional wood burners, there are means for removing the ash formed. Rubber wood has a relatively high ash content and in using it for fuel, it may be necessary to remove the ash formed more often than for other wood species. The problem of ash does not arise in fluidised-bed combustion as it is removed by the interaction between the wood and the inert material. An incinerator-type wood burner, similar to the one used here, is obviously not suitable for the burning of Rubber wood as there are no provisions for ash removal.

8.2.4 Mass Balance

A mass balance was carried out for Run No.1 (Rubber wood). It was confined to the first day of experiment as combustion of the wood in the second day was not very satisfactory. As the rate of burning and also the composition of the flue gas varied during the run, it was decided to use the mean values for the material inputs. The average rate of burning of the wood during this period was 1.27 kg/h and the mean concentrations of the various gases in the flue gas, on a weight basis, were : CO_2 26.20%, CO 3.21%, CH_4 0.36%, C_2H_6 0.17%, O_2 0.76% and N_2 69.30% (by difference).

The flowsheet for the burning of the wood is shown in Figure 132. In this diagram, A, B, C, D, E, F, G and H denote the average hourly flowrates of air, N_2, CO_2, CO, CH_4, C_2H_6, O_2 and water (formed from combustion reactions) respectively. Unlike those of the other gases, the inlet air flowrate was constant as there was change in the draught used during the

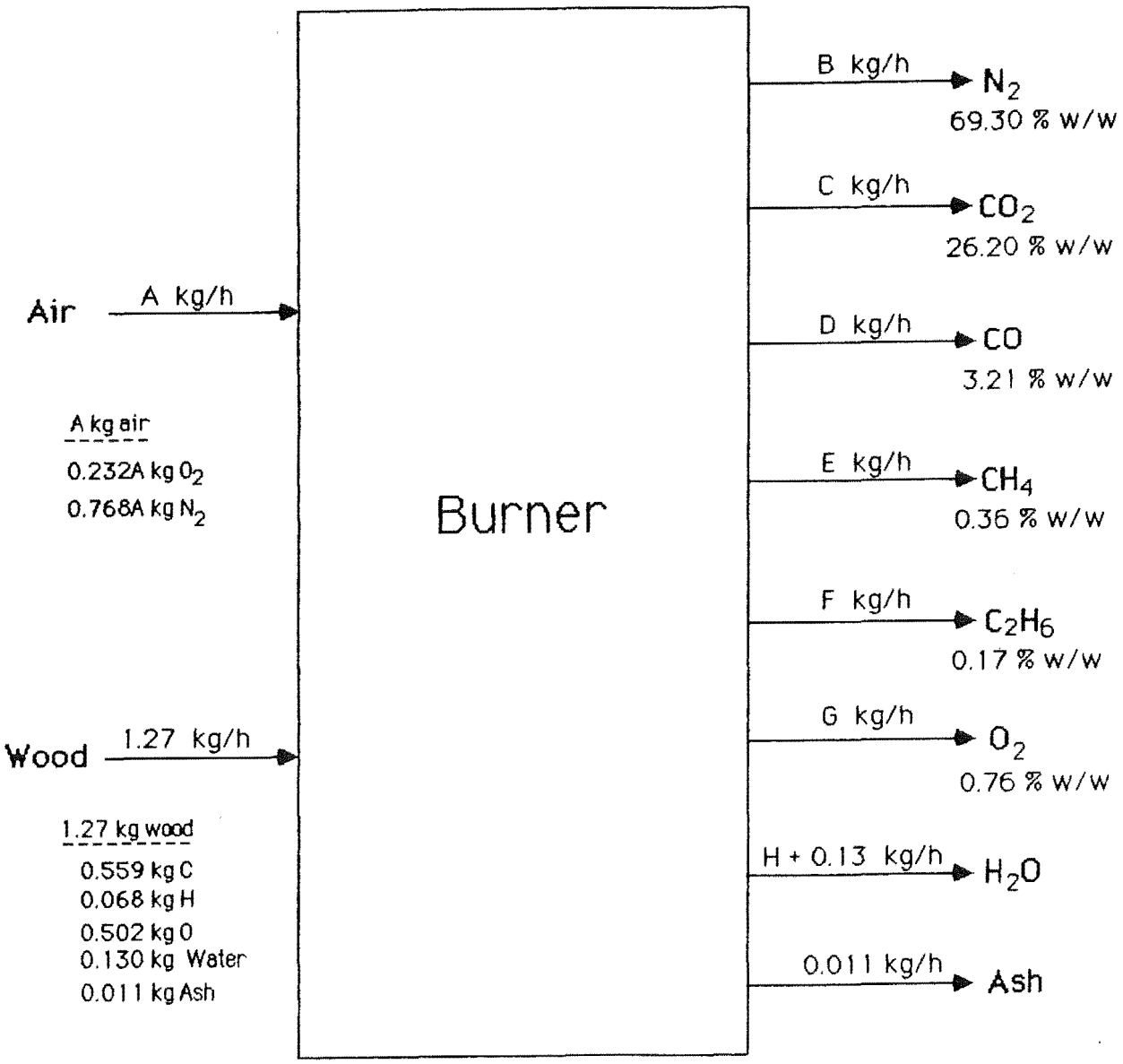

Figure 132. Flow sheet for Run No.1 (Rubber wood)

experiment. The test blocks contained 11.55% free water which did not play any part in the combustion reactions. Thus, on a dry basis, an average of 1.14 kg of wood, consisting of 0.559 kg C, 0.068 kg H and 0.502 kg O and 0.01 kg ash, was burnt every hour. As air contains 23.2% by weight of oxygen, 0.232A kg of oxygen and 0.768A kg of nitrogen entered the burner per hour.

Mass balance for C :

$$0.559 = 12C/44 + 12D/28 + 12E/16 + 24F/30 \quad .....(1)$$

Mass balance for H :

$$0.068 = 2H/18 + 6F/30 + 4E/16 \quad .....(2)$$

Mass balance for O :

$$0.232A + 0.502 = 32C/44 + 16D/28 + G + 16H/18 \quad ....(3)$$

Mass balance for N :

$$0.768A = B \quad .....(4)$$

From the composition of the flue gas, the following equations were obtained :

$$3.21B = 69.30D \quad .....(5)$$

$$3.21C = 26.20D \quad .....(6)$$

$$3.21E = 0.36D \quad .....(7)$$

$$3.21F = 0.17D \quad .....(8)$$

and

$$3.21G = 0.76D \quad .....(9)$$

Combining Equations (1), (6), (7) and (8),

$$0.559 = (12x26.20D/44x3.21)+(12D/28)+(12x0.36D/16x3.21) +(24x0.17D/30x3.21)$$

$$= 2.226D + 0.429D + 0.084D + 0.042D$$

$$= 2.781D$$

$$\therefore D = 0.559/2.781$$

$$= 0.201$$

From Equation (5), $B = 69.30x0.201/3.21 = 4.339$

From Equation (6), $C = 26.20x0.201/3.21 = 1.641$

From Equation (7), $E = 0.36x0.201/3.21 = 0.023$

From Equation (8), $F = 0.17x0.201/3.21 = 0.011$

From Equation (9), $G = 0.76 \times 0.201/3.21 = 0.048$

From Equation (2),

$$0.068 = (2H/18)+(6\times0.011/30)+(4\times0.023/16)$$
$$= 2H/18+0.002+0.006$$
$$2H/18 = 0.068-0.002-0.006$$
$$= 0.060$$
$$\therefore H = 18\times0.060/2 = 0.540$$

From Equation (4), $0.768A = 4.339$

$$\therefore A = 4.339/0.768$$
$$= \underline{5.650}$$

From the above calculations, the inlet air flowrate was found to be 5.650 kg/h. The theoretical air requirement for complete combustion of 1 kg of dry Rubber wood is estimated at 5.81 kg (Appendix 11). For 1.14 kg of dry Rubber wood, 6.62 kg of air is required for complete combustion. The air supply was therefore short of the theoretical requirement for complete combustion, by 0.97 kg/h or around 17%. In reality, the shortage was greatest in the initial stage and decreased with time, in the same way as the rate of burning. Towards the end of the day, when the rate of burning dropped to around 0.6 kg/h, there was actually an excess of air supply.

The final results are presented below :

Materials in		Materials out	
1.27	kg wood	4.339	kg N_2
5.650	kg air	1.641	kg CO_2
		0.201	kg CO
Total : 6.920	kg	0.023	kg CH_4
		0.011	kg C_2H_6
		0.048	kg O_2
		0.670	kg H_2O
		0.011	kg ash
		Total : 6.944	kg

There was a discrepancy of 0.3% between the material inputs and material outputs. The cause of this discrepancy is not entirely clear.

8.2.5 Heat Balance

Due to incomplete combustion, a certain percentage of the heat content of the wood remained untapped in the unburnt hydrocarbons, namely CO, CH_4 and C_2H_6. The magnitude of this heat loss can be calculated quite easily. The heats of combustion of CO, CH_4 and C_2H_6 are 10100 kJ/kg, 50050 kJ/kg and 47500 kJ/kg respectively (Perry and Chilton, 1973). Using the same mean gas flowrates as in the mass balance, the heat contents of the individual unburnt hydrocarbons were determined and are as follows : CO 2030 kJ/h, CH_4 1150 kJ/h and C_2H_6 520 kJ/h. The total heat content of the unburnt hydrocarbons was 3700 kJ/kg. Taking the heat of combustion of wood to be 18,500 kJ/kg (see Section 6.4.3), the heat content of 1.14 kg of dry Rubber wood was calculated at 21,100 kJ. Thus the energy lost due to incomplete combustion of the wood amounted to 18% of its heat content. This would mean that only 82% of the energy input or 17,400 kJ was actually released in the burner. This is depicted in Figure 133.

(i) Heat Loss around Heat Exchanger

The heat loss from the heat exchanger was determined by conducting a heat balance around it as follows :

<u>Temperatures</u>

Air inlet temperature	:	25°C
Air outlet "	:	130°C (mean value)
Mean air "	:	78°C
Flue gas inlet temperature	:	619°C (mean value)
Flue gas outlet "	:	227°C (" ")
Mean flue gas "	:	423°C

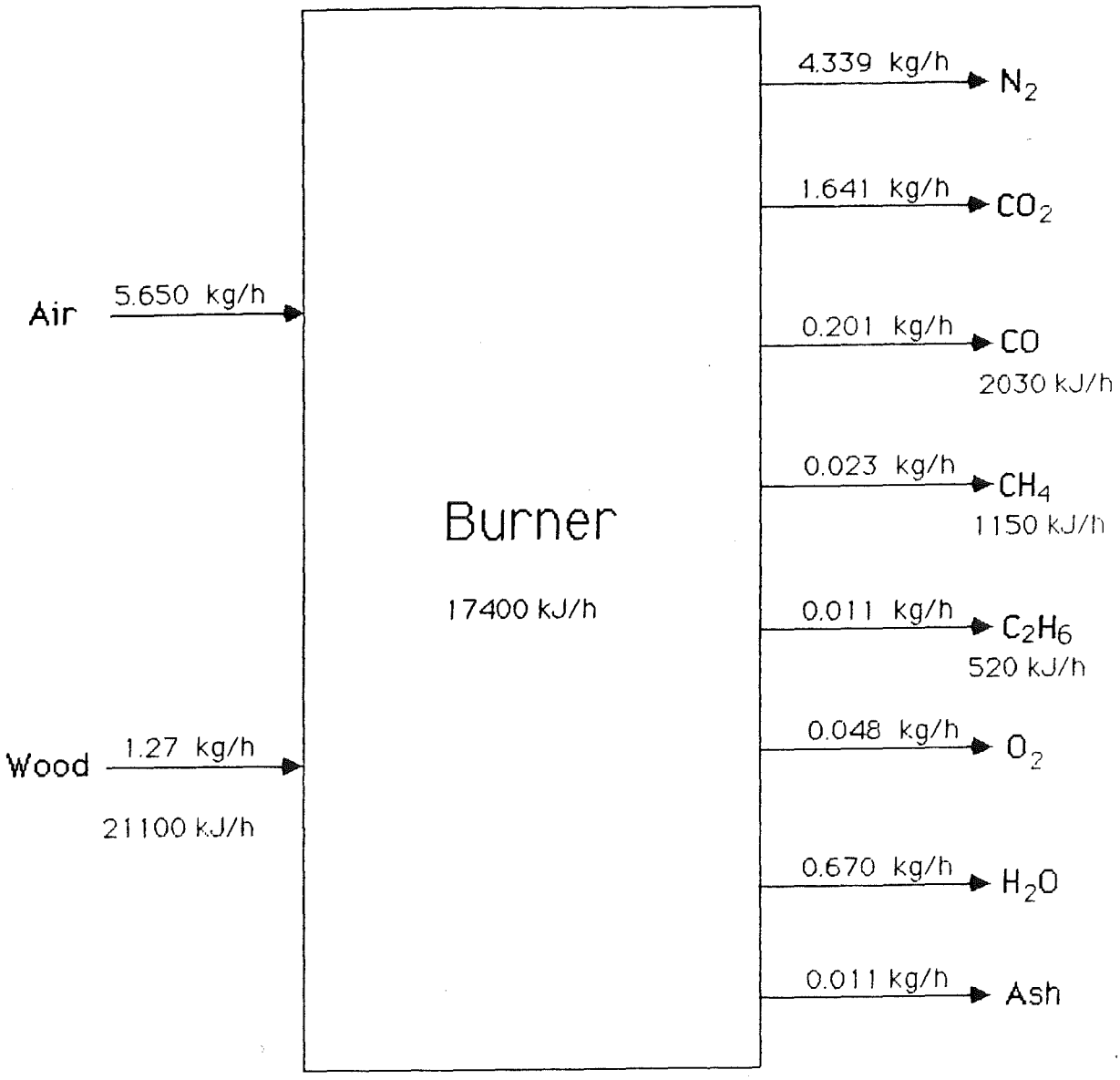

Figure 133. Heat balance for Run No.1 (Rubber wood)

Specific Heats

Specific heat of air at 78°C : 1.047 kJ/kgK
" " " " 423°C : 1.089 kJ/kgK
Specific heat of steam at 423°C : 2.0935 kJ/kgK
(Kern, 1950)

The specific heat of the flue gas was assumed to be the same as that of air. Since the specific heat of steam is around twice that of air, it was decided to work out the heat lost by the steam and the permanent gases in the flue gas separately to be more accurate.

Heat gained by air = 5.635x1.047x105 kJ
= 620 kJ
Heat lost by steam in flue gas = 0.67x2.0935x392 kJ
= 550 kJ
Heat lost by permanent gases = 6.263x1.089x392 kJ
= 2670 kJ
Total heat lost by flue gas = 3220 kJ
∴ nett heat loss of the flue gas around the heat exchanger = 2600 kJ

(ii) Heat Loss from Other Parts of Burner

The heat content of the flue gas coming out of the heat exchanger was calculated as follows :

Enthalpy of steam at 227°C 1 atm. = 2926 kJ/kg.
(Rogers and Mayhew, 1980)
Specific heat of air at 126°C = 1.05 kJ/kg K
Heat content of steam in the flue gas = 0.67x2926 kJ
= 1960 kJ
Heat content of the permanent gases = 6.263x1.05x202 kJ
= 1330 kJ
∴ heat content of the flue gas = 3290 kJ
Thus heat loss from other parts of the burner, including the fuel drum = 17400-2600-3290 kJ
= 11510 kJ

The total heat loss from the burner amounted to 14100 kJ, which represents around 80% of the heat released from the burning of the wood. The bulk of the heat loss was by radiation from the burner's outer surface.

(iii) Radiative Heat Loss from Heat Exchanger

The radiative heat loss from the heat exchanger through its outer tube can be calculated since its surface temperature is known. The equation governing the radiation of energy from a heat source to a relatively large enclosure is:

$$Q = \varepsilon \sigma A(T_1^4 - T_2^4)$$

where Q = heat flow
ε = emissivity of surface
σ = Stefan-Boltzmann constant
A = surface area
T_1 = surface temperature (K)
and T_2 = ambient temperature (K)

Mean surface temperature = $78^{\circ}C$ or 351 K
Ambient " = $25^{\circ}C$ or 298 K
Surface area = $\pi \times 0.1 \times 0.99 = 0.311\ m^2$
The emissivity of stainless steel Grade AISI 304 (18Cr 8Ni) at $78^{\circ}C$ = 0.48 (Kern, 1950)
and $\sigma = 5.67 \times 10^{-8}\ W/m^2K^4$

Thus, $Q = 0.311 \times 0.48 \times 5.67 \times 10^{-8}(351^4 - 298^4)$ W
= 61.8 W or 220 kJ/h, which is relatively small.

Most of the heat losses from the burner must have occurred through the walls of the two combustion chambers where the temperatures are comparatively high. The heat loss from the burner can be cut down substantially by insulating it with a suitable insulator, especially on the outside of the combustion chambers.

CHAPTER 9

DISCUSSION AND CONCLUSIONS

The apparatus built was well suited for the thermal studies of wood in both inert and oxidative environments. No major problems were encountered. The only constraint associated with its use lies in the heating rate which was restricted to a maximum of 6°C/min due to the large thermal capacity of the reactor. Therefore, experiments involving higher heating rates could not be carried out in this apparatus. Although this invariably limited the scope of the present investigation, it was, however, not a serious problem. As a matter of fact, a low heating rate is preferred in DTA runs in an oxidative environment as it gives a better resolution of the reaction peaks. Again, because of its large thermal capacity, it took the reactor just as long to cool down as to heat up. As a consequence, only two to three runs could be conducted in a day. Another disadvantage was the large amount of carrier or fluidising gas used in each run - around 70 litres in the case of nitrogn and around 360 litres in the case of air, with or witout blending with oxygen. This compared with only 1-1.5 litre required by the conventional static bed apparatus operating, for example, at 12°C/min heating rate and 30 ml/min gas flowrate. Against these drawbacks are the advantages that a larger sample size and also larger wood pieces can be used, allowing (1) gaseous and liquid pyrolysis products to be collected for analysis and (2) the effect of particle size on the thermal behaviour of wood to be studied.

The results of most of the experiments described in this thesis have already been discussed in some detail in the relevant sections. The main points are presented here and references are made to the more detailed discussions in the text.

In DTA of Rubber wood in an inert environment, particle sizes ranging from 150 mesh to 19 mm diameter were used. The sample remained stationary throughout the run, while the reference bed was fluidised. It was not mixed with an inert material and fluidised because the heat of pyrolysis was not high enough to produce well-defined reaction peaks under those circumstances. The shape of the resultant curve depended on the particle size of the sample, for the same gas flowrate. Generally, pyrolysis of the larger wood pieces had an overall exothermic effect while the picture was not so clear in the case of the smaller particles (Section 4.4.2). Very little difference was found in the thermal behaviours of the outer and the inner wood of a 19 mm diameter piece, although a small temperature difference existed between them due to time lag in heat transfer. It was noted that decreasing the gas flowrate produced almost the same effect as increasing the particle size (Section 4.4.3). This may be explained by the fact that, with a lower gas flowrate, the volatile products spend a longer time within the sample bed before escaping, in the same way as those in a big piece. Internal reactions between these materials is believed to be partly the cause of the variation in thermal analysis of Rubber wood of different particle sizes and using different flowrates.

The study also showed that for comparison of the thermal behaviours of different wood species, it is desirable to use larger test pieces in order to bring out the difference more clearly. Very little information is available in the literature regarding the effect of the extractives on the thermal behaviour of wood. In as far as Rubber wood is concerned, they exert quite a strong influence (Section 4.4.4). It has been shown that the thermal response of wood is simply the sum of the thermal responses of its components (Shafizadeh and DeGroot, 1977). The study conducted here showed this to be true only for small particle sizes.

The pyrolysis products of Rubber wood were collected for

analysis. The liquid fraction was the biggest of the three components (slightly over 50% w/w) and the gaseous products the smallest (around 15% w/w). It was noted that about a quarter of the gases released or 4% (w/w) of the sample's weight was CO, which is a highly poisonous gas. Although the amount of CO produced may vary under different experimental conditions, it is nevertheless important that care should be taken when working in places where wood is being pyrolysed, for example, in charcoal kilns. Like CO2, CO is released mainly within the temperature range 300-400 C, peaking at around 370 C. The bulk of these gases are formed from the degradation of cellulose, as evident from the results obtained from DTA and thermogravimetric analysis of the individual wood components (Sections 4.3 and 7.3.1).

Fluidised-bed DTA in the presence of oxygen proved to be a useful tool for studying the combustion characteristics of wood. Each DTA curve in air contained two exothermic peaks, the first one attributed to the volatiles and the second one to the char. The locations and heights of the two reaction peaks in the curve varied from species to species. Generally, the denser species took a longer time to burn to completion compared with the lighter species (Section 6.4.4). In runs in 80% O_2 (v/v), ignition occurred in only five of the twenty wood species under study, resulting in flaming combustion. Each of their DTA curves contained only one peak, as opposed to two in those of the other samples which did not ignite. The absence of a second peak in these curves is because burning of the char in the runs concerned occurred almost immediately after flaming combustion subsided. The order of the burning times of the various wood species in 80% O_2 was about the same as that obtained from the runs in air.

An interesting observation made in experiments with Rubber wood was that the tendency for ignition to occur increased with particle size of the sample (Section 6.4.2). This is thought to be due to a greater concentration of the

combustibles in one area as the particle size is increased. This line of reasoning is supported by the fact that the flaming combustion was localised, i.e. confined to individual pieces.

The DTA apparatus may also be used to evaluate chemical compounds for their fire-retarding properties. For example, in the present study, the combustibility of Rubber wood was found to be greatly reduced by treatment with a 20% borax solution (w/w) for a few hours (Section 6.4.7). The chemical treatment resulted in a reduction in the rate of production of the volatile products, making the fuel mixture less flammable. In addition, the char of the treated wood was more stable thermally than that of the untreated wood.

A further advantage of the apparatus used is that it enables the amount of heat released by the test sample to be determined through an internal electrical calibration (Section 6.4.3). Basden (1967b) used a similar apparatus to determine the specific heats of coal. These determinations are more difficult with the conventional static apparatus. It is, however, not so suitable for thermal studies of wood involving fine solids because of possible entrainment during the experiment, i.e. the particles may be carried away by the fluidising gas.

Thermogravimetry is a complementary technique to DTA and they are often used alongside each other. The results obtained from TG runs of the wood components and Rubber wood in N_2 helped confirm the conclusions drawn in DTA experiments under the same environment. They also gave the char yields of the individual wood components. It was noted that those species which burst into flame in DTA runs gave out more volatile products on pyrolysis than the other species (Section 7.3.2). This is to be expected since the volatile products are responsible for flaming combustion. These same species also had the shortest burning times in TG runs in air (with

the sample remaining stationary). This is consistent with the results obtained from DTA runs in air or in 80% O_2. Furthermore, the order of the burning times of the various wood species was about the same as that obtained from DTA runs. In other words, the relative combustibility of each wood species was unchanged in fluidised-bed and fixed-bed combustions. It should, however, be added that the above holds only for experiments involving small wood pieces. The situation may be quite different if larger wood pieces are used, as explained in the next paragraph.

The combustion experiments carried out in the fluidised-bed reactor and the down-draught incinerator represent the two extreme forms of wood combustion. In fluidised-bed combustion, the wood pieces are constantly in motion and the ash formed is rubbed off the surface of the wood as soon as it is formed by the inert material. The problems caused by the ash, therefore, do not arise. In the other combustion system, the wood pieces are stationary and burn from top to bottom. The ash formed remains on top of the fuel bed and can seriously affect combustion of the fuel, especially if it has a high ash content. This explains why the rate of burning of Rubber wood in the incinerator dropped faster than those of the other species used, as it has a higher ash content (Section 8.2.1). Each system, of course, has its other advantages and disadvantages. In general, wood combustion systems may be classified under three categories, viz (1) pile burning, (2) suspension burning and (3) fluidised-bed combustion. For each system, there are numerous designs. In addition, there are special equipments for burning sawdust. Fluidised-bed combustion of wood and related materials is a relatively recent development. Several units are in operation in New Zealand, mainly to supply hot air for drying forest products. The results obtained from the DTA runs in an oxidative environment are more applicable to this combustion system than to pile burning unless the ash formed is removed constantly.

Although most of the work described in this thesis was carried out using oven-dried wood, it must be noted that the moisture content of wood has an effect on its combustion. If the wood is too wet, combustion becomes unstable and the fire can be put out. Energy is also wasted unnecessarily in driving away the water. The moisture content of freshly cut Rubber wood is usually between 60-70% (expressed as a percentage of the oven-dried wood), which is relatively low, but what is more important is that it is comparatively fast drying (Anon, 1974; Tan et al., 1980). It therefore does not have to be stored for too long before use.

The DTA curves presented in this thesis were re-plotted from the original charts with the aid of a digitiser, a computer and a plotter. Instruments (data acquisition units) are now available in this department which can be connected to the thermocouples so that their outputs are fed directly into a computer, besides being recorded on a chart recorder. In this way, a considerable amount of time would be saved as the laborious process of digitising each curve would not be required.

From the results obtained in this work, the following conclusions may be drawn :

(1) The combustion characteristics of wood vary from species to species, with the lighter species generally easier to burn.
(2) Rubber wood is relatively easy to burn, from the viewpoint of initiating flaming combustion and the burning time.
(3) There is very little difference, if any, in the combustion characteristics of Rubber wood from the four trees chosen in this study. The same is true between the fresh and the mouldy wood from each of them.
(4) Rubber wood has a comparatively high ash content (around 1%) which may affect its combustion if not removed.
(5) The bark of the rubber tree is relatively difficult to burn, besides having a high ash content (around 7%).

Suggestion for Further Work

It would be useful to know why some wood species are easier to burn than others. It is thought that this is related to the porosity of the wood, or more specifically, the ease with which fluids flow in and out of the wood. This view is supported by the fact that Rubber wood, which burns quite easily, is relatively easy to impregnate with chemical solutions, even in the semi-dry state, and dries fairly quickly (Stevens et al., 1980; Tan et al., 1980). This is one area where further work may be carried out.

REFERENCES

1. ANON (1974) Towards a Wider Use of Rubber Wood. **Plrs. Bull. Rubb. Res. Inst. Malaysia No.135**, 181.

2. ARSENEAU, D.F.(1961) The Differential Thermal Analysis of Wood. **Can. J. Chem., 39**, 1915.

3. BASDEN, K.S.(1960a) Fluidised-bed Differential Thermal Analysis. **Fuel, 39**, 270.

4. BASDEN, K.S.(1960b) Low Temperature Reactions in Fluidised Bed Coal Analysis. **FUEL, 39**, 359.

5. BASDEN, K.S.(1967a) A Fluidised-bed Differential Thermal Calorimeter. In **Physical Aspects of Coal Carbonisation** (KIROV, N.Y. and STEPHENS, J.N., eds), 153. Research Monograph. Department of Fuel Technology, University of New South Wales, Sydney.

6. BASDEN, K.S.(1967b) An Experimental Technique for the Determination of the Specific Heats of Coals. In **Physical Aspects of Coal Carbonisation** (KIROV, N.Y. and STEPHENS, J.N., eds), 163. Research Monograph. Department of Fuel Technology, University of New South Wales, Sydney.

7. BEALL, F.C., MERRILL, W., BALDWIN, R.C. and WANG, J.H. (1976) Thermogravimetric Evaluation of Fungal Degradation of Wood. **Wood and Fiber**, 8(3), 159.

8. BERKOWITZ, N.(1957) On the Differential Thermal Analysis of Coal. **FUEL, 36**, 355.

9. BROIDO, A.(1976) Kinetics of Solid-phase Cellulose Pyrolysis. In **Thermal Uses and Properties of Carbohydrates and Lignins** (SHAFIZADEH, V.F. SARKANEN, K.V. and TILLMAN, D.A., eds.), 19. Academic Press, New York.

10. BROWNING, B.L.(1967) Methods of Wood Chemistry. Vols I and II. John Wiley and Sons, New York.

11. CHOW, S.Z. and PICKLES, K.J.(1971) Thermal Softening and Degradation of Wood and Bark. **Wood and Fiber**, 3(3), 166.

12. DOMBURG, G., SERGEEVA, V., KALNINSH, A., KOSHIK, M. and KOZMAL, F.(1968) New Aspects and Tasks of Differential Thermal Analysis in Wood Chemistry. In **Proceedings of the Second International Conference on Thermal Analysis**, held in Worcester, Massachusetts. Vol I, 623.

13. EICKNER, H.W.(1962) Basic Research on the Pyrolysis and combustion of Wood. **Forest Products J., 12**, 194.

14. EVANS, M., VITHANADURAGE, I. and WILLIAMS, A.(1981) An Investigation of the Combustion of Wood. **Journal of the Institute of Energy, 179,** 179.

15. FANG, P., MCGINNIS, G.D. and PARISH, E.J.(1975) Thermogravimetric Analysis of Loblolly Pine Bark Components. **Wood and Fiber,** 7(2), 136.

16. FENGEL, D. and WEGENER, G.(1984) Wood - Chemistry, Ultrastructure, Reactions. Walter de Gruyter, Berlin and New York.

17. Findly, W.P.K.(1960) Boron Compounds for the Preservation of Timber against Fungi and Insects. **Pest Technol.,** 2(6), 124.

18. HARRIS, E.M.(1979) Utilisation of Wastewood as Fuel and Chemical Resources. **Plrs' Bull. Rubb. Res. Inst. Malaysia No.160,** 118.

19. KERN, D.Q.(1950) Process Heat Transfer. McGraw-Hill Book Company, Inc..

20. KHOO, T.C.(1982) Private Communication. The Rubber Research Institute of Malaysia, Kuala Lumpur.

21. KOSIK, M., LUZAKOVA, V. and REISER, V.(1972) **Cellul. Chem. Technol.,** 6, 589.

22. KUNII, D. and LEVENSPIEL, O.(1969) Fluidisation Engineering. John Wiley and Sons, New York.

23. LEE, Y.H., CHIK, Engku.A.R, and CHU, Y.P.(1965) The Strength Properties of Some Malaysian Timbers. Revised by CHU, Y.P.(1979) **Timber Trade Leaflets No.34,** The Malaysian Timber Industry Board, Kuala Lumpur.

24. LEONG, S.K.(1983) Determination of Calorific Values and Energy Contents of **Hevea** Trees. **J. Rubb. Res Inst. Malaysia,** 31(1), 1.

25. LEVA, M.(1959) Fluidization. McGraw-Hill Book Company, New York.

26. MACKENZIE, R.C.(1971) Further Recommendations for Nomenclature in Thermal Analysis. In **Proceedings of the Third International Conference on Thermal Analysis,** held in Davos, Switzerland. Vol I, 609.

27. MCADIE, H.G.(1967) Recommendations for Reporting Thermal Analysis Data. **Anal. Chem.,** 39(4), 543.

28. MILLER, B. and TURNER, R.(1976) **Appl. Polym. Symp., 28,** 855.

29. NGUYEN, T., ZAVARIN, E. and BARRALL II, E.M.(1981) Thermal Analysis of Cellulosic Materials. Part I : Unmodified Materials. **J. Macromol. Sci.- Rev. Macromol. Chem., C20**(1), 1.

30. PERRY, R.H. and CHILTON, C.H.(1973) Chemical Engineers' Handbook. Fifth edition. McGraw-Hill Kogakusha Ltd., Tokyo.

31. PEEL, J.D.(1956) Rubber Wood as a Raw Material for Paper Pulp or Building Materials. **Plrs' Bull. Rubb. Res. Inst. Malaya No.23**, 29.

32. ROGERS, D.E.(1984) Differential Thermal Analysis Study of Lignite Hydrogenation. **FUEL, 63**, 1610.

33. ROGERS, G.F.C. and MAYHEW, Y.R.(1980) Thermodynamic and Transport Properties of Fluids. Third edition. Basil Blackwell, Oxford.

34. ROTHERMAL, R.C.(1976) Forest Fires and the Chemistry of Forest Fuels. In **Thermal Uses and Properties of Carbohydrates and Lignins** (SHAFIZADEH, F., SARKANEN, K.V. and TILLMAN, D.A., eds.), 245. Academic Press, New York.

35. SCHWENKER, R.F., Jr.(1968) Analytical Methods for a Textile Laboratory, 2nd edition (WEAVER, J., ed.). AATCC Monograph No.3, 385.

36. SHAFIZADEH, F.(1978) Combustion, Combustibility and Heat Release of Forest Fuels. **AIchE Symposium Series No.177, 74**, 76.

37. SHAFIZADEH, F. and DEGROOT, W.F.(1976) Combustion Characteristics of Cellulosic Fuels. In **Thermal Uses and Properties of Carbohydrates and Lignins** (SHAFIZADEH, F., SARKANEN, K.V. and TILLMAN, D.A., eds.), 1. Academic Press, New York.

38. SHAFIZADEH, F and DEGROOT, W.F.(1977) Thermal Analysis of Forest Fuels. In **Fuels and Energy from Renewable Resources**(TILLMAN, D.A., SARKANEN, K.V. and ANDERSON, L.L., eds.), 93. Academic Press, New York.

39. SHAFIZADEH, F., BRADBURY, A.G.W., DEGROOT, W.F. and AANERUD, T.W.(1982) Role of Inorganic Additives in the Smoldering Combustion of Cotton Cellulose. **Ind. Eng. Chem. Prod. Res. Dev., 21**(1), 97.

40. SHIMIZU, K.(1975) **Ringyo Shikenjo Kenko Hokoku, 272**, 1.

41. SJOSTROM, E.(1981) Wood Chemistry - Fundamentals and Application. Academic Press, New York.

42. SMOTHERS, W.J. and CHIANG, Y.(1966) Handbook of Differential Thermal Analysis. Chemical Publishing Company, Inc., New York.

43. STEVENS, M., TAN, A.G., SUJAN, M.A. and SCHALCK, J.(1980) Preservative Treatment of Rubber Wood (**Hevea brasiliensis**) by Pressure Impregnation - Chemical and Biological Evaluations. **Material und Organismen**, 15(4), 305.

44. STOTT, J.B. and BAKER, O.J.(1953) Differential Thermal Analysis of Coal. **FUEL**, **32**, 415.

45. SUSOTT, R.A., DEGROOT, W.F. and SHAFIZADEH, F.(1975) Heat Contents of Natural Fuels. **J. Fire Flammability**, **6**, 311.

46. TAN, A.G. and CHANG, W.P.(1973) Construction of SMR Pallets from Rubber Wood. **Technology Series Report No.1.** The Rubber Research Institute of Malaysia, Kuala Lumpur.

47. TAN, A.G., CHONG, K.F. and TAM, M.K.(1980) Evaluation of Three Preservative Treatment Methods for Rubber Wood (**Hevea brasiliensis**). **J. Sains IPGM**, Kuala Lumpur, 4(1), 52.

48. TAN, A.G., SUJAN, M.A. and SIM, H.C.(1981) Rubber Wood for Furniture Manufacture. **Planter**, Kuala Lumpur, **57**, 649.

49. TANG, W.K.(1972) Forest Products. In **Differential Thermal Analysis** (MACKENZIE, R.C., ed.). Vol II, 523. Academic Press, London and New York.

50. TILLMAN, D.A.(1978) Wood as an Energy Resource. Academic Press, New York.

51. WEN, C.Y. and LEVA, M.(1956) Fluidized-bed Heat Transfer: A Generalised Dense-phase Correlation. **A.I.Ch.E. Journal**, **2**, 482

52. WENDLANDT, W.W.(1974) Thermal Methods of Analysis. 2nd edition. Wiley, New York.

53. WENZL, H.F.J.(1970) The Chemical Technology of Wood. Translated from German by BRAUNS, F.E. and BRAUNS, D.A. Academic Press, New York and London.

54. WONG, H.Y.(1977) Handbook of Essential Formulae and Data on Heat Transfer for Engineers. Longman Inc., New York.

APPENDICES

Appendix 1. Densities and Moisture Contents of Rubber Wood Pieces

(1) Fresh Wood

Piece No.	Initial density kg/m^3	Moisture content %
Tjir 1		
1	643	7.86
2	668	7.50
3	660	7.22
4	676	7.57
5	612	7.85
6	622	7.99
PR 107		
1	714	8.44
2	679	8.54
3	664	7.74
4	705	8.18
5	685	8.35
6	714	8.14
RRIM 605		
1	677	8.35
2	656	8.11
3	651	8.19
4	712	7.90
5	581	7.78
6	653	8.55
RRIM 623		
1	640	8.20
2	626	8.14
3	620	8.12
4	608	8.25
5	648	8.47
6	621	8.39

contd.

(2) Mouldy Wood

Piece No.	Initial density kg/m^3	Moisture content %
Tjir 1		
1	610	7.88
2	647	7.90
3	563	7.73
4	636	7.93
5	640	8.20
6	620	8.09
PR 107		
1	576	7.63
2	626	8.14
3	615	8.26
4	649	8.58
5	631	7.98
6	647	8.63
RRIM 605		
1	585	8.09
2	573	8.82
3	566	8.50
4	574	8.28
5	556	8.13
6	632	8.35
RRIM 623		
1	565	8.33
2	578	7.89
3	581	8.51
4	563	8.63
5	576	8.00
6	563	8.17

Appendix 2. Variance Analysis

1. Between densities of fresh and mouldy wood pieces of Tjir 1

	Density, kg/m3		
	Fresh Pcs	Mouldy Pcs	Pooled Data
	643	610	
	668	647	
	660	563	
	676	636	
	612	640	
	622	620	
Sum	3881	3716	7597
Mean Density, kg/m3	646.833	619.333	633.083
Std. Deviation, kg/m3	25.7517	30.7522	
Coef. of Variation, %	3.9812	4.96538	
Unadjusted SS, $X10^6$	2.51368	2.30617	4.81985
Correction Term, $X10^6$	2.51036	2.30145	4.81181
Error SS	3315.75	4728.5	8044.25
Treatment SS			2277

ANALYSIS OF VARIANCE TABLE

Source of Variation	Degrees of Freedom	Sums of Squares	Mean Square	F
Between Discs	1	2277	2277	2.83059
Within Discs	10	8044.25	804.425	
Total	11	10321.3		

$$F_{.05}(1,10) = 4.96$$

Since 2.83059 < 4.96 , difference is not significant at the 5 % level of significance

2. Between densities of fresh and mouldy wood pieces of PR 107

	Density, kg/m3		
	Fresh Pcs	Mouldy Pcs	Pooled Data
	714	576	
	679	626	
	664	615	
	705	649	
	685	631	
	714	647	
Sum	4161	3744	7905
Mean Density, kg/m3	693.5	624	658.75
Std. Deviation, kg/m3	20.6216	26.7974	
Coef. of Variation, %	2.97355	4.29445	
Unadjusted SS, $X10^6$	2.88778	2.33985	5.22762
Correction Term, $X10^6$	2.88565	2.33626	5.22191
Error SS	2126.25	3590.5	5716.75
Treatment SS			14489

ANALYSIS OF VARIANCE TABLE

Source of Variation	Degrees of Freedom	Sums of Squares	Mean Square	F
Between Discs	1	14489	14489	25.3448
Within Discs	10	5716.75	571.675	
Total	11	20205.8		

Since 25.3448 > 4.96 ,difference is significant at 5 % level of significance

3. Between densities of fresh and mouldy wood pieces of RRIM 605

	Density, kg/m3		
	Fresh Pcs	Mouldy Pcs	Pooled Data
	677	585	
	656	573	
	651	566	
	712	574	
	581	556	
	653	632	
Sum	3930	3486	7416
Mean Density, kg/m3	655	581	618
Std. Deviation, kg/m3	42.9628	26.754	
Coef. of Variation, %	6.5592	4.60481	
Unadjusted SS, $X10^6$	2.58338	2.02895	4.61232
Correction Term, $X10^6$	2.57415	2.02537	4.59952
Error SS	9229	3578.88	12807.9
Treatment SS			16425.5

ANALYSIS OF VARIANCE TABLE

Source of Variation	Degrees of Freedom	Sums of Squares	Mean Square	F
Between Discs	1	16425.5	16425.5	12.8245
Within Discs	10	12807.9	1280.79	
Total	11	29233.4		

Since 12.8245 > 4.96 , difference is significant at 5 % level of significance

4. Between densities of fresh and mouldy wood pieces of RRIM 623

	Density, kg/m3		
	Fresh Pcs	Mouldy Pcs	Pooled Data
	640	565	
	626	578	
	620	581	
	608	563	
	648	576	
	621	563	
Sum	3763	3426	7189
Mean Density, kg/m3	627.167	571	599.083
Std. Deviation, kg/m3	14.5224	8.21888	
Coef. of Variation, %	2.31556	1.43938	
Unadjusted SS, $X10^6$	2.36108	1.95658	4.31767
Correction Term, $X10^6$	2.36003	1.95625	4.31628
Error SS	1054.5	337.75	1392.25
Treatment SS			9463.5

ANALYSIS OF VARIANCE TABLE

Source of Variation	Degrees of Freedom	Sums of Squares	Mean Square	F
Between Discs	1	9463.5	9463.5	67.9727
Within Discs	10	1392.25	139.225	
Total	11	10855.8		

Since 67.9727 > 4.96 , difference is significant at 5 % level of significance

```
10 LPRINT TAB(26);"Appendix 2.  Variance Analysis"
20 LPRINT TAB(26);"------------------------------"
30 LPRINT
40 LPRINT "1. Between densities of fresh and mouldy wood pieces of Tjir 1"
50 LPRINT "-------------------------------------------------------------------"
60 LPRINT
63 LPRINT TAB(32);"Density, kg/m3"
66 LPRINT TAB(25);"---------------------------"
70 LPRINT TAB(25);"Fresh Pcs";TAB(43);"Mouldy Pcs";TAB(62);"Pooled Data"
80 LPRINT TAB(25);"----------";TAB(43);"-----------";TAB(62);"-----------"
90 B1=0
100 B2=0
130 C1=0
140 C2=0
170 R=2
180 C=6
185 F=4.96
190 DIM A(R,C)
200 FOR I=1 TO R
210 FOR J=1 TO C
220 READ A(I,J)
230 NEXT J,I
240 FOR J=1 TO C
250 B1=B1+A(1,J)
260 B2=B2+A(2,J)
290 C1=C1+A(1,J)[2
300 C2=C2+A(2,J)[2
330 LPRINT TAB(27);A(1,J);TAB(46);A(2,J)
340 NEXT J
350 FOR J=1 TO C
360 LPRINT TAB(25);"----------";TAB(43);"-----------";TAB(62);"-----------"
370 LPRINT "Sum";TAB(26);B1;TAB(45);B2;TAB(64);B1+B2
380 LPRINT
385 LPRINT
390 LPRINT "Mean Density, kg/m3 ";TAB(26);B1/C;TAB(45);B2/C;TAB(64);(B1+B2)/(R*C
)
400 LPRINT
410 T1=C1-B1[2/C
420 T2=C2-B2[2/C
450 S1=SQR(T1/(C-1))
460 S2=SQR(T2/(C-1))
490 LPRINT "Std. Deviation, kg/m3 ";TAB(26);S1;TAB(45);S2
500 LPRINT
510 LPRINT "Coef. of Variation, % ";TAB(26);100*S1*C/B1;TAB(45);100*S2*C/B2
520 LPRINT
530 LPRINT
540 LPRINT "Unadjusted SS, X10";TAB(26);C1/10[6;TAB(45);C2/10[6;TAB(64);(C1+C2)/
10[6
550 LPRINT
560 LPRINT "Correction Term, X10";TAB(26);B1[2/C/10[6;TAB(45);B2[2/C/10[6;TAB(64
);(B1[2+B2[2)/C/10[6
570 LPRINT
580 P=C1-B1[2/C+C2-B2[2/C
590 LPRINT "Error SS";TAB(26);C1-B1[2/C;TAB(45);C2-B2[2/C;TAB(64);P
600 LPRINT
610 Q=(B1[2+B2[2)/C-(B1+B2)[2/R/C
620 LPRINT "Treatment SS"; TAB(64);Q
640 LPRINT
660 LPRINT
670 LPRINT TAB(30);"ANALYSIS OF VARIANCE TABLE"
```

```
680 LPRINT TAB(30);"--------------------------"
690 LPRINT
700 LPRINT TAB(5);"Source of";TAB(25);"Degrees of";TAB(40);"Sums of";TAB(55);"Me
an"
710 LPRINT TAB(5);"Variation";TAB(26);"Freedom";TAB(40);"Squares";TAB(54);"Squar
e";TAB(73);"F"
720 LPRINT TAB(5);"------------------------------------------------------------
-------------"
740 F1=Q*R*(C-1)/(R-1)/P
750 LPRINT TAB(5);"Between Discs ";TAB(28);R-1;TAB(40);Q;TAB(54);Q/(R-1);TAB(69)
;F1
760 LPRINT TAB(5);"Within Discs ";TAB(27);R*(C-1);TAB(40);P;TAB(55);P/R/(C-1)
770 LPRINT TAB(5);"------------------------------------------------------------
-------------"
780 LPRINT TAB(7);"Total";TAB(27);R-1+R*(C-1);TAB(39);P+Q
790 LPRINT TAB(5);"------------------------------------------------------------
-------------"
800 LPRINT
805 LPRINT TAB(27);"F  (1,10) = 4.96"
810 LPRINT
820 IF F1>F THEN 840
830 LPRINT TAB(8);"Since";F1;"<";F;", difference is not significant at the 5 % l
evel of significance"
835 GOTO 850
840 LPRINT TAB(8);"Since";F1;">";F;", difference is significant at the 5 % level
 of significance"
850 END
900 DATA 643,668,660,676,612,622
910 DATA 610,647,563,636,640,620
```

Appendix 3. Selection of Gas Flowrate

(1) Calculation of minimum fluidising velocity, u_{mf}

The general equation for the calculation of u_{mf} for the whole range of Reynolds number, as given in Kunii and Levenspiel (1969), is

$$\frac{d_p u_{mf} \rho_g}{\mu} = \left(33.7^2 + 0.0408 \frac{d_p^3 \rho_g (\rho_s - \rho_g) g}{\mu^2} \right)^{\frac{1}{2}} - 33.7 \quad \ldots\ldots(i)$$

where d_p = the particle diameter

u_{mf} = the superficial fluid velocity (measured on an empty tube basis) at minimum fluidising conditions

ρ_g = the gas density

ρ_s = the solid density

μ = the gas viscosity

and g = the acceleration of gravity

The Reynolds number, Re_p, is given by

$$Re_p = \frac{d_p \rho_g u_o}{\mu}$$

where u_o = the superficial fluid velocity (measured on an empty tube basis) through a bed of solids.

For small particles, with Re_p smaller than 20, Equation (i) is simplified to :

$$u_{mf} = \frac{d_p^2 (\rho_s - \rho_g) g}{1650 \mu}$$

In the DTA runs, it was decided to use beach sand of particle size -85+100 mesh as the inert material. For this fraction,

$$d_p = 1.65 \times 10^{-4} \text{ m}$$

$$\rho_s = 2590 \text{ kg/m}^3 \text{ (Leva, 1959)}$$

Also μ at 25°C = 1.18 kg/m^3 (Wong, 1977)

$$\rho_g = 1.983 \times 10^{-5} \text{ kg/ms (Wong, 1977)}$$

$$\therefore u_{mf} = \frac{1.65^2 \times 10^{-8} \times (2590-1.18) \times 9.81}{1650 \times 1.983 \times 10^{-5}} \text{ m/s}$$

$$= 0.0211 \text{ m/s}$$

$$\text{and } Re_p = \frac{1.65 \times 10^{-4} \times 1.18 \times 10^{-3} \times 0.0211}{1.983 \times 10^{-5}}$$

$$= 0.21$$

Since Re_p is less than 20, the use of the simplified equation for calculating u_{mf} is justified.

(2) Calculation of u_o/u_{mf} for several gas flowrates

Internal diameter of reaction tubes = 2.664×10^{-2} m

Flow area of each tube $= \frac{\pi}{4} \times 2.664^2 \times 10^{-4}$ m^2

$= 5.57 \times 10^{-4}$ m^2

Now, Flowrate = Area x Velocity

or Velocity = Flowrate/Area

(1 lit/min = 1.667×10^{-5} m^3/s)

The following tabulation gives the superficial gas velocities and the corresponding values of u_o/u_{mf} for gas flowrates of 1, 2, 3 and 4 lit/min.

Flowrate, lit/min	u_o, m/s	u_o/u_{mf}
1	0.030	1.42
2	0.060	2.84
3	0.090	4.26
4	0.120	5.68

Since u_o/u_{mf} is greater than 1 for all the flowrates, it would appear that anyone of them may be used. To find out which one of them is the most suitable, trial runs were carried out.

(3) Trial runs

First of all, blank runs were carried out to determine the heights of the expanded beds for different gas flowrates and at different temperatures. To facilitate measurement of bed height, the steel frames were not used in these runs. Each bed contained 30 gm of sand of height in the unfluidised state of 40 mm. In one bed was inserted a chromel/alumel thermocouple to measure its temperature. The reactor was heated up at about 5.5°C/min and air was passed through the two tubes at the desired flowrate. The expanded bed height was measured by lowering a graduated steel wire with a thin, circular plate welded horizontally to its end into the bed without a thermocouple. The reading on the scale when sand began to be collected on the plate was taken and from it the bed height was determined. The results of the blank runs for air flowrates of 2, 4, 6 and 8 lit/min (combined flowrates) are plotted in Figure A1. With a gas flowrate of 2 lit/min, fluidisation did not occur until about 100°C. The bed height increased by about 20% over that of the static bed at 250°C and by about 50% at 500°C. Fluidisation was rather sluggish. With a flowrate of 4 lit/min, fluidisation occurred from the outset. The bed height increased by about 25% at ambient temperature, by about 55% at 250°C and by about 90% at 550°C. Fluidisation was generally smooth and steady. With gas flowrates of 6 lit/min and 8 lit/min, fluidisation was rather

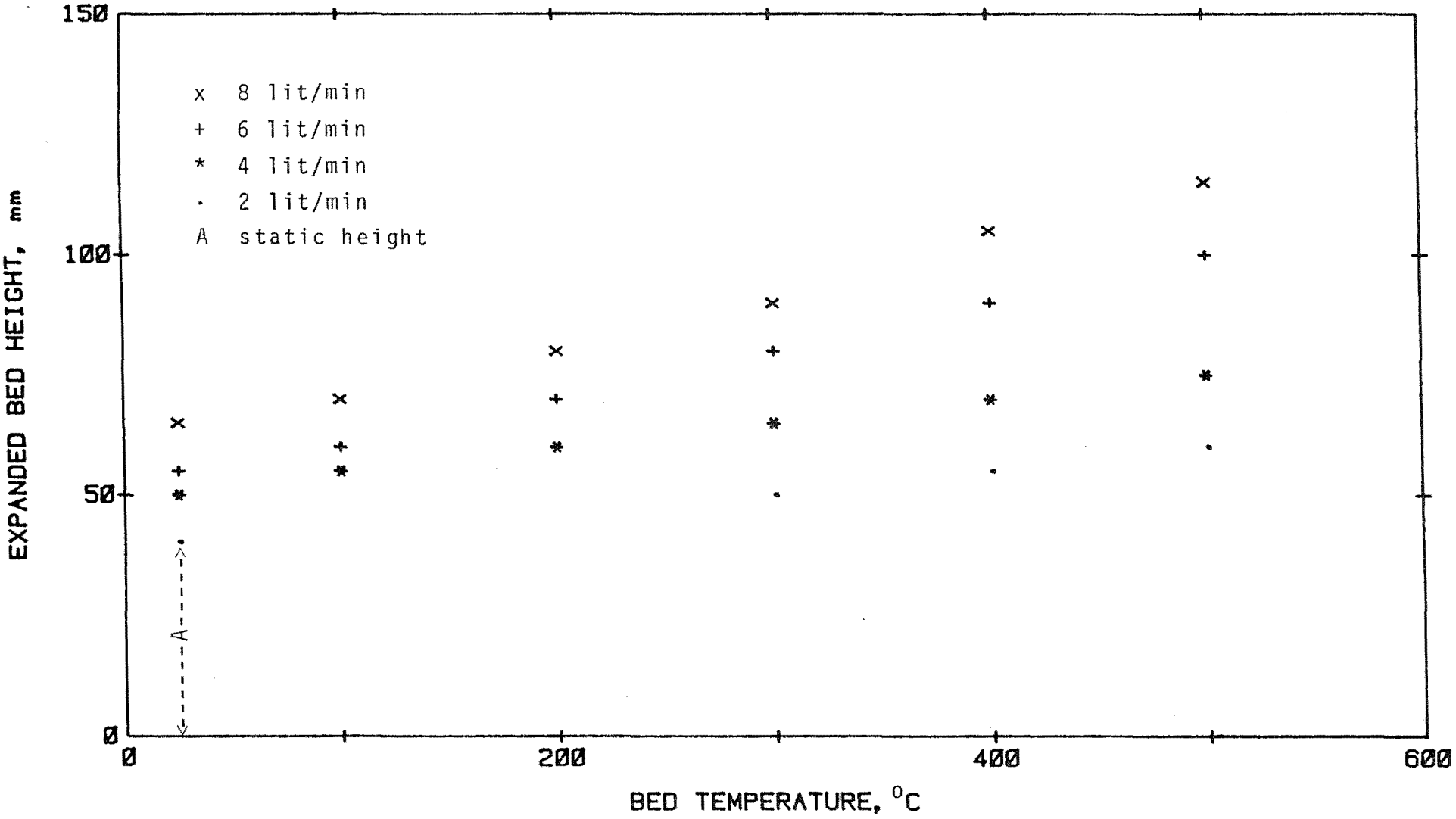

Figure A1. Height of expanded bed versus gas flowrate at different temperatures

violent, especially at high temperatures. To help make a final choice, trial runs were carried out using Rubber wood as samples. From the observations made, the suitability of the last two flowrates was ruled out for the following reasons:

(1) there is a tendency for the smaller particles to be pushed up the bed if the gas flowrate is too high,

(2) with a high gas flowrate, the distributor runs the risk of being forced up the tube despite being sandwiched between two steel frames.

The above problems did not arise when a flowrate of 4 lit/min was used. There was very little disruption to the experiment and it was clearly the best choice.

Appendix 4. DTA Curves in Air and in 80% O2 of some Tropical Wood Species

Figure A3 : Balau
" A4 : Bark of rubber tree
" A5 : Chengal
" A6 : Coconut wood
" A7 : Jelutong
" A8 : Kempas
" A9 : Keruing
" A10 : Mengkulang
" A11 : Meranti, dark red
" A12 : Meranti, light red
" A13 : Merbau
" A14 : Mersawa
" A15 : Nyatoh
" A16 : Oil palm wood
" A17 : Pulai
" A18 : Ramin
" A19 : Sepetir
" A20 : Tembusu
" A21 : Tualang

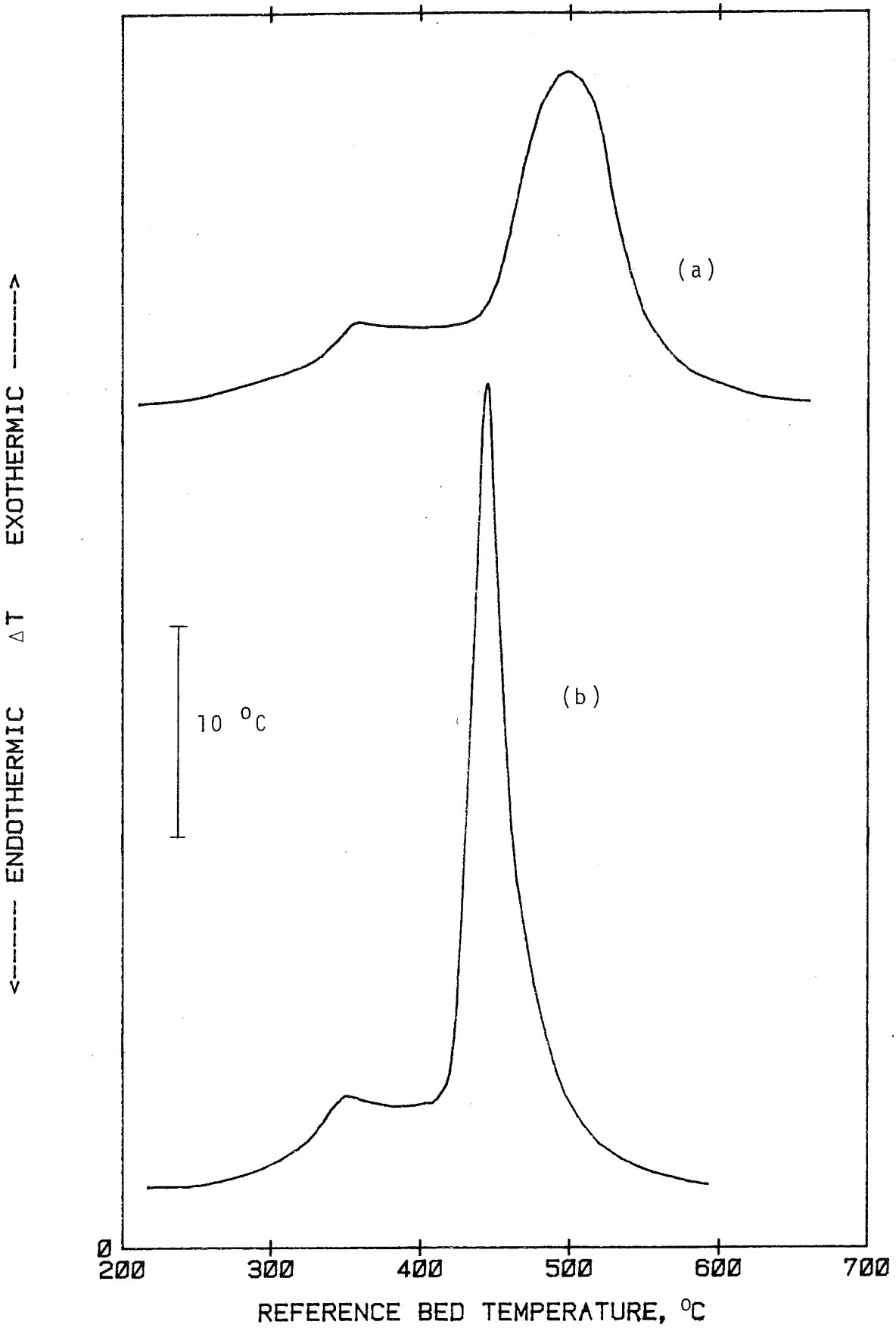

Fig. A3. DTA curves of Balau:(a) in air and (b) in 80% O_2

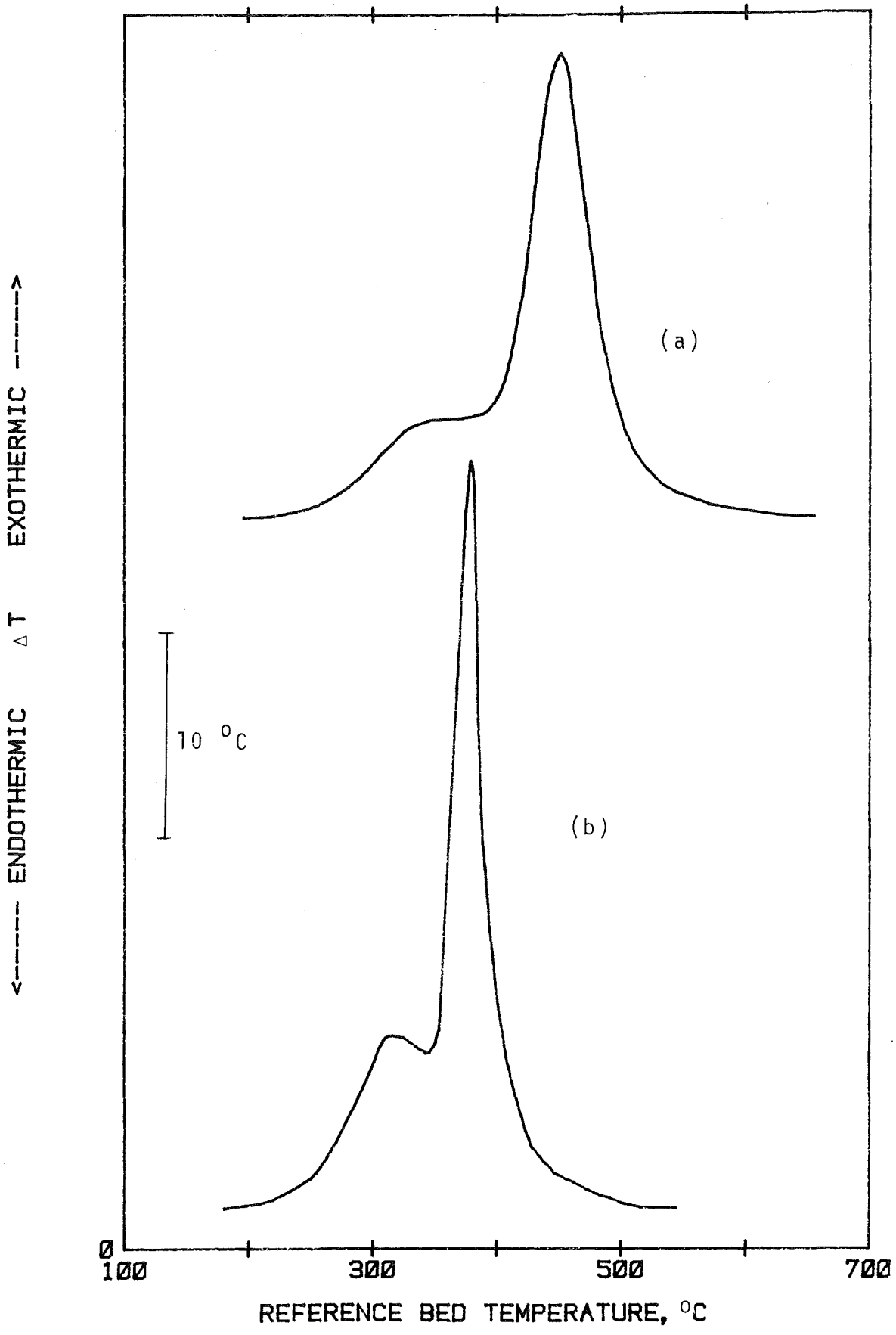

Fig. A4. DTA curves of rubber tree bark:(a) in air and (b) in 80% O_2

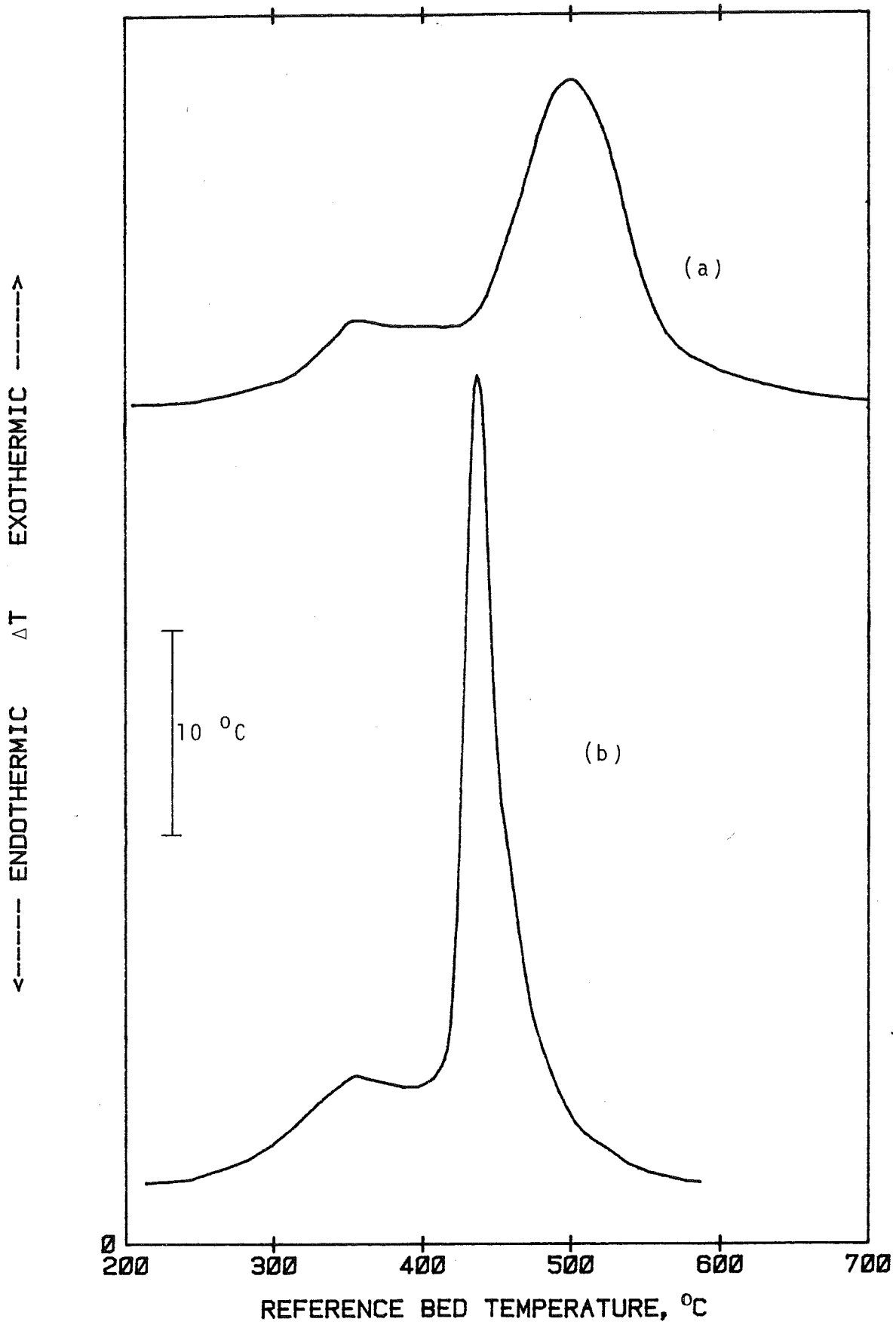

Fig. A5. DTA curves of Chengal:(a) in air and (b) in 80% O_2

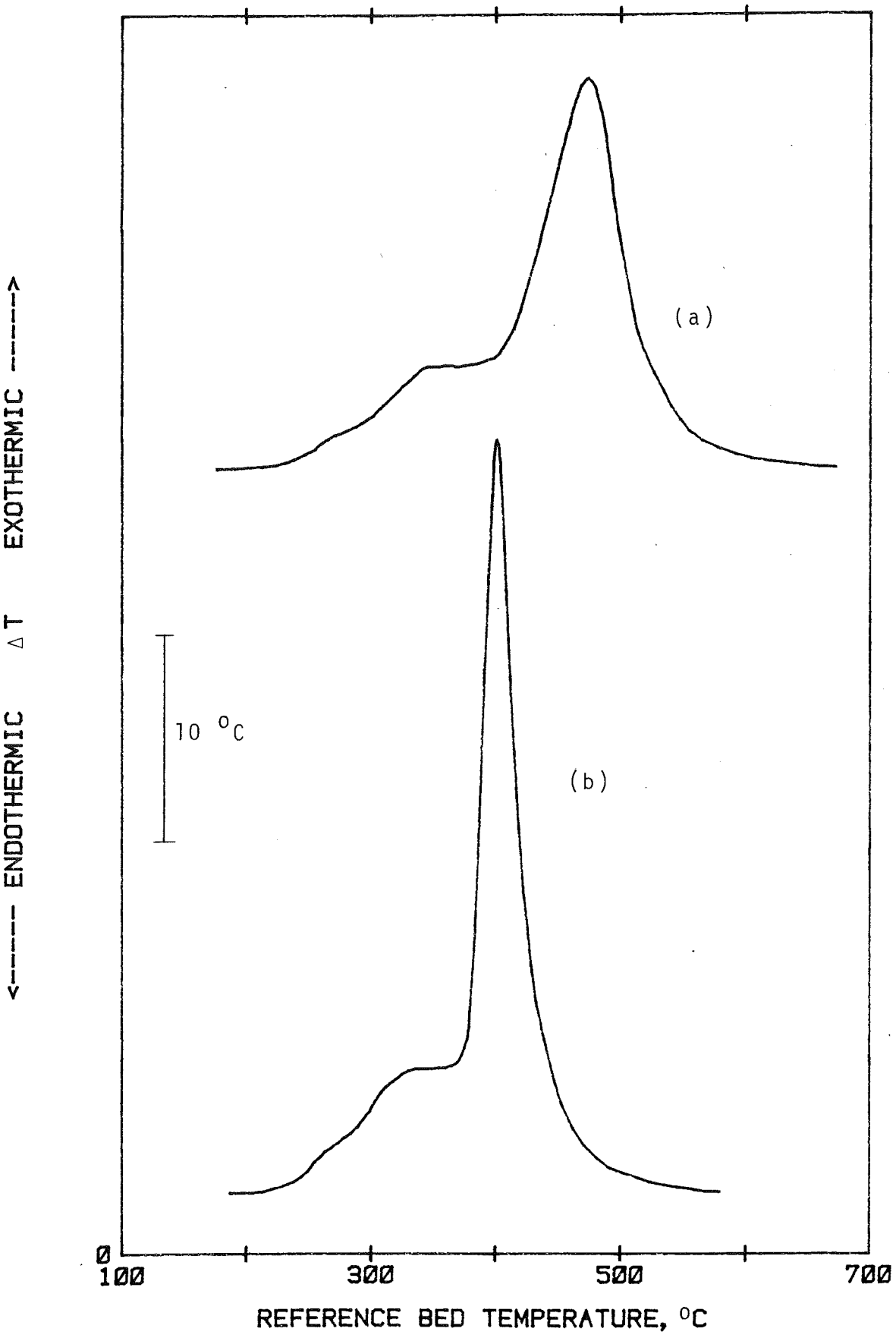

Fig. A6. DTA curves of Coconut wood:(a) in air and (b) in 80% O_2

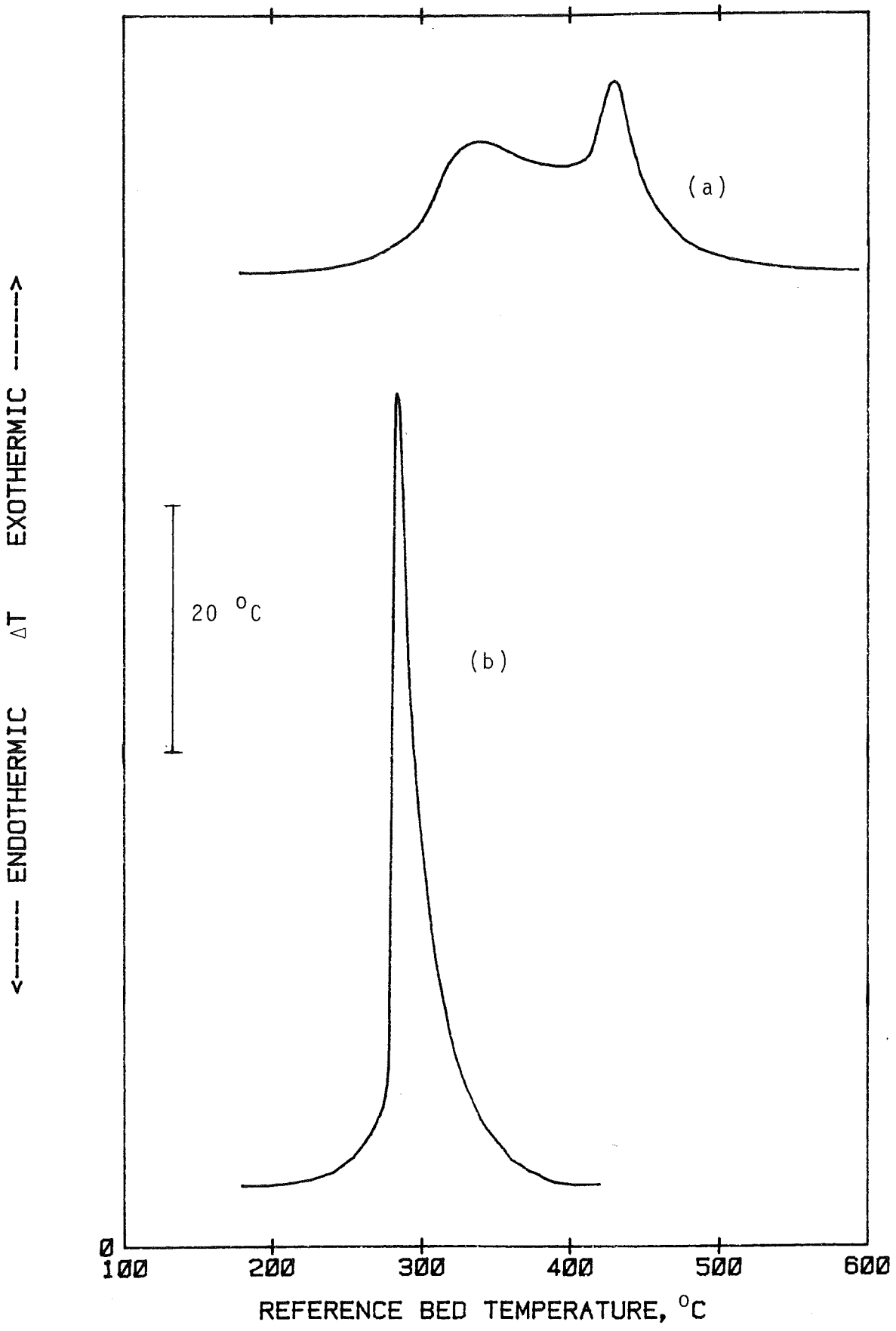

Fig. A7. DTA curves of Jelutong: (a) in air and (b) in 80% O_2

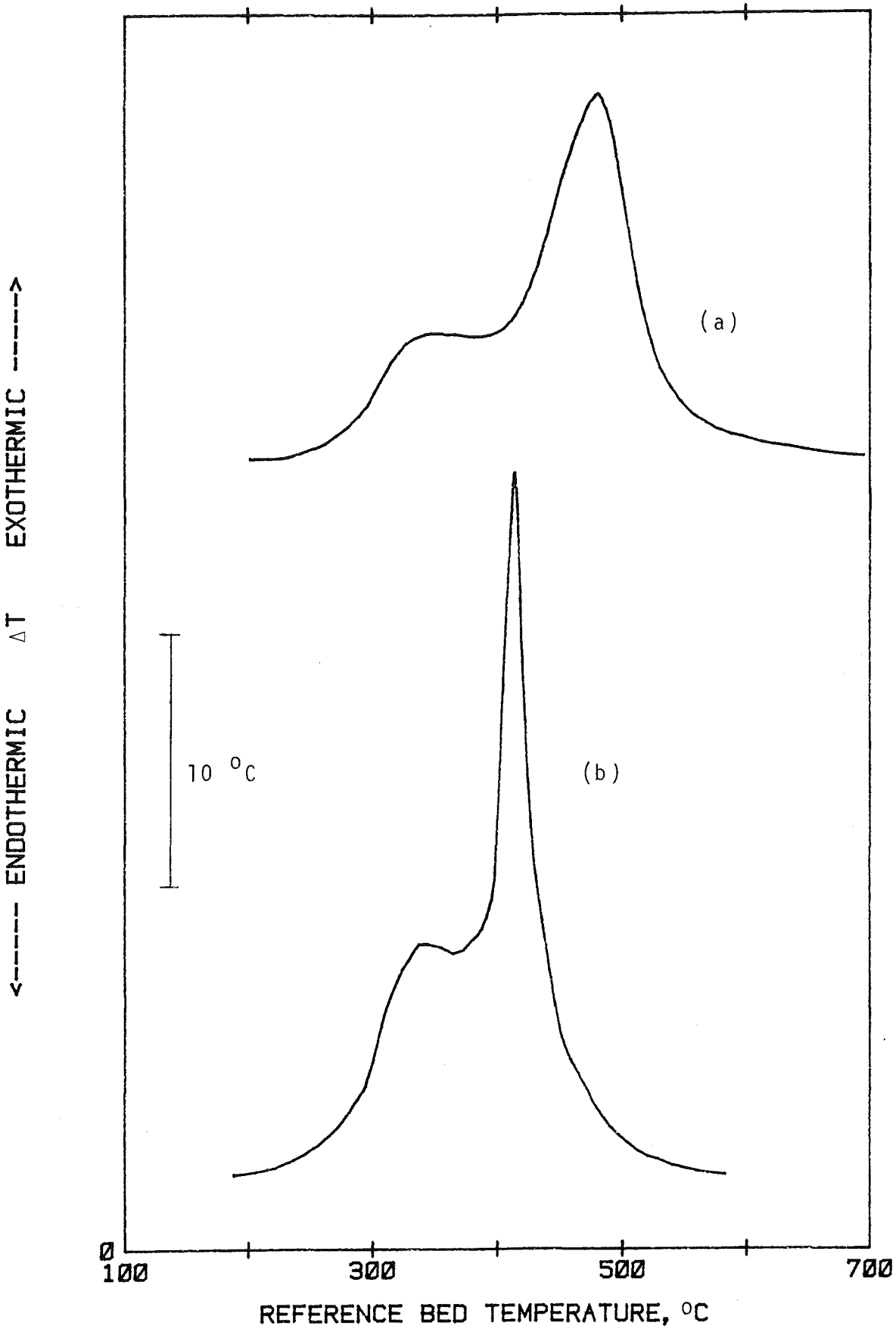

Fig. A8. DTA curves of Kempas:(a) in air and (b) in 80% O_2

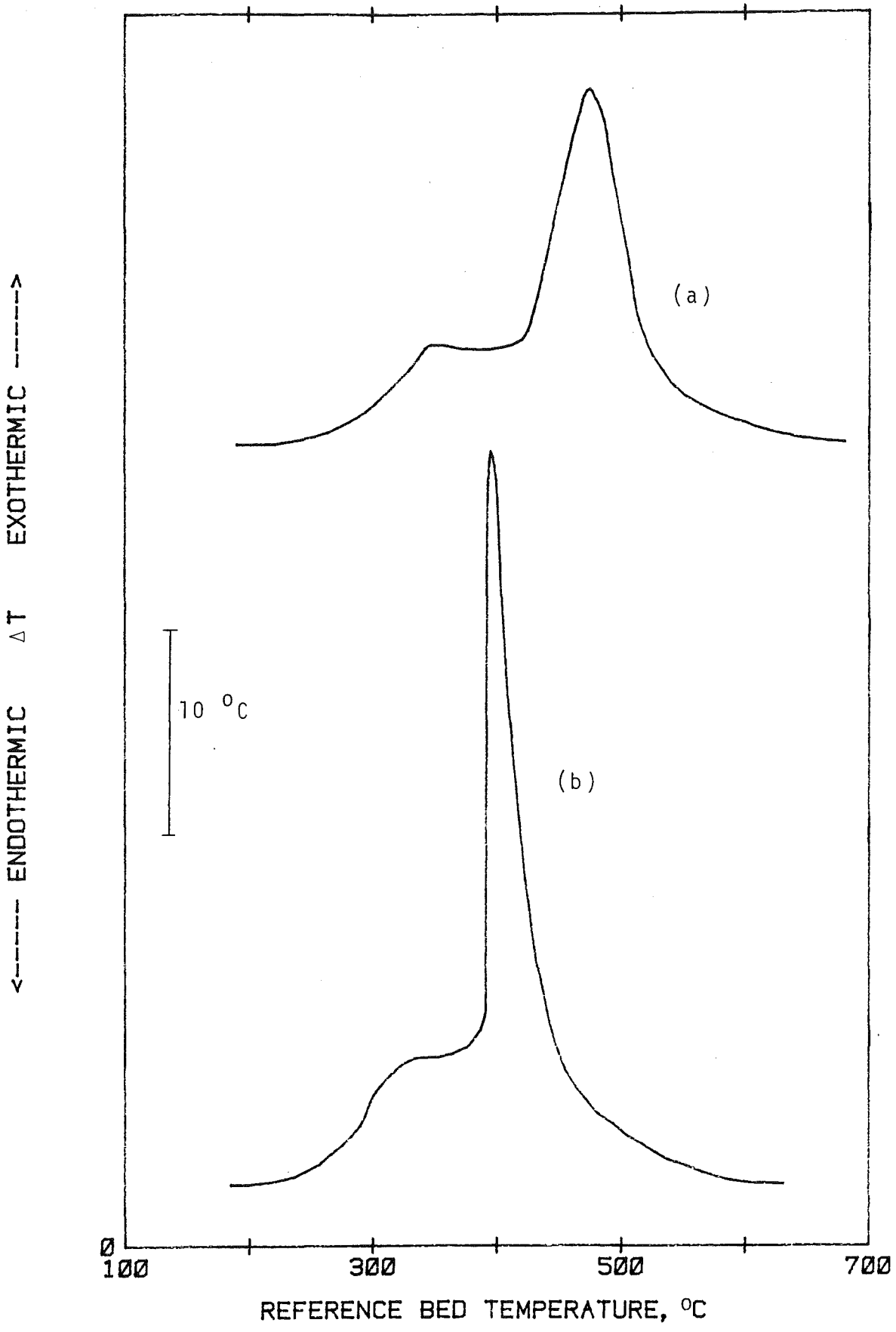

Fig. A9. DTA curves of Keruing:(a) in air and (b) in 80% O_2

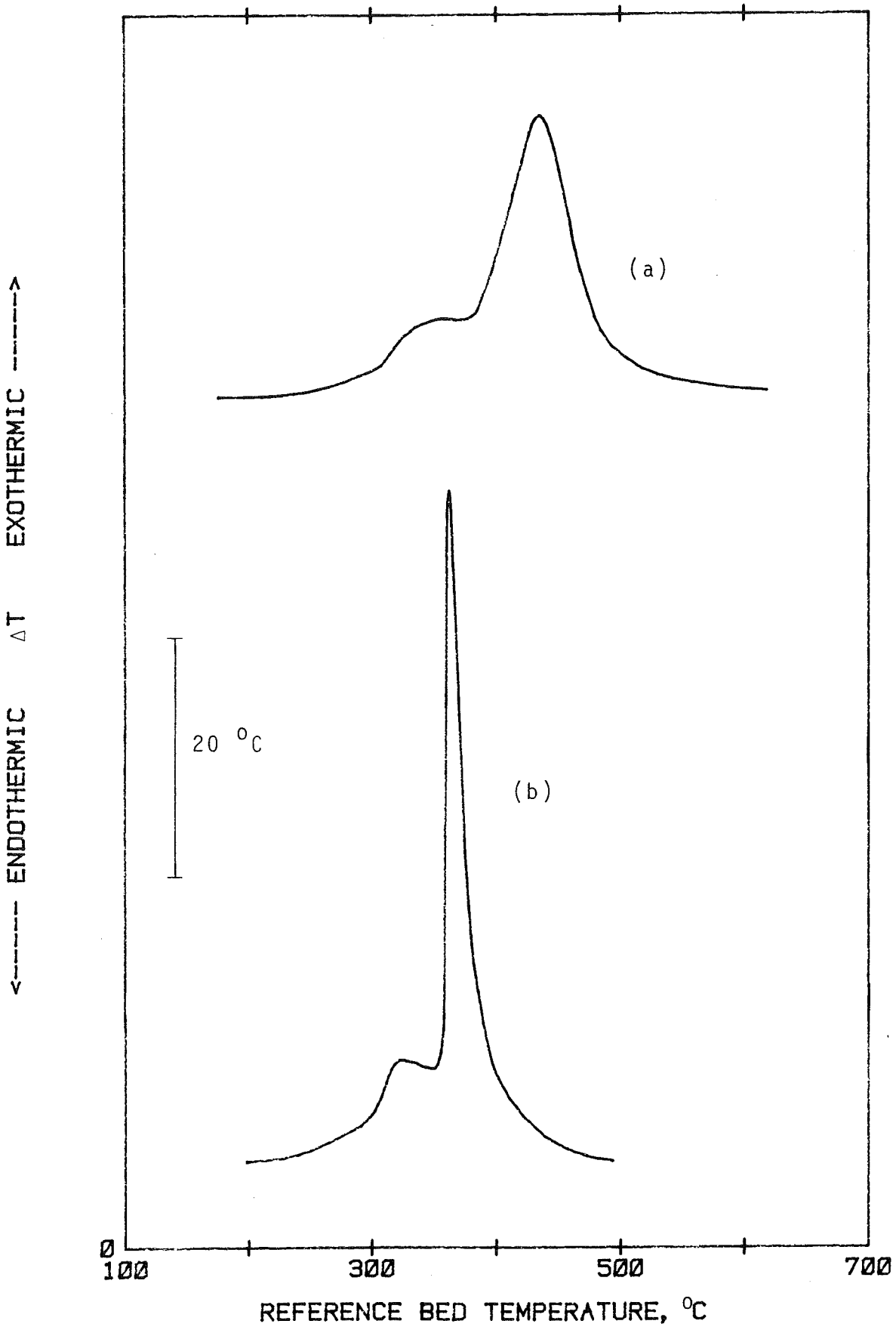

Fig. A10. DTA curves of Mengkulang:(a) in air and (b) in 80% O_2

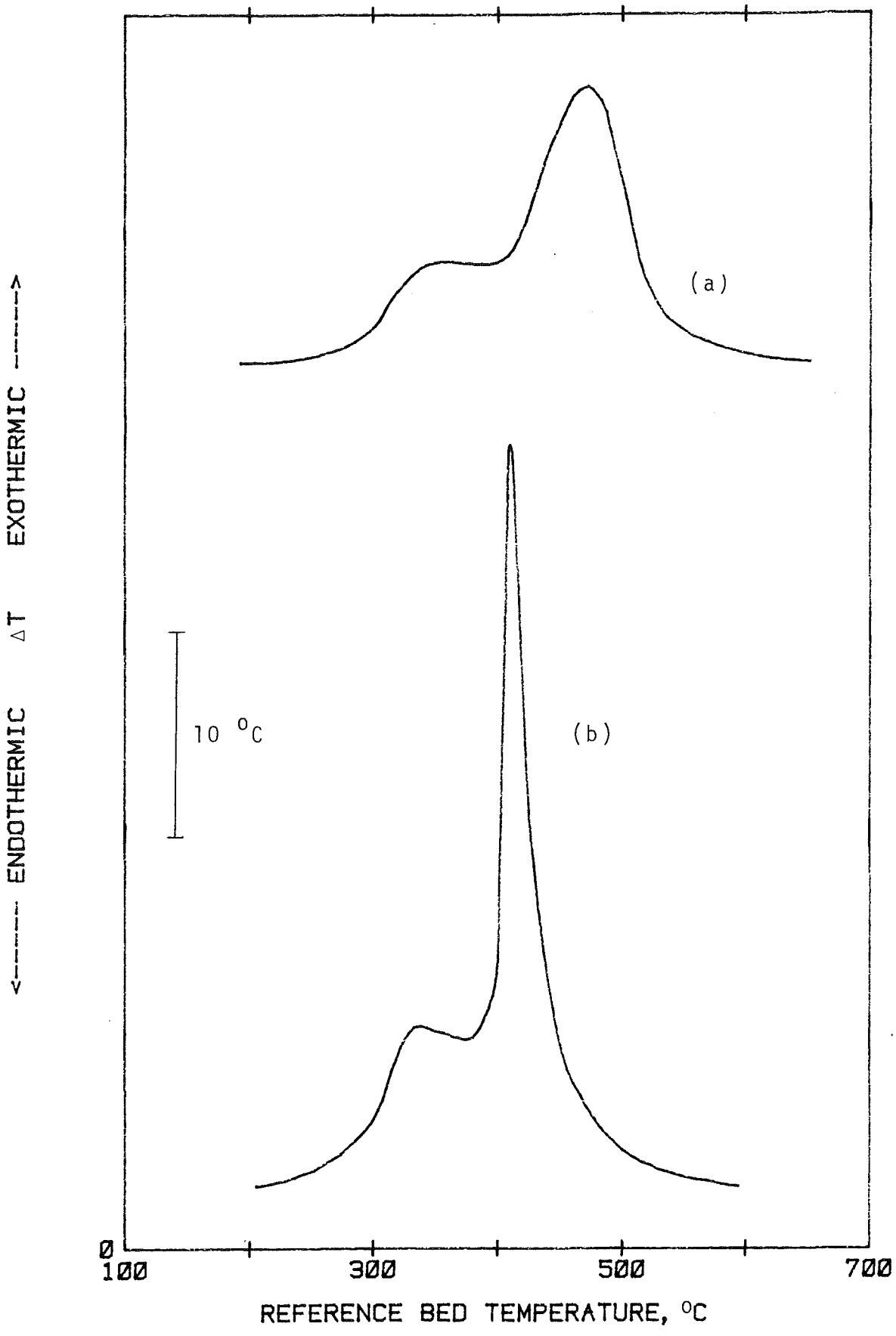

Fig. A11. DTA curves of dark red Meranti:(a) in air and (b) in 80% O_2

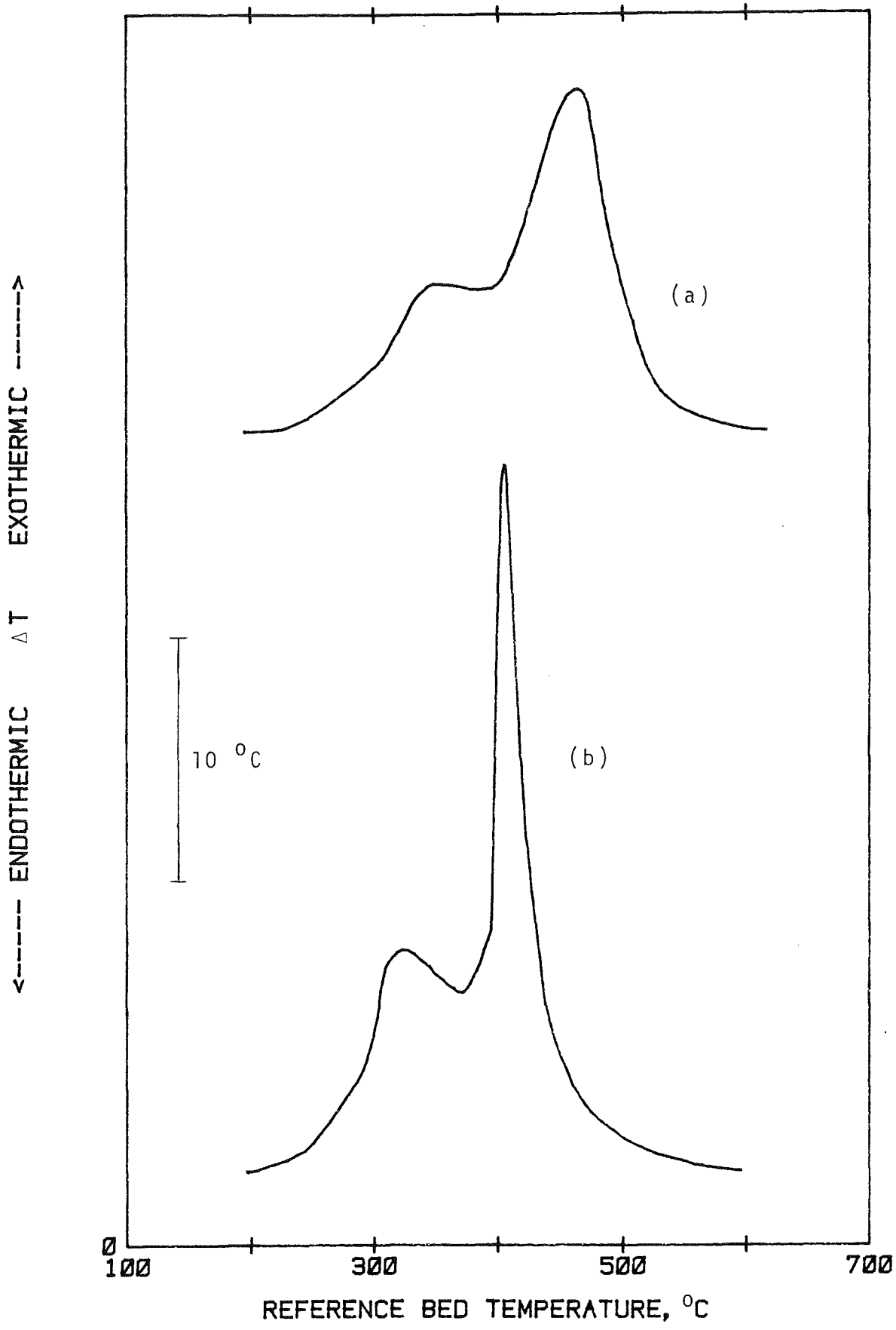

Fig. A12. DTA curves of light red Meranti:(a) in air and (b) in 80% O_2

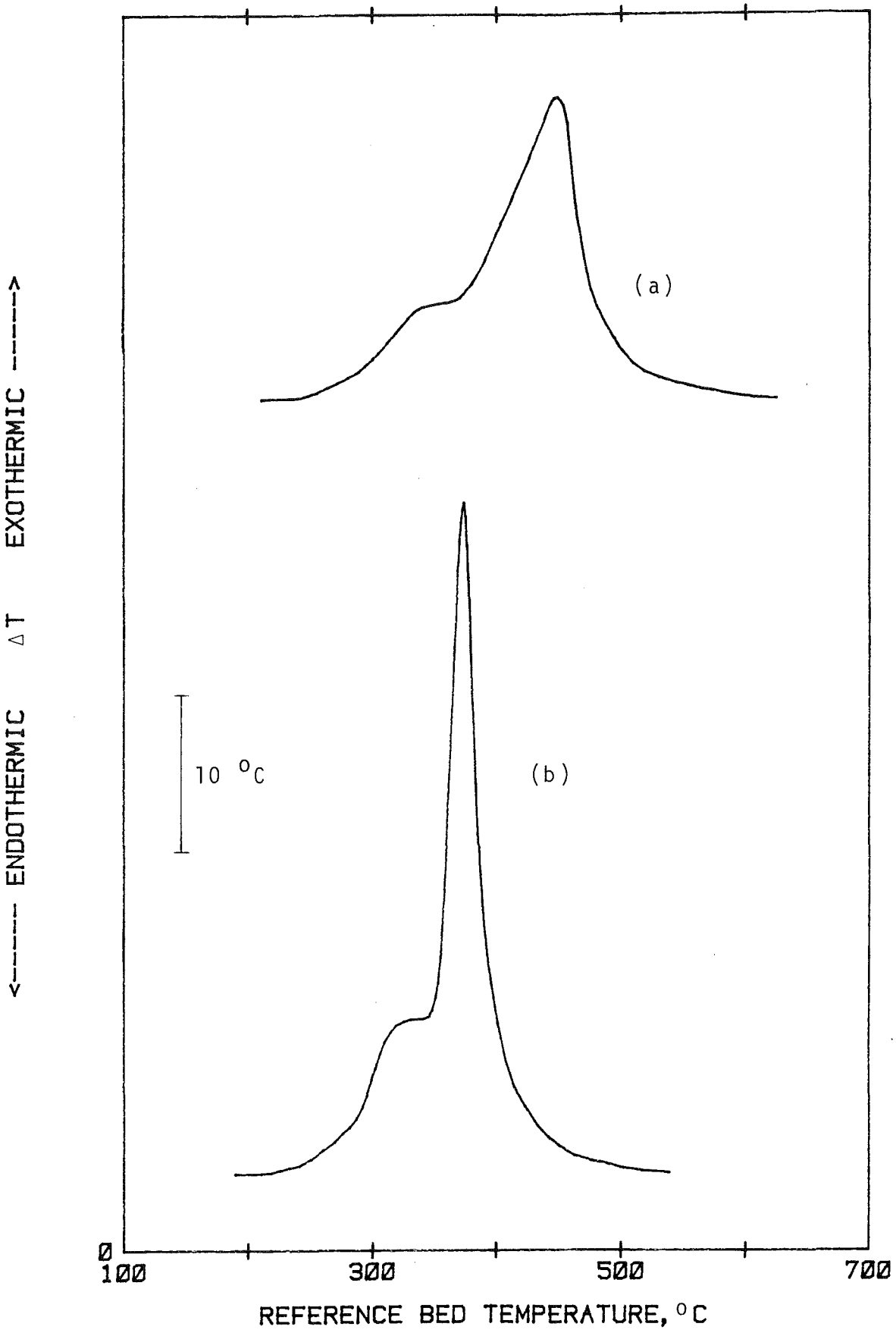

Fig. A13. DTA curves of Merbau:(a) in air and (b) in 80% O_2

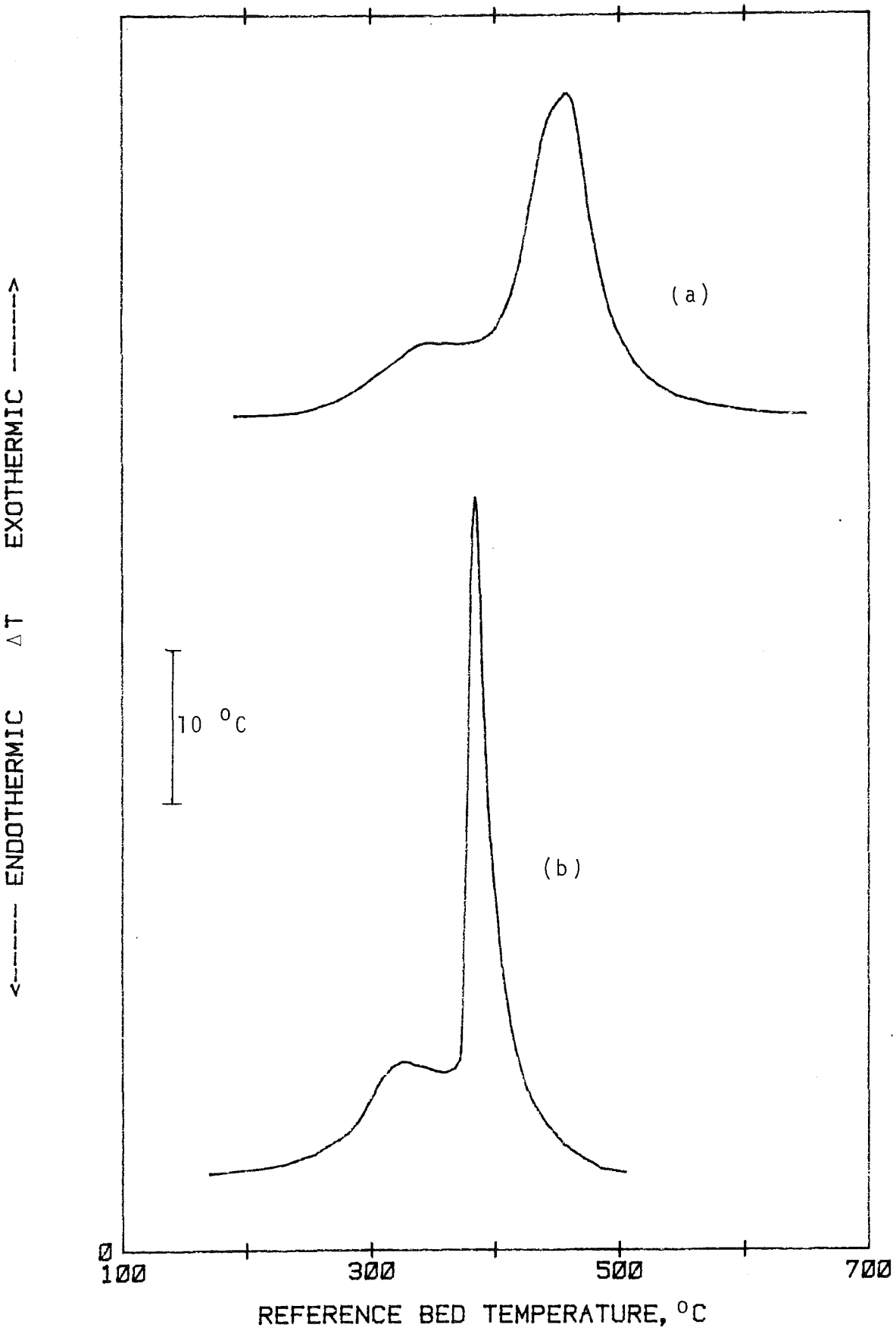

Fig. A14. DTA curves of Mersawa:(a) in air and (b) in 80% O_2

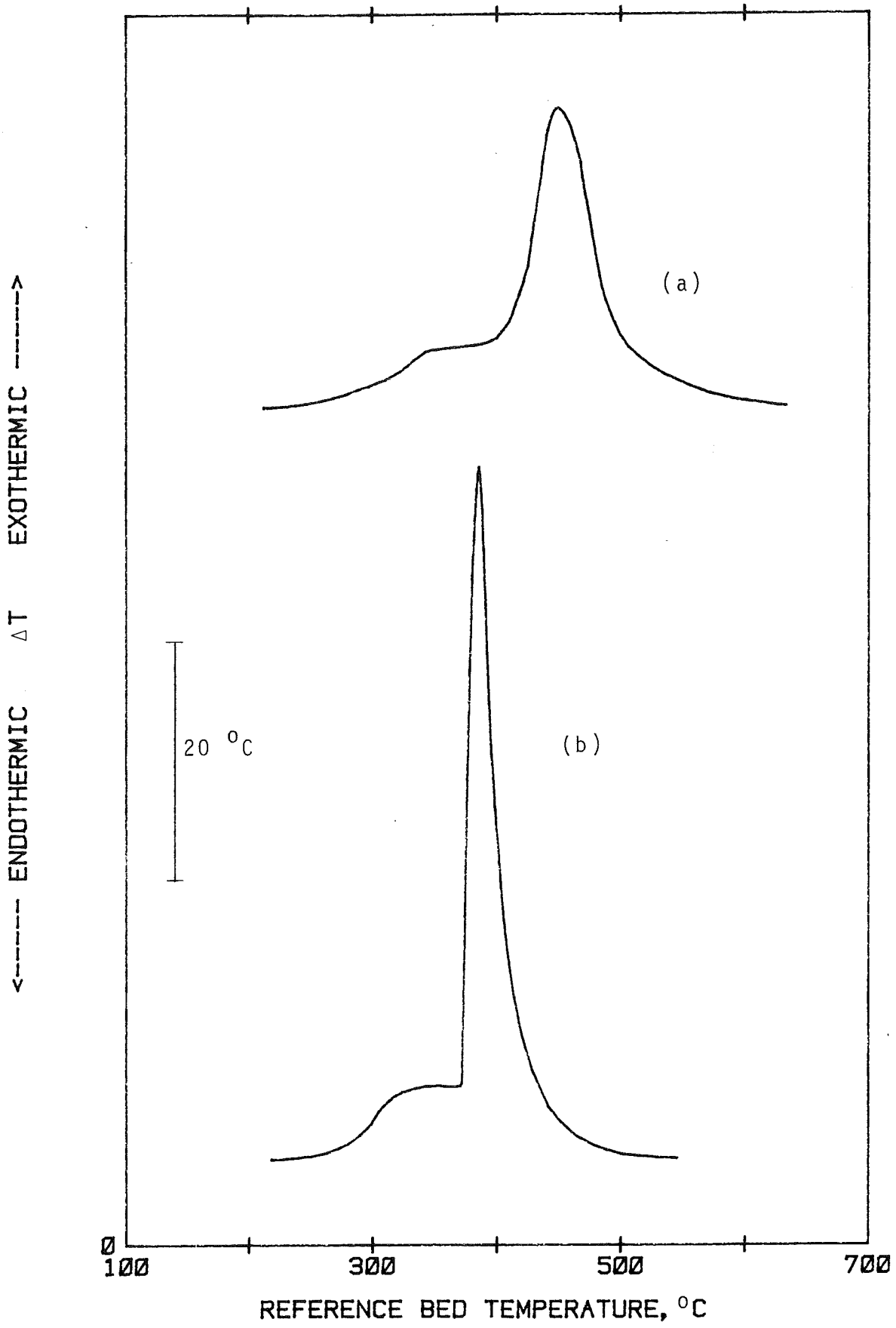

Fig. A15. DTA curves of Nyatoh:(a) in air and (b) in 80% O_2

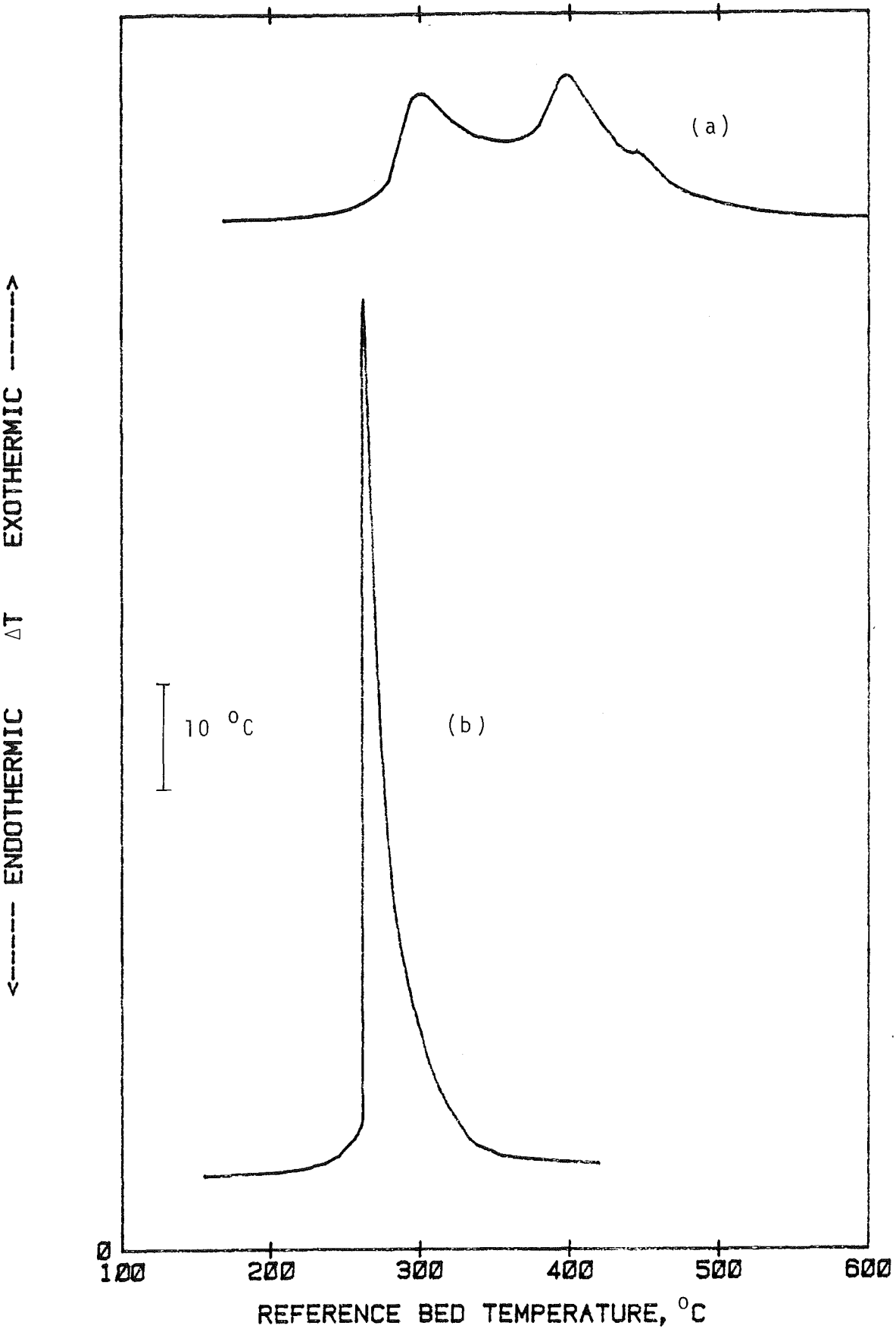

Fig. A16. DTA curves of Oil palm wood:(a) in air and (b) in 80% O_2

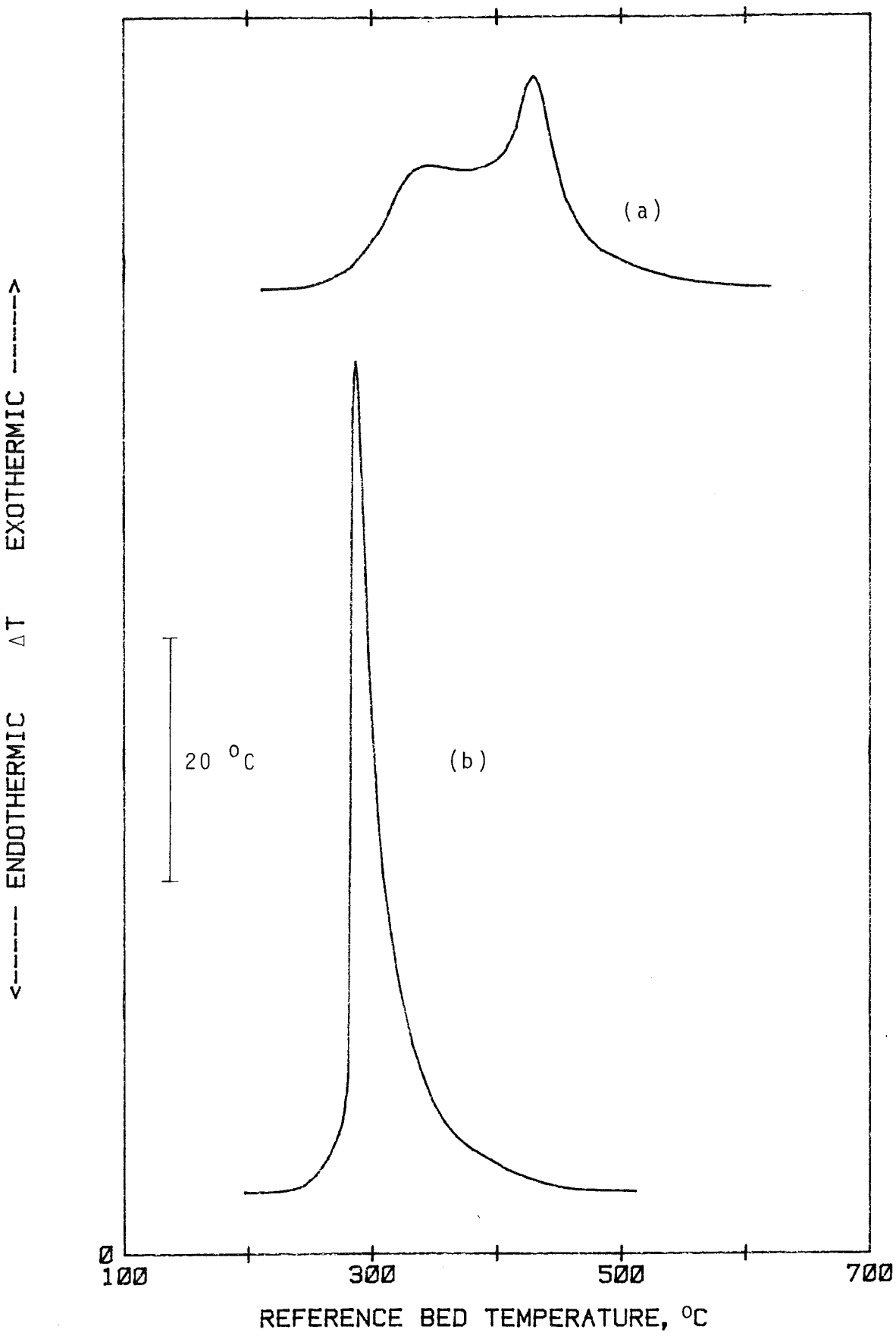

Fig. A17. DTA curves of Pulai:(a) in air and (b) in 80% O_2

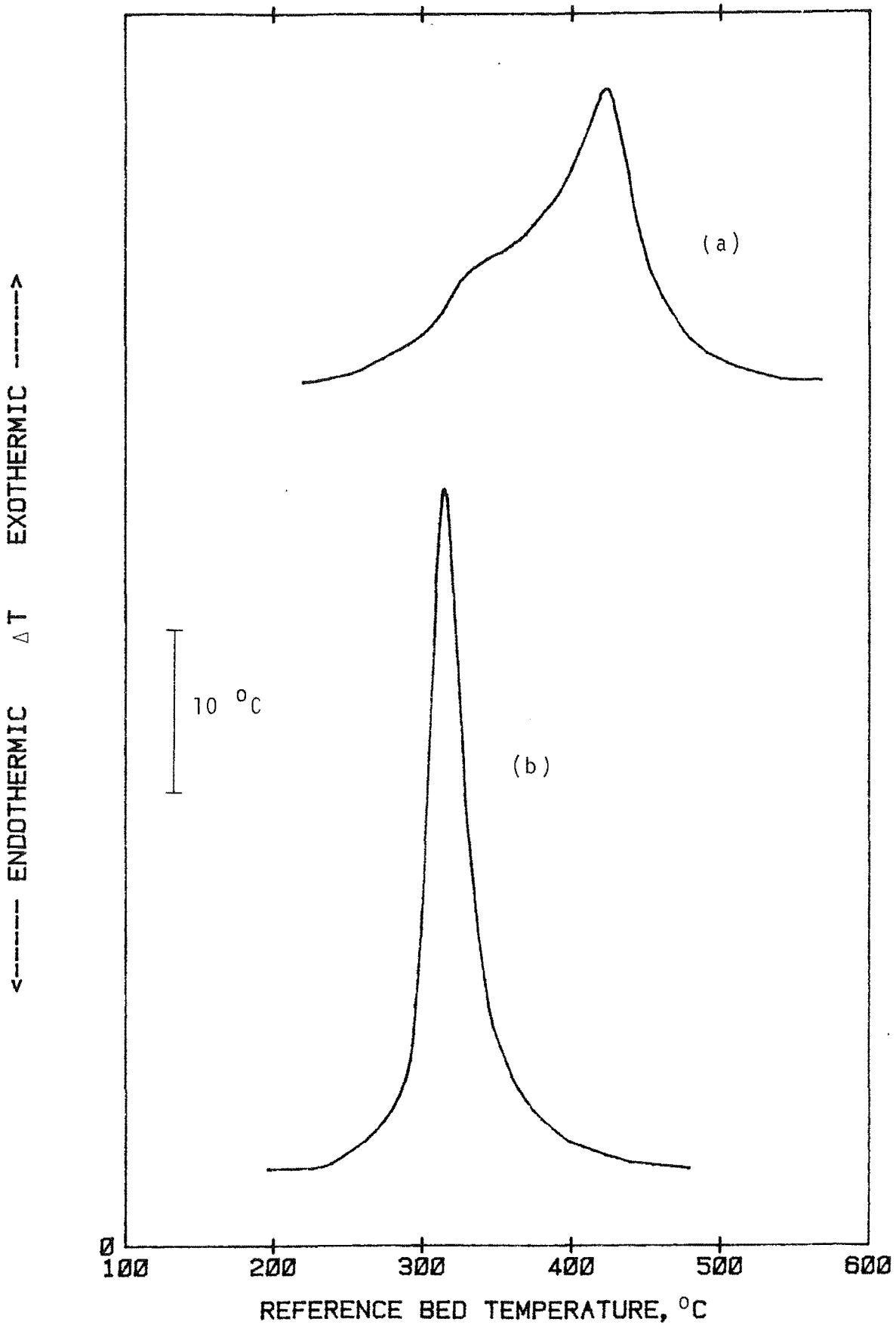

Fig. A18. DTA curves of Ramin:(a) in air and (b) in 80% O_2

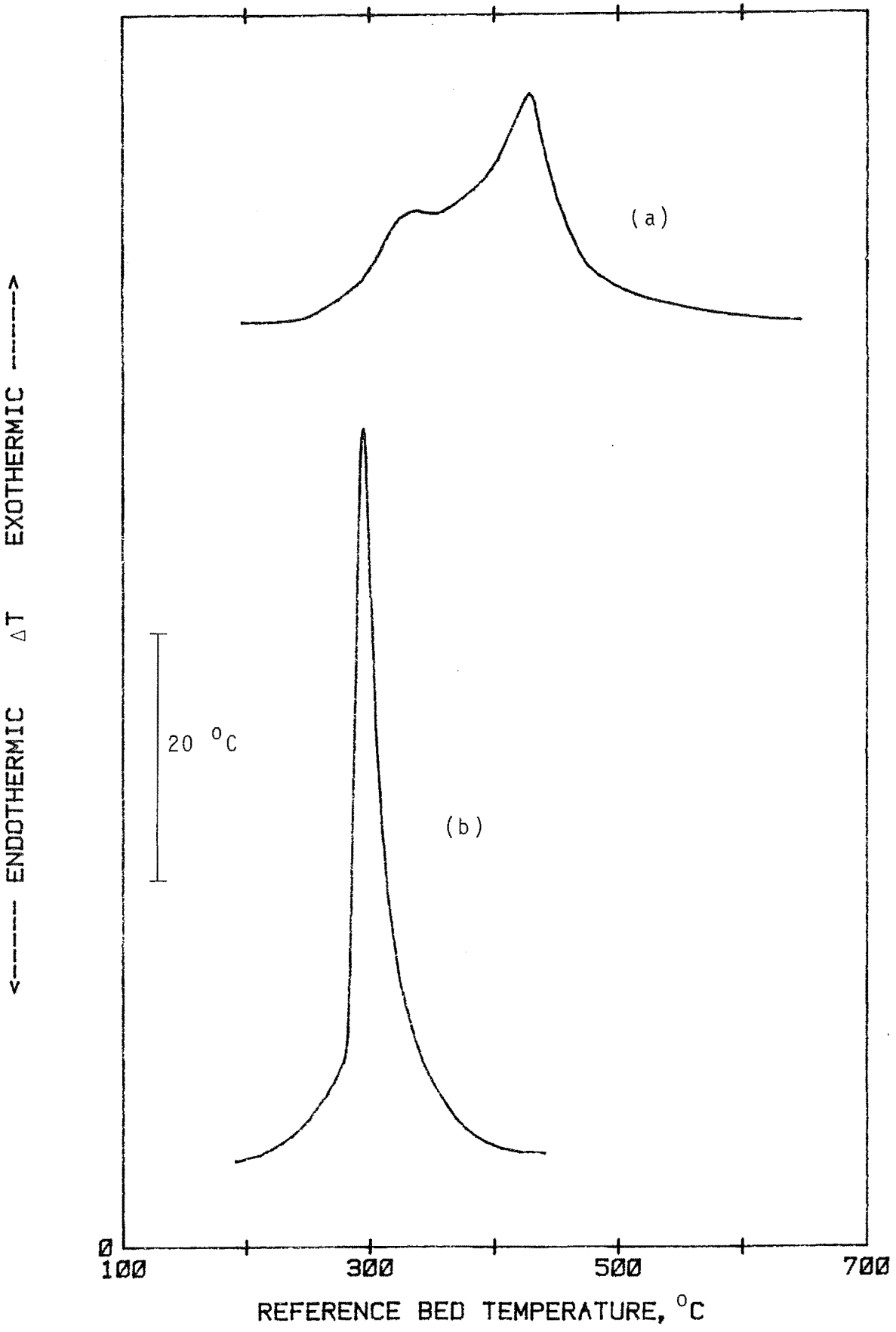

Fig. A19. DTA curves of Sepetir:(a) in air and (b) in 80% O_2

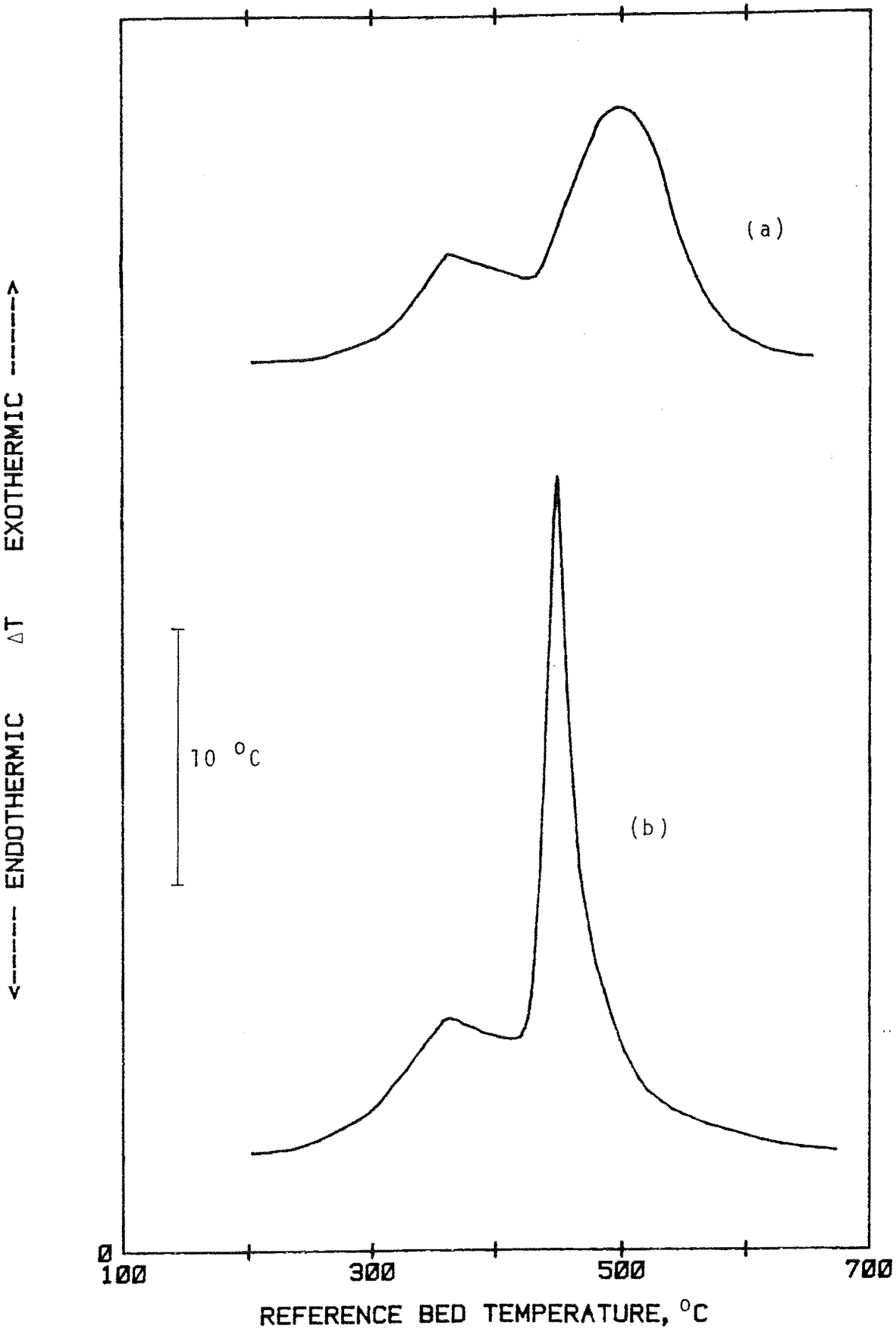

Fig. A20. DTA curves of Tembusu:(a) in air and (b) in 80% O_2

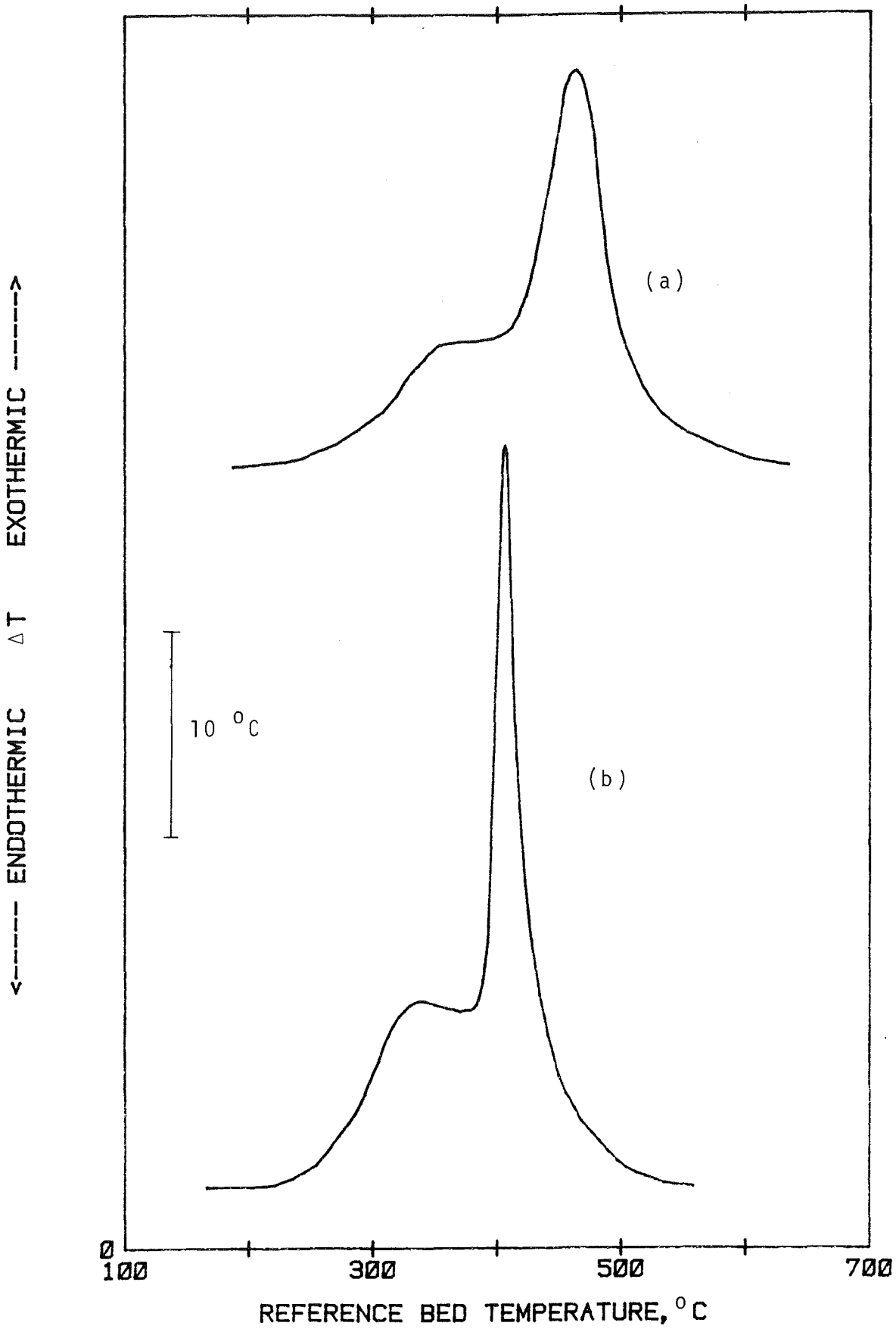

Fig. A21. DTA curves of Tualang:(a) in air and (b) in 80% O_2

Appendix 5. Calculation of Temperature Drop across Reactor

(i) Temperature drop from wall to bed

Weight of sand = 30×10^{-3} kg

Specific heat of sand = 800 J/kgK (Perry and Chilton, 1973)

Thermal capacity of sand = $30 \times 800 \times 10^{-3}$ J/K

= 24.00 J/K

Weight of frame = 23.20×10^{-3} kg

Specific heat of steel at 400°C = 640 J/kgK (Kern, 1950)

Thermal capacity of frame = $23.20 \times 640 \times 10^{-3}$ J/K

= 14.85 J/K

Total thermal capacity of bed = (24.00+14.85) J/k

= 38.85 J/K

Rate of temperature rise = 5.5°C/min or 0.0917°C/s

Heat flux from reactor tube to bed (Q_w) = 38.85x0.0917 W

= 3.56 W

Now, $Q_w = h_w A_w \Delta T_w$

where h_w = wall-bed heat transfer coefficient

= 218 W/m^2K (Appendix 6)

A_w = heat transfer area, wall-to-bed

= 5.85×10^{-3} m^2 (Appendix 7)

ΔT_w = temperature drop, wall-to-bed

$\therefore 3.56 = 218 \times 5.85 \times 10^{-3} \Delta T_w$

and $$\Delta T_w = \frac{3.56}{218 \times 5.85 \times 10^{-3}} \ ^\circ C$$

$$= 2.79^\circ C$$

(ii) Temperature drop across reactor tube

Density of SANDVIK 253MA steel = 7800 kg/m^3
(from catalogue)

Volume of reactor tube of length 70 mm

$$= \frac{\pi}{4}(33.4^2-26.6^2)\times70\times10^{-9}\ m^3$$

$$= 22.43\times10^{-6}\ m^3$$

Weight of section of tube = $7800\times22.43\times10^{-6}$ kg
$= 174.95\times10^{-3}$ kg

Specific heat at 400°C = 560 J/kgK (from catalogue)

Thermal capacity of section of tube = $174.95\times560\times10^{-3}$ J/K
= 97.97 J/K

Heat flux from magnesia to reactor tube (Q_t)
= Rate of temperate rise x total heat capacity inside
= 0.0917(97.97+38.85) W
= 12.55 W

Mean heat flux in reactor tube = $\frac{1}{2}(Q_w+Q_t)$
$= \frac{1}{2}(3.56+12.55)$ W
= 8.055 W

$$\text{Now,}\quad 8.055 = \frac{k_t A_t}{L_t}\Delta T_t$$

where k_t = thermal conductivity of SANDVIK steel
= 20 W/mK at 400°C (from catalogue)

A_t = heat transfer area of tube
$= 6.58\times10^{-3}\ m^2$ (Appendix 7)

L_t = thickness of tube
= 0.00338 m

and ΔT_t = temperature drop across tube

$$\therefore\ \Delta T_t = \frac{8.055\times0.00338}{20\times6.58\times10^{-3}}\ °C$$

$$= 0.21°C$$

(iii) Temperature drop across magnesia

Bulk density of magnesia = 400 kg/m^3 (as determined)

Volume of magnesia within section

$$= \frac{\pi}{4}(39.4^2-33.4^2)\times70\times10^{-9}\ m^3$$

$$= 24.03\times10^{-6}\ m^3$$

Weight of magnesia = $400\times24.03\times10^{-6}$ kg

$= 9.61\times10^{-3}$ kg

Specific heat of magnesia at 400°C = 942 J/kgK

(Perry and Chilton, 1973)

Heat capacity of magnesia = $9.61\times942\times10^{-3}$ J/K

= 9.05 J/K

Heat flux from heat sink to magnesia (Q_m)

= 0.0917(97.97+38.85+9.05) W

= 13.38 W

Mean heat flux in magnesia = $\frac{1}{2}(Q_t+Q_m)$

$= \frac{1}{2}(12.55+13.38)$ W

= 12.965 W

$$\text{Now,}\quad 12.965 = \frac{k_m A_m}{L_m}\Delta T_m$$

where k_m = thermal conductivity of magnesia

= 0.606 W/mK (Kern, 1950)

A_m = heat transfer area of magnesia layer

$= 7.98\times10^{-3}\ m^2$ (Appendix 7)

L_m = thickness of magnesia layer

= 0.003 m

and ΔT_m = temperature drop across magnesia layer

$$\therefore\ \Delta T_m = \frac{12.965\times0.003}{0.606\times7.98\times10^{-3}}\ °C$$

$$= 8.04°C$$

(iv) Temperature drop across heat sink

Weight of one side of steel block = 10.75 kg

Height of steel block = 0.297 m

Weight of a section of length 70 mm = 2.53 kg

Specific heat of steel at 400°C = 640 J/kgK

Heat capacity of section = 2.53x640 J/K

= 1619 J/K

Heat flux from furnace to heat sink (Q_s)

= 0.0917(97.97+38.85+9.05+1619) W

= 161.84 W

Mean heat flux in heat sink = $\frac{1}{2}(Q_m+Q_s)$

= $\frac{1}{2}$(13.38+161.84) W

= 87.61 W

Now, $$87.61 = \frac{k_s A_s}{L_s}\Delta T_s$$

where k_s = thermal conductivity of steel

= 20.8 W/mK (Wong, 1977)

A_s = heat transfer area of heat sink

= 13.39×10^{-3} m^2 (Appendix 7)

L_s = thickness of heat sink

= 0.0248 m

and ΔT_s = temperature drop across heat sink

$$\therefore \Delta T_s = \frac{87.61\times0.0248}{20.8\times13.39\times10^{-3}} \ ^\circ C$$

$$= 7.80^\circ C$$

Total temperature drop across the four regions

= (2.79+0.21+8.08+7.80) °C

= 18.84°C

Appendix 6. Calculating bed-wall heat transfer coefficient

The bed-wall heat transfer coefficient was calculated using the generalised correlation of Wen and Leva (1956) which is given below :

$$\frac{h_w d_p}{k_g} = 0.16 \left(\frac{C_{pg}}{k_g}\right)^{0.4} \left(\frac{d_p \rho_g u_o}{\mu}\right)^{0.76} \left(\frac{\rho_s C_{ps}}{\rho_g C_{pg}}\right)^{0.4} \left(\frac{u_o^2}{g d_p}\right)^{-0.2} \left(\eta \frac{L_{mf}}{L_f}\right)^{0.36}$$

where h_w = bed-wall heat transfer coefficient

d_p = diameter of solids

ρ_s = density of solids

C_{ps} = specific heat of solids

ρ_g = density of fluids

k_g = thermal conductivity of fluids

C_{pg} = specific heat of fluids

μ = viscosity of fluid

u_o = superficial velocity of fluid

η = efficiency factor

L_{mf} = bed height at minimum fluidising conditions

L_f = height of fluidised-bed

In the present case, the solids are sand and the fluid r. The physical properties of these two substances at 400°C ...d the bed heights are as follows :

$d_p = 1.65 \times 10^{-4}$ m

$\rho_s = 2590$ kg/m^3 (Leva, 1959)

$C_{ps} = 800$ J/kgK (Perry and Chilton, 1973)

$\rho_g = 0.523$ kg/m^3 (Wong, 1977)

k_g = 0.05092 W/mK (Wong, 1977)

C_{pg} = 1070 J/kgK (Wong, 1977)

μ = 3.25×10^{-5} kg/ms (Wong, 1977)

u_o = 0.135 m/s (Appendix 8)

L_{mf} = 0.04 m

L_f = 0.07 m

Determination of η

For small particles, the superficial fluid velocity at minimum fluidising conditions, u_{mf},

$$= \frac{d_p^2(\rho_s - \rho_g)g}{1650\mu} \quad \text{(Kunii and Levenspiel, 1969)}$$

$$= \frac{1.65^2 \times 10^{-8} \times 2590 \times 9.81}{1650 \times 3.25 \times 10^{-5}} \text{ m/s}$$

$$= 1.29 \times 10^{-2} \text{ m/s}$$

$$\frac{u_o}{u_{mf}} = \frac{0.135}{1.29 \times 10^{-2}} = 10.47$$

The efficiency factor, η, corresponding to u_o/u_{mf} of 10.47 d d_p of 1.65×10^{-4} m is read from a chart (Figure A2) and uals 0.6.

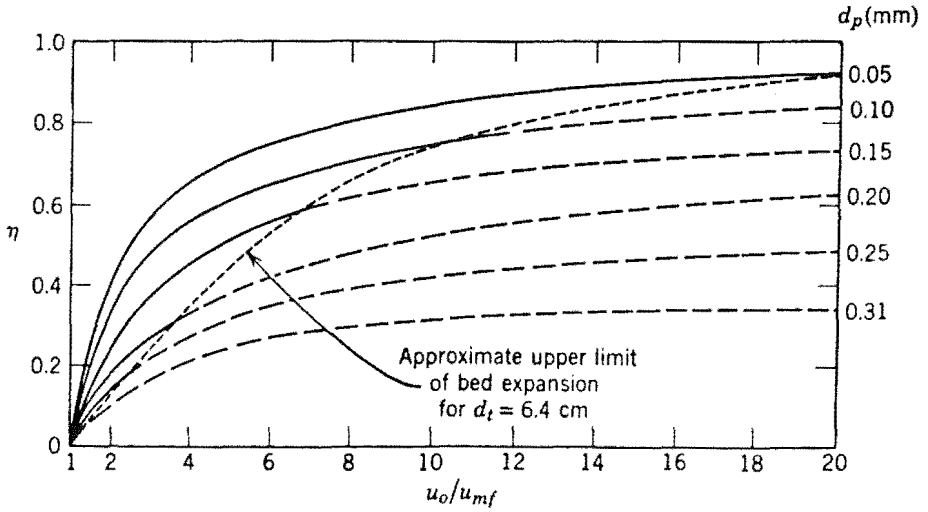

Figure A2. Chart for determining η

Calculation of each term

$$\left(\frac{C_{pg}\mu}{k_g}\right)^{0.4} = \left(\frac{1070 \times 3.25 \times 10^{-5}}{0.05092}\right)^{0.4}$$

$$= \underline{0.859}$$

$$\left(\frac{d_p \rho_g u_o}{\mu}\right)^{0.76} = \left(\frac{1.65 \times 10\text{-}4 \times 0.523 \times 0.135}{3.25 \times 10^{-5}}\right)^{0.76}$$

$$= \underline{0.458}$$

$$\left(\frac{\rho_s C_{ps}}{\rho_g C_{pg}}\right)^{0.4} = \left(\frac{2590 \times 800}{0.523 \times 1070}\right)^{0.4}$$

$$= \underline{26.80}$$

$$\left(\frac{u_o^2}{g d_p}\right)^{-0.2} = \left(\frac{0.135^2}{9.81 \times 1.65 \times 10^{-4}}\right)^{-0.2}$$

$$= \underline{0.616}$$

and $$\left(\eta \frac{Lmf}{Lf}\right)^{0.36} = \left(0.6 \times \frac{0.04}{0.07}\right)^{0.36}$$

$$= \underline{0.68}$$

lculation of h_w

$$\frac{h_w d_p}{k_g} = 0.16 \times 0.859 \times 0.458 \times 26.80 \times 0.616 \times 0.680$$

$$= 0.707$$

and $$h_w = \frac{0.707 \times 0.05092}{1.65 \times 10^{-4}} \text{ W/m}^2\text{K}$$

$$= 218 \text{ W/m}^2\text{K}$$

Appendix 7. Calculation of Heat Transfer Areas

This was done for one side of the reactor and for a section of length 70 mm, corresponding to the height of the expanded bed at 400°C.

(1) Heat Sink

The heat sink is treated as a complete cylinder

Outside diameter = 0.0890 m

Inside diameter = 0.0394 m

$$\text{Log mean diameter} = \frac{0.0890-0.0394}{\ln(0.089/0.0394)}\ \text{m}$$

$$= 0.0609\ \text{m}$$

$$\text{Heat transfer area} = \pi \times 0.0609 \times 0.07\ \text{m}^2$$

$$= 13.39 \times 10^{-3}\ \text{m}^2$$

(2) Magnesia Layer

Outside diameter = 0.0394 m

Inside diameter = 0.0334 m

$$\text{Log mean diameter} = \frac{0.0394-0.0334}{\ln(0.0394/0.0334)}\ \text{m}$$

$$= 0.0363\ \text{m}$$

$$\text{Heat transfer area} = \pi \times 0.0363 \times 0.07\ \text{m}^2$$

$$= 7.98 \times 10^{-3}\ \text{m}^2$$

3) Reactor Tube

Outside diameter = 0.0334 m

Inside diameter = 0.0226 m

$$\text{Log mean diameter} = \frac{0.0334-0.0266}{\ln(0.0334/0.0266)}\ \text{m}$$

$$= 0.0299 \text{ m}$$

$$\text{Heat transfer area} = \pi \times 0.0299 \times 0.07 \text{ m}^2$$

$$= 6.58 \times 10^{-3} \text{ m}^2$$

(4) Wall-bed Boundary Layer

Inside diameter of reactor tube = 0.0266 m

$$\text{Heat transfer area} = \pi \times 0.0266 \times 0.07 \text{ m}^2$$

$$= 5.85 \times 10^{-3} \text{ m}^2$$

Appendix 8. Calculating superficial gas velocity at 400°C

Air flowrate (in each tube) at 25°C = 2 lit/min

$$\text{Air flowrate at } 400^{\circ}C = \frac{2 \times 673}{298} \text{ lit/min}$$

(from $V_1/T_1 = V_2/T_2$)

$$= 4.52 \text{ lit/min}$$

$$\text{or } 0.753 \times 10^{-4} \text{ m}^3/\text{s}$$

$$\text{Flow area of each tube} = \frac{\pi}{4} \times 2.664^2 \times 10^{-4} \text{ m}^2$$

$$= 5.575 \times 10^{-4} \text{ m}^2$$

Now, Flowrate = Area x Velocity

$$\therefore u_o \text{ at } 400^{\circ}C = \frac{0.753 \times 10\text{-}4}{5.575 \times 10\text{-}4} \text{ m/s}$$

$$= \underline{0.135 \text{ m/s}}$$

Appendix 9. TG Curves in N2 and in air of some Tropical Wood Species

Figure A22 : Balau
" A23 : Bark of rubber tree
" A24 : Chengal
" A25 : Coconut wood
" A26 : Jelutong
" A27 : Kempas
" A28 : Keruing
" A29 : Mengkulang
" A30 : Meranti, dark red
" A31 : Meranti, light red
" A32 : Merbau
" A33 : Mersawa
" A34 : Nyatoh
" A35 : Oil palm wood
" A36 : Pulai
" A37 : Ramin
" A38 : Sepetir
" A39 : Tembusu
" A40 : Tualang

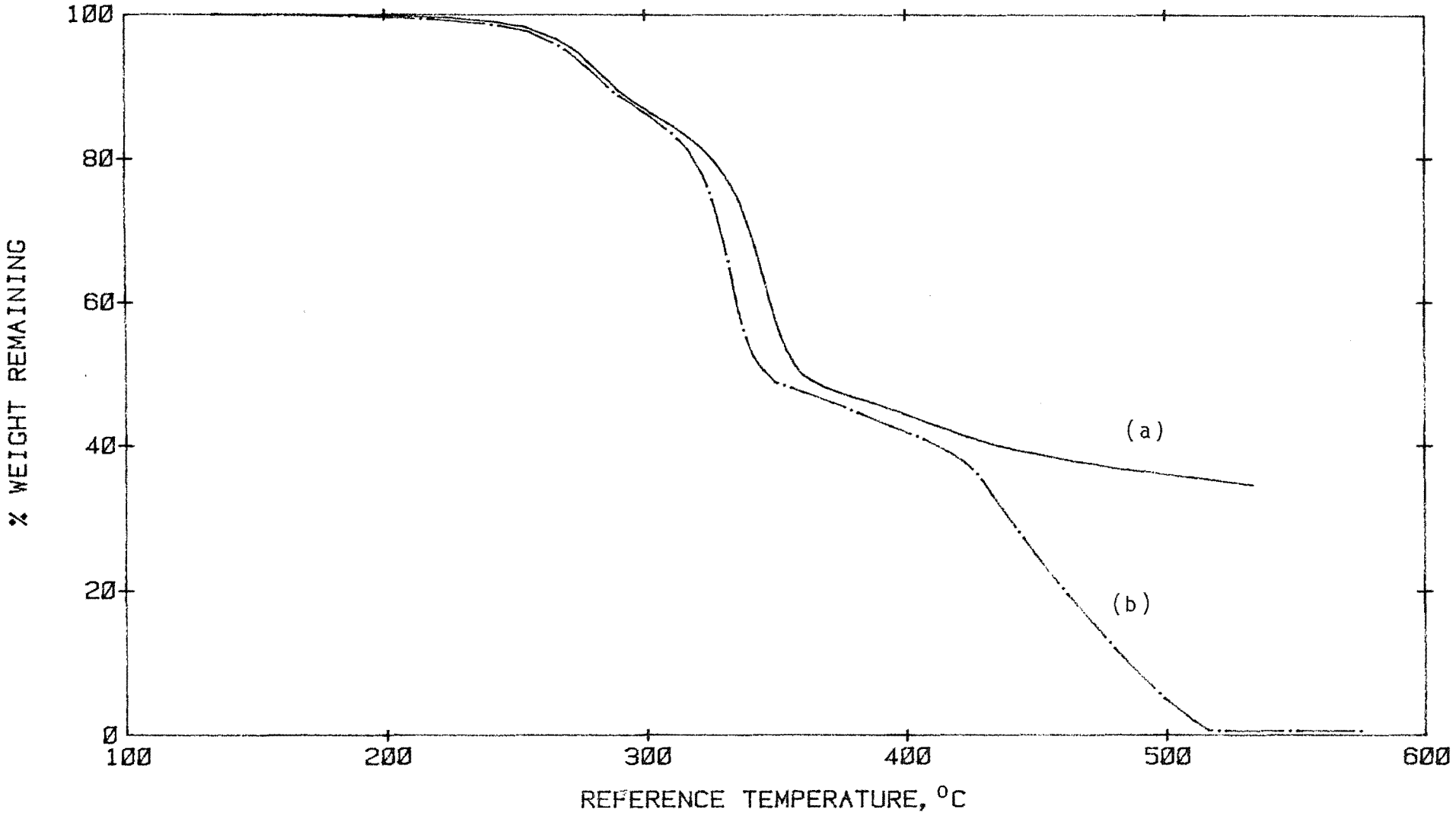

Fig. A22. TG curves of Balau:(a) in N_2 and (b) in air

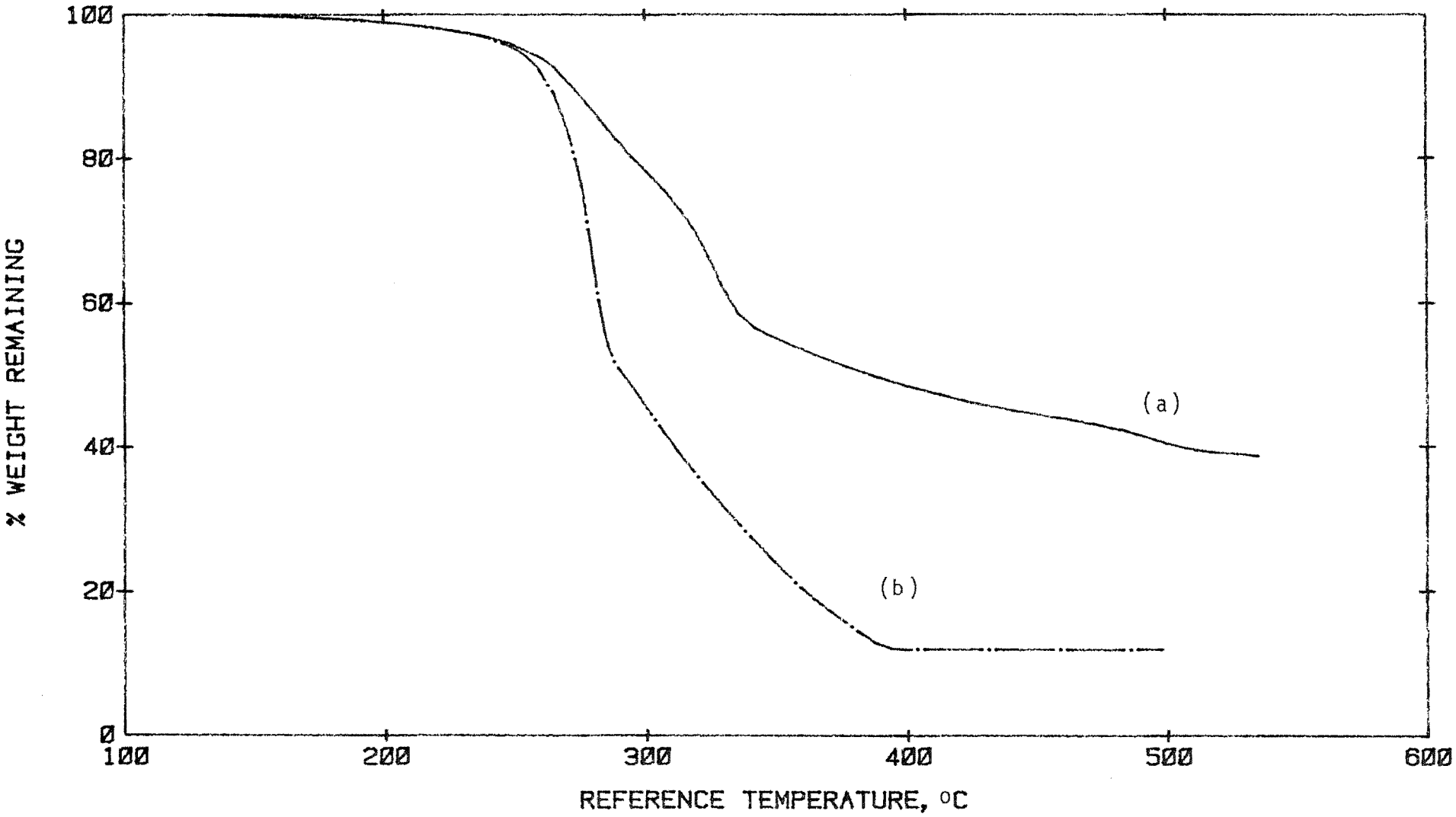

Fig. A23. TG curves of rubber tree bark:(a) in N_2 and (b) in air

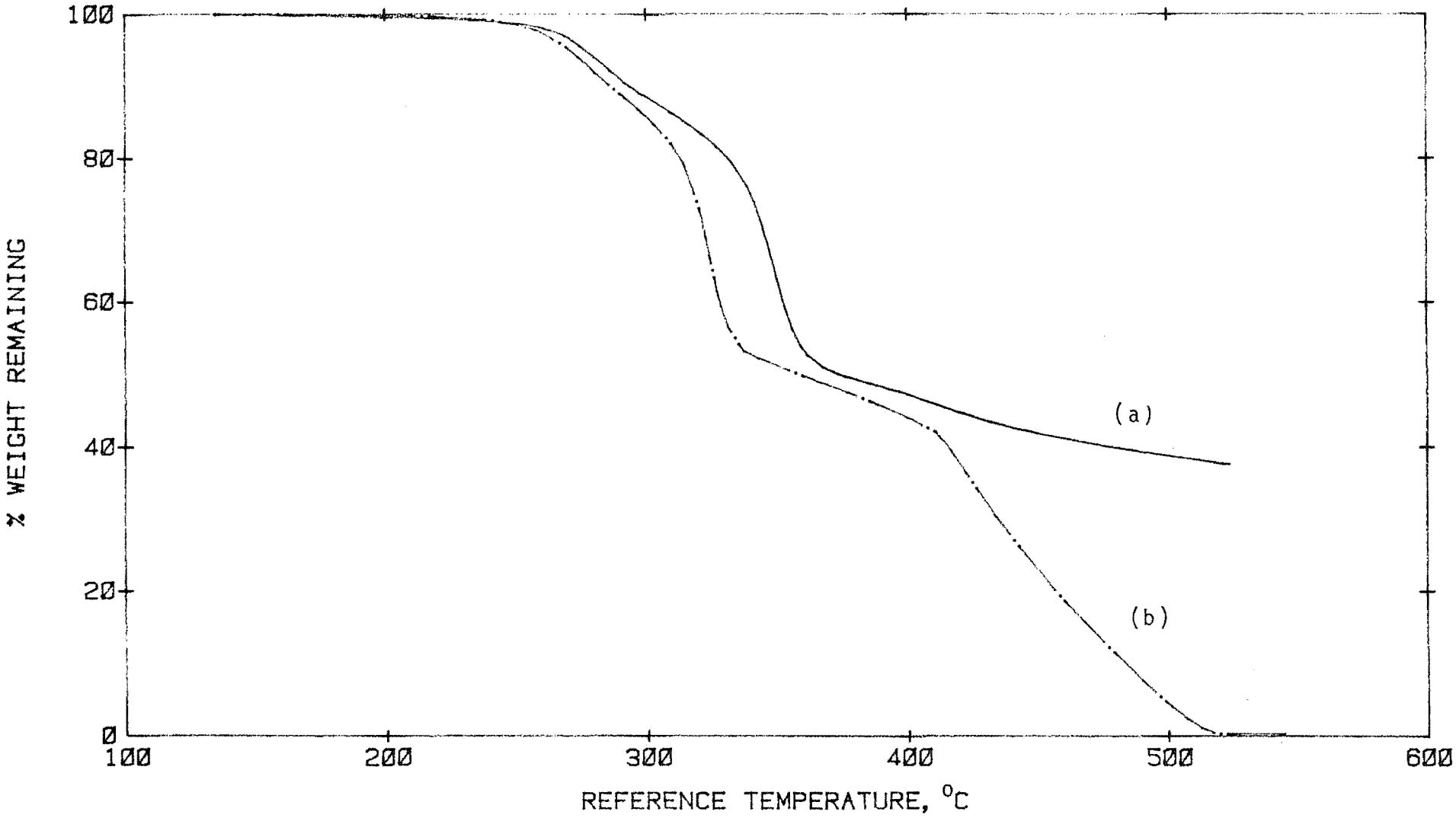

Fig. A24. TG curves of Chengal:(a) in N_2 and (b) in air

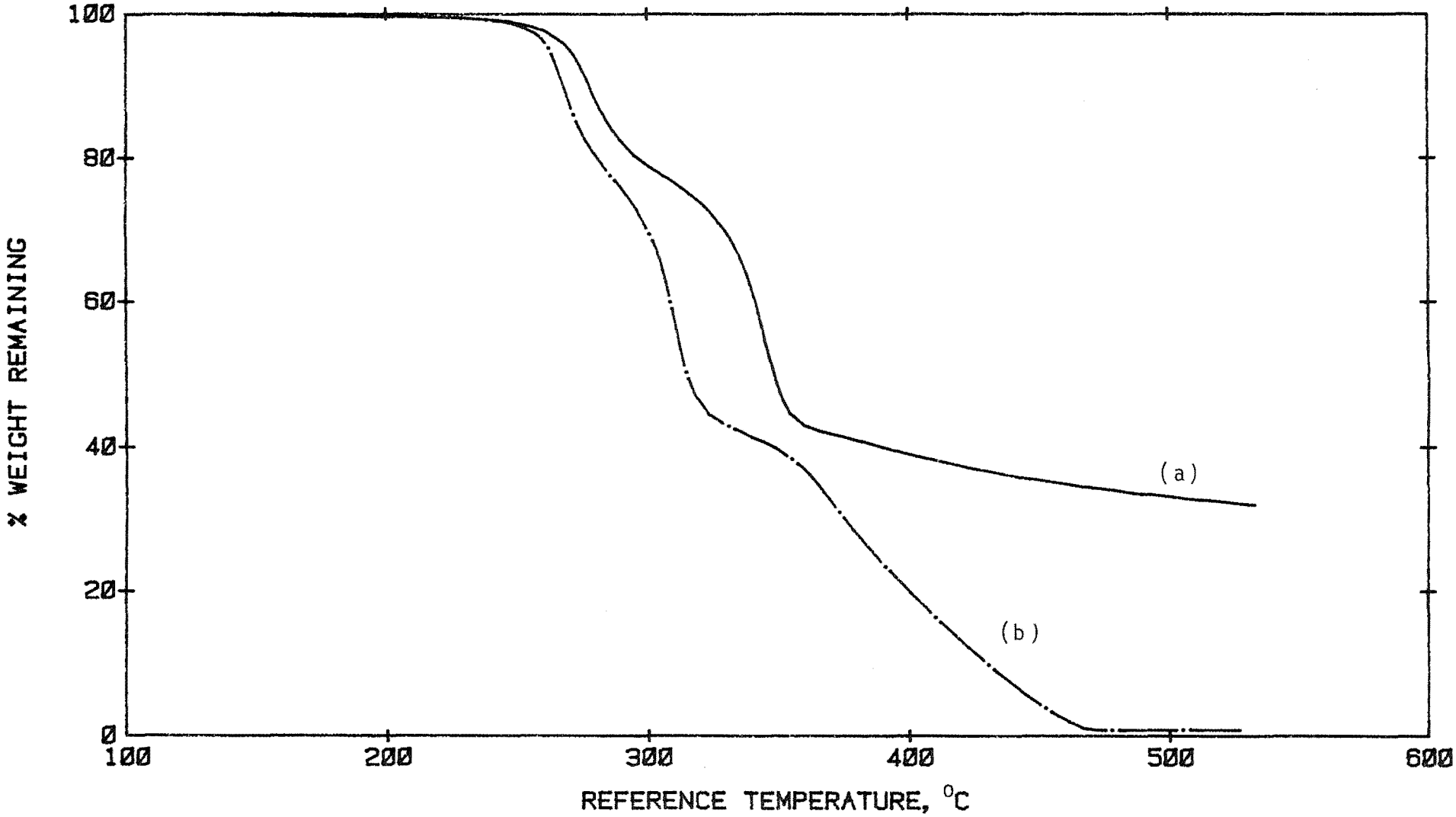

Fig. A25. TG curves of Coconut wood:(a) in N_2 and (b) in air

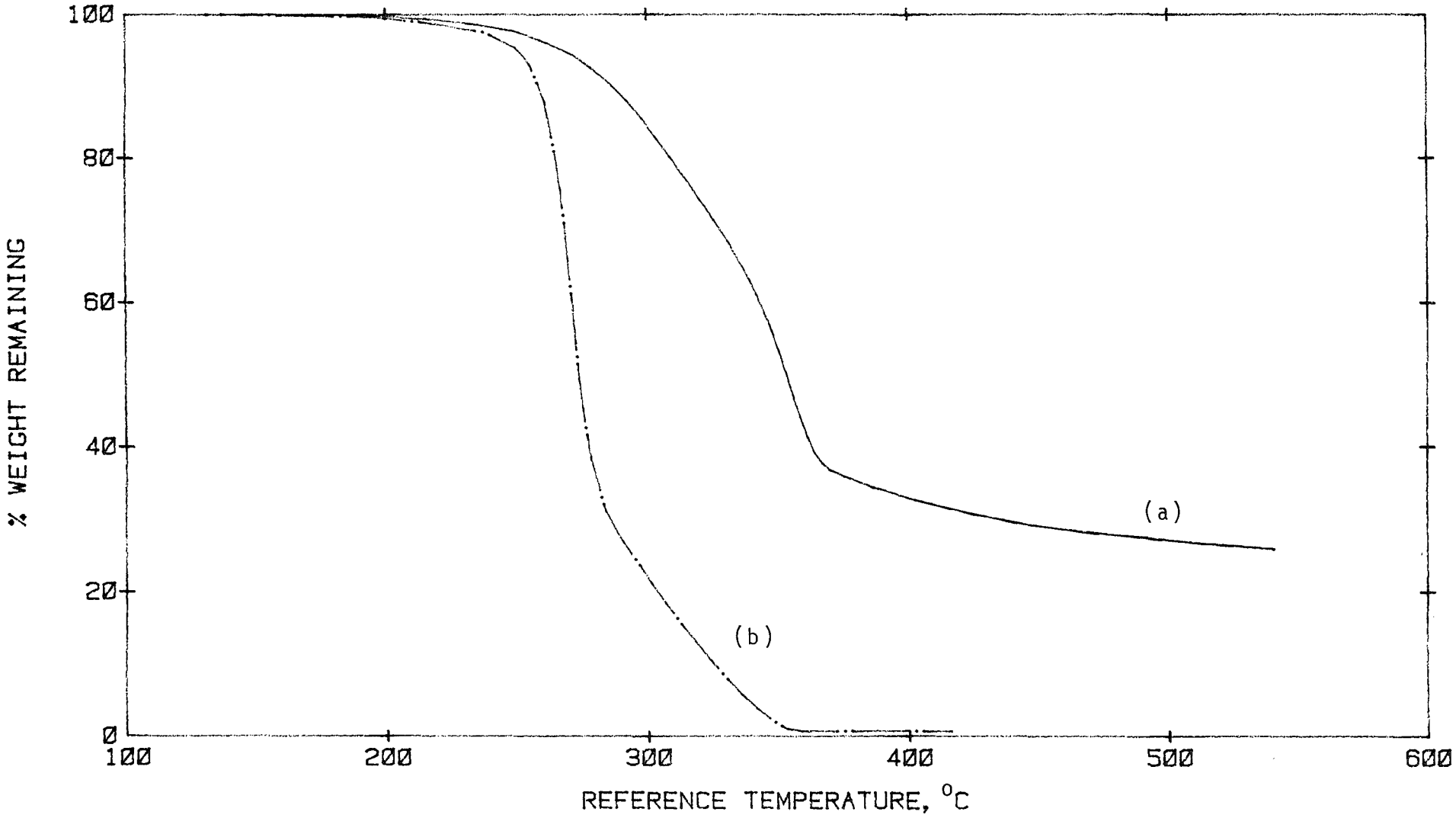

Fig. A26. TG curves of Jelutong:(a) in N_2 and (b) in air

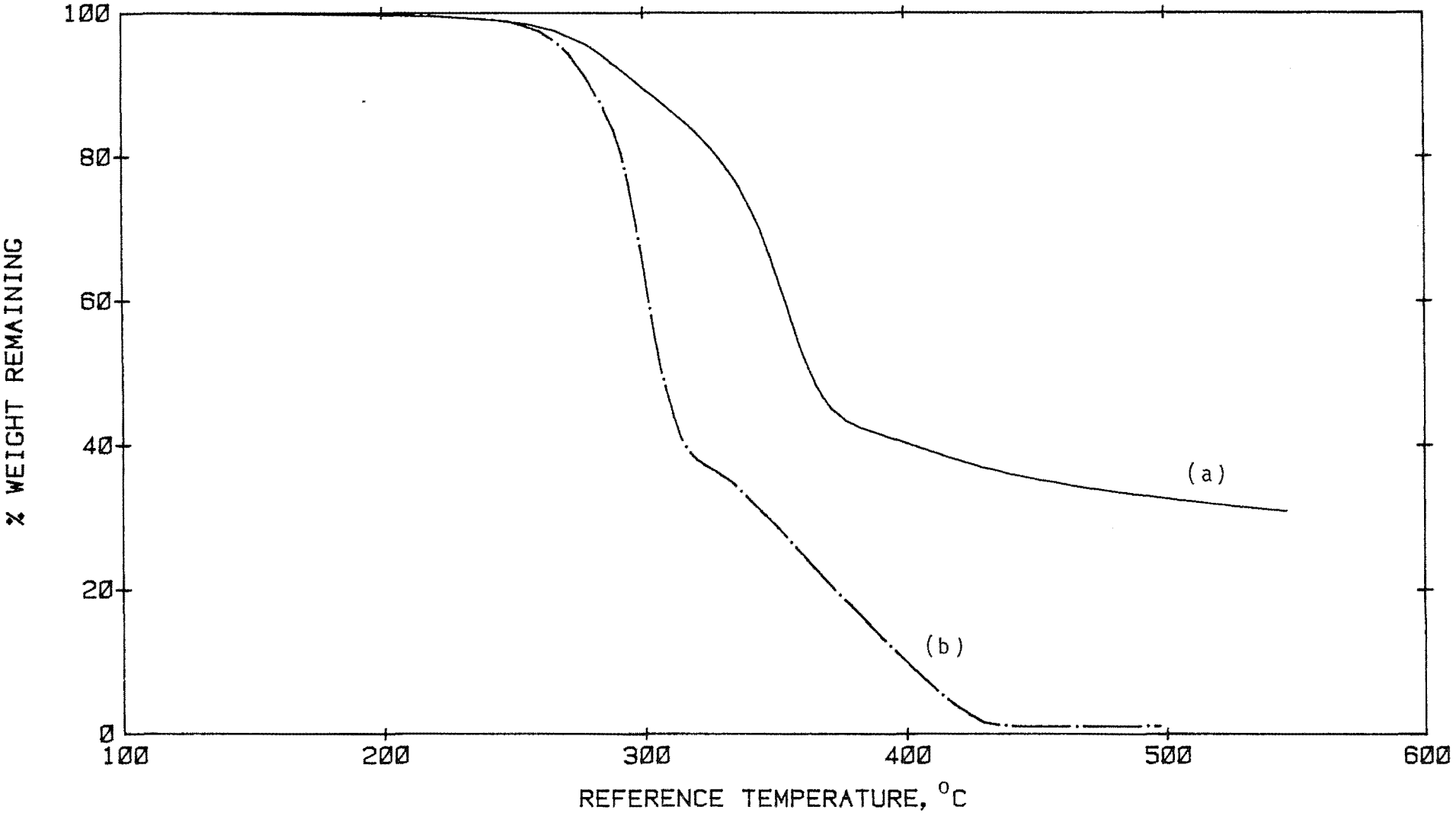

Fig. A27. TG curves of Kempas:(a) in N_2 and (b) in air

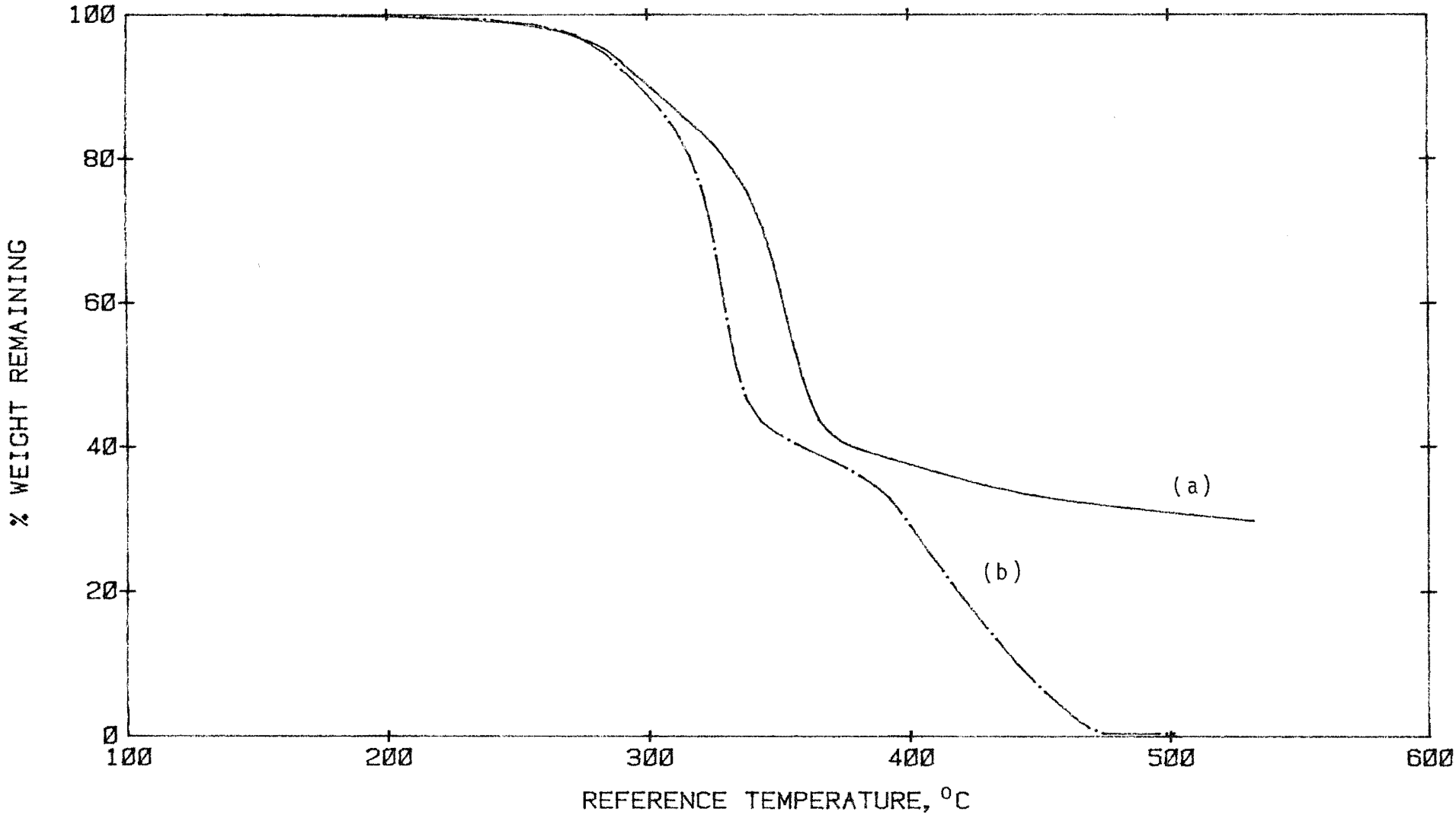

Fig. A28. TG curves of Keruing:(a) in N_2 and (b) in air

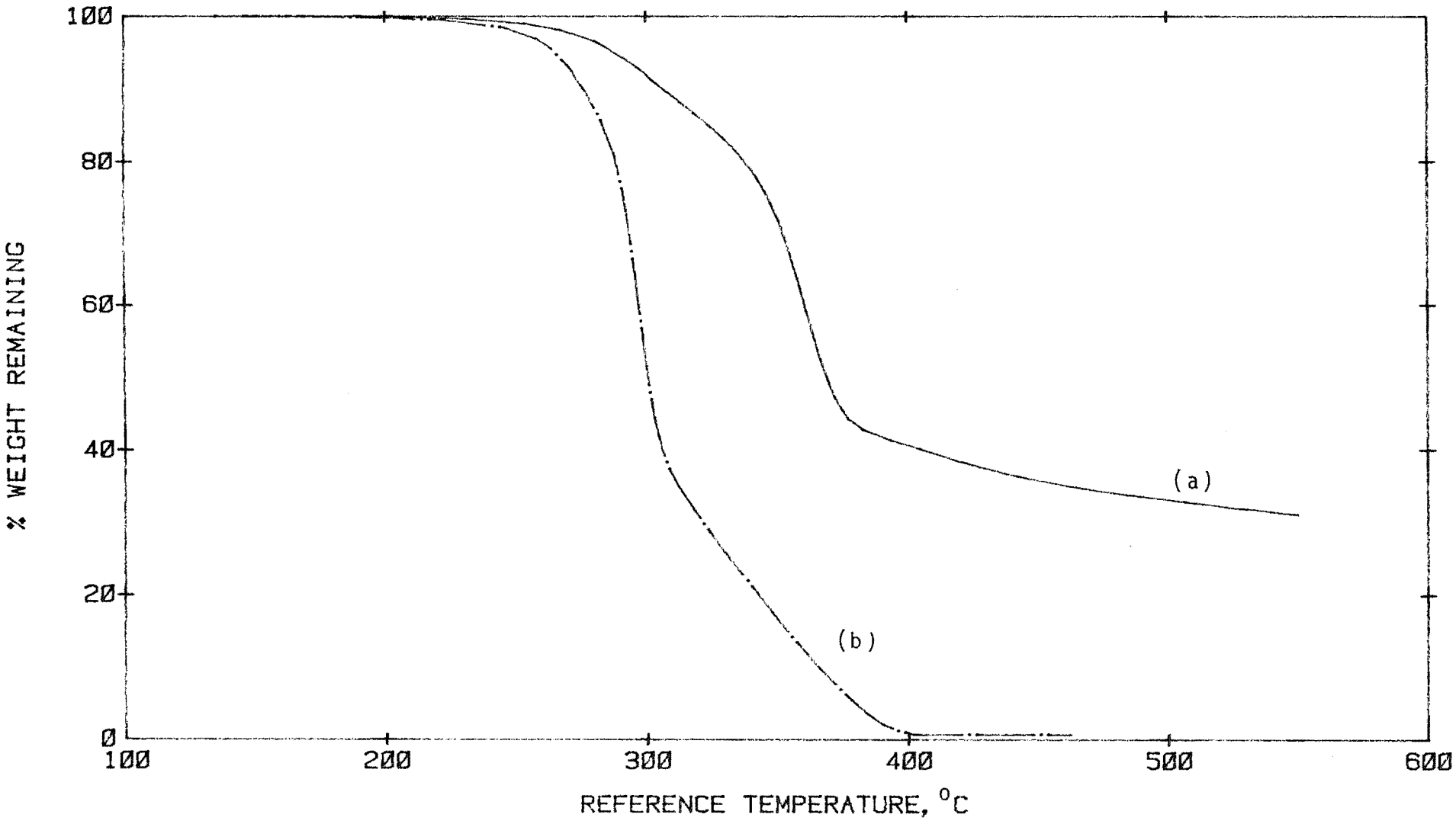

Fig. A29. TG curves of Mengkulang:(a) in N_2 and (b) in air

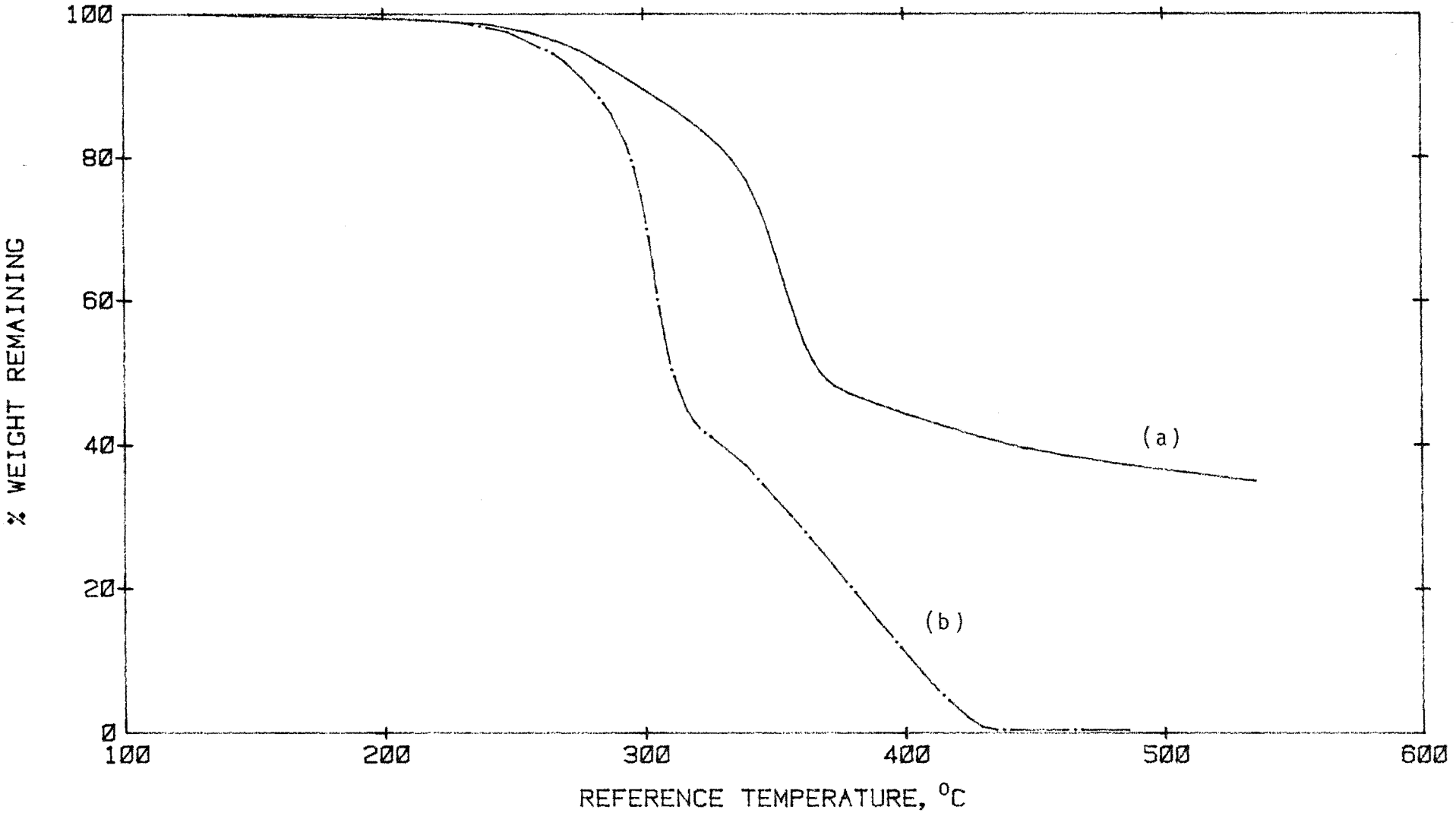

Fig. A30. TG curves of dark red Meranti:(a) in N_2 and (b) in air

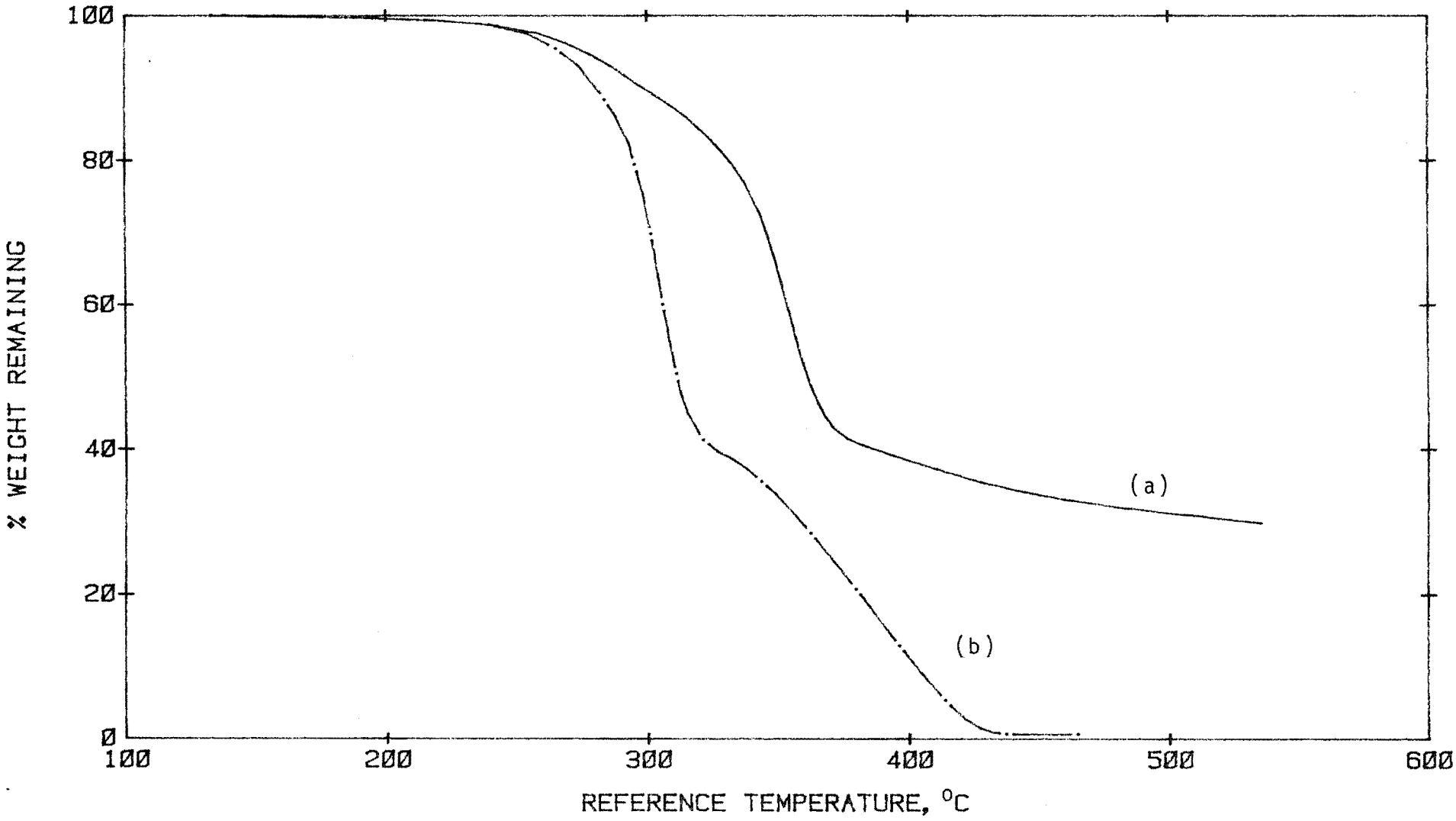

Fig. A31. TG curves of light red meranti:(a) in N_2 and (b) in air

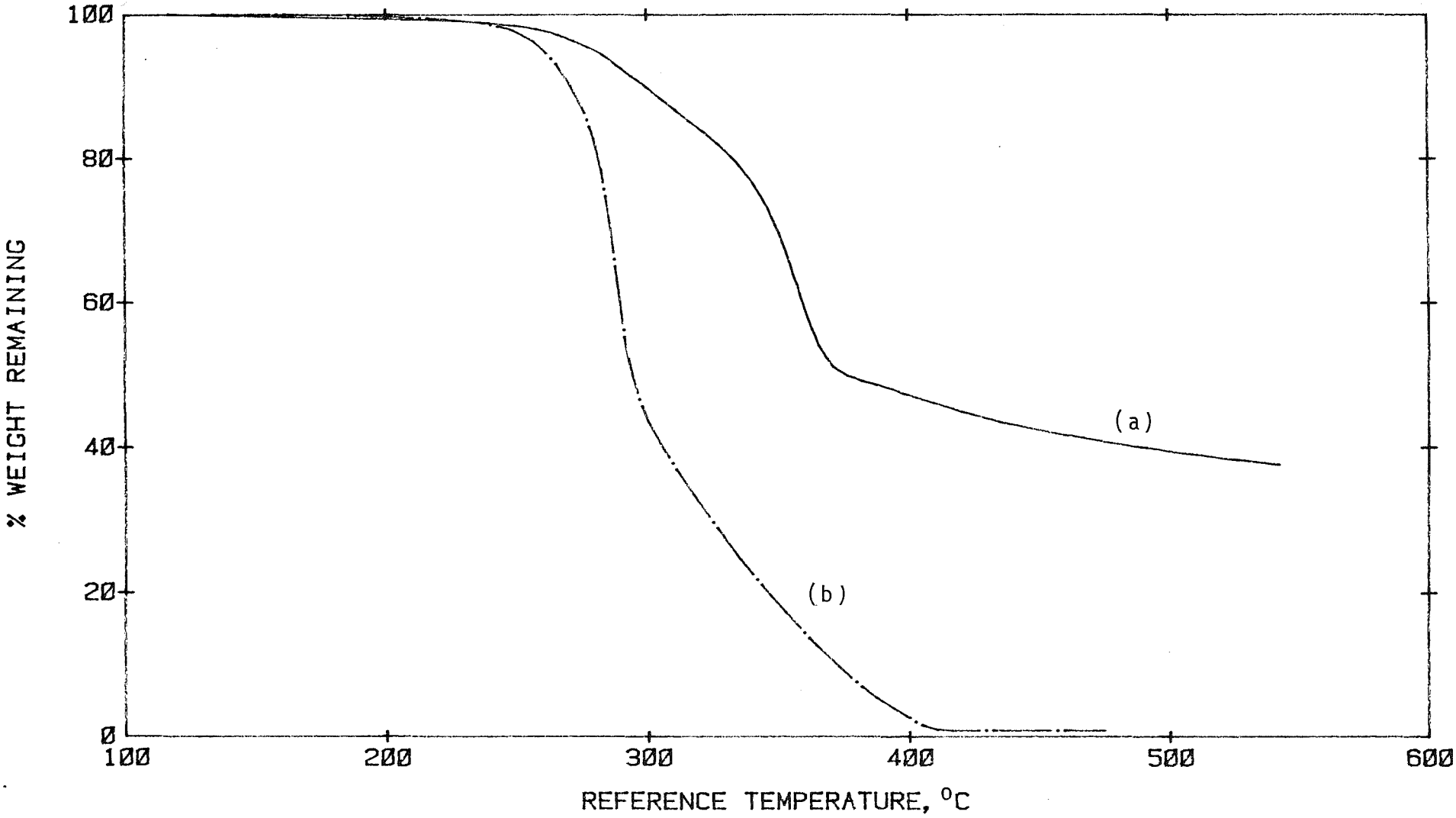

Fig. A32. TG curves of Merbau:(a) in N_2 and (b) in air

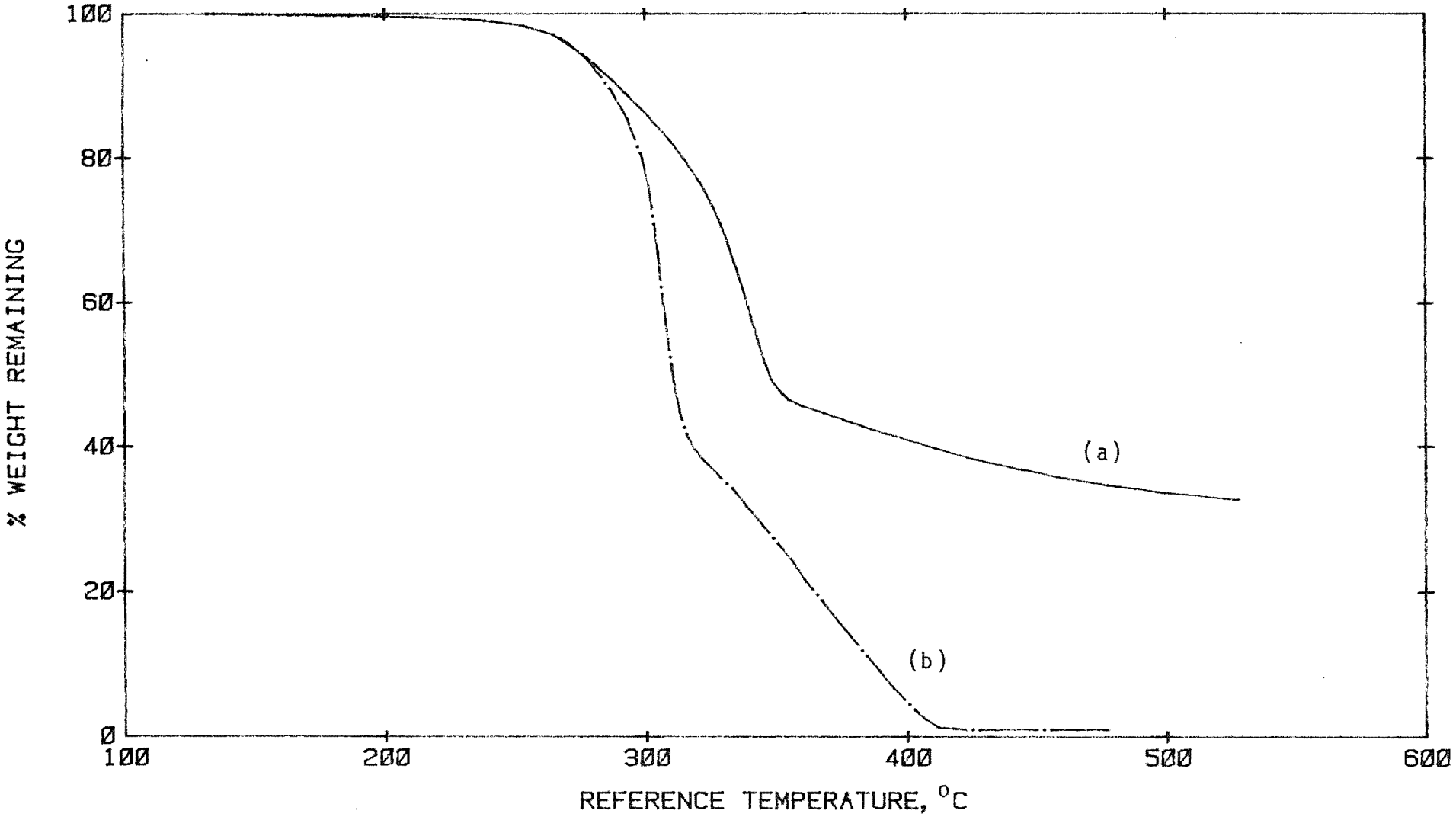

Fig. A33. TG curves of Mersawa:(a) in N_2 and (b) in air

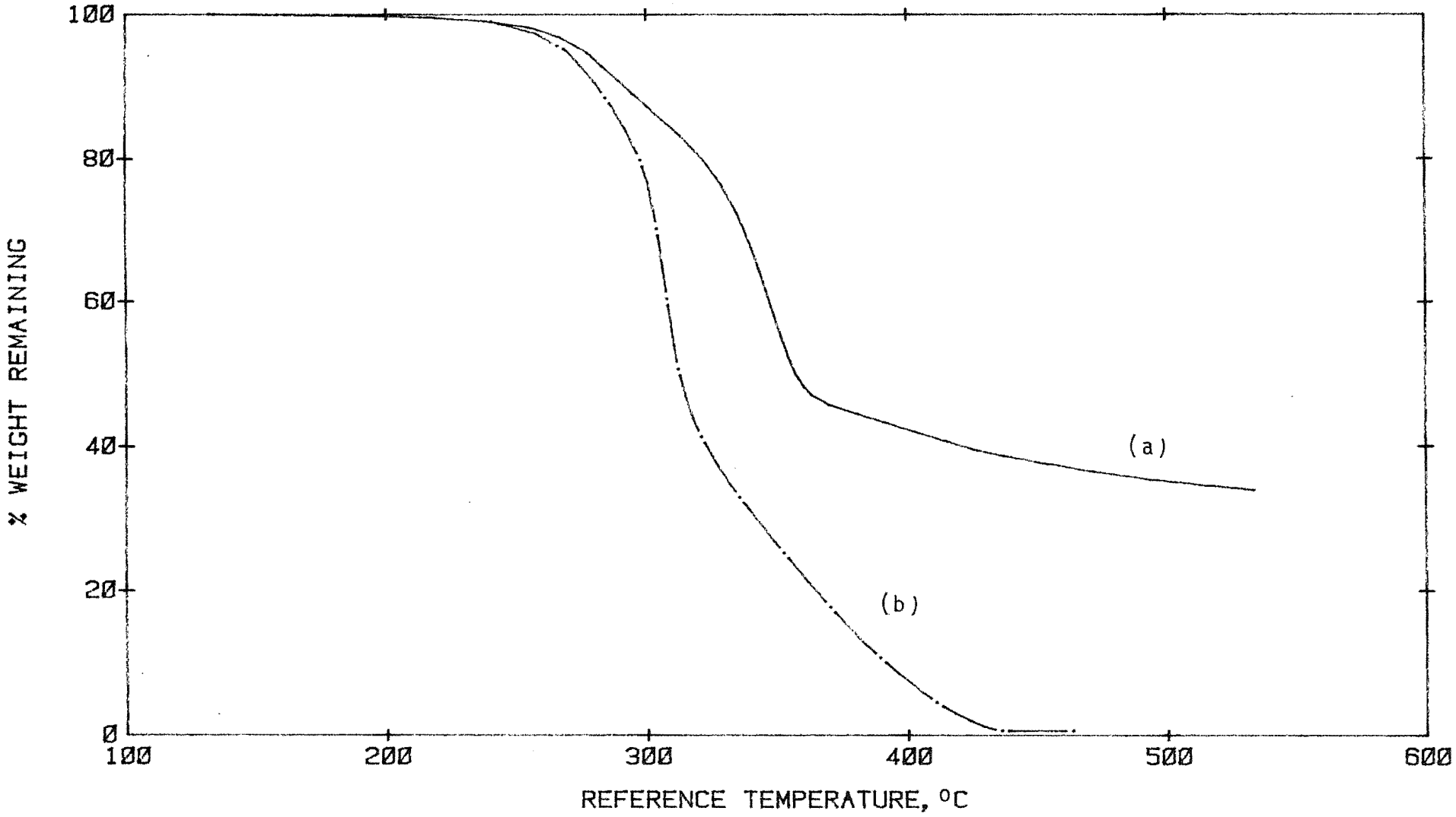

Fig. A34. TG curves of Nyatoh:(a) in N_2 and (b) in air

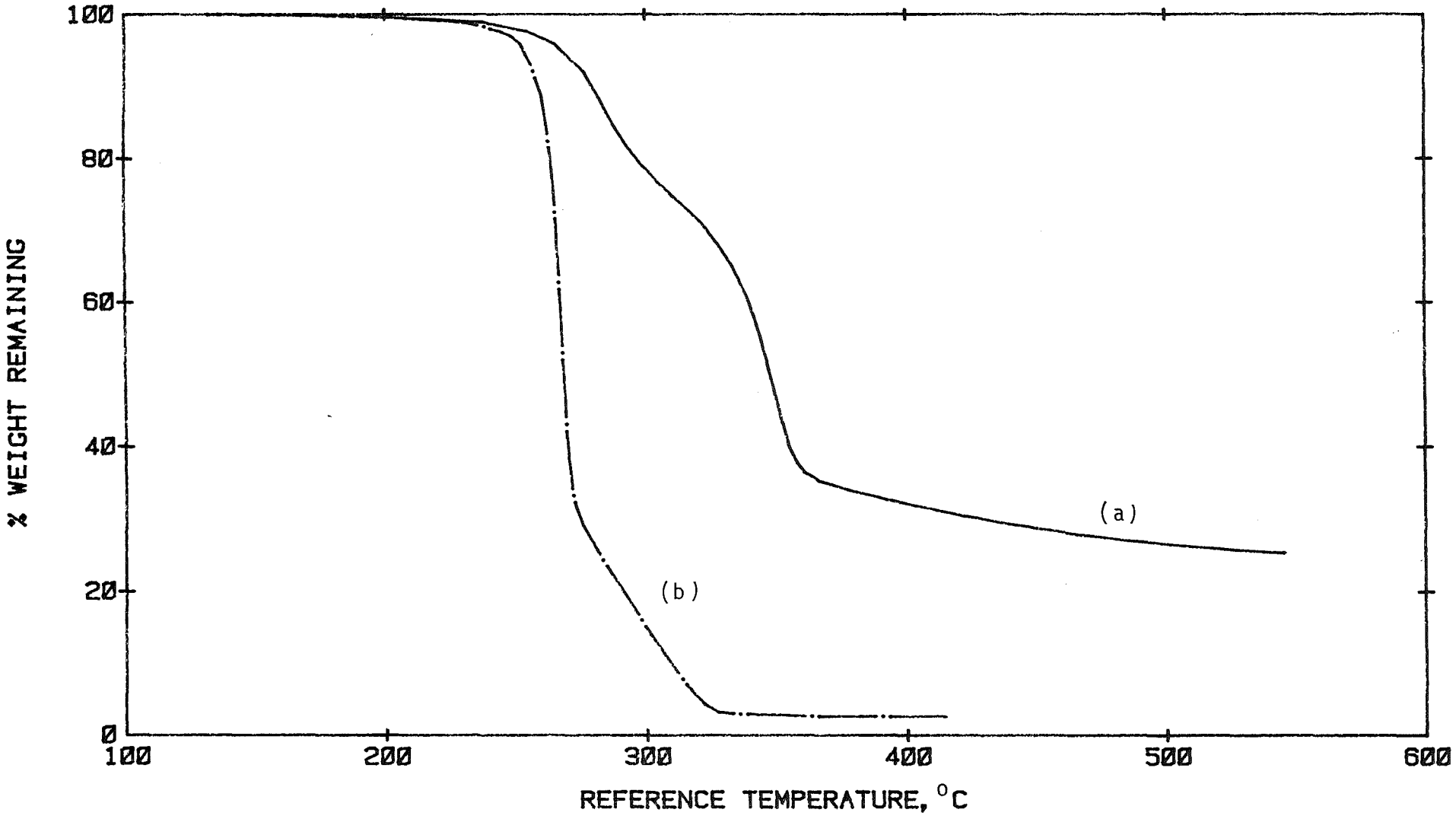

Fig. A35. TG curves of Oil palm wood:(a) in N_2 and (b) in air

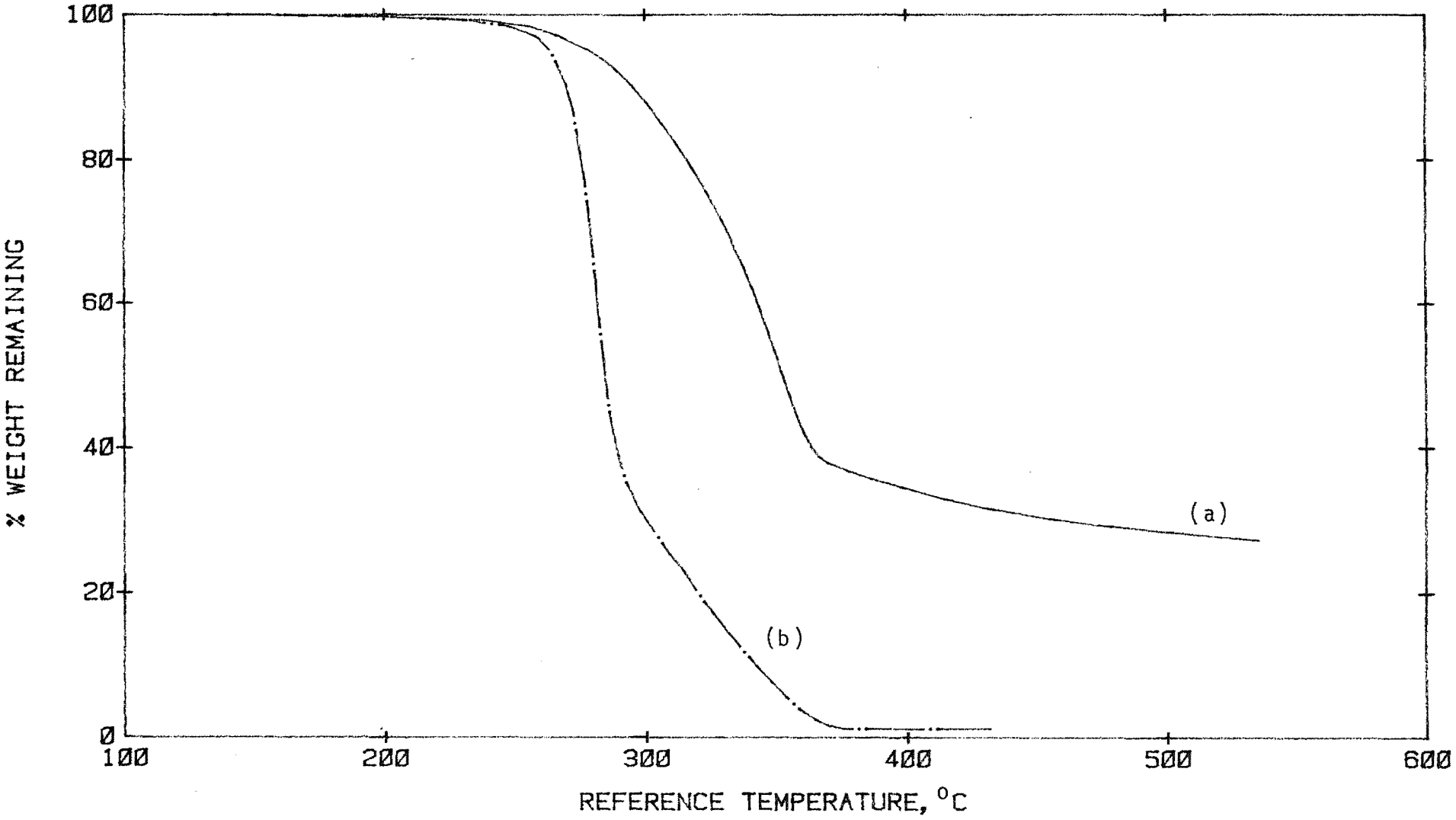

Fig. A36. TG curves of Pulai:(a) in N_2 and (b) in air

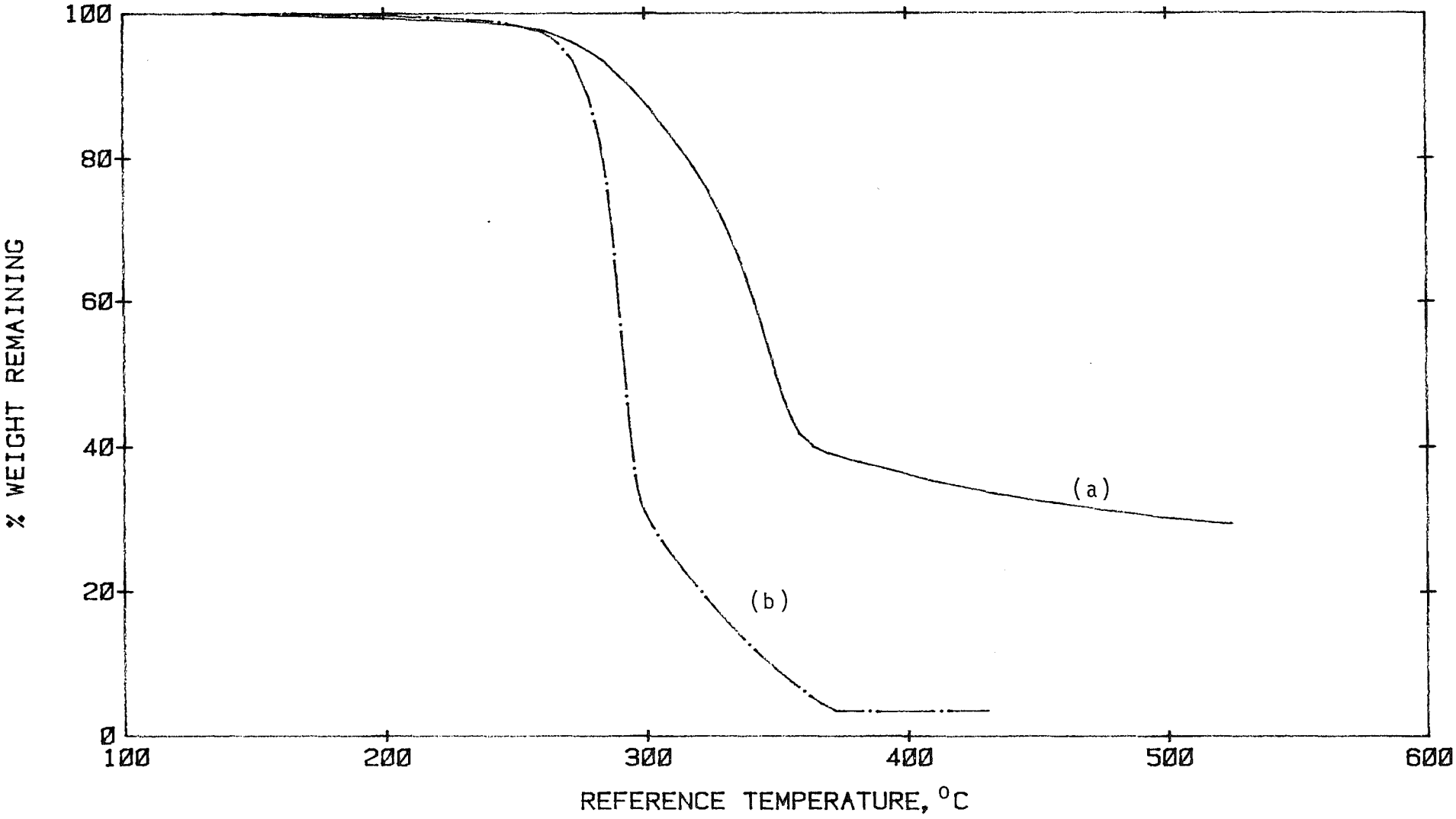

Fig. A37. TG curves of Ramin:(a) in N_2 and (b) in air

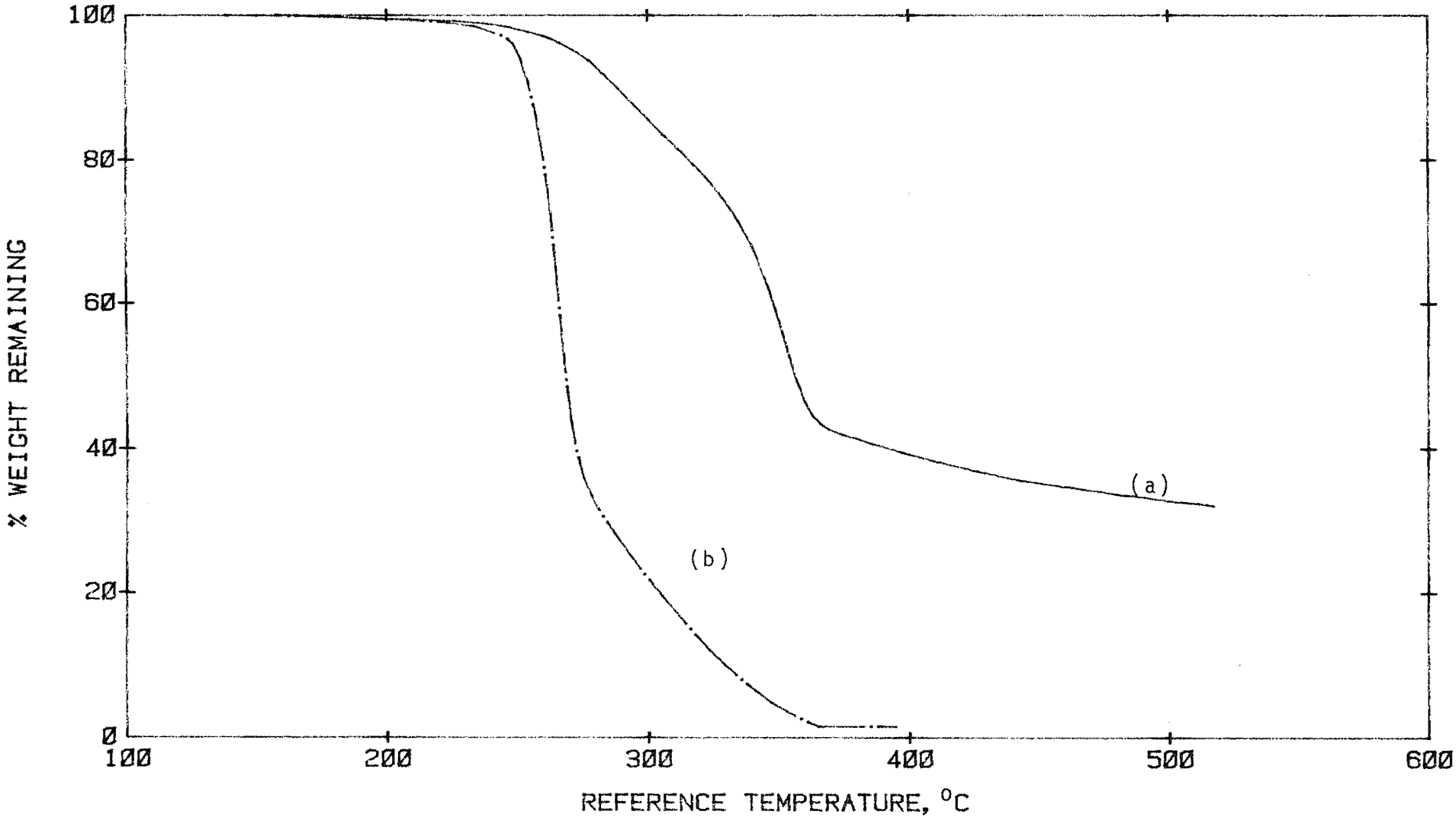

Fig. A38. TG curves of Sepetir:(a) in N_2 and (b) in air

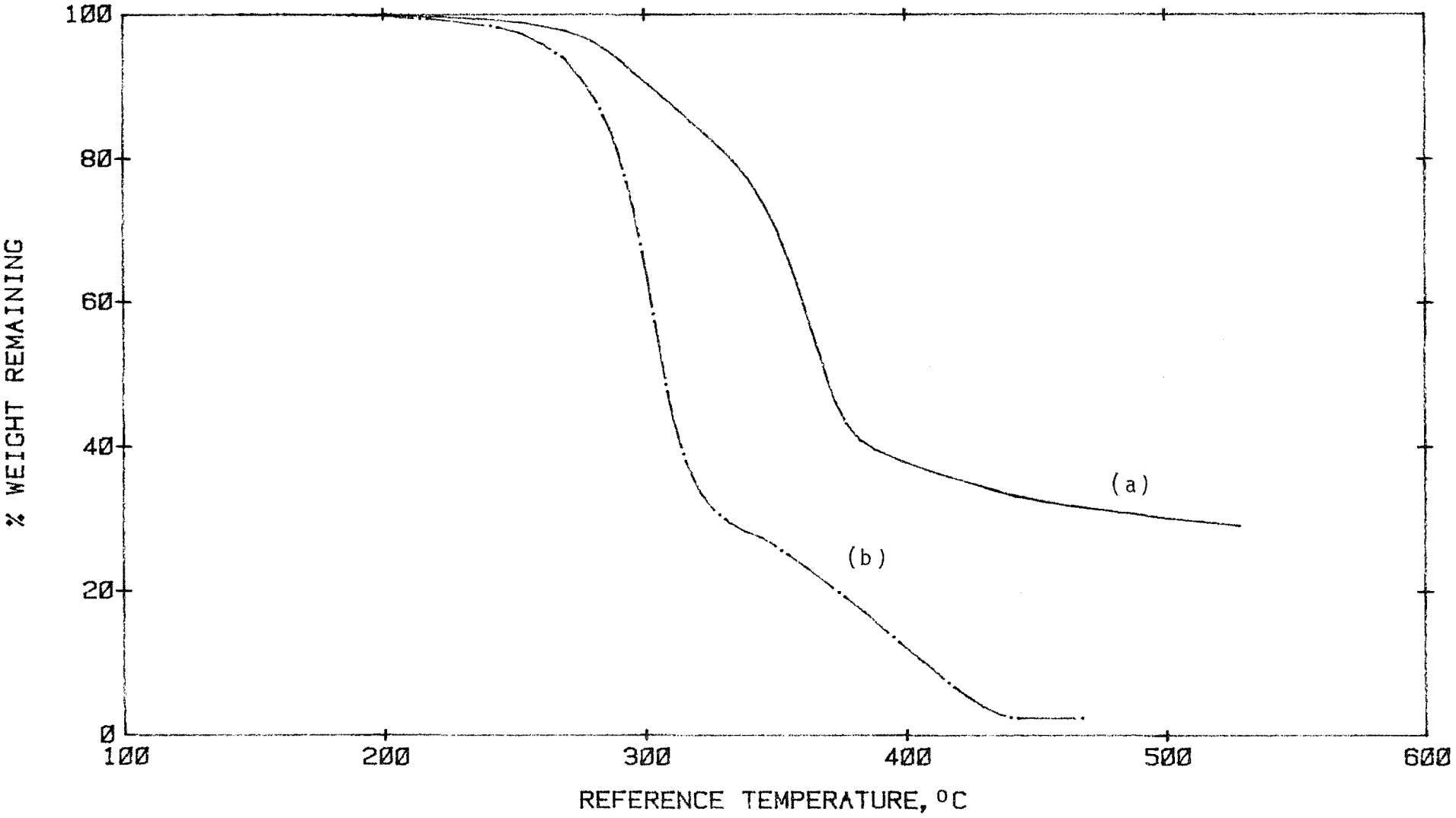

Fig. A39. TG curves of Tembusu:(a) in N_2 and (b) in air

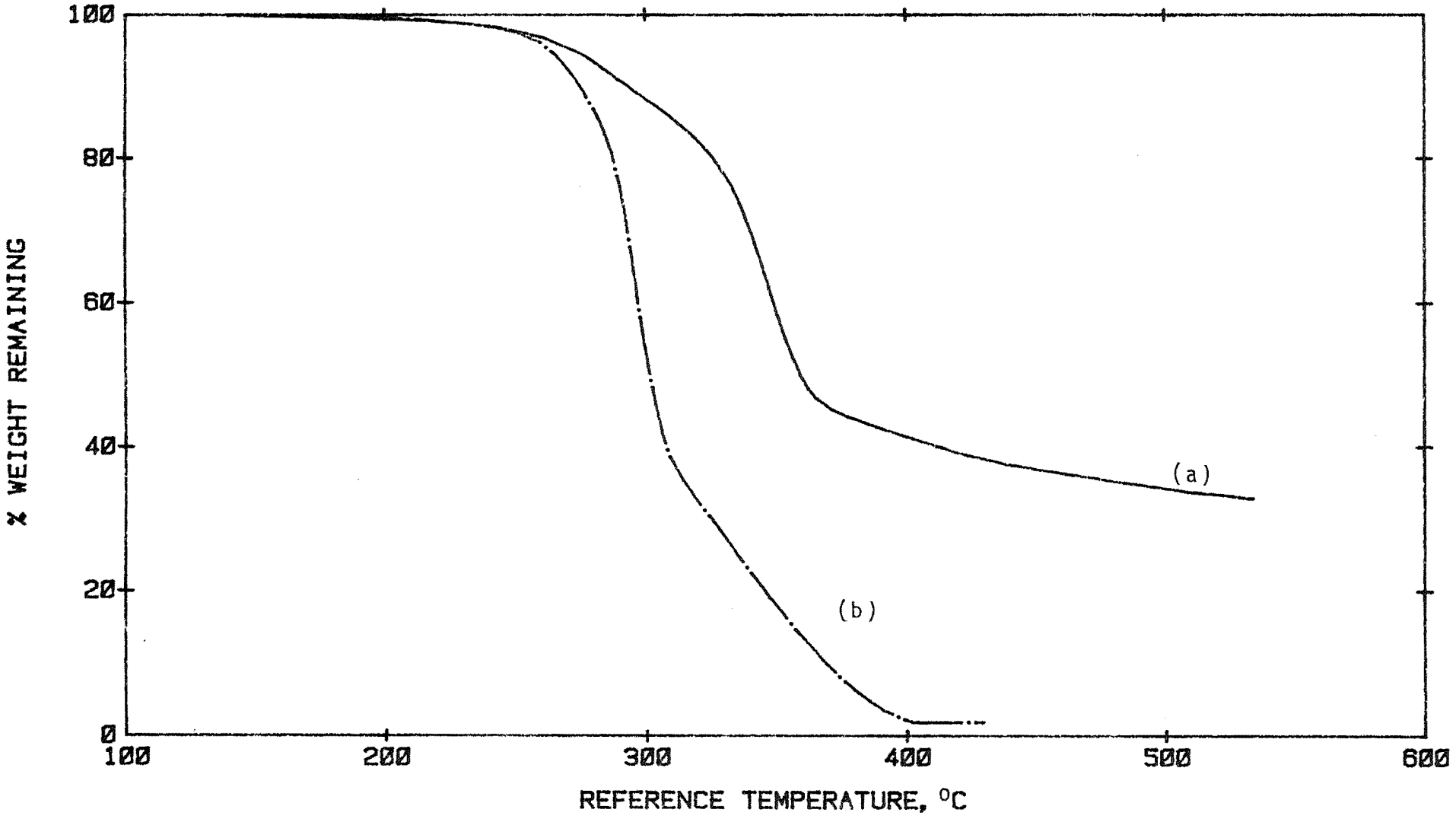

Fig. A40. TG curves of Tualang:(a) in N_2 and (b) in air

Appendix 10A. Individual Ash Contents - Rubber Wood

Sample No.	Ash content, % of oven-dried wood
Tjir 1	
1	1.23
2	1.08
3	1.17
4	1.26
5	1.12
PR 107	
1	1.52
2	1.36
3	0.97
4	1.10
5	1.17
RRIM 605	
1	1.07
2	1.07
3	0.60
4	0.73
5	1.12
RRIM 623	
1	1.14
2	0.89
3	0.92
4	0.97
5	1.08

Mean ash contents

Tjir 1 - 1.17%

PR 107 - 1.22%

RRIM 605 - 0.92%

RRIM 623 - 1.00%

Appendix 10B. Individual Ash Contents - Other Wood Species

Species	Ash content, % of oven-dried wood
BARK	6.20
"	8.48
"	7.64
"	6.14
Ramin	2.01
"	2.12
"	2.24
Oil palm wood	1.53
"	1.52
"	1.50
Sepetir	1.33
"	1.20
Tualang	1.24
"	1.23
Mersawa	0.93
"	1.07
Pulai	0.77
"	0.70
Coconut wood	0.47
"	0.43
"	1.08
"	0.55
"	0.74
Jelutong	0.53
"	0.51
Merbau	0.53
"	0.51
Mengkulang	0.54
"	0.48

contd.

Species	Ash content, %
Nyatoh	0.38
"	0.50
Keruing	0.30
"	0.37
Radiata pine	0.23
"	0.21
Tembusu	0.19
"	0.18
Kempas	0.14
"	0.12
Meranti, dark red	0.09
"	0.09
Meranti, light red	0.09
Balau	0.08
"	0.18
"	0.04
Chengal	0.07
"	0.08

Appendix 11. Theoretical Oxygen Requirement for Complete Combustion

The theoretical oxygen requirement for the complete combustion of a unit weight of Rubber wood is calculated.

The elemental compositon of Rubber wood is as follows (see Section 3.2.1) :

C	49.0 % w/w
O	44.0 % w/w
H	6.0 % w/w
Ash	1.0 % w/w

Basis : 1 kg of oven-dried wood

The reactions involved are :

$$C + O_2 \text{ ------> } CO_2$$
$$12 \quad 32 \qquad 44$$
$$H_2 + \tfrac{1}{2}O_2 \text{ ------> } H_2O$$
$$2 \quad 16 \qquad 18$$

Amount of oxygen required to burn 0.49 kg of carbon
= 0.49x32/12 kg
= 1.307 kg

and amount of oxygen required to burn 0.06 kg of hydrogen
= 0.06x16/2 kg
= 0.480 kg

Total oxygen requirement = 1.307+0.480 = 1.787 kg

Since 0.44 kg of oxygen is available in the wood, oxygen to be supplied = 1.787-0.44 = 1.347 kg

Thus, amount of air to be supplied = 1.347x100/23.2 kg
= 5.806 kg

(air contains 23.2 % by weight of oxygen)

Combustion Products

Amount of CO_2 formed = 0.49x44/12 = 1.80 kg
Amount of H_2O formed = 0.06x18/2 = 0.54 kg
Amount of N_2 in flue gas = 0.768x5.86 = 4.50 kg

A flowsheet for the burning of the wood using the theoretical amount of air required for complete combustion is shown in Figure A41.

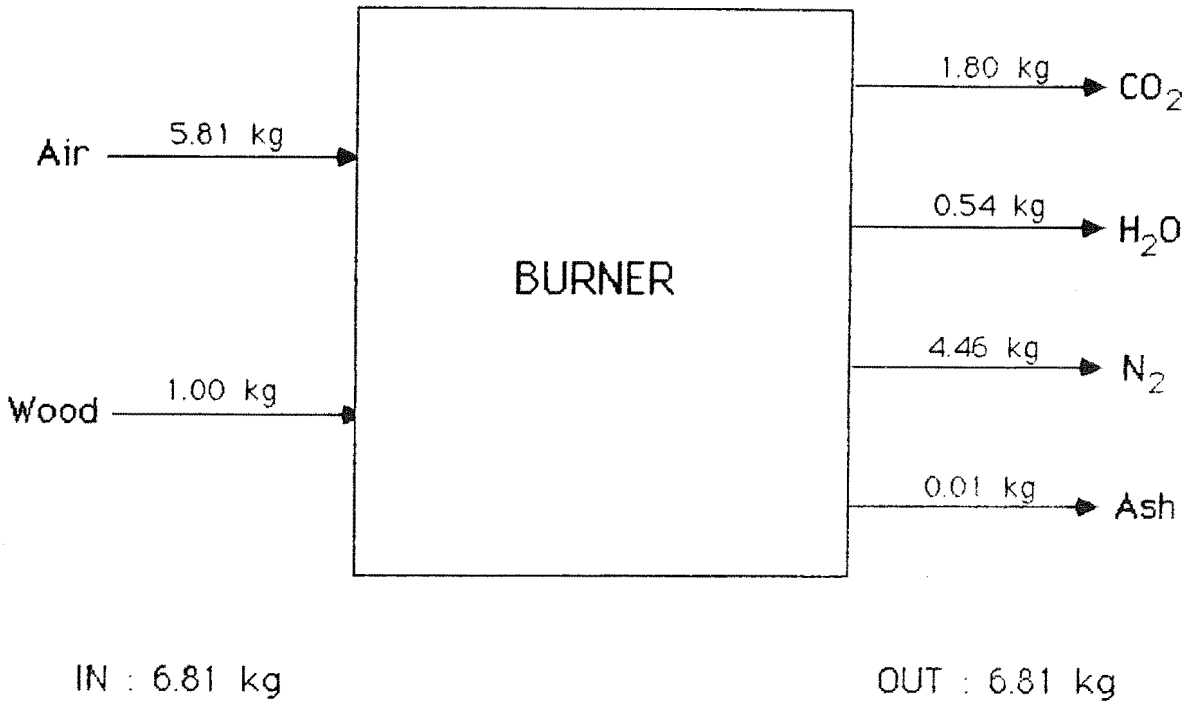

Figure A41. Flow-sheet for combution of wood